Polymeric Nucleic Acid Delivery Systems for Reviving TRAIL Therapy for Breast Cancer

by

Bindu Thapa

A thesis submitted in partial fulfillment of the requirements for the degree of

Doctor of Philosophy

in

Pharmaceutical Sciences

Faculty of Pharmacy and Pharmaceutical Sciences

University of Alberta

Abstract

Targeting a single pathway is not enough to treat cancer because of compensatory mechanisms against anticancer therapy via alternative molecular pathways for survival and proliferation of malignant cells. Given the unacceptable toxicity associated with conventional therapy, nucleic acids such as plasmid DNA (pDNA), messenger RNA (mRNA) and small interfering RNA (siRNA) and their combinations could be a potential approach for specifically killing cancer cells. The idea of nucleic acid combination therapy is to simultaneously target multiple intracellular signalling pathways via overexpressing therapeutic proteins with pDNA and mRNA while silencing unwanted proteins with siRNAs. Nucleic acids, however, cannot enter cells on their own. Therefore, this thesis explored the delivery of nucleic acids and their combinations in *in vitro* and *in vivo* model using non-viral delivery systems. We first explored the galactose-based glycopolymers for the gene delivery. Optimization on size, composition (cationic vs galactose) and architectures (block vs statistical) was essential for gene delivery. Galactose containing block copolymer delivered pDNA specifically to asialoglycoprotein receptor (ASGPR) expressing hepatocytes (e.g. HepG2, Huh7.5). However, transfection efficiency of these polymers was negligible in ASGPR deficient cells. Instead, small hydrophobe and longer aliphatic lipid modified low molecular weight polyethyleneimine (PEI) were explored which efficiently delivered nucleic acid into breast cancer cells. The amount, length, and type of substitution as well as type of bond between hydrophobic group and PEI had significant impact on the transfection efficiency. Small hydrophobe propionic acid (C3) substitution on 1.2 PEI (PEI1.2-PrA) resulted higher pDNA delivery efficiency at modest substitution (0.5 to 1 PrA/PEI, mol/mol) while higher substitutions were detrimental. pDNA transfection efficiency of PEI1.2-PrA was higher than linoleic acid (C18) substituted 1.2PEI (1.2PEI-LA). However, 1.2PEI-PrA was unable to deliver siRNA while

aliphatic lipid linoleoyl (LA) and linolenoyl (αLA) substitution resulted higher siRNA transfection efficiencies. To target different pathways simultaneously, co-delivery of pDNA and siRNA was then explored which is more challenging due to differences in their size and structure. LA-modified thioester linked polymer (PEI1.2-tαLA) was able to co-deliver both pDNA and siRNA in *in vitro* and *in vivo* breast cancer models. Using 1.2PEI-αLA, siRNA library against 446 human apoptosis related proteins were screened and we identified, among others, two siRNAs silencing BCL2 like 12 (BCL2L12) and superoxide dismutase 1 (SOD1) which enhanced the tumor necrosis factor receptor apoptosis inducing ligand (TRAIL) induced apoptosis in breast cancer cells. Using 1.2PEItαLA, a TRAIL encoding plasmid (pTRAIL) and siRNAs targeting BCL2L12 and SOD1 were then employed as synergistic pair for breast cancer therapy. We found that co-delivery resulted higher breast cancer cell death than separate delivery without affecting normal cells. Furthermore, co-delivery of pTRAIL and BCL2L12 siRNA significantly retarded growth of breast cancer xenografts in mice. The enhanced anticancer activity was attributed to increased *in situ* secretion of TRAIL and sensitization of breast cancer cells against TRAIL by the co-delivered siRNAs. To mitigate the problems associated with pDNA including immunogenicity, mutagenesis due to possibility of permanent integration into genome and need for nuclear transport, all leading to low transfection efficiency, we explored mRNA delivery using PEI1.2-tαLA. Messenger RNA transfection resulted earlier and higher protein expression as compared to pDNA. Messenger RNA encoding TRAIL (mTRAIL) resulted higher cell death than pTRAIL in breast cancer cells and hBMSC modified with mTRAIL were able to kill breast cancer cells after co-culture. Overall, these studies identified polymers suitable for delivery of individual types of nucleic acids or their combination and established importance of nucleic acid combinations to support TRAIL induced apoptosis in breast cancer cells.

Preface

Versions of the literature review and research results presented in this thesis were published as described below. All chapters (apart from **Chapter 2**, see below) were conceptualized, researched and written by Bindu Thapa under the supervision of H. Uludağ, the primary supervisory author. Additional contributions and acknowledgements are listed at the respective chapters. The ethics approval to use animals in this thesis was obtained from Animal Care and Use Committee: Heath Sciences at the University of Alberta (Study ID: AUP00000423) in accordance with the directions of the Canadian Council on Animal Care. **Chapter 1** contains a review on the delivery of nucleic acids which is included within the manuscript published as R. KC, B. Thapa, J. Valencia-Serna, H. M. Aliabadi, H. Uludağ, "Nucleic Acid Combinations: A New Frontier for Cancer Treatment", *Journal of Controlled Release*, 2017, 256, 153–169. Only the portions of described paper that I contributed (Section 1.2 Nucleic Acid Combination and section 1.3 Delivery of Nucleic Acid Combinations with Nano-assembled Non-Viral Carriers) were included in the thesis. Figure 1 is of courtesy of R. KC. This section is followed by an overview on therapeutic effects of TRAIL on cancer, which was not published previously.

Chapters 2 and **3** are research papers focused on the gene delivery to cancer cells using non-viral vectors. **Chapter 2** was published as B. Thapa, P. Kumar, H. Zeng, R. Narain, "Asialoglycoprotein Receptor-mediated Gene Delivery to Hepatocytes Using Galactosylated Polymers", *Biomacromolecules,* 2015, 16*,* 3008-3020. As the lead author, I designed, performed and analyzed the studies and wrote the manuscript. P. Kumar and H. Zeng edited the manuscript. R. Narain provided research guidance and edited the manuscript and was the responsible author for study direction. **Chapter 3** was published as B. Thapa, S. Plianwong, B. Rutherford, R. B. KC, H. Uludag, "Small Hydrophobe Substitution on Polyethylenimine for Plasmid DNA Delivery:

Optimal Substitution is Critical for Effective Delivery", *Acta Biomaterialia*, 2016, 33, 213-224. I was responsible for the data collection and analysis as well as writing the manuscript. S. Plianwong, B. and Rutherford assisted with characterization of particles and R. KC synthesized the polymers and contributed to manuscript editing.

Chapter 4 was published as B. Thapa, R. B. KC, Hasan Uludag, "Novel targets for sensitizing breast cancer cells to TRAIL induced apoptosis with siRNA delivery", *International Journal of Cancer*, 2017, 142, 597-606. I was responsible for the experiment design, data collection, and analysis and manuscript composition. R.B. KC synthesized the polymers and contributed to edit manuscript.

Chapter 5 involved co-delivery of nucleic acids which is under review now for publication as B. Thapa, R. B. KC, M. Hitt, A. Lavasanifar, O. Kutsch, D. W. Seol, H. Uludağ, "Breathing a new life into TRAIL: Co-delivery of TRAIL plasmid and complementary siRNA for breast cancer treatment." As a lead author, I was involved in the experiment design, data collection, analysis and writing the manuscript. R. B. KC synthesized the polymers and assisted in manuscript composition. M. Hitt and A. Lavasanifar provided research guidance. O. Kutsch provided GFP positive MDA-MB-231 cells and D. W. Seol provided the secretable TRAIL plasmid, which was expanded in-house. **Chapter 6** involved the utilizing an mRNA encoding TRAIL protein for treatment of breast cancer and will be submitted for publication. As a lead author, I was involved in the experiment design, data collection, analysis and writing the manuscript. R. B. KC synthesized the polymers and assisted in manuscript composition, Liu Xin and Wei Fu synthesized mRNA incoding TRAIL. I conclude with **Chapter 7** that is focused on the conclusions and future directions of my thesis work. This chapter includes portions of research articles described above as well as new content derived from the knowledge gained from the work presented in the thesis.

Appendix F was published as B. Thapa, R. B. KC, H. Uludağ, "siRNA Library Screening to Identify Complementary Therapeutics Paris in Triple-Negative Breast Cancer Cells", *RNA Interference and Cancer Therapy: Methods and Protocols in Molecular Biology*, 2019, 1974, 1-19. I was responsible for manuscript composition. R. KC synthesized the polymers and contributed to manuscript edits.

Acknowledgements

I have had the opportunity to be supported by scholarship funding over the course of my graduate studies. I would like to acknowledge and thank following institutions for their support: Alberta Innovates for providing me Alberta Innovates Graduate Studentships, University of Alberta for Doctoral recruitment scholarship, NSERC CREATE Program for regenerative medicine for Graduate studentship, Faculty of Pharmacy and Pharmaceutical Sciences for Shoppers Drug Mart Graduate Scholarship. I have also been supported to present research work at several conferences and would like to thank the supporting agencies; GSA, University of Alberta for Mary Louise Imrie Graduate Student Award, Faculty of Pharmacy and Pharmaceutical Sciences for Travel award. During the course of my PhD study, I have had the opportunity to work with many talented researchers within our lab as well as in others across the University of Alberta. I would specifically like to thank my lab colleagues at the Dr. Uludag lab (past and present). Especially I would like to thank Dr. Remant KC, whom I enjoyed working together on many experiments, Cezary Kucharski for guidance in cell culture studies. I would like to thank lab colleagues, Dr. Juliana Valencia-Serna, Dr. Major Parmar, Eleni Tsekoura, Anyeld Ubeda, Daniel Nisakar Sundaram, Aysha Ansari, Mahsa Mohseni, Adam Manfrin, Teo Atz Dick, whom I enjoyed working with and provided critical insight into my studies in our group meetings and haphazard discussions. I would like to thank my previous supervisor, Dr. Ravin Narain and colleagues at Dr. Narain's lab at the time; Dr. Yinan Wang and Stephen Quan. I would also like to thank visiting PhD student from Thailand, Samarwadee Pilangwong and summer student Janine Schmitke who worked with me on some studies. I would like to thank a visiting scholar from China, Dr. Liu Xin and collaborator from China, Dr. Wei Fu for helping on synthesis of mRNA encoding TRAIL. I would like to again acknowledge my co-authors in my publications and those listed in the

acknowledgement section of my publications for their valuable contributions. I would specially thank my thesis committee members Dr. Hasan Uludag, Dr. Afsaneh Lavasanifar and Dr. Mary Hitt for their continuous suggestions and guidance to complete this thesis work. I would like to thank my family and friends for their support, encouragement and entertainment during my studies. Lastly, I greatly appreciate the opportunity, support and mentorship I received from my supervisor Dr. Hasan Uludağ. I would like to thank Dr. Hasan Uludag for his strong academic support he provides, patience, and the positive laboratory environment he maintains, which made my 5 years in his lab an enjoyable experience.

Table of Contents

List of Tables

List of Figures

Chapter 1

Chapter 2

Chapter 3

Chapter 4

Chapter 5

Chapter 6

List of Abbreviations

Abbreviation	Name
^{1}H NMR	Proton nuclear magnetic resonance
AAVs	Adeno-associated viruses
ABD	Albumin binding domain
ACVA	4,4-azobis (4-cyanovaleric acid)
AEMA	2-aminoethyl methacrylamide
ANOVA	Analysis of variance
Apaf-1	Apoptotic protease-activating factor 1
ASF	Asialofetuin
ASGPR	asialoglycoprotein receptor
AT-MSG-TRAIL	Adipose tissue derived MSC modified with TRAIL gene
AV	Adenoviruses
bak	bcl-2 homologous antagonist/killer
bax	bcl-2 associated X protein
Bcl-2	B-cell lymphoma2
BCL2L1	Bcl-2 like 1
BCL2L12	BCL2-like-12
bcl-XL	B-cell lymphoma-extra large
BID	BH3 interacting domain
BIR	Baculovirus IAP repeat
CDC	Cell cycle protein
CDK9	Cyclin dependent kinase 9
cFLIP	Cellular FLICE-inhibitory protein
$CHCl_3$	Chloroform
CS	Chitosan
CsiRNA	Control siRNA
CTC	Circulating tumor cells
CTMP	Carboxyl-terminal modulator protein

CTP	4-Cyanopentanoic acid dithiobenzoate
DAPI	4,6-diamino-2-phenylindole
DcR1	Decoy receptor 1
DcR2	Decoy receptor 2
DD	Death domain
DISC	Death-inducing signaling complex
DLS	Dynamic light scattering
DMEM	Dulbecco's Modified Eagle Medium
DMF	*N,N′*-dimethylformamide
DMSO	Dimethyl sulfoxide
DNA	Deoxyribonucleic acid
DOTAP	*N*-(1-(2,3-dioleoyloxy)propyl)-*N,N,N*-trimethylammonium chloride
DR	Death receptor
DsiRNA	Dicer substrate siRNA
EDC	1-ethyl-3-(3-dimethylaminopropyl) carbodiimide
EGFR	Epidermal growth factor receptor
ER	Estrogen receptor
FADD	Fas-associated protein with death domain
FBS	Fetal bovine serum
GC	Glycol chitosan
GM-CSF	Granulocyte-macrophage colony-stimulating factor
GFP	Green Fluorescent Protein
GPC	Gel permeation chromatography
GPCS	Galactosylated poly (ethylene glycol)-chitosan-graft-spermine
gWIZ-GFP	GFP expressing plasmid
HSLAS	Health Sciences Laboratory Animal Services
HA	Hyaluronic acid
hBMSC	Human bone marrow stromal cells
HBSS	Hank's balanced salt solution
HCC	Hepatocellular carcinoma
HER-2	Human epidermal growth factor receptor 2

HSV-tk	Herpes simplex virus thymidine kinase
HUMSC	human umbilical cord mesenchymal stem cell
HUVEC	Human umbilical vein cells
IAP	Inhibitor of apoptosis
IGF-IR	Insulin-like growth factor I(IGF-I) receptor
IL2	Interleukin-2
IP	intraperitoneal
IV	Intravenous
JAK	Janus Activated Kinase
KSP	Kinesin spindle protein
LA	Linoleic acid
LAEMA	2-lactobionamidoethyl methacrylamide
LETM1	Leucine zipper/EF hand-containing transmembrane-1
LKB1	Liver kinase B1
LMW	Low molecular weight
LMW PEI	Low molecular weight polyethyleneimine
mAB	Monoclonal antibodies
Mcl-1	Myeloid cell leukemia-1
MDM2	Murine double minute-2
MEK	Mitogen-activated extracellular signal-regulated kinase
MeOH	Methanol
mGM-CSF	Mouse granulocyte macrophage colony- stimulating factor
mIL-2	Mouse interleukin-2
miRNA	Micro ribonucleic acid
modRNA	Chemically modified messenger RNA
MPA	Mercaptopropionic acid
mPEG-*b*-PCL-*b*-PPEEA	poly(ethylene glycol)-b-poly(ε-caprolactone)-b-poly(2-aminoethyl ethylene phosphate)
mRNA	Messenger ribonucleic acid
MSC	Mesenchymal stem cells
MTT	3-(4,5-dimethylthiazol-2-yl)-2,5-diphenyltetrazolium bromide

MW	Molecular weight
ncRNA	Non coding RNA
NET-1	Neuroepithelial cell-transforming gene 1
NF-κB	nuclear factor κB
NHS	N-hydroxysuccinimide
NSCLC	Non–small cell lung cancer
OMEM	Opti-MEM
ONPG	O-Nitrophenyl β-D-galactopyranoside
OPG	Osteoprotegerin
ORF	Open reading frame
PAMAM	Polyamidoamine
PARP	poly ADP-ribose polymerase
PBS	Phosphate buffer saline
PC	Prostate cancer
PCL	Polycaprolactone
PCR	Polymerase chain reaction
pDMAEMA	Poly[2-(dimethyamino)ethyl methacrylate]
pDNA	Plasmid dexocy ribonucleic acid
PEG-*b*-PCL	Poly(ethylene glycol)-b-poly(ε-caprolactone)
PEI	Polyethyleimine
PEI25	Polyethylenimine (Mw. 25,000 Da)
PEI-L	Lipid grafted polyethyleneimine
PGCS	Poly(ethylene glycol)-chitosan-graft-spemine
PI-3K	Phosphatidylinositol 3-kinase
PKC	Protein kinase C
PLA	Polylactic acid
PLGA	poly(D,L-lactide-co-glycolide
PLL	Poly-L-lysine
PrA	propionic acid
PrA-PEI	Propionic acid grafted polyethyleneimine
PTEN	Phosphatase and tensin homolog

pTRAIL	Plasmid expressing TRAIL
RAFT	Reversible addition-fragmentation chain transfer
RES	Reticuloendothelial system
RIP	Receptor interacting protein
RNAi	RNA interference
ROS	Reactive oxygen species
SC	Subcutaneous
scFv	Single-chain variable fragments
SD	Standard deviation
shRNA	Small hairpin ribonucleic acid
siRNA	Small interfering ribonucleic acid
SMAC	Second mitochondria-derived activator of caspases
SOD1	Superoxide dismutase 1
STAT 3	Signal transducer and activator of transcription 3
tCS	Thiolated chitosan
TNF	Tumor necrosis factor
TNFRSF10D	Tumor necrosis factor receptor soluble factor superfamily member 10D
TRA	TRAIL receptor agonist
TRAF2	TNF Receptor Associated Factor 2
TRAIL	Tumor necrosis factor-related apoptosis-inducing ligand
TRAIL-R1	Tumor necrosis factor-related apoptosis-inducing ligand receptor 1
TRAIL-R2	Tumor necrosis factor-related apoptosis-inducing ligand receptor 2
UTR	5’ untranslated region
VEGF	Vascular endothelial growth factor
VEGF-A	Vascular endothelial growth factor-A
VEGF-C	Vascular endothelial growth factor-C
WGA	Wheat germ agglutinin
XIAP	X-linked inhibitor of apoptosis
α-LA	α-Linolenoyl

Scope

The objective of my thesis is to explore new nucleic acid-based combination therapy of cancer using non-viral gene delivery. The main idea behind the combination therapy is (i) to simultaneously target multiple intracellular signalling pathways in transformed cells since tumorigenesis involves mutation and abnormal expression of multiple genes or proteins, and (ii) to overcome the ability of cancer cells to compensate against anticancer therapies via recruitment of alternative molecular pathways for their survival and proliferation. In addition, intolerable toxicities associated with non-specific action of conventional therapy on healthy tissues is of significant concern. Given the unacceptable toxicities associated with conventional therapy (especially at advanced stage disease), combination of nucleic acids comprising a plasmid DNA (pDNA) and a small interfering RNA (siRNA) could be a potential approach for specifically killing the cancer cells. Beneficial effects of this approach will be achieved in this thesis via forced expression of apoptosis inducing protein such as the TRAIL (Tumor necrosis factor receptor apoptosis inducing ligand) with pDNA and sensitizing the action of TRAIL with specific siRNAs via silencing over-expressed pro-survival proteins. Among several anti-apoptotic or pro-survival proteins, identification of key regulator of TRAIL induced apoptosis is of paramount important to achieve synergistic anticancer activity from pDNA/siRNA combination. Therefore, we hypothesize that co-delivery of pDNA encoding TRAIL and siRNA that sensitize TRAIL induced apoptosis will be effective to kill the breast cancer cells without affecting non-malignant cells. Nucleic acids, however, are highly unstable in serum due to presence of serum nucleases and the high negative charge density prevents intracellular uptake on their own. Incorporating both pDNA and siRNA in single complexes is additionally challenging due to differences in the size and the chemical properties of these nucleic acids.

This thesis explored the delivery of nucleic acids as a single or in combination using polymeric delivery systems to kill the cancer cells. The main objectives of the thesis are: 1) Optimizing polymeric systems for pDNA and siRNA delivery; 2) Identifying complementary siRNAs which sensitize the breast cancer against TRAIL-induced apoptosis, 3) Identifying polymers for co-delivery of pDNA and siRNA, and 4) Development of an effective therapy through co-delivery of TRAIL encoding plasmid (pTRAIL) and specific siRNAs by using *in vitro* and *in vivo* models of human breast cancer. 5) Explore the messenger RNA (mRNA) encoding TRAIL delivery in vitro and in vivo models of human breast cancer. The work within this thesis provides thorough details on the conceived nucleic acid combination therapy, rationale for selecting therapeutic nucleic acid pairs and studies to address the objectives of the thesis. Below is the content of the thesis chapters.

Chapter 1 introduces combinatorial therapy of cancer by articulating on nucleic acid combinations and their delivery focussing on TRAIL and its complementary approaches to induce apoptosis. This chapter covers a literature survey on nucleic acid combination therapy including its successes in cancer treatment using non-viral delivery systems, a review of TRAIL mediated apoptotic pathway, clinical application of TRAIL therapy, mechanisms of TRAIL resistant and current approaches to enhance the TRAIL induced apoptosis. **Chapter 2** and **Chapter 3** summarize attempts to develop new polymeric delivery systems for gene delivery to different cancer cells. In **Chapter 2,** synthesis, characterization and use of galactosylated cationic polymer for gene delivery to hepatocytes is explored. It covers rational design of a library of galactosylated polymers with different architectures, compositions and molecular weight and their effects on gene delivery efficacy. **Chapter 3** further explored preparation and characterization of a new type of polymer

for gene delivery, but this time specifically for breast cancer cells. This chapter covers the modification of low molecular weight PEI with a small hydrophobe, propionic acid (PrA) and their gene delivery efficiency into breast cancer cells. I further explored the effect of substitution on physicochemical features of polymer, resultant complexes, and their functional performance.

Next, I identified several siRNA targets, which sensitized TRAIL-induced apoptosis by screening a human siRNA library of 446 apoptosis-related siRNAs in MDA-MB-231 cells. Detailed methodology of the siRNA library screening to identify complementary therapeutic targets is explained in **Appendix F.** Results of the siRNA library screening were presented in detail in **Chapter 4.** This chapter includes the design of new polymer prepared by grafting α-linolenic acid (αLA) onto low molecular weight PEIs and its application to deliver siRNA to breast cancer cells followed by outcomes of the siRNA library screening. Efficacy of combination therapy of TRAIL protein and most effective siRNAs silencing BCL2L12 and SOD1 to retard breast cancer cells growth and their effect on the non-malignant cells is explained in detail. After identification of siRNA targets that sensitize the TRAIL induced apoptosis, I pursued the co-delivery of pTRAIL and specific siRNAs using lipopolymers to enhance the breast cancer cell death *in vitro* and *in vivo* breast cancer model and outcomes are summarized in **Chapter 5.** This chapter focuses on the optimization of polymeric delivery systems for co-delivery of pDNA and siRNA and beneficial effects of co-delivery versus separate delivery is thoroughly studied with highlighting the mechanism. **Chapter 6** builds on this expertise and presents a series of studies where pTRAIL has been replaced with modRNA, a modified mRNA encoding for the trimeric TRAIL protein. Finally, I conclude this thesis with **Chapter 7** summarizing the key findings and contribution to nucleic acid combination therapy for breast cancer and future directions.

Chapter 1

Combination therapy for cancer treatment

A version of sections of this chapter was published in:

Remant KC, Bindu Thapa, Juliana Valencia-Serna, Hamidreza Montezari Aliabadi, Hasan Uludag, Nucleic acid combinations: A new frontier for cancer treatment. Journal of Controlled Release, 2017, 256: 153-169.

1.1. Background and Rationale

Conventional view of gene therapy, hereditary single gene defects corrected with functional copies, has been expanded to treatment of both acquired gene defects and infectious diseases [1-4]. In case of cancer, where hereditary and acquired defects, as well as infectious agents can cause cellular transformations, nucleic acid-based gene therapy is presenting a potential alternative for traditional chemotherapy. Therapeutic limitations of the latter approach are due to robustness in signaling networks that includes redundancies, extensive crosstalk, compensatory and neutralizing activities associated with disease-causing cells [5-11]. This realization is shifting the drug development paradigm from conventional broad-spectrum cytotoxic compounds to molecular agents selective for specific targets. In many aggressive cancers, strategies to target individual signaling pathways is not sufficient to block the abnormal proliferation and metastasis due to cellular plasticity to restore the activities of interfered pathways or employ alternative pathways for vital cellular activities [6]. To this end, a new strategy employing combination therapy, which comprise of co-delivery of different types of therapeutic agents (e.g., nucleic acids, drugs, and their combinations) via a single carrier, is emerging. This strategy promises the navigation of the joint payload through multi-dimensional transport pathways in cells [11] and it is intended to trigger synergistic effect(s) via complementary pathways (**Figure 1.1**), generating a greater effect than the sum of the constituent components [12, 13]. Synergistic combination of therapeutic agents may further overcome the possible toxicities associated with the clinical doses of individual drugs by allowing lower doses of components to be employed [14, 15]. In an ideal combination therapy, each component displays independent pharmacodynamics, with minimal overlapping of toxicity spectra associated with constituent drugs.

Heterogeneity in transformed cell population and a complex web of signaling pathways continuously limits the outcome of one-dimensional therapies. The major aim of combinational therapy is to (i) maximize inhibition of a specific target (e.g., antibodies and small molecules antagonists), (ii) abolish multiple components in a given pathway, and (iii) interfere with multiple mechanisms in tumor growth and metastasis [13]. The overall goal is to generate a better efficacy with minimal side effect by delivering different types of therapeutic agents including nucleic acid, drugs and molecular inhibitors **(Figure 1.1**). While mono-therapies are effective to some extent, corresponding combinations can be synergistic, additive, or co-alistic [16], where individual agents are inactive but shows efficacy in combination [17, 18]. The expected synergism of combination therapy is expressed by a combination index (CI; CI < 1) [11]. CI for synergistic pairs of A and B is quantified based on following equation:

$$CI = \frac{IC_{50}\ (A)\ Pair}{IC_{50}\ (A)} + \frac{IC_{50}\ (B)\ Pair}{IC_{50}\ (B)}$$

where IC_{50} is the concentration (for an individual drug or a drug used in combination with another agent) for 50% inhibition of cell growth.

In general synergistic pairs are identified by exploring mechanistic insights or high-throughput screening without introducing a bias in the selection process [19-21]. The objective is to identify the intracellular targets associated with network of signaling pathways which regulate the signals at gene or protein levels. Generally, a combination pair generate synergistic effect in cancer cells while in normal cells, it often exhibits an additive or antagonistic due to variation in proteins expression [22, 23]. Since cancer cells over-express specific mediators, the higher the available target levels, the greater the effects via synergy. This usually avoids the synergistic side

effects. In many cases, it is believed that inter-connectivity of signaling pathways does not allow sufficient effect by simple shutting off a single target since cell can re-store signals via alternate proteins and/or functional mutations [24, 25]. Combination therapy that address different mechanisms to inhibit cancer development may overcome this limitation by simultaneously blocking multiple pathways. One can envision co-delivery of combination drugs in a single carrier, delivery in a mixture of distinct (separate) carriers, or subsequent delivery of an agent (probably in free form) following by the other [26, 27].

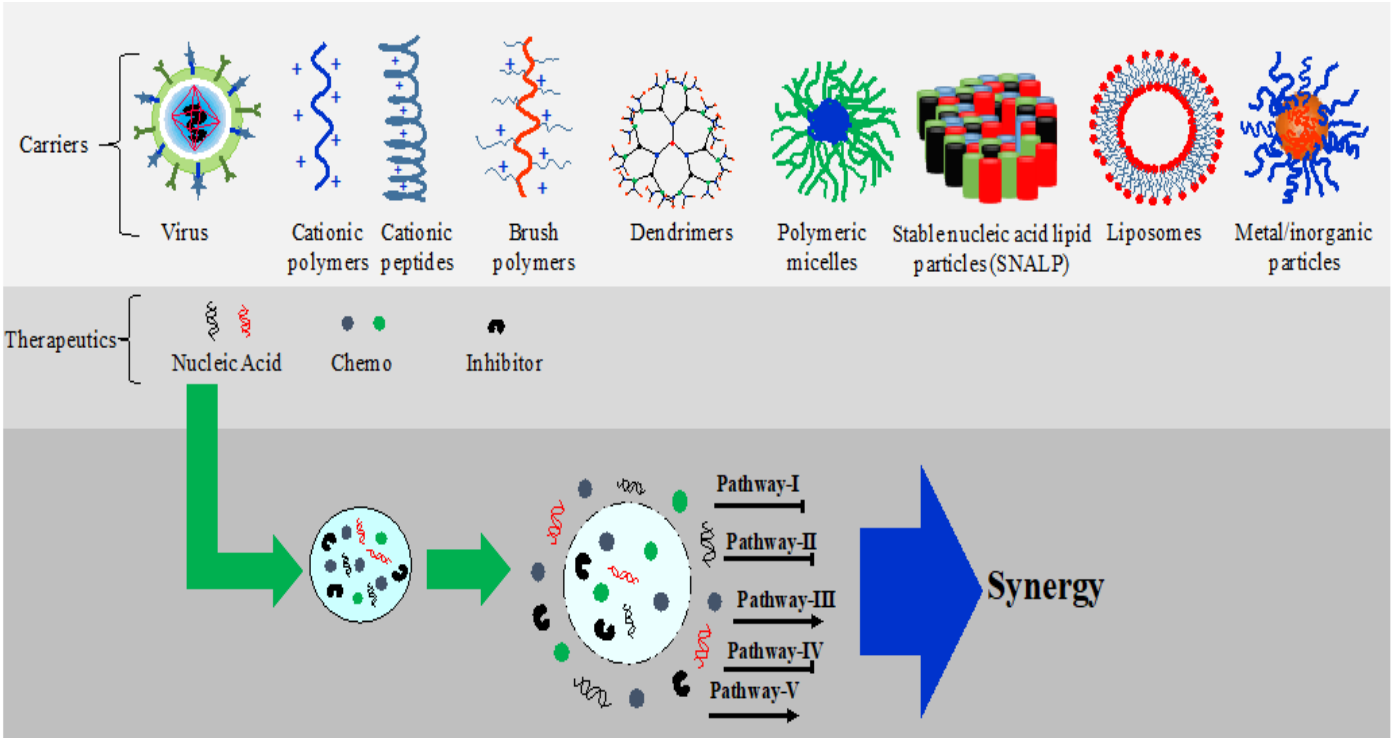

Figure 1.1. An illustration of combination therapy. Vectors and therapeutics form nano-complexes that enter cells, pass through multiple cellular compartments and finally release the cargo intracellularly. Each cargo generates substantial effect on the corresponding target which generates synergistic therapeutic effects. Figure courtesy of Remant KC.

1.2. Current therapeutic modalities of breast cancer

According to World Health Organization, breast cancer is the leading cause of cancer-related deaths among women affecting 2.1 million women each year. In 2018, nearly 627,000 women died from breast cancer accounting about 15% of all cancer deaths among women. Recently, mortality rate has generally declined worldwide due to early diagnosis and screening [28]. Survival rate is high with early detection of breast cancer. Based on the size, type and amount the tumor penetration into tissue, breast cancer stage is referred to a number on a scale of 0 to IV. Stage 0 is noninvasive stage where cancer remains within location of origin. Stage I describes invasive breast cancer where microscopic invasion of breast cancer may occur. Stage II is also invasive breast cancer where tumor is found in axillary lymph nodes or in sentinel lymph nodes. Tumor larger than 5 cm but have not reach to the axillary lymph nodes is also classified as stage II. After invasion into axillary lymph nodes or lymph nodes near breast bone, it is referred as Stage III. Stage IV is advanced metastatic stage of breast cancer where breast cancer has spread to other organ including lung, distant lymph node, skin or liver [29].

Different therapeutic modalities such as targeted therapy, hormonal therapy, surgery, radiation therapy and chemotherapy have been employed in the treatment of breast cancer based on the stage and molecular subtypes. Commonly explored intrinsic or molecular subtypes of breast cancer are luminal A, luminal B, human epidermal growth factor receptor (HER-2) enriched, Triple-negative/basal-like and Normal-like breast cancer cells [30]. Luminal A breast cancer is hormone-receptor [estrogen-receptor (ER) and/or progesterone-receptor (PR) positive], HER2 negative and low levels of protein Ki-67. Luminal A breast cancer has best prognosis and grow slowly. Luminal B breast cancer is hormone-receptor (estrogen-receptor and/or progesterone-receptor) positive with or without HER2 and has high levels of Ki-67. Growth of Luminal B is

faster than Luminal A breast cancer. Third type is triple-negative/basal like breast cancer. These are hormone-receptor (estrogen-receptor and progesterone-receptor) and HER2 negative. HER2-enriched breast cancer is HER2 positive and does not have hormone-receptor (estrogen-receptor and progesterone-receptor). It has poor prognosis and grows faster than luminal cancers. Normal-like breast cancer is estrogen-receptor and/or progesterone-receptor positive, HER2 negative and has low level of Ki-67 protein. Although it is similar to luminal A breast cancer, its prognosis is slightly worse than luminal A cancer's prognosis. The molecular markers such as (HER2), estrogen-receptor progesterone-receptor were utilized for treatment of breast cancer. Anti-estrogen such as tamoxifen, raloxifene, toremifene were employed to treat ER positive breast cancer [29, 31]. Monoclonal antibody called Trastuzumab and pretuzumab are directed against the HER2 positive breast cancer [32]. However, breast cancer is heterogeneous. Some breast cancer called triple negative breast cancer does not express those markers are difficult to treat [33, 34].

Surgery is main strategy for breast cancer treatment which has not spread to other areas of body. Lumpectomy and mastectomy are two main kinds of breast cancer surgery. Lumpectomy involves removal of tumor along with some healthy tissues and surrounding lymph nodes leaving major part of the breast. While mastectomy is removal of entire breast [35]. Although mastectomy is considered the most effective to remove most of affected breast tissue, most women experienced loss of self-image and depression due to loss of breast [36]. In addition, surgery can not completely cure disease and chances of reoccurrence is high. Radiation therapy is another option which is often combined with lumpectomy at early stages of breast cancer [37]. The side effects including breast pain, stiffness and swelling, fatigue, redness and peeling of skin are main concern with radiotherapy. These local treatments; surgery and radiation are not enough if tumor has spread to other tissues.

Chemotherapy and endocrine therapy are systemic treatment for breast cancer where small molecule drugs are delivered through blood stream. Anthracyclines (doxorubicin, epirubicin), taxanes (paclitaxel, docetaxel), platinum agents (cisplatin, carboplatin), Vinorelbine (Navelbind), liposomal doxorubicin (Doxil), cyclophosphamide are some examples of chemotherapeutics [29, 38]. Chemotherapy is given for treatment of metastatic cancer. It is also used as adjuvant therapy after mastectomy and lumpectomy to eradicate remaining cancer cells and prevent recurrence. Chemotherapy destroys all the quickly dividing malignant and non-malignant cells. Due to non-specific effects of chemotherapy, severe side effects including neuropathy, bone marrow suppression, destruction of hair follicles, lining of mouth and intestines, nausea, vomiting, fatigue are most common side effects [38]. Due to incomplete eradication and tremendous side effect of these well-established therapies of breast cancer, novel treatment that specifically kills the breast cancer without affecting non-malignant cells is needed. Therefore, we explored nucleic acid combination therapy as alternative to conventional therapeutic modalities in this thesis.

1.3. Nucleic Acid Combination

Various combinations of DNA and RNA molecules are being explored to achieve synergistic effect(s) at the molecular level. **Table 1.1** summarizes several examples of nucleic acid combinations identified from a literature search. Combination of nucleic acid in cancer therapy employs multiple pathways associated in cellular cross-talk such as; the phosphatidylinositol 3-kinase (PI3K)/Akt, nuclear factor κB (NF-κB), Janus-activated kinase/signal transducers (JAKs) and various activators of transcription, apoptosis, growth/invasion and angiogenesis [39]. Apoptosis inhibition by over-expressed anti-apoptotic mediators including Mcl-1, Bcl-2 and survivin, and mutation in drug targets, such as MEK, Epidermal Growth Factor Receptor (EGFR) and BCR-Abl, are associated with cellular resistance against conventional therapeutics [40-45].

Targeting these pathways with nucleic acid combinations generate synergistic anticancer activity. Several combinations of nucleic acid are possible. Among the nucleic acid combinations, siRNAs are gaining upper hand to complement the action of a DNA-based expression system [46].

Table 1.1. Summary of nucleic acid combinations for retarding the proliferation of malignant cells.

Therapeutic Combination	**Cancer type/Model**	**Vehicle**	**Activity**	**Outcomes**	**Ref.**
LETM1/CTMP	Hepatocellular Carcinoma *In vivo*: H-ras12V mice	GPCS	Activated AMPK and Akt1 pathways	Induced mitochondria-mediated apoptosis	[47]
VEGE-siRNA/Bcl2-siRNA	Prostate cancer *In vitro*: PC-3 cells *In vivo*: Mouse model	GC	Synchronized VEGF and Bcl-2 silencing	Increased apoptosis, Inhibited tumor growth	[48]
VEGF-siRNA/Bcl2-siRNA	Epithelial carcinoma *In vitro*: HeLa cells	PEI	Downregulation target mRNA and protein levels	Induced apoptosis	[49]
shRNA-STAT3/ LKB1	Ovarian cancer *In vitro*: SKOV3 cells *In vivo*: BALB/c mice	Lipofectamine 2000	Expressed shRNA-STAT3 and LKB1	Reduced cancer cell invasion, migration and tumor growth	[50]
LKB1/FUS1	Lung cancer *In vitro*: A549 and H460 Cells *In vivo*: BALB/c mice	DOTAP: Cholesterol nanoparticles	Expression of LKB1 and FUS1	Reduced Metastatic and enhanced survival of mice	[51]
FUS1 and p53	Lung cancer *In vitro*: NSCLC cells *In vivo:* H322 lung cancer mouse	DOTAP: Cholesterol nanoparticles	Downregulated MDM2 and activated expression of P53 and Apaf-1	Induced apoptosis and suppressed tumor growth	[52]
shRNA-EGFR/PTEN	Glioblastoma *In vitro*: U251-MG cells *In vivo:* BALB/c mice	Lipofectamine 2000	Down regulated EGFR and up-regulation of PTEN	Induced apoptosis and suppressed tumor growth	[53]
miR-34/let-7	Lung cancer *In vitro*: NSCLC cells *In vivo:* Mice model	Dharmafect 1	Repressed oncogene expression	Inhibited cell proliferation and tumor growth	[54]

VEGF-siRNA/HER2-siRNA	Breast cancer *In vitro*: MCF7	Lipofectamine 2000	Silencing of VEGF, HER2	Inhibited tumor invasion, proliferation and induced apoptosis	[55, 56]
NET-1 siRNA/VEGF siRNA	Hepatocellular carcinoma *In vitro*: HepG2 cells *In vivo*: BALB/c mice	Lipofectamine 2000	Down regulated VEGF mRNA and protein levels	Inhibited growth and angiogenesis of HCC, suppressed tumor growth	[57]
VEGF-siRNA/KSP-siRNA	Hepatocellular carcinoma *In vitro*: Hep3B cells	Lipofectamine RNAiMAX	Downregulated VEGF and KSP mRNA and protein levels	Inhibited growth, migration, invasion and induced apoptosis of HCC cells	[58]
Bcl2-siRNA /SURVIVIN-siRNA	Human bladder cancer *In vitro*: T24 cells	Lipofectamine 2000	Up-regulateed caspase-3 activities	Inhibited cell proliferation and induced apoptosis	[59]
IGF-IR-siRNA/EGFR-siRNA	Colorectal cancer *In vitro*: DLD-1, Caco2 cells		Up-regulated caspase-3/7 activities	Inhibited cell proliferation and induced apoptosis	[60]
pU6-EGFR-shRNA/pU6-IGF1R-shRNA	Nasopharyngeal cancer *In vitro*: CNE2 and TW03 cells	Lipofectamine 2000	Downregulated EGFR and IGF1R mRNA and protein expression	Induced apoptosis and chemo-sensitivity	[61]
HSV-tk/mIL-2	Colon Carcinoma *In vivo*: BALB/c Mice	Virus	Expressed HSV-tK/mIL-2	Reduced Metastasis of colon carcinoma into liver	[62]
tk/mGM-CSF/mIL-2	Colon cancer *In vivo*: BALB/c Mice	Virus	Expressed tk/mGM/mIL-2	Enhanced antitumor immunity	[63]
GC-CSF/IL-2	Squamous cancer *In vitro*: SCCVII *In vivo*: C3H/HeJ mice	Virus	Secreted GC-CSF/IL-2	Suppressed tumor growth	[64]
IL-12, pro-IL-18, and ICE cDNA	*In vivo*: BALB/c mice	Gene gun	Induced INF-γ pathway	Enhanced antitumor activity	[65]
psiRNA-VEGF-C/psiRNA-VEGF-A	Mammary cancer *In vitro*: BJMC3879 cell *In vivo*: BALB/c mice	Electrotransfer	Down regulated VEGF-C and VEGF-A expression	Reduced Metastatis and enhanced survival of mice	[66]

1.4. Delivery of Nucleic Acids and their Combinations with Nano-assembled Non-Viral Carriers

Non-viral delivery of pDNA for transgene expression is the most extensively studied approach, as the initial foundation of gene therapy approach to cancer. More recently, siRNA delivery has been explored for post-transcriptional knockdown of specific gene expression which are responsible for the disease. The nucleic acids can not enter cell on their own due to negative charge and physiological digestion. Therefore, effective delivery systems are required. We are mainly interested in non-viral vectors in order to avoid the toxicity and immunogenicity associated with the viral vectors [67, 68]. The critical features of non-viral vectors essential for an effective delivery includes; i) the ability to condense negatively charged nucleic acid into a positively charged nano-complexes that can interact with plasma membrane and enable subsequent cellular uptake because negatively charged nucleic acid can not enter cells ii) protect delivery cargo from extracellular/intracellular enzymatic/non-enzymatic digestion while navigating in physiological system, iii) circumnavigate intracellular compartments to unload the nucleic acid cargo in the targeted sub-cellular domain, and iv) minimize off-target associated toxicity including genotoxicity, immunogenicity and cytotoxicity. Non-viral carriers for the delivery of nucleic acid was previously reviewed elsewhere [69, 70], therefore, I focused on non-viral vectors used for co-delivery of nucleic acids.

Depending on the mechanism action of nucleic acid and targeting proteins and pathways, one can envision different combinations of nucleic acid (**Figure 1.2**). For example, simultaneous expression of two therapeutic proteins can be achieved with combination of pDNAs where as siRNAs/shRNAs combination leads to silencing of proteins. Similarly, combination of pDNA and siRNA/shRNA enables simultaneous knockdown of undesirable proteins with siRNA/shRNA and

forced expression of desirable proteins with pDNA [71]. To achieve the therapeutic benefits, one can deliver nucleic acid combinations using different approaches; co-delivery of nucleic acid combination, separate delivery with distinct (separate) carriers, or subsequent delivery in a mixture an agent following delivery of another agent [26]. While synergistic agents can be delivered using either a single or mixed carrier, co-delivery through a single carrier is preferred from a convenience perspective. It delivers payload at the proper balance to a target site at the same time (if desirable) and generates cumulative activities. In addition, this approach will synchronize the pharmacokinetics of the bioactive agents, and targeted cells will be exposed with both therapeutics at a defined ratio, thereby increase the therapeutic efficacy.

Nucleic acids have anionic phosphodiester backbones which allows electrostatic interaction with cationic molecules (polymers or lipids) and forms complexes, polyplexes or lipoplexes, respectively. Therefore, the delivery mechanisms such as; complexation, condensation, protection and endosomal release, involved in pDNA delivery are more or less identical with other nucleic acids delivery. However, differences in size, charge density, mechanism and site of action of nucleic acid should always be considered. For example, site of action of siRNA is on cytoplasm whereas further transport is required for pDNA. If the size and chemical structure of nucleic acids are prominently different, identifying a single carrier for different nucleic acids is difficult. For example, co-delivery of pDNA and siRNA where pDNAs are long (>3000 base pairs) flexible molecules while siRNAs are short (<30 base pairs) rigid molecules, could be challenging. In general, electrostatic strength of polycations or polyanions increases with size. Therefore, electrostatic strength of siRNA might be about one hundredth of the electrostatic strength of pDNA to bind with the polycations, indicating need of higher molecular weight polycation or high polycation/siRNA ratio [72]. However, some studies took advantage of their unique characteristics

such as size, charge to co-deliver the pDNA and siRNA. Enhanced transfection of both nucleic acid (pDNA and siRNA) was achieved in one study [73], while stability of siRNA polyplexes were enhanced by pDNA when co-delivered in another study [72].

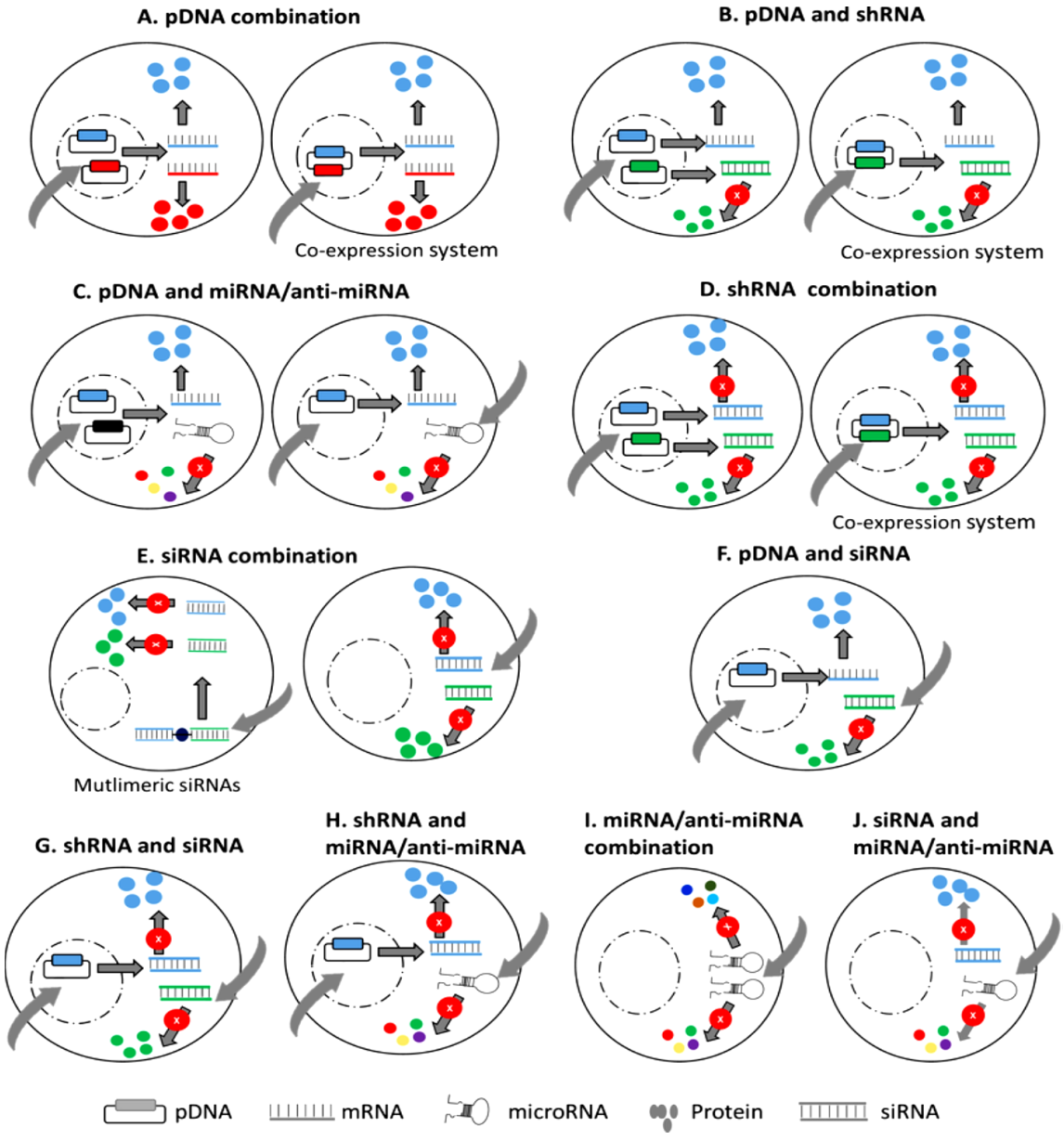

Figure 1.2: Schematic representation of possible nucleic acid combinations. (A) Therapeutic protein combination. (B) Therapeutic protein and shRNA combination. (C) Therapeutic protein and miRNA combination. (D) Therapeutic protein and siRNA combination. (E) shRNA combination. (F) shRNA and miRNA combination. (G) shRNA and siRNA combination. (H) siRNA combination composed of individual siRNAs or multimeric siRNAs (I) siRNA and miRNA

combination. In the case of pDNA driven expression systems (proteins, shRNA and miRNA), either independent expression systems or co-expression systems could be used. In the case of miRNA delivery, it is possible to deliver miRNA or anti-miRNA reagents to exert a desired therapeutic effect.

For co-delivery of nucleic acids, several strategies were employed. In one approach, multiple genes were constructed into eukaryotic co-expression plasmid and delivered by viral vector. Co-expression of LKB1 and FUS1 with an eukaryotic co-expression plasmid synergistically inhibited lung cancer cell growth and prolonged the survival of lung tumor-bearing mice [51]. Co-expression plasmid vector was also used for delivery of the shRNA and pDNA combination. Co-expression of STAT3 specific shRNA and liver kinase B1 (LKB1, a tumor suppressor) has shown an effective synergism to inhibit ovarian cancer cell growth, invasion and migration, induced cell apoptosis when compared with monotherapy [50]. In the study by Cho et. al., two mitochondrial targeting genes, LETM1 and CTMP, were linked together by 2A peptide and delivered using galactosylated poly (ethylene glycol)-chitosan-graft-spermine into liver cancer (HCC) mice model [47]. The delivery overexpresses the constituent genes and consequently reduced the incidence of tumorigenesis by generating morphological changes in mitochondria. Similarly, siRNA molecules can be crosslinked together into multimerized siRNA with cleavable bond like disulfide [74]. Two 5'-end dithiol-end modified siRNAs silencing VEGF and Bcl-2 were randomly copolymerized in a single siRNA polymer and delivered into human prostate cancer cell (PC-3) tumor bearing mice using glycol chitosan nanoparticles [48].

1.4.1. Liposomes and Lipoplexes

Liposomes, the lipid-based nano-carriers, are the earliest delivery formulation established to introduce exogenous genes to host cells [75, 76]. Liposomes were made using cationic and

helper lipids. Liposomes could be tailored by varying cationic charge density, hydrophobic tail conformation and spacer length of cationic lipids. These structural components yield specific conformations of an interior aqueous phase and a lipid envelope. Cationic head groups are particularly responsible for complexation with nucleic acids, thereby incorporating the nucleic acids into liposomes. The mechanistic studies shows that liposomes mediate gene delivery primarily through membrane fusion or endocytosis, followed by destabilization of endosomal membranes via a flip-flop reorganization of phospholipid layers [77]. Lipoplexes, on the other hand, are formed by complexation of anionic nucleic acids with cationic lipids under aqueous conditions, forming homogeneous lipophilic interpenetrating complexes. These complexes are small enough (~100 nm) for cellular uptake [76, 78, 79].

For gene delivery both unmodified (e.g. Lipofectmine, DOTAP etc) as well as chemically modified form (e.g. PEI-DOTAP, PEG-DOTAP etc) of cationic lipids were used [80, 81]. Commercial lipofection reagents (e.g., Lipofectamine® 2000, Oligofectamine®, DharmaFECT®, etc.) and DOTAP:cholesterol based cationic liposomes are most effective among lipid-based delivery agents [50, 51, 54, 60]. With non-ionic formulations, the aqueous core makes it possible to entrap multiple nucleic acids at desired ratios; however, unlike small molecule drugs, nucleic acids cannot penetrate the lipid membrane and the liposome needs to be destabilized in order to release its payload. DOTAP/cholesterol liposomes were employed for successful co-expression of functionally synergistic tumor suppressor genes, FUS1/p53 in human non-small cell lung carcinoma (NSCLC) cells and its xenograft model [52]. The commercial reagent Lipofectamine® 2000 (not recommended for animal models) has been most commonly used in combinational delivery, though other carriers (**Table 1.1**) have also shown effective performance in *in vitro* and

in vivo models. Cationic charge density, hydrophobic tail conformation and the spacer length could be optimized for co-entrapment and co-delivery, but chemically-modified lipids especially with cationic functionalities (e.g., polyethyleneimine (PEI), polyamidoamine (PAMAM) and polylysine (PLL) derivatives) are particularly attractive to tailor the liposomes for nucleic acid payloads [80, 81]. Being localized at the inner and outer aqueous interfaces of liposomes, the cationic moieties could act as binding sites for anionic nucleic acids through electrostatic interactions [80, 82]. The cationic groups can also provide a spacer for anchoring specific motifs and binding ligands to generate cell specificity for active targeting. With liposomes that bear nucleic acids on the outside surface, displacement of nucleic acids with other anionic species such as heparin sulfate [83] is always a concern, which results in premature release of the payload, as well as its rapid digestion of nucleic acids in serum. While maintaining proper balance of active agents after loading multiple nucleic acids in carriers is always a concern in combinational delivery, having a secondary nucleic acid may lead to improved pharmaceutical effects; DNA supplementation in short interfering RNA (siRNA) formulations of liposomes were noted to enhance the silencing activity of siRNA, not due to gross morphological changes in liposomes but possibly due to altered dissociation/release of the nucleic acids from the lipoplexes [84]. Systemic nano-delivery (using commercial DharmaFECT1 reagent) of combination of two biologically relevant tumor suppressive microRNAs, miR-34 and let-7, resulted in superior ability to prevent proliferation and invasion of cancer *in vitro* and to suppress tumor growth *in vivo* conferring a prolonged survival in non-small lung cancer mouse model [54].

1.4.2. Nanoparticles and Micelles: Cationic Polymers and Dendrimers

Nanoparticles and micelles are another set of versatile carriers explored in combination therapy [85, 86]. Structural geometry and biodegradability had led these carriers to the most sophisticated and potential delivery system for combination therapy [85-88]. These carriers are formulated using biodegradable amphiphilic polymers, cationic polymers or dendrimers which ideally self-assembled into a core-shell geometry in aqueous systems, or electrostatically interact with nucleic acids to form nano-sized particles. They exhibit the ability to simultaneous delivery of nucleic acids to cells after systemic administration and exerts maximal effect [89]. Cationic polymers are the most studied material in non-viral gene delivery due to their high cationic charge density, facile chemistry, cost effective and safe toxicity profiles [90, 91]. Electrostatic interactions between the positively charged amino groups of the polymers and negatively charged phosphate groups of nucleic acids (DNA/RNA) result the formation of poly-ionic complexes (polyplexes). These complexes can protect the encapsulated payload from enzymatic/non-enzymatic degradation, avoid the clearance by nonspecific uptake through reticuloendothelial system (RES) and interaction with blood components and enhance cellular uptake via the interaction with anionic cell surface proteoglycans [90, 91]. Cationic polymers can be configured into multiple forms, including micelles, hollow polymersomes and homogenous nanoparticle polyplexes [88, 92, 93].

Over the last few decades, polyethylenimine (PEI, branched/linear), poly(L-lysine) (PLL), poly[2-(dimethyamino)ethyl methacrylate] (pDMAEMA), poly(amidoamine) (PAMAM) and chitosan (CS) are the most common cationic polymers employed for nucleic acid delivery. Dendrimers are another group of cationic polymers used as non-viral gene delivery. Biodegradability, molecular hierarchy and buffering capacity in a wide range of pH value makes

dendrimers (e.g. PAMAM) as a potential alternative of cationic polymers [94]. The particular interest of dendrimers in gene delivery is due to their customizable structure which provides high functionalization space to anchor multiple ligands [94-97]. Cell selectivity is generated in dendrimers by grafting targeting ligands (e.g. β-cyclo-dextrin, amino-acids, etc.) specific to cell surface receptors [98]. Dendrimers are routinely coupled with hydrophobe/or polyester polymers (PCL, PLA etc.) to generate duel functionality. These hybrid polymers form unique cationic micelles in aqueous system that possess sufficient binding capacity with nucleic acids and promises co-delivery of therapeutic pairs [93].

Another group of polymers used in nucleic acid delivery are polyester based amphiphilic polymers that can form micelles in aqueous system and can undergo degradation due to hydrolytic breakdown of ester linkages. Some examples are poly(ethylene glycol)-b-poly(ε-caprolactone)-b-poly(2-aminoethyl ethylene phosphate) [mPEG-*b*-PCL-*b*-PPEEA], poly(D,L-lactide-co-glycolide) [PLGA], poly(ethylene glycol)-b-poly(ε-caprolactone) [PEG-*b*-PCL], poly(ethylenimine)-g-poly(ε-caprolactone) [PEI-*b*-PCL] [85-87, 99]. In some cases, cationic polymers (e.g. PEI) and polyester polymers (e.g. PLGA) are blended together along with nucleic acids that leads the formation of a hybrid nanoparticles [87]. Selection of appropriate pair of therapeutics as well as their most efficient carrier are critical for clinical translation of nucleic acid therapy [100].

Low molecular weight PEI (LMW; <2 kDa) was derivatized with a broad range of hydrophilic and hydrophobic moieties to transform them into effective carriers [101-103]. Kim et al introduced the cholesteryl chloroformate into low molecular weight PEI for first time which

enhanced the transfection efficacy [103] which was followed by modification with dodecyl and hexadecyl derivatives [104]. Our group modified low molecular PEI with aliphatic lipids including caprylic, myristic, palmitic, stearic, oleic and linoleic acid [102]. Hydrophobic modification of LMW PEIs with aliphatic/aromatic moieties imparts lipophilicity to already existing buffering capacity. Synergism between these features enables improved self-assembly during complexation with nucleic acids while enhancing binding to hydrophobic domains of plasma membrane that ultimately enhances internalization [105, 106]. LMW PEIs grafted with aliphatic lipids (C8 to C18) generate relatively non-toxic PEI derivatives, and even small hydrophobes (C3) appear to be functional for nucleic acid delivery [107]. As with single agents, these polymeric derivatives displayed superior delivery of siRNA cocktails with a single carrier and enabled down-regulation of target genes without interfering each other [108, 109]. Lipid modified LMW PEI efficiently co-delivered siRNAs (silencing Mcl-1 and P-glycoprotein) *in vitro* and siRNA (silencing Mcl-1 and ribosomal protein S6 kinase) *in vivo* breast cancer model [108, 110]. Chemical modification of higher MW PEI (10 kDa) with the natural polyanion hyaluronic acid (HA) was proposed to generate more compatible derivative, since it can neutralize excess cationic charge density to decrease cellular cytotoxicity, while still preserving siRNA encapsulation capacity [111]. PEI-HA was utilized to formulate a dual-functional (CD44/EGFR-targeting) nano-carrier for systemic delivery of p53- and miR-125b expressing plasmid in a mouse model of lung cancer [112]. Arginine modified PEI co-delivered the pDNA and siRNA where co-delivery resulted increase in pDNA transfection [73]. Jeon *et al.* (2012) co-used PEI modified poly (lactide-co-glycolic acid) nanoparticle to co-deliver SOX9 expressing pDNA and a Cbfa-1 siRNA [113]. Beneficial effects of SOX9 gene and anti Cbfa-1 siRNA combination was evident.

Chitosan (CS) is another natural cationic polymer extensively studied as an alternative to PEI due to its perceived biocompatibility. Chitosan derivatives, galactosylated poly(ethylene glycol)-chitosan-graft-spemine (GPCS) copolymer and thiolated chitosan (tCS), are typical CS derivatives employed in co-delivery of nucleic acids [47, 48]. Here GPCS was utilized to deliver two different tumor suppressor genes to hepatocellular carcinoma and tCS was used to deliver poly(siRNA) to prostate cancer cells. In both approaches, CS derivatives were able to generate significant anti-cancer activity. Similarly, poly(L-lysine) with or without oligomeric sulfadiazine [72] and polymer coated gold nanoparticles [114] were reported to co-deliver DNA and siRNA as a proof of principle. Addition of pDNA resulted in more compact particles than the siRNA particles with the poly(L-lysine) based carriers [72].

1.5. TRAIL Therapy in Cancer Treatment

1.5.1. TRAIL Induced Apoptosis

TNF-related apoptosis-inducing ligand (TRAIL, also known as Apo2L) is a type II transmembrane protein that was initially identified based on the sequence homology of its extracellular domain with CD95L (28% identical) and tumor necrosis factor (TNF) (23% identical) [115], however, its carboxyl-terminal extracellular end can be proteolytically cleaved from cell surface in vesicle-associated or in a soluble form [116]. TRAIL acquires the unique capacity to induce apoptosis in a variety of tumor cell lines, but not in most normal cells highlighting its potential therapeutic application in cancer treatment [116-118]. TRAIL induces apoptosis after binding with two TRAIL receptors; TRAIL-R1 (also known as DR4) and TRAIL-R2 (also known as Apo2, KILLER, DR5 or TRICK2). Binding of TRAIL to TRAIL-R1 and/or TRAIL-R2 induced the formation of death-inducing signaling complex (DISC). This complex consists of trimerized

receptor and the adaptor protein called Fas-associated protein with death domain (FADD). FADD in turn, recruits procaspase-8 to DISC. Caspase 8 is activated by auto-catalytic cleavage and formation of homodimers. Upon release from DISC, activated caspase 8 cleaves and activates caspase 3 and leads to apoptosis. In addition, it cleaves BID into tBID, which translocates to mitochondria leading to release of cytochrome c and Smac/DIABLO.

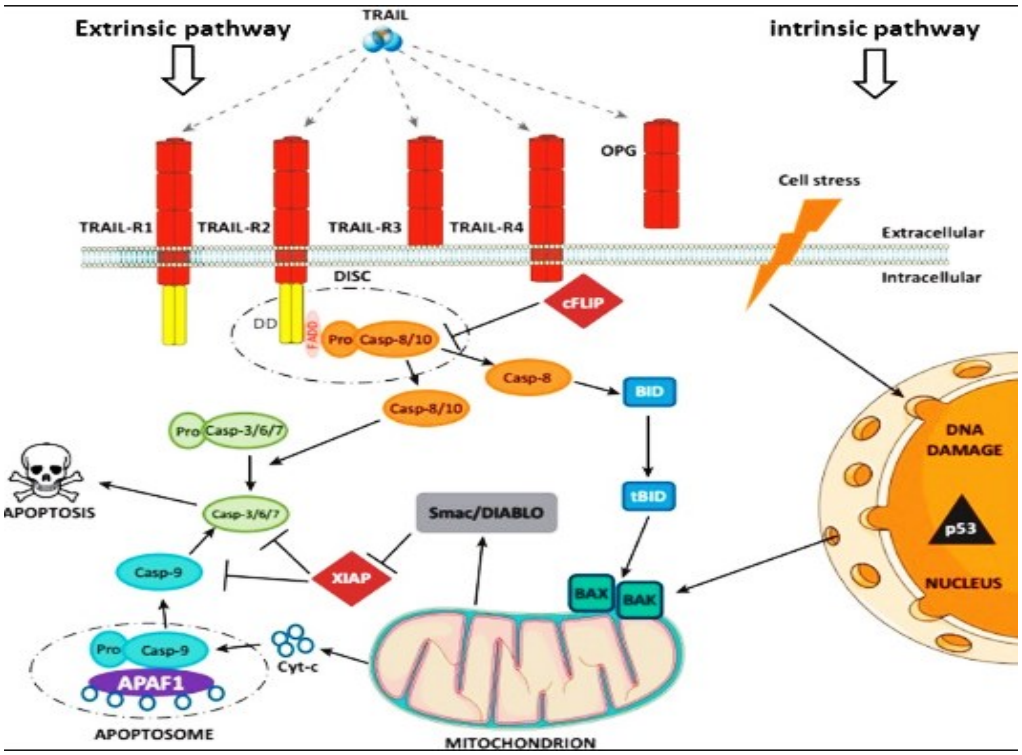

Figure 1.3: Schematic representation of extrinsic and intrinsic apoptotic pathways. Extrinsic or death receptor mediated pathway is initiated by ligation of specific death receptors by their ligands including TRAIL, Fas ligand. Then caspase 8 is activated which induced apoptosis by activating caspase 3. Activated caspase 8 also cleaves bid (BH3 interacting domain death agonist) resulting in mitochondrial dysfunction and subsequent release of cytochrome C and activation of caspase 9 and 3. Chemotherapy and radiotherapy induce apoptosis via intrinsic (mitochondrial) pathway. This pathway is partly influenced by bcl family members bound to the mitochondrial membrane. Among them bax (bcl-2 associated X protein), bak (bcl-2 homologous antagonist/killer) and bid are proapoptotic which promote cytochrome C release from mitochondria and bcl-2, bcl-XL are antiapoptotic proteins which inhibit its release. (Reprinted from reference [119], Copyright with permission from Elsevier).

Cytochrome c and Apaf-1 together activate caspase-9, which then activates caspase 3 (**Figure 1.3**). Recently, activation of DR was suggested to program cells in a caspase-independent, necrotic way of cell death, called programmed necrosis or necroptosis [120]. Necroptosis depends on the formation of complex called necrosome containing kinases RIP1 and RIP3. The complex mainly forms when caspase-8 is absent or non-functional. Necrosome recruits and phosphorylates the pseudokinase MLKL which is required for necroptosis induction [121]. Although it was not fully understood, MLKL was believed to be recruited to plasma membrane where it forms pores resulting in membrane permeabilization [122]. In addition to TRAIL-R1 and TRAIL-R2, TRAIL can also bind to 2 non-DD-containing membrane bound receptors called TRAIL-R3 (known as decoy receptor 1 (DcR1) [123, 124] and TRAIL-R4 (known as DcR2) [124, 125]. TRAIL-R3 is glycosyl-phosphatidyl-inositol-anchored receptor without an intracellular domain and TRAIL-R4 contains a truncated, non-functional DD in its intracellular domain. TRAIL-R3 was found highly expressed in normal cells including peripheral blood lymphocytes, spleen. Lung, heart, liver, kidney, bone marrow, placenta as compared to most transformed cell lines [123]. Although extracellular domains of these receptors are highly homologous to those of TRAIL-R1 and TRAIL-R2, they are incapable to induce apoptosis (**Figure 1.4**). Indeed, TRAIL-R3/4 compete with the apoptosis-inducing DD-containing TRAIL-Rs for ligand binding and inhibit TRAIL-induced apoptosis when overexpressed [126, 127].

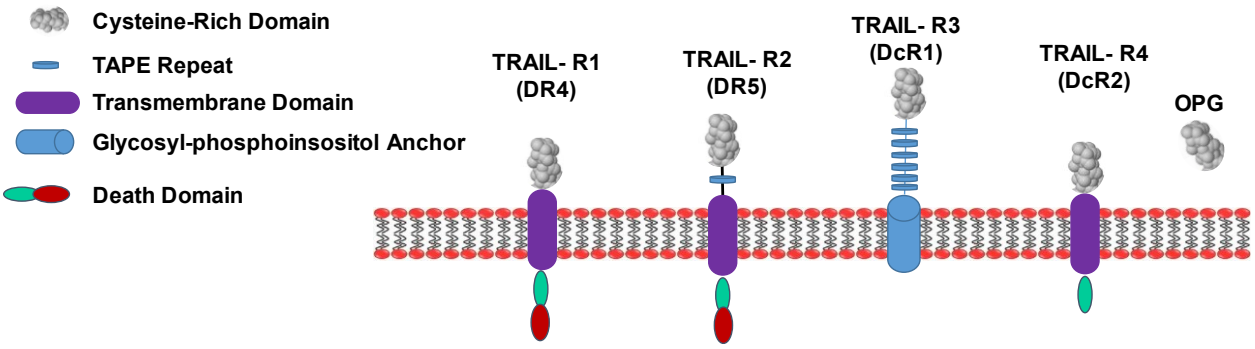

Figure 1.4: Receptors for TRAIL in humans. TRAIL induce apoptosis after binding to TRAIL-R1 (DR4) and TRAIL-R2 (DR5). In contrast, binding to TRAIL-R3 (DcR1) and TRAIL-R4 (DcR2) and soluble receptor osteoprotegerin (OPG) is incapable of inducing apoptosis because of lack of functional death domain (DD). Adapted from reference [124].

1.5.2. Clinical Testing of TRAIL Therapy

Activation of death receptors by TNF and CD95L for anticancer activity was dampened due to severe toxicity after systemic application. Therefore, targeting death receptors (DR4 and DR5) using TRAIL has become attractive alternative approach for cancer therapy. Ability of TRAIL to induce apoptosis in various tumor cell, but not in normal cells, made it as a promising anticancer agent [117, 128]. Currently, TRAIL and TRAIL receptor mediated anticancer therapy comprises two types of pharmacological agents; i) recombinant forms of TRAIL protein and ii) TRAIL-R1 or TRAIL-R2 receptor agonist antibodies. Efficiency of TRAIL receptor agonist in preclinical studies advanced it to clinical trials for treatment of several cancers [119, 124]. Clinically tested TRAIL receptor agonists in patients with advanced solid tumors include soluble recombinant TRAIL (Dulanermin) [129], TRAIL-R1 mAb agonist Mapatumumab [130] and TRAIL-R2 mAb agonist Tigatuxumab, Lexatumumab and Apomab [119, 124, 131, 132]. To date, Mapatumumab has been the most promising as a monotherapy, which entered a Phase II clinical trial in patients with non-hodgkin lymphoma and resulted in 3 responses with 1 complete recovery out of 40 patients [133]. However, there was no remission in vast majority of patients although

they well tolerated the treatment (**Table 1.2**). Although clinical trials revealed the safety and broad tolerability for all TRAIL-R1 and TRAIL-R2 agonist mAb when used alone or in combination with chemotherapy or the proteasome inhibitor bortezomib, no statistically significant anticancer activity was attained by addition of any of these TRAIL-R1 and TRAIL-R2 agonist. Recombinant TRAIL Dulanermin was found also safe and well tolerated with few partial or complete clinical response in a subset of patients in several Phase I clinical trial when used as monotherapy or in combination with chemotherapy or the CD20-targeting antibody rituximab. However, anticancer activity attributed to Dulanermin was insignificant in two randomized controlled trial; one in non-small-cell lung cancer comparing Dulanermin/chemotherapy to chemotherapy alone [134] and another in non-Hodgkin's lymphomas comparing Dulanermin/rituximab to rituximab alone [124]. Based on these clinical Trials, it was concluded that recombinant TRAIL and TRAIL-Rs agonist were well tolerated but produced minimal anticancer activity. Several factors were found associated with resistance to TRAIL induced apoptosis (discussed later). Therefore, combination therapy containing TRAIL and its sensitizer can be effective approach to enhance TRAIL induced apoptosis.

Table 1.2: Effects of recombinant TRAIL and TRAIL receptor agonist in clinical trials.

Cancer	**Combination**	**Clinical trial**	**Dose (mg/kg/day)**	**Efficacy on clinics**	**Ref.**
Dulanermin (recombinant, soluble TRAIL)					
Advanced cancers	-	Phase I	0.5 to 30	Safe, among 71 patients tested only 2 showed partial response	[129]
Colorectal	Chemotherapy+ bevacizumab	Phase I	4.5 or 9	Safe, Among 23 patients 13 showed partial response	[135]
Lung	Chemotherapy+ bevacizumab	Phase I	4 or 8	Safe, among 24 patients, it was effective in one patient and 13 showed partial response	[136]
Lung	Chemotherapy+ bevacizumab	Phase II	8 or 20	Safe but addition of dulanermin showed no significant anticancer activity	[134]
Mapatumumab (TRAIL-R1 agonistic antibody)					

Advanced cancers	-	Phase I	0.01 to 10	Safe, no responses observed on 49 patients tested	[137]
Advanced cancers		Phase I	0.01 to 20	Safe, no response among 41 patients tested	[130]
Advanced cancers	Chemotherapy	Phase I	1 to 30	Safe, among 49 patients, 12 showed partial response	[138]
Lung	Chemotherapy	Phase II	10 or 30	Safe but no significant anticancer activity with addition of TRAIL receptor agonist in randomized controlled trial	[139]
Colorectal	-	Phase II	20 followed by 10	Safe, no response in 38 patients	[140]
Conatumumab (AMG-655) TRAIL-R2- agonistic antibody					
Advanced cancers	-	Phase I	0.3 to 20	Safe, only one partial response among 37 patients	[141]
Non-small cell lung cancer	Chemotherapy	Phase II	3 or 15	Safe, no advantage of TRA on chemotherapy in 172 patients tested in randomized controlled trial	[142]
Pancreatic cancer	Chemotherapy	Phase II	10	Safe, no additive anticancer activity of TRA in 83 patients tested in randomized controlled	[143]
Lexatumumab (TRAIL-R2- agonistic antibody)					
Advanced cancer	-	Phase I	0.1 to 20	Safe, no responses in 37 patients	[144]
Advanced cancer	Chemotherapy	Phase I	0.1 to 10	Safe, no anticancer activity with addition of TRA in 41 patients	[145]
Pediatric solid tumors		Phase I	3, 5, 8 or 10	Safe but no response in 24 patients tested	[146]
Tigatuzumab (TRAIL-R2- agonistic antibody)					
Carcinoma or lymphoma	-	Phase I	1 to 8	Safe, no responses in 17 patients	[131]
Pancreatic	Chemotherapy	Phase II	8 followed by 3	Safe, only 8 patients showed partial responses among 61 patients	[147]
Lung cancer	Chemotherapy	Phase II	10 followed by 8	Safe, no advantage of adding TRA in randomized controlled TRAIL	[148]
Drozitumab (PRO95780) (TRAIL-R2- agonistic antibody)					
Colorectal	Chemotherapy	Phase I	5 followed by 3.5 or 10 followed by 7	Safe, only 2 partial response among 9 patients, number of patients were less to draw any conclusion	[149]
Advanced cancer	-	Phase I	1 to 20	Safe, no responses in 50 patients tested in different dose	[150]
LBY-135 (TRAIL-R2- agonistic antibody)					
Advanced cancer	Chemotherapy	Phase I/II	0.3 to 40	Safe, only 2 responses among 73 patients tested and anticancer activity was not significant that chemotherapy alone	[151]

1.5.3. Resistance Mechanism to TRAIL Induced Apoptosis

Resistance of normal cells and tissues to TRAIL-induced apoptosis and the sensitivity of variety of cancer cells to TRAIL raised the possibility of using TRAIL treatment for cancer therapy. However, despite promising preclinical results and safe profile, TRAIL therapy that have been tested so far clinically failed to exert a robust anticancer activity in patients. Cancer cells were found to have mixed response to TRAIL induced apoptosis in in *vitro* models [117, 152]. To avoid the apoptosis induction by TRAIL, several mechanisms exists in normal cells and these mechanisms are frequently deployed in cancer cells to avoid TRAIL-induced apoptosis.

1.5.3.1. Resistance mechanism(s) in cancer cells

Breast cancer cells showed mixed response to TRAIL. TRAIL induced apoptosis in some breast cancer cells while others are resistant to TRAIL mediated apoptosis [152-154]. Eight of eleven triple-negative breast cancer cell lines were sensitive to TRAIL with IC_{50} ranging from 10-250 ng/ml, while five of estrogen receptor (ER) positive cell lines tested in one study were resistant to TRAIL induced apoptosis and two of five cell lines with HER-2 amplification were modestly sensitive to TRAIL with IC_{50} of ~1000 ng/ml [155]. Initially, it was believed that TRAIL resistant was mediated by the non-functional decoy receptors (DcR1 and DcR2) via competing with functional receptors DR4 and DR5 for TRAIL binding. Several studies had shown that TRAIL sensitivity in normal cell was determined by the ratio of expression of death receptor and decoy receptors [156]. Transfection of TRAIL-R3 cDNA into TRAIL sensitive lines conferred resistance against TRAIL-induced apoptosis, indicating a dynamic regulatory mechanism to resist TRAIL action. High expression of TRAIL-R3 is found in many primary gastrointestinal cancers [157] and is related to poor prognosis in breast cancer [158]. However, other studies failed to prove consistent

correlation of TRAIL sensitivity with expression of death receptors and decoy receptors in cancer cells suggesting that decoy receptor is not the only mechanism of TRAIL resistant [159, 160].

Regulating function and expression of pro-apoptotic and anti-apoptotic proteins is another mechanism to regulate TRAIL induced apoptosis. Overexpression of the several anti apoptotic proteins have been associated with TRAIL resistance. Studies have shown that resistance to TRAIL can occur through defects at every level of the TRAIL signaling pathways from ligand binding to cleavage of the effector caspases [152, 161]. At DISC, cellular FLICE-inhibitory protein (cFLIP) inhibits the activation of caspase-8 by interacting with the adaptor protein FADD. FLIP is structurally similar to caspase-8 and caspase-10 and exists in three splice variants; long ($cFLIP_L$), short ($cFLIP_S$) and Raji ($cFLIP_R$) [162, 163]. $cFLIP_S$ and Raji $cFLIP_R$ are short variants which lack caspase-like domain whereas $cFLIP_L$ contains long c-terminal caspase-like domain without catalytical activity. $cFLIP_S$ and $cFLIP_R$ inhibit pro-apoptotic activity of DISC by competing with caspase-8 and caspase-10 for binding to DISC thereby preventing activation. In contrast, the function of $cFLIP_L$ is more complex. Depending on the amount, $cFLIP_L$ can exert a pro-apoptotic or an anti-apoptotic function. When expressed at high level, $cFLIP_L$ has anti-apoptotic function by preventing binding of caspases to DISC. When expressed at lower level, $cFLIP_L$ has pro-apoptotic function by enhancing pro-caspase-8 recruitment at the DISC [164]. Expression of FLIP is controlled by transcription factor NF-kB. Activation of NF-kB upregulates the FLIP thus increasing resistant to death ligand mediated apoptosis [165]. In addition, Akt, PKCs and MAPK pathways regulate the FLIP expression [166]. High level of $cFLIP_L$ was found in human cancer cells, including colorectal carcinoma, hepatocellular carcinoma, pancreatic carcinoma, prostate

carcinoma, melanoma and metastatic cutaneous melanoma lesions from human patients and has been associated with resistance to TRAIL-induced apoptosis [167-170].

TRAIL also induces mitochondrial apoptosis pathway by cleaving BID to tBID. TRAIL induced mitochondrial apoptosis is regulated by anti-apoptotic Bcl-2 family members such as Bcl-2, Bcl-B, Bcl-w, Bfl-1, Bcl-xL and Mcl-1 via inhibiting pro-apoptotic Bax-Bak-mediated MOMP. Hydrophobic domain of these protein binds to BH3-only proteins and to the pro-apoptotic Bcl-2 family members; Bad, Bak and Bax and inhibits the apoptosis [171]. Overexpression of anti-apoptotic Bcl-2 family members or loss of expression of pro-apoptotic members are common in cancers which are rendered resistant to apoptosis induction [124]. Finally, at level of effector caspase, TRAIL induced apoptosis is halted by the inhibitors of apoptosis (IAPs) via inhibiting catalytic activity of effector caspase after direct interaction with them [124]. IAPs carry a functional baculovirus IAP repeat (BIR) domain. Until now, eight family members have been identified including survivin, c-IAP1, c-IAP2, and X-linked inhibitor of apoptosis (XIAP). Several IAPs including XIAP, survivin are abundantly expressed in a variety of cancer cells and are associated with the resistant of cancer cells to various apoptotic stimuli (reviewed by Altieri et al.) [124, 172]. In an independent study, 76% of TRAIL-resistant cell lines (13 out of 17) expressed only one of anti-apoptotic proteins (cFLIP, Bcl-2 or XIAP) at high levels ($\geq$ 1.2 fold higher than the mean expressed across all cell lines) supporting that tumor cell rely on a single antiapoptotic protein to block the apoptotis induction [173].

1.5.3.2. Resistant Mechanism in Non-Transformed Cells

The attractive aspect of TRAIL is due to its property of inducing apoptosis selectively in cancer cells, but not in non-transformed cells. This attribute of TRAIL was further validated by pre-clinical and Phase 1 studies, which demonstrated no systemic toxicity of TRAIL even at very high doses [117, 124]. Although, understanding mechanism of TRAIL resistance in cancer cells has greatly increased in last decade, the mechanism of TRAIL resistance in normal, non-transformed cells is poorly understood. Early study showed higher expression of decoy receptors (DcR1 and DcR2) in non-transformed cells than in cancer cells, which was believed to be mechanism of TRAIL resistance in normal tissues [174, 175]. However, DR5 receptor agonistic antibodies selectively induced apoptosis in DR5 expressed cancer cells while sparing non-transformed cells; hepatocytes, dermal fibroblasts and umbilical artery smooth muscle cells suggesting involvement of other mechanism of TRAIL resistant in normal cells [173]. In addition, another study failed to show correlation between TRAIL resistant and DcRs in melanoma cell lines [176]. Human primary fibroblasts and smooth muscle cells were found protected from the TRAIL-induced apoptosis via multiple inhibitors of apoptosis such as cFLIP, anti-apoptotic Bcl-2 proteins and XIAP. Interestingly, removal of only one of these proteins was unable to induce TRAIL sensitivity. Only simultaneous loss of cFLIP and XIAP or cFLIP and anti-apoptotic Bcl-2 reversed TRAIL resistance [173]. However, many cancer cells utilize single resistance mechanism and silencing of single anti-apoptotic protein was sufficient to sensitize the cancer cells against TRAIL induced apoptosis (described above). Another study showed protective role of TAK1 against TRAIL-induced apoptosis in keratinocytes. TRAIL induced the ROS accumulation, activation of DISC and degradation of cFLIP in TAK1 deficiency keratinocytes and fibroblasts [177].

Differentiating the mechanisms of TRAIL resistant in normal and cancer cells allows to selectively induce TRAIL mediated apoptosis in cancer cells.

1.5.4. Strategies to Enhance TRAIL Induced apoptosis

In addition to development of intrinsic or acquired resistant to TRAIL therapy, other mechanism responsible for ineffective TRAIL therapy are; i) the poor pharmacokinetic profile of recombinant TRAIL proteins (i.e., low systemic availability), and ii) weak apoptosis induction by TRAIL receptor agonistic antibodies. Because of small molecular weight and instability of non-covalently linked trimeric structure, systemically administered recombinant TRAIL protein is rapidly cleared via renal elimination resulting into very short plasma half-life [178-180]. Trimerization of TRAIL receptors is prerequisite for efficient apoptosis induction by TRAIL. Therefore, the inherent bivalent nature of antibodies permits only crosslinking of two TRAIL receptors and allows inefficient DISC formation resulting in weak apoptotic signal [124]. Therefore, several strategies were employed to increase the bioavailability of TRAIL and better sensitize the TRAIL-induced apoptosis.

1.5.4.1. **Combination Therapy to Enhance TRAIL Induced Apoptosis**

Many studies investigated the combination of a wide range of chemotherapeutic drugs with TRAIL to enhance cell death. For example cisplatin in combination with a TRAIL encoding retrovirus produced higher anticancer activity in ovarian carcinoma cells *in vitro* and in xenografts [181]. Similarly, most commonly used standard chemotherapeutic agents including gemcitabine, irinotecan, doxorubicin, 5-FU and platinum-based chemotherapeutics have been shown to synergize TRAIL action [124]. Various mechanisms have been proposed for synergistic effect of

chemotherapeutics and TRAIL including increased DISC formation, upregulation of death domain receptors (DR4 and DR5), activation of caspases, upregulation of pro-apoptotic and suppression of anti-apoptotic proteins [124, 152]. However, none of the randomized clinical trials conducted to date, showed clinical benefits attributed to TRAIL or TRAIL receptor agonist (TRA) in combination with chemotherapy **(Table 1.2).** The lack of efficacy of TRAIL or TRA and chemotherapy combination might be due to insufficient agonistic activity of TRA, or insufficient sensitization to TRAIL-induced apoptosis [124].

In addition, studies were performed to identify the potent sensitizer of TRAIL. Inhibition of proteasome using bortezomib and histone deacetylases inhibitors also synergized the TRAIL induced apoptosis [182, 183]. Recently, it was found that selective inhibition of cyclin dependent kinase 9 (CDK9) sensitized TRAIL induced apoptosis in variety of cancer cells by down regulating cFLIP and Mcl-1 [184]. Another class of agents that suppressed apoptosis in combination with TRAIL are IAPs such as XIAP, cIAP1, cIAP2 and survivin. High expression of these proteins in cancer is associated with tumor progression and therapy resistance [124]. Small molecular Smac mimetics or IAP antagonists have been developed which inhibit the IAPs and are promising anticancer agents alone or in combination with anticancer agents. These molecules mimic the XIAP-binding site of the endogenous XIAP antagonist Smac. Smac is normally a mitochondrial protein and released into cytosol when the cells undergo apoptosis and binds to IAPs preventing them from inhibiting caspase activation. Smac mimetics increased apoptosis induced by TRAIL *in vitro* and *in vivo* in a variety of cancer [185, 186] **(Table 1.3)**. To overcome the mitochondrial apoptosis, BH3 mimetic small molecules such as ABT-199, ABT-263, ABT-373 have been

developed that antagonize the function of anti-apoptotic Bcl-2 family proteins. These BH3 mimetic small molecules have also sensitized cancer cells to TRAIL *in vitro* [187, 188].

Table 1.3: Combination therapy with TRAIL and a variety of agents to induce apoptosis.

TRAIL name	**Modification**	**Combination therapy**	**Tumor type (in vitro/vivo)**	**Comments and clinical development**	**Ref.**
LZ-TRAIL	Addition of leucine zipper to recombinant TRAIL	-	Mammary adenocarcinoma	Improved stability and activity in vitro and in vivo animal model	[189]
rhTRAIL	cross-linked by adding an anti histidine mAB	bortezomib	Esophageal squamous cell carcinoma in vitro	Bortezomib resulted in more efficient recruitment of caspase-8 FADD complex and downregulation of cFLIP and anticancer activity was improved	[190]
rhTRAIL	-	bortezomib	Glioblastoma in vitro	P65/NF-κB DNA-binding activity was abolished by bortezomib and sensitize the TRAIL induced apoptosis	[191]
rhTRAIL		ABT 373	Renal, prostate and cancer cell line in vitro	Upregulation of death receptor 5 and enhanced apoptosis	[192]
rhTRAIL		XIAP-small molecule inhibitors	Pancreatic cancer in vitro	Enhanced apoptosis by activation of downstream effector caspases	[193]
rhTRAIL		Smac peptide	Malignant glioma tumor model in vivo	Smac peptide sensitized tumor cells including resistant cells for TRAIL induced apoptosis	[185]
TRAIL		Smac mimetic small molecule	Human glioblastoma in vitro	Binds to XIAP, cIAP-1 and cIAP-2 and synergized the apoptosis induced by TRAIL	[186]
TRAIL	-	shRNA against XIAP or small molecule XIAP inhibitor	Childhood acute leukemia cells in vitro	XIAP inhibitors enhanced TRAIL-induced activation of caspases, loss of mitochondrial membrane potential, and cytochrome c release in a caspase-dependent manner, and even overcome Bcl-2-mediated resistance to TRAIL by enhancing Bcl-2 cleavage and Bak conformational change.	[194]
TRAIL		BH3I-2' and HA14-1(Bcl-2 inhibitors)	Lymphoblastic leukemina in vitro	Overcame resistant to TRAIL induced apoptosis after increased reactive oxygen species and	[195]

				mitochondrial respiration resulting release of cytochrome C	
Mouse rTRAIL	-	PS- 341	Murine myeloid leukemia, murine renal cancer cells in vitro	Long term tumor inhibition in mice and enhanced survival	[196]
NP-TRAIL	TRAIL conjugated to magnetic ferric oxide nanoparticle	γ-radiation or bortezomib	Glioblastoma in vivo and in vitro	Enhanced anticancer activity of NP-TRAIL as compared to TRAIL alone. γ-radiation or bortezomib sensitized glioblastoma cells to TRAIL induced apoptosis in vivo and in vitro	[197]
NT-TRAIL	TRAIL loaded onto PLGA nanoparticles	-	Hela cells in vitro and in vivo xenograft model in mice	Enhanced apoptosis in vitro and tumor growth in an in-vivo xenograft model in mice was inhibited without any loss of body weight.	[198]
S-TRAIL-GFP	Fusion of extracellular domain of Flt3L and isoleucine zipper to N terminus and GFP in c terminus	-	Primary glioma cells in vitro	Enhanced apoptosis via bystander effect and stabilized oligomerization of TRAIL.	[199]
Transferrin-PEG-TRAIL	PEGylated TRAIL attached to transferrin	-	HCT 116 cells in vitro and in vivo mouse model	Enhanced efficacy and combined the tumor targeting properties	[200]
pORF-hTRAIL	TRAIL gene (pORF-TRAIL) and Doxorubicin loaded into nanoparticle	Doxorubicin	Glioblastoma cells, orthotopic human glioblastoma model in mice	Enhanced antiglioma efficacy in vivo	[201]
Ad-stTRAIL	Adenoviral vector carrying secretable trimeric TRAIL gene	-	Human glioma xenograph tumor model in animal	Supressesed tumor growth without detectable side effects and secretable TRAIL expressed by Ad-stTRAIL persisted in tumor tissues for more than 4 days after intratumoral injection	[202]
Ad5-TRAIL	Adenovirus encoding human TRAIL gene	-	Human prostate carcinoma cell in vitro	Tumor cell death was observed with activation of caspase – 8	[203]
AAV.TRAIL	Adeno-associated virus encoding TRAIL	-	Human colorectal tumor in mouse model	Significantly inhibited the growth of tumor	[204]

1.5.4.2. TRAIL Sensitization by RNA Interference

TRAIL usually induces apoptosis via the extrinsic pathway; however, when a cell is additionally stressed, it can trigger the intrinsic pathway, resulting in enhanced apoptosis. In so called type-I cells, activation of DISC is strong and stable enough to trigger caspase-8 activation and in turn, directly and fully activate effector caspase-3, resulting in apoptosis. While in type II cells, DISC induced activation of caspase-3 is not sufficient enough to induce apoptosis [124]. Therefore, additional triggering of intrinsic pathway is required to induce apoptosis. Over-expression of several anti-apoptotic proteins led to resistance to TRAIL-induced therapy as described above. Several chemotherapeutics and small molecules reduced the expression of such aberrant anti-apoptotic protein(s) and induced cellular stress or inhibited the oncogene to restore the sensitivity of cancer cells to TRAIL induced apoptosis (**Table 1.3**). Alternatively, short interfering RNAs (siRNAs) that participate in and trigger RNA interference (RNAi) mechanism have been developed as a new line of therapeutics to silence transcripts of unwanted proteins specifically. An siRNA targets a specific messenger RNA (mRNA) and employs endogenous RNAi pathway to degrade the transcript or block translation. Recently, U.S. Food and Drug Administration approved first-of-its kind siRNA called ONPATTRO (Alnylam Pharmaceuticals) for treatment of the polyneuropathy of hereditary transthyretin-mediated (hATTR) amyloidosis in adults. This shows a promise on siRNA use as a new era in patient care. Effective siRNA targets can be selected either from high-throughput screening of human siRNA libraries or by exploring mechanistic insights into the apoptosis pathways from the literature and choosing the appropriate targets. To reveal regulator(s) of TRAIL induced apoptosis, several siRNA libraries targeted against kinases, phosphatases, apoptosis related genes and unknown genes were screening in cancer cells in presence or absence of recombinant TRAIL. A siRNA library directed against 510

genes which included 380 known and predicted kinases, 20 known genes of interest, 100 genes of unknown function, 10 well-characterized genes known to play a role in apoptosis and TRAIL-mediated signaling pathways were screened in HeLa cells in presence or absence of TRAIL to reveal genes that regulate the TRAIL-induced apoptosis [205]. This screening revealed several TRAIL-enhancer siRNAs which silences kinases including p38 substrate kinases MKNK1 and MAPKAPK2, PAK1, RPS6KA5, MEK5 and its specific target BMK1/ERK5, the well-known antiapoptotic kinase AKT1, and SRC family kinases LYN and FGR, FLJ21802, the JNK inhibitory kinase JIK, and the semaphoring receptor PLXNB1[205]. Recently, an independent study identified several positive and negative regulators of TRAIL action by screening an siRNA library containing human kinome (691 genes), phosphatome (320 genes) and 300 additional genes in the triple negative breast cancer MDA-MB-231 cells. This study identified 150 genes including 83 kinases, 4 phosphatases and 63 nonkinases as inhibitors of TRAIL induced apoptosis [206]. In our recent screening of 446 human apoptosis-related siRNA library, 16 siRNAs were identified which sensitized the TRAIL induced apoptosis in the same MDA-MB-231 cells. siRNAs silencing BCL2L12, SOD1 BCL2L1 (BCL-XL) and BIRC4 (XIAP) TNFRSF10D (tumor necrosis factor receptor superfamily member 10d) and TRAF2 were top sensitizer of TRAIL induced apoptosis [207]. It was interesting to note that there was minimal overlap on the outcomes of these studies, which could be due to differences between types of cells used, endpoint assays, delivery systems and type of siRNA library (i.e., chemical nature of siRNAs). Besides the siRNA library screening, several studies used siRNAs to silence negative regulator of apoptosis based on literature searches.

Expression of decoy receptors (e.g., DcR1, DcR2 and DcR3) is one of the extracellular mechanisms by which cells diminish the death receptor induced apoptosis. Therefore, silencing

decoy receptor with siRNA is one approach to clear the blockage of apoptosis. Enhanced TRAIL-induced apoptosis in pancreatic cells after siRNA mediated silencing of DcR3 is one example [208]. After binding of TRAIL to the TRAIL receptor, downstream apoptosis induction is regulated by cellular FLICE-like inhibitory protein (cFLIP) which is studied as one of the negative regulators of the death receptor mediated apoptosis [169]. Silencing cFLIP reversed TRAIL resistance in the FLIP over-expressing cancer cells. To silence the FLIP, transfection with siRNA [168] or with short hairpin RNA (shRNA) encoding plasmids [169, 170] were employed. Silencing of FLIP enhanced TRAIL-induced apoptosis in several cancer cell lines (**Table 1.4**). In melanoma cells (A375), siRNA mediated inhibition of FLIP led to enhanced TRAIL mediated apoptosis via increasing activity of caspase-3, -8, -9 [168]. Human renal carcinoma was also sensitized against TRAIL therapy after siRNA mediated silencing of cFLIP [209]. Similarly, plasmid encoding shRNA against c-FLIP enhanced the sensitivity of human osteogenic sarcoma cells (U2OS) [169] and hepatocellular cell lines [170] to TRAIL induced apoptosis. Another bottleneck for apoptosis pathway is IAPs and anti-apoptotic Bcl-2 family members such as Bcl-2, Bcl-xL and Mcl-1, as mentioned before. siRNA mediated inhibition of XIAP sensitized the canine tumor cells lines (BDE, Pll4 and Di7) and breast cancer cells (MCF-7) for TRAIL [210, 211]. Similarly, down-regulation of survivin with siRNA enhanced the TRAIL sensitivity even at low concentration (1 to 2 ng/ml) in hepatoma Huh-7 cells [212]. Lung cancer cell (H460 cell) was also sensitized to TRAIL induced apoptosis after siRNA mediated silencing of survivin [213]. In TRAIL-resistant melanoma cells, siRNA mediated silencing of Bcl-2, FLIP, XIAP and survivin sensitized the TRAIL-induced apoptosis, where silencing XIAP and survivin were more potent than silencing Bcl-2 and FLIP [168].

In addition to proteins which directly involved in apoptotic pathway, siRNA mediated silencing of other proteins also sensitized TRAIL-induced apoptosis. Lentiviral mediated HIF-1α knockdown sensitized the tumor cells (HeLa, A549, SNU-638 and SK-N-SH) against TRAIL in hypoxic conditions [214]. However, HIF-1α silencing did not increase sensitivity of pancreatic cancer cells to TRAIL therapy [215]. PKCδ, one of the isoforms of protein kinase C (PKC) is pro-survival molecule which regulates the TRAIL induced apoptosis; siRNA mediated silencing of PKCδ sensitized the TRAIL-resistant HT1080 cells against the TRAIL protein [216]. siRNA mediated silencing of several other mediators including HIFs, WEE1, melanoma-associated antigen (MAGE-D2), TAK1, HSP27, DNA-PKcs enhanced the TRAIL induced apoptosis in various cancer cells [177, 215, 217-220]. Although these proteins do not participate in the apoptosis pathway, they enhanced TRAIL-induced apoptosis via regulating death receptors, caspases and pro- and anti-apoptotic proteins. Surface expression of death receptors was increased by siRNA mediated silencing of WEE1 in basal/triple negative breast cancer cells [217], MAGE-D2 in melanoma [218], DNA-PKcs in leukemic cell, K562 [221] which sensitized the TRAIL activity. Direct activation of caspases is another mechanism to overcome TRAIL resistance. siRNA mediated silencing of WEE1 in basal/triple negative breast cancer cells increased the caspase-8, -9 and -3 activation [217]. Caspase-8 activity was also enhanced by siRNA mediated silencing of HSP27 in human lung cancer cells (A549) [219] and expression of caspase 3 and 9 was increased after silencing DNA-PKcs in K562 cells [221]. Silencing DNA-PKcs decreases the expression of c-FLIP (c-$FLIP_L$ and c-FLIPs) in K562 cells [221]. siRNA mediated silencing of TAK1 induced TRAIL-dependent downregulation of cIAP and accumulation of reactive oxygen species (ROS), which facilitates TRAIL-induced cell death in moderately TRAIL resistant HeLa and TRAIL resistant Saos2 cells [177]. Silencing of HSP27 sensitized the human lung cancer A549

against TRAIL induced apoptosis via down-regulating protein level of Bcl-2 and increasing protein level of Bax, Bak and p53 [219]. shSNAIL carrying lentivirus sensitized the TRAIL resistant HCC (eg HuH-7) against TRAIL where TRAIL was expressed by adenoviral vectors. Here, enhanced cell death was observed through upregulating p53 protein and regulating related gene of NF-kB pathway including Bcl-xl, cIAP2, survivin and Raf-1 protein [222]. siRNA mediated silencing of HIF-2α enhanced susceptibility of pancreatic cancer cell lines, Panc-1 and AsPC-1 to TRAIL induced cells death under normoxic and hypoxic conditions via downregulating expression of survivin. Mouse xenograft model with HIF-2α shRNA expressing cells were more sensitive to TRAIL *in vivo* [215].

Table 1.4: siRNAs used to sensitize cancer cells against TRAIL-induced apoptosis

Cancer type/cell line	siRNA Dose	Target	Delivery vector	Outcome	siRNA Sequences	Ref.
siRNA targeting Decoy receptors						
Human Pancreatic cells (AsPC-1, MiaPACa-2)	10nM	DcR3	Lipofectamine LTX reagent	Enhanced proapoptotic effect of TRAIL (100ng/mL)	5'-CGCUGCAGCCUCUUGAUGGAGAUGUCC-3′	[208]
The human prostate tumor cell lines, DU145 and LNCaP,	(0.3 μg)	DcR2	Lipofectamine plus reagent	DcR2 siRNA-mediated knockdown of DcR2, followed by Ad5hTRAIL infection, dramatically reduced the in vitro tumorigenic potential of prostate cancer cells	Strand A: GGAUGGUCAAGGUCAGUAA; Strand B: CCCUAUCACUACCUUAUCA; Strand C: GCUUGGGAAUGGUGUGAAA.	[223]
siRNAs targeting antiapoptotic proteins						
Human osteogenic sarcoma (U2OS)	-	cFLIP	pSUPER RNAi Vector (pSUPER. puro) FuGENE® HD	FuGENE® HD transfection reagent Enhanced proapoptotic effect of TRAIL (100ng/mL)	Transfected with plasmid encoding siRNA 5'-GGAGCAGGGACAAGUUACA(dTdT)- 3'(sense); 5'-UGUAACUUGUCCCUGCUCC(dTdT)- 3'(antisense).	[169]

			transfection reagent			
Melanoma cells (A375)	20-40 nM	cFLIP	Lipofectamine	Enhanced the apoptosis induction by TRAIL (100ng/ml) by increasing caspase-3, -8, -9 activity	5*AACUGCUCUACAGAGUGAGGC-3* (Dharmacon)	[168]
Human renal carcinoma cells	-	FLIP	Lipofectamine 2000	sensitized cells to TRAIL-mediated apoptosis	nucleotides 472–492 (h1-FLIP) and 908–928 (h2-FLIP) of FLIP-L	[209]
Hepatocellular carcinoma (Hep3b, HepG2TR)	-	FLIP	Fugene 7	Sensitized the TRAIL induced apoptosis	siRNA sequences cloned into pSUPER.gfp/neo	[170]
Renal carcinoma (ACHN, CAKI-1, SN12C)	-	FLIP	Lipofectamine	Sensitized the TRAIL induced apoptosis	nucleotides 472–492 (h1-FLIP) and 908–928 (h2-FLIP) of FLIP-L (ac.-no. U97074) as described by Siegmund et al.	[209]
SV80 and KB	150 nM	cFLIP	Electroporation	Sensitized the tumor cells for TRAIL induced apoptosis by increasing activation of Caspase-8	nucleotides 472–492 (siRNA-F1) and 908–928 (siRNA-F2) of FLIP-L	[166]
GBM cell linesMZ18	1 µg	Bcl-2	Lipofectamine TM 2000	Enhanced apoptosis by TRAIL (100ng/ml)	-	[224]
Melanoma cells (A375)	20 nM	Bcl-2	Lipofectamine 2000	Enhanced apoptosis by TRAIL (100ng/ml)	Dharmacon cat # M-003307-00-05	[168]
Hepatoma cell (Huh-7)	4pmol/104 cells	Survivin	Oligofectamine	Sensitized the TRAIL induced cells at 1 to 2 ng/ml	5'-GCAAUUUUGUUCUUG GCUCTT-3' (antisense)	[212]
Small lung cancer cells (A460)	20 nM	Survivin	INTERFERinTM	Sensitized the TRAIL induced cell death at 75 ng/ml	survivin small interfering RNA (siRNA) were from Cell Signaling (Beverly, MA).	[213]
Melanoma cells (A375)	20–40 nM	survivin	Lipofectamine 2000	increased caspase-9, caspase-8 and caspase-3 activity. Increased TRAIL induced apoptosis	5-AAGGCUGGGAGCCAGAUGACG-3	[168]
siRNAs targeting inhibitors of Apoptosis (IAPs)						

canine tumor cells lines (BDE, Pll4 and Di7)	50 nM	XIAP	Magnet assisted transfection in combination with Lipofectamine	Sensitized the TRAIL induced cells death	XIAP silencing (5'-CCAUGUGCUAUACAGUCAUUACUUU- 3')	[210]
Brest cancer cells MCF-7	25-40 pmo	XIAP	Lipofectamine RNAiMAX	Sensitized the TRAIL induced cells death	5'-CCAGAAUGGUCAGUACAAAGUUGAA-3', HSS100564: 5'-ACACUGGCACGAGCAGGGUUUCUUU-3', HSS100565: 5'-GAAGGAGAUACCGUGCGGUGCUUUA-3')	[211]
Melanoma cells (A375)	20nM	XIAP	Lipofectamine 2000	cleavage of Bid, activation of caspase-9 and cleavage of PARP (poly ADP-ribose polymerase).	5AAGUGGUAGUCCUGUUUCAGC-3	[168]
Other siRNAs						
Imatinib resistant K562		Bcr-Abl	Oligofectamine (Invitrogen)	Enhanced TRAIL-induced apoptosis via down regulation of cFLIP	(5_-CAGAGUUCAAAAGCCCUUCdTdT-3_)	[225]
Breast cancer cells (MDA-MB-231, HCC38, BT549, BT747, MCF7, Hs578T, and SKBR3)	50 nM	WEE1	oligofectamine	Enhanced expression of death receptor and caspase-8,9,3 which sensitized TRAIL induced apoptosis	SMARTpool siRNA (siWEE1, L-005050-00)	[217]
Melanoma cells (Mel-JD, MM200, Mel-FH, ME4405, Mel-RM, Mel-CV, Mel-RMu,ME1007 and IgR3)	50-100 nM	Melanoma-associated antigen (MAGE-D2)	lipofectamine	enhanced formation of TRAIL death-inducing signaling complex and up-regulation of TRAIL-R2 100ng/ml	MAGE-D2 siGENOME SMARTpool (M-017284-00-0010)	[218]
HeLa and Saos2 cells	1 uM	TAK1	Electroporation	TAK1 silencing led to TRAIL mediated accumulation o f ROS and cFLIP degradation	TAK1 siRNA, 5′-GAGUGAAUCUGGACGUUUA-3′	[177]

human lung adenocarcinoma cell line A549		HSP27	PEI polymers	cells transfected with HSP27 siRNA underwent typical apoptotic morphological changes upon TRAIL treatment at a low dose (40 ng/ml)	pRNAT-U6.1/neo vector, a RNA polymerase III-based plasmid HSP27 cDNA (GenBank accession No NM 001540), with sense (5_-CTGCAAAATCCGATGAGAC-3_) and antisense (5_-GTCTCATCGGATTTTGCAG-3_) sequences	[219]
Hepatocellular carcinoma HuH-7		SNAIL	Lentiviral vector	SNAIL silencing enhanced the pp53 expression and regulate NF-kB via supressing Bcl-xl, cIAP2, survivin and Raf-1 protein	Lentiviral expressing shSNAIL	[222]
Pancreatic cancer cells Panc-1 and AsPC-1		HIF-2α	Lipofectamine RNAiMAX	Enhanced TRAIL induced apoptosis via reducing survivin expression	HIF-2α siRNA (Invitrogen	[215]
Cervical cancer cell HeLa, prostate cancer cell (DU145)		HIF-1α	Lipofectamine RNAiMAX	Enhanced TRAIL induced apoptosis	HIF-1α siRNA (Santa Cruz Biotechnology [SCB]),	[215]
HeLa, A549, SNU-638 and SK-N-SH		HIF-1α	Lentiviral	Enhanced TRAIL induced apoptosis		[214]
K562	0.2uM	DNA-PKcs	Oligofectamine	Enhanced TRAIL induced apoptosis via decreasing expression of c-FLIP, increasing expression of caspase 3 and 9, upregulation of death receptors	(50- CAGUCUUAGUCCGGAUCAU dTdT-30)	[221]
HIF-2α shRNA lentiviral vectors in the pLKO.1-puro plasmid (Sigma-Aldrich) in Panc-1, pancreatic cancer cells		HIF-2α	lentivirus	More susceptible to TRAIL in vivo		[215]
Human fibrosarcoma cell lines (HT1080)	50 uM	PKCδ,	Lipofectamine 2000	Enhanced cell death.		[216]

1.5.4.3. Enhancing Pharmacokinetics of TRAIL

Major drawback of using soluble recombinant human TRAIL is its low pharmacokinetic profiles, especially short serum half-life: only 3-5 min in rodents and 23-31 min in nonhuman primates [180]. Because of its small sizes, systemically delivered recombinant TRAIL is rapidly cleared via kidneys [226]. Therefore, repeated administration or alternate delivery methods is required to maintain therapeutic level in circulation. Increasing the total size of the peptide by addition of peptide 'tags' has been used as one approach to retard *in vivo* renal clearance. Addition of FLAG tag (FLAG-TRAIL) [227], poly-Histidine tag (His-TRAIL) [228], leucine or isoleucine zipper (LZ-TRAIL) [189] iz-TRAIL[229] resulted in increased stability and often enhanced its activity *in vitro* (**Table 1.3**). Addition of leucine and isoleucine zipper motifs resulted trimerized form of TRAIL, which is more active than unmodified TRAIL. Unfortunately, both FLAG-TRAIL and His-TRAIL were toxic to primary human hepatocytes [230, 231]. Alternatively, recombinant TRAIL, when covalently linked to human serum albumin [232] and polyethylene glycol [233], displayed increased plasma half-life while maintaining antitumor activity. Another strategy employed a 46-amino acid albumin binding domain (ABD) derived from streptococcal protein G where ABD was genetically fused to the amino or carboxy-terminal of TRAIL. Circulatory half life of ABD fused-TRAIL was increased due to its binding to albumin which resulted in elimination of circulating tumor cells (CTC) as evident from notably reduced chances of secondary lung cancer development in mice [234]. In addition to recombinant TRAIL, monoclonal antibodies (mAbs) that target specific TRAIL receptors were used to induce apoptosis. As compared to recombinant TRAIL, antibodies have a longer half-life. Clinical trials have been conducted with these antibodies targeting TRAIL-R1 and TRAIL-R2. However, recruitment of immune cells is always the potential concern while using antibodies.

Alternative strategy to improve the pharmacokinetics and pharmacodynamics of recombinant TRAIL is via using NP-based delivery systems such as liposomes and micelles and microspheres. To develop TRAIL containing NP, different polymers and lipids have been used such as; poly (lactic-co-glycolic) acid (PLGA) microspheres [198], a combination of PEGylated heparin and poly-L-lysine [179], liposomes [235] and ferric oxide nanoparticles [197]. TRAIL is either encapsulated inside these NPs allowing constant release from the NP or attached on the surface of NP resembling the physiological membrane-bound TRAIL protein. Both strategies resulted improved stability and pharmacokinetic of TRAIL and consequently, enhanced apoptotic effect [179, 197, 198, 235]. NP containing TRAIL were further functionalized with the different targeting molecules such as single-chain variable fragments (scFv) [236], transferrin [237], angiopep-2 [238] to tailor its delivery specifically to cancer cells. TRAIL gene therapy is another approach to prolong the TRAIL exposure to tumor site which is achieved via sustained expression of TRAIL at the site of action. TRAIL gene, however, requires efficient vectors for expression. Both viral and non-viral vector were used for TRAIL gene therapy. TRAIL gene has been incorporated into adeno-associated viruses (AAVs) and adenoviruses (AVs) and used to treat variety of cancers [119, 239, 240]. However, immunogenicity of viral vectors and instability of transgene expression limit their use especially in a clinical setting. Nano-assembled complexes with cationic lipid, polymer, peptide and other organic nanoparticles are alternative carriers as described before. Cationic liposomes were used to deliver the TRAIL gene into the glioma cells both *in vitro* and *in vivo* model [238].

Recently, a variety of adult stem cells which were engineered to express soluble TRAIL were used as delivery agents [119]. Mesenchymal stem cells (MSC) were modified with TRAIL gene using both viral or non-viral vectors and their effects were evaluated in different cancer cells.

Adipose tissue derived MSC modified with TRAIL gene (AT-MSG-TRAIL) using retro-viral vector induced apoptosis in different osteosarcoma *in vitro* and Ewing's Sarcoma xenotransplants *in vivo* [241] and in human cervical carcinoma, pancreatic and colon cancer cells [242]. Bone marrow derived MSCs modified with TRAIL efficiently killed the human malignant mesothelioma tumors *in vivo* [243]. Similarly, human umbilical cord mesenchymal stem cell (HUMSCs) engineered to secrete TRAIL via adenoviral transduction were effective in killing glioma cells *in vitro* and prolonged the survival of nude mice with human glioma xenograft model [244]. Other studies used lentiviral vector and oncolytic adenovirus secreting TRAIL to modify human MSCs which showed significant cell death in different cancer cells lines [245, 246]. Alternatively, several non-viral vectors were used to engineer the human stem cells to secrete the TRAIL. Low molecular weight PEI linked to β-cyclodexin [247], and Lipofectamine 2000 [248] was used to modify MSC cells with TRAIL plasmid.

1.6. Concluding Remarks and Prospective

It is well accepted now that cancer is a heterogeneous disease which involves mutation or abnormal expression of multiple proteins. Therefore, no matter what therapeutics we select, a sub-population of cells would be unresponsive to the therapy which will continue to grow. On the other hand, the plasticity of the malignant cells results resistant to any treatment. Inherent heterogeneity and plasticity certainly necessitates combination therapeutic approaches. The growing interest on combination therapy arises from the potential of synergism between selected therapeutics. Combination of chemotherapeutics is routine in treatment of cancer. However, intolerable toxicity associated with chemotherapeutics at advanced stages of the disease warrants the alternative therapeutic approach. Nucleic acid combination allows targeting multiple pathways to specifically

inhibit the growth of cancer cells. Combination of nucleic acid can not be employed without appropriate delivery systems. Cationic, lipophilic carriers will be vital for success of nuleic acid combination since they can incorporate multiple nucleic acids and facilitate intracellular delivery through lipophilic plasma membrane. In nucleic acid combination therapy selection of therapeutic pair is of paramount importance. Combination of plasmid DNA encoding TRAIL and its complementary siRNA will be ideal to induce cell death in cancer cells. TRAIL has the unique capacity to induce apoptosis in a variety of tumor cell lines, but not in most non-malignant cells highlighting its potential therapeutic application in cancer treatment [117, 128]. Currently, TRAIL and TRAIL receptor mediated anticancer therapy comprise two types of pharmacological agents; i) recombinant forms of TRAIL protein and ii) TRAIL-R1 or TRAIL-R2 receptor agonist antibodies. These TRAIL therapies in combination with chemotherapeutics were safe but failed to exert anticancer activity in clinics [124]. Increasing the exposure of TRAIL to the cancer cells and sensitization of cancer cells to TRAIL-induced apoptosis would be most effective to irradicate the cancer cells. Many antiapoptotic proteins were found overexpressed in cancer. These antiapoptotic proteins block the apoptotosis induction by TRAIL [168]. RNAi is ideal to silence these unwanted antiapoptotic proteins. RNAi allows specific silencing of the aniapoptotic proteins to target cancer cells sparing vital normal cells. Identification of the most effective siRNA target that sensitized the breast cancer cells to TRAIL induced apoptosis without affecting normal cells remains to be identified.

Chapter 2

Asialoglycoprotein Receptor-Mediated Gene Delivery to Hepatocytes using Galactosylated Polymers

Versions of this chapter was published in:

Bindu Thapa, Piyush Kumar, Hongbo Zeng, Ravin Narain, "Asialoglycoprotein receptor-mediated gene delivery to hepatocytes using galactosylated polymers", *Biomacromolecules,* 2015, 16*,* 3008-3020.

2. 1. Introduction

Success of gene therapy depends on the safe, specific and effective delivery systems of therapeutic gene to the target cells. Recently, gene therapy using non-viral vectors has been investigated extensively because of their capacity to deliver large DNA, facile chemistry, flexible manufacturing, low immune response and safe toxicity profiles. However, the clinical outcome is limited due to low efficiency of the carrier. A wide range of cationic polymers including poly(ethyleneimine) (PEI), poly(L-lysine) and poly(amidoamines) have been synthesized and explored in gene therapy over the last few decades and significant progress has also been reported [249]. The electrostatic interaction between cationic charge of these polymers and negative charge of nucleic acid is the basis of non-viral gene delivery and it generates nano- to submicron-sized complexes. Strong cationic charge density, however, creates unnecessary cell surface disruption and cellular toxicity. In addition, non-specific cellular interaction, poor colloidal stability and low transfection are major hurdles that can hamper delivery capability of non-viral carriers to specific cells [90, 249]. Lately, significant attention has been given to the development of non-viral gene delivery carrying specific ligands targeting cell surface receptors [250, 251].

Receptor mediated endocytosis is among the promising approaches to deliver therapeutic gene to specific cells and tissues types. Cell surface receptor-specific ligands including galactose [250, 252], mannose [253], folate [254], antibody [255], asialofetuin [251] have been conjugated onto the non-viral gene delivery vectors. Among these asialoglycoprotein receptor (ASGPR) seemed most promising for receptor targeting gene deliver because of its high affinity and rapid internalization rate [256]. Successful *in vivo* gene delivery specifically into hepatocytes by exploring ASGPRs therefore appears to be of great therapeutic potential since hepatocytes are

responsible for the synthesis of a wide variety of proteins. Moreover, it can be a most promising tool to deliver therapeutic gene into hepatocytes to treat hepatocellular carcinoma (HCC), which is one of the most common malignancies and third leading cause of cancer-related deaths in the world. More than one million cases of HCC are reported each year with a poor 5-year survival rate of about 7% in spite of treatment [257-259]. ASGPRs are exclusively expressed in hepatoma cell lines such as HepG2, Huh 7.5 cells; [260, 261] therefore strategy of exploiting these receptors for targeted therapy may have reduced toxicity in other tissues. ASGPR selectively binds to galactose or N-acetylgalactosamine residues of deacetylated glycoproteins and then internalize them [262]. Galactose has been focused for gene and drug delivery into liver cells.

We have previously reported a series of block and statistical carbohydrate-based copolymers which exhibited high gene delivery efficacy with lower toxicity than conventional transfection agents [263-265]. Sizes, compositions and architectures of these cationic carbohydrate copolymers were found to impact DNA condensation and transfection efficiency [263-265]. Use of carbohydrates and their cationic analogues for gene delivery is nature-inspired approach to produce biocompatible gene delivery vectors. Carbohydrate residues can facilitate the condensation of DNA via hydrogen bonding, thus reducing the need of excess cationic charge and eventually decreasing the toxicity of vector system [266, 267]. In this study, we have synthesized a series of galactose containing block and statistical cationic copolymers of different sizes and compositions via reversible addition-fragmentation chain transfer polymerization (RAFT) technique. Subsequently, their transfection efficiencies were evaluated in ASGPR expressing and non-expressing hepatocytes.

2.2. Materials and methods

2.2.1. Materials

O-Nitrophenyl β-D-galactopyranoside, (ONPG)(enzymatic), asialofetuin, formalin, β-mercaptoethanol,3-(4,5-dimethylthiazol-2-yl)-2,5-diphenyltetrazolium bromide (MTT), hyperbranched polyethyleneimine (PEI)(M_w = 25 kDa) and4,4-azobis(4-cyanovaleric acid) (ACVA)were purchased from Sigma Aldrich. Cell Culture media Dulbecco's Modified Eagle Medium (DMEM; high glucose with glutamine and sodium pyruvate), Opti-MEM (OMEM), penicillin (10,000 U/mL), streptomycin (10 mg/mL), 0.25% trypsin and fetal bovine serum (FBS) were obtained from Invitrogen. Micro BCA assay kit was obtained from Fisher Scientific. Gwiz *β*-galactosidase plasmid was purchased from Aldervon. Cy3 plasmid labeling dye was purchased from Bio Mirus. 4-Cyanopentanoic acid dithiobenzoate (CTP), 2-aminoethyl methacrylamide (AEMA) and 2-lactobionamidoethyl methacrylamide (LAEMA) were synthesized according to previously reported procedure [268-270]. All other chemicals used were of reagent grade.

2.2.2. Experimental Section

2.2.2.1. Polymer Synthesis and Modifications

The polymers of varying degree and architecture were synthesized via RAFT polymerization according to previously reported protocols [271]. The statistical copolymers of AEMA and LAEMA were prepared at 70 °C in the presence of initiator 4,4'-azobis(4-cyanovaleric acid) (ACVA) and chain transfer agent 4-cyanopentanioc acid dithiobenzoate (CTP). Briefly, for the polymer of targeted M_n = 30 kDa and DP_n= 100, AEMA (0.130 g, 0.78 mmol) and LAEMA (0.370 g, 0.79 mmol) were dissolved in 5 mL double distilled water followed by addition of CTP (3.99 mg, 0.014 mmol) and ACVA (1.995 mg, 0.0071 mmol) in 1 mL of *N,N′*-dimethylformamide

(DMF). Then the mixture was degassed with nitrogen gas for 45 min and maintained at 70 °C for 12 h under constant stirring. The polymerization was quenched with liquid nitrogen and precipitated in acetone followed by washing with methanol and DMF. The structural composition was analyzed by ^{1}H-NMR spectroscopy (Varian 500 NMR). Molecular weight and molecular weight distribution of the polymers was determined by GPC (Viscotek GPC system) using 0.5 M sodium acetate/0.5 M acetic acid buffer as eluent at a flow rate of 1.0 mL/min at 22 °C. Pullulan standards (M_w = 6.2–113 kDa) were used for calibration.

For the di-block copolymerization, macroCTA of AEMA was prepared and then used in the polymerization of LAEMA. In a typical reaction of macroCTA of AEMA (M_n= 20 kDa), AEMA (0.5 g, 3.02 mmol) was dissolved in double distilled water (4 mL), followed by addition of CTP (7.049 mg, 0.025 mmol) and ACVA (3.52 mg, 0.013 mmol) in 1,4-dioxane (2 mL). The mixture was degassed with nitrogen gas for 45 min and placed in oil bath at 70 °C with constant stirring for 6 h. The polymerization was quenched with liquid nitrogen. Polymer was precipitated in acetone, extensively washed with methanol and dried. Molecular weight and molecular weight distribution was determined by GPC as described above. The obtained macroCTA (0.2 g, 0.01 mmol) and LAEMA (0.201 g, 0.43 mmol) were dissolved in double distilled water (5 mL), followed by addition of ACVA (1.4 mg, 0.005 mmol) in DMF (1 mL). The mixture was degassed with nitrogen for 45 min and polymerization was carried out at 70 °C for 12 h. The polymerization was then stopped by quenching in liquid nitrogen, precipitated in acetone and extensively washed with DMF and methanol. The final product was dried and analyzed by GPC as described above.

2.2.2.2. Formulation of Polymer/DNA Complex and Characterization

Polyplexes were formed by mixing polymer with β-galactosidase plasmid in OMEM medium. Briefly;1.2 µg of *β*-galactosidase plasmid was added to varying concentrations of polymer (depending on type of polymer) in OMEM medium, lightly vortexed and incubated at 22 °C (RT) for 30 min to obtain polyplexes. Polyplexes were diluted with OMEM and the size and surface charge of polyplexes were measured using Brookhaven Zeta Plus (zeta potential and particle size analyzer) instrument. In order to study stability, polyplexes were diluted with complete medium and incubated at room temperature. Then size was measured in designated time. Formation of Polyplexes was confirmed by agarose gel electrophoresis. Polyplexes were loaded in 0.8% agarose gel containing 1 µg/mL ethidium bromide in 1X tris acetate/EDTA buffer at 120 V for 45 min. The gel was illuminated with UV light to reveal the relative position of complexed and naked DNA using UV transilluminator (Alpha Innotech; San Leandro, CA).

2.2.2.3. Cell culture

Hep G2, SK hep1, Hela and Huh 7.5 cells were maintained in high glucose DMEM with 10% FBS and 1% penicillin/streptomycin in a humidified atmosphere in the presence of 5% CO_2 at 37°C. Cells were trypsinized with 0.25% trypsin and sub-cultured in tissue culture plates upon 80% confluence.

2.2.2.4. Determination of lethal dose (LD_{50}) values

Toxicity of polymers was determined by 3-(4,5-dimethylthiazol-2-yl)-2,5-diphenyltetrazolium bromide (MTT) assay. Hep G2 cells were seeded in 96 well plates at the density of 10,000 cells per well and incubated overnight in DMEM with 10% FBS and 1%

antibiotic in humidified atmosphere containing 5% CO_2 at 37 °C. The media was replaced with fresh one containing varying concentration of polymers. After 24 h, media in each well was replaced with 100 µl of MTT reagent (1 mg/mL) and incubated at 37 °C for 2 h. The crystal formed was dissolved in 100 µL of dimethylsulfoxide: Isopropanol (1:1) and absorbance was measured at 570 nm using Tecan Microplate reader. This experiment was done in triplicate. Untreated cells were used as positive control and based on this % of cell viability was calculated. LD_{50} values for different polymers were calculated using Origin Pro software and data were fit into sigmoidal fit using Boltzmann function.

2.2.2.5. Gene expression

HEP G2, HeLa and SK Hep1cells (100,000 cells/well) and Huh 7.5 cells (150,000 cells/ well) were seeded in 24 well plates. Cells were allowed to adhere overnight, and then media was replaced with 10% FBS OMEM containing polyplexes formulated as described above. After 4 h of incubation, they were replaced with fresh serum containing DMEM media and then the cells were further allowed to grow for 48 h. The cells were lysed with Triton X lysis buffer, followed by three freeze-thaw cycle. Transgene expression was determined by analyzing β-galactosidase activity [271]. The transfection efficiency of each polymer was done in triplicate and mean and standard deviation was determined and t-test was performed to determine the significance. Branched PEI was used as positive control and cells without any treatment, as negative control.

2.2.2.6. Toxicity after transfection

Hep G2 cells were seeded in 24 well tissue culture plates and treated with polyplexes in similar ways to transfection condition as described above. After 48 h, media was replaced with

200 µl of MTT reagent (1 mg/mL) per well and incubated at 37°C for 2 h. Medium was removed and dimethylsulfoxide: isopropanol (1:1, v/v, 200 µL) was added to each well and the absorbance was read at 570 nm using TECAN plate reader. This experiment was also performed in triplicate. The untreated cells were used as positive control to calculate the percent of cell viability.

2.2.2.7. Uptake of Polyplexes using confocal microscopy and flow cytometry

Gwiz plasmid was labeled according to the manufacturer protocol. Plasmid (1 µg) was incubated with DNA labeling buffer and Cy3 fluorescent dye at 37 °C for 2 h followed by purification. Cellular uptake of polyplexes was analyzed using Cy3-labelled plasmid via confocal microscopy and flow cytometry. Hep G2 cells were seeded in 6 well tissue culture plates containing glass coverslips overnight. Upon 80% of confluence, media was replaced by OMEM medium containing polyplexes with Cy3 labeled plasmid. Media was removed after 4 h of incubation and washed with PBS buffer at a pH 7.4 thrice, followed by fixation using 3.7% formalin in PBS (pH 7.4). The cells containing slides were fixed on microscope slide and analyzed using a Fluoview FV 10i Olympus confocal microscope. Samples were excited at 550 nm and detected at 570 nm.

For the flow cytometry studies, Hep G2 and SK Hep 1 cells were seeded in 24 well plate (100,000 cells per well) and allowed to adhere overnight. The media was replaced with a media containing polyplexes prepared with Cy3 labeled DNA and incubated for 4 h in triplicate. The cells were rinsed (3X) with PBS, trypsinized and fixed with 3.7% formalin. The uptake of polyplexes was quantified using FACSCaliburMACPro acquisition flow cytometer using FL-2 channel. The untreated cells were used as negative controls.

2.2.2.8. Asialofetuin (ASF) competition assay

Hep G2 cells were seeded onto 24 well plates (100,000 cells/well) and allowed to adhere overnight. Cells were incubated with 500 µl of 1 mg/mL of asialofetuin in fresh media. After 1 h, media was replaced with the media containing polyplexes and incubated. In another group, cells were treated with polyplexes along with 1 mg/mL asialofetuin. After 4 h of incubation, media was replaced with the fresh DMEM media and the cells were allowed to grow for 48 h. β-Galactosidase expressed was determined as described above.

2.3. Results and Discussion

Use of natural cationic polysaccharides as gene delivery vehicles is hindered by their polydisperse nature, and the gene delivery efficacy is dependent on their architecture, size and composition. Therefore, a facile approach to synthesize cationic glycopolymers of well-defined size and flexible architecture (block versus random polymers) with narrow polydispersity is necessary. Recent advances in the field of polymer chemistry have made it possible to produce well-defined and non-toxic cationic polymers with desired molecular weights and compositions, which allow a clearer improved understanding of structure-functionality relationships of non-viral gene delivery vehicles [267, 272-275]. Careful engineering of materials has therefore enabled us to overcome some of the major drawbacks of previously studied vectors leading to major advances in the field of therapeutic gene delivery [271, 276]. Our previous studies demonstrated that gene delivery efficacy, toxicity and DNA binding properties of polymers were affected by the parameters including composition, architecture and molecular weight [263, 271, 276]. In addition, composition of carbohydrate segment was critical which determines the gene delivery efficacy and toxicity of polymer [271].

A library of galactose containing cationic glycopolymers was synthesized via RAFT polymerization. Schemes 1 and 2 illustrate the synthesis of block and statistical cationic glycopolymers. RAFT polymerization approach allows the synthesis of various cationic polymers of controlled dimensions and architecture in the absence of metal catalysis [271, 277, 278]. Several linear and hyperbranched cationic copolymers of block and statistical architecture were synthesized by RAFT and their gene delivery efficacy was evaluated [271, 276].

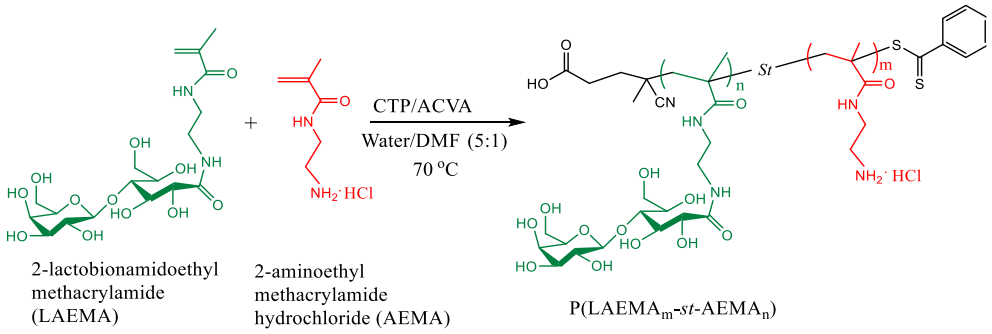

Scheme 1. Synthesis of statistical cationic glycopolymer using 4-cyanopentanoic acid dithiobenzoate (CTP) as chain transfer agent and 4,4' – azobis(4-cyanovaleric acid) (ACVA) as initiator via the RAFT polymerization technique.

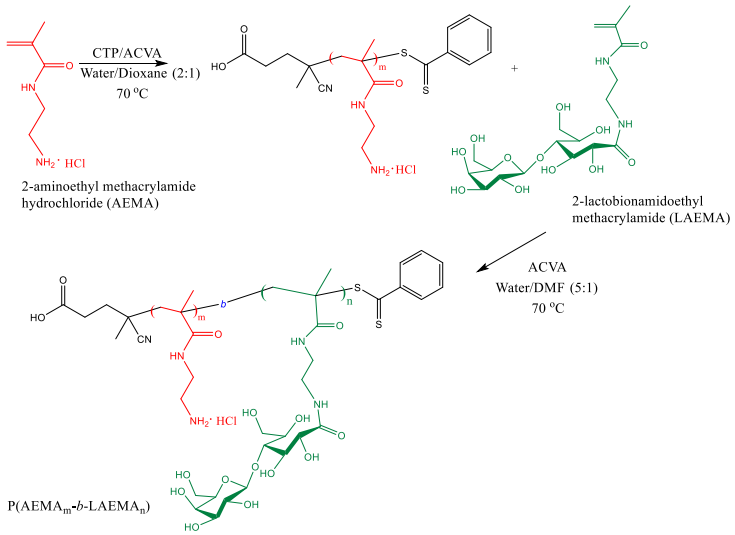

Scheme 2. Synthesis of cationic block glycopolymer using 4-cyanopentanoic acid dithiobenzoate (CTP) as chain transfer agent and 4,4'–azobis(4-cyanovaleric acid) (ACVA) as initiator via RAFT polymerization technique.

A series of cationic homopolymer and copolymer with block and statistical architecture of varying molecular weights and compositions were synthesized by RAFT using 2-lactobionamidoethyl methacrylamide (LAEMA) and 2-aminoethylmethacrylamide (AEMA) as monomers (Scheme 1 and 2). Statistical copolymers of AEMA and LAEMA were synthesized by RAFT polymerization in the presence of CTP and ACVA (Scheme 1). For block copolymer, LAEMA was polymerized in the presence of P(AEMA) macroCTA and ACVA by RAFT polymerization (Scheme 2). The resulting statistical and block polymers were characterized by gel permeation chromatography (GPC) for molecular weights, polydispersities (PDI), and molecular weight was revealed to be between 6.8 to 41 kDa (**Table 2.1**). For comparison, homopolymer of AEMA (M_n = 15 kDa) was synthesized. Furthermore, compositions of polymers were calculated by ^{1}H NMR spectroscopy. **Figure S 2.2** is a representative of ^{1}H NMR spectra of statistical copolymer.

Table 2.1. Molecular weight distribution of polymers and their Lethal Dose 50 (LD_{50}) obtained by MTT assay in HepG2 cells.

Polymer composition	GPC M_n(kDa)	M_w/M_n	LD_{50} (μM)
Homopolymer			
P($AEMA_{90}$)	15	1.3	17.12±1.67
Statistical copolymers			
P($AEMA_{10}$-st-$LAEMA_{11}$)	6.8	1.2	>1470
P($AEMA_{22}$-st-$LAEMA_{22}$)	14	1.2	>714
P($AEMA_{43}$-st-$LAEMA_{42}$)	26	1.5	>384
P($AEMA_{74}$-st-$LAEMA_{62}$)	41	1.3	172±14
P($AEMA_{81}$-st-$LAEMA_{58}$)	41	1.3	56.87±8.29
Block copolymers			
P($AEMA_{17}$-b-$LAEMA_{17}$)	11	1.5	68.85±3.19
P($AEMA_{42}$-b-$LAEMA_{48}$)	30	1.3	94.65±11
P($AEMA_{58}$-b-$LAEMA_{56}$)	36	1.4	84.52±7.094
PEI[a]			2.334±0.57

[a]Commercially available branched polyethyleneimine of M_w~25kDa. Values are mean ± SD (n=3).

In order to investigate the role of polymer size and carbohydrate segment in gene delivery and masking toxicity, molecular weight and carbohydrate content were varied in both statistical and block copolymers (**Table 2.1**). The resulting polymers were studied for their DNA complexation and gene delivery efficacy. Toxicity of polymer plays a crucial role in their use as gene carrier in vivo. Toxicity of polymers were performed by using an MTT assay in Hep G2 cells and lethal dose 50 (LD_{50}) was determined (**Table 2.1**).Toxicity of polymers was found to be dependent on the architecture and carbohydrate content of polymers, which is in accordance with previous reports [271, 279]. As expected, homopolymer, $P(AEMA)_{90}$ is most toxic, and the toxicity decreases as carbohydrate content of polymer increases. Incorporation of carbohydrate residues in the copolymer decreased the toxicity significantly and copolymer with LD_{50} more than 1470 μM was achieved. However, higher molecular weight polymers were found to be more toxic than lower molecular weight polymers despite the presence of carbohydrate moieties. LD_{50} of polymer $P(AEMA_{74}\text{-st-}LAEMA_{62})$ of M_n- 41 kDa was found to be higher than $P(AEMA_{81}\text{-}st\text{-}LAEMA_{58})$ of same molecular weight (172±14 versus 56.87±8.29 respectively) which confirms decrease in toxicity with increasing carbohydrate content. Block copolymers were found to be more toxic than their corresponding statistical copolymers. For example, block copolymer $P(AEMA_{42}\text{-}b\text{-}LAEMA_{48})$ with LD_{50} of 94.65±11 μM is more toxic than $P(AEMA_{43}\text{-}st\text{-}LAEMA_{42})$ with LD_{50} of more than 384 μM in spite of higher content of carbohydrate in first one. Similar trends were observed in our previous study [271]. Increase in the LAEMA content is expected to decrease the net positive charge of the cationic polymer, thus reducing the toxicity. Huang *et al.* also showed increase in toxicity with increasing cationic charge density of *β*-cyclodextrin conjugated poly(amidines) polymers [280]. Furthermore, block copolymers are not that capable to mask the cationic component, which makes them more toxic. This leads to valuable information that toxicity

of polymer depends not only on the type and composition of monomers and molecular weight, but also on the architecture of polymers. As shown in **Table 2.1**, all resulting cationic glycopolymers were less toxic than polyethyleneimine (PEI) (M_w = 25 kDa) which has LD_{50} value of 2.334±0.57 μM in Hep G2. In spite of demonstrating high transfection efficiency, use of PEI as non-viral gene delivery vehicles was compromised due to its toxicity. Hence, resulting galactose based glycopolymers were safer than PEI for in vivo use as gene delivery agents.

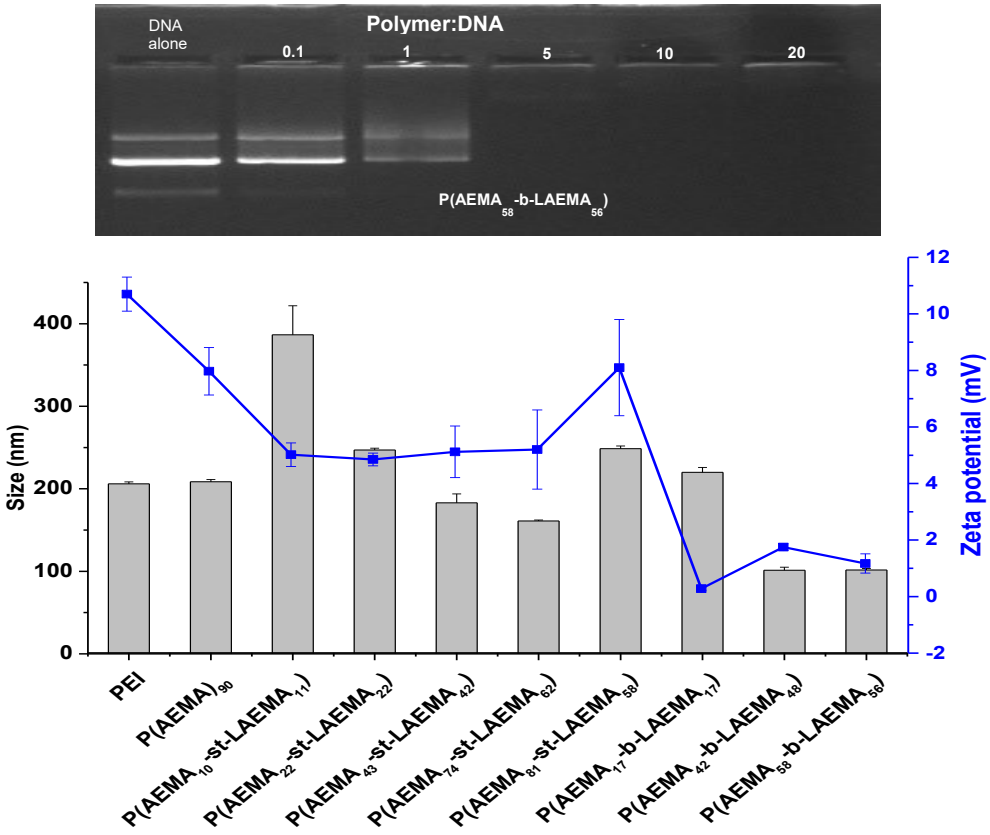

Figure 2.1. Binding of polymers, size and surface charge of complexes. Agarose gel electrophoresis showing complexation of polymer with *β*-galactosidase plasmid (top). Dynamic light scattering (DLS) and zeta potential data for the glycopolymer- *β*-galactosidase plasmid polyplexes (bottom). All samples were at fixed plasmid concentration, while polymer concentrations were varied to obtain stable particles. Polymer to plasmid ratios were similar to that used for transfection.

The polymers produced were complexed with the β-galactosidase plasmid for 30 min at 22 °C, and the sizes and charges of the resulting complexes were determined. Binding of polymer with plasmid was characterized by gel electrophoresis shift assay (**Figure 2.1**). Although gel electrophoresis shift assay showed formation of complexes at very low polymer to plasmid ratio, higher ratios were used to obtain stable and nanometer sized particles which are essential criteria for high transfection efficiency. N/P ratios of the polyplexes used for transfection are listed in supporting information **Table S 2.1**.Net surface charge and size of polyplexes at polymer/plasmid ratio (showing optimum gene expression) were measured. Surface charge of polyplexes varies as a function of sizes, compositions and architectures of polymers. As expected, the surface charge is the highest for the cationic homopolymer based polyplexes and is lower for the copolymer based polyplexes (**Figure 2.1**). Net surface charge of statistical copolymer-based polyplexes is higher than that of the block copolymer-based polyplexes, which proves the higher binding efficiency of the block copolymers and is in accordance with previous study [271]. In addition, polyplexes with block copolymers contain most of the condensed DNA in the core displaying higher carbohydrate content on the shell, contributing to a reduction in net positive charge on the polyplexes surface. Therefore, zeta potentials of block copolymer based polyplexes were found to be close to zero. In contrast, for polyplexes made with statistical copolymers, there is an equal possibility of displaying carbohydrate and cationic segment on the surface displaying net positive charge on the surfaces.

Polyplexes with different polymers showed size between 100 to 400 nm with net positive zeta potential values (**Figure 1.1**). In general, size of polyplexes decreases with increasing molecular weight of polymers, and the size of block copolymer based polyplexes were found to be smaller than their corresponding statistical copolymers (**Figure 2.**1). These results are in

agreement with the previous report where effects of carbohydrate compositions and architectures of copolymers on size, charge and transfection efficiencies were studied [271]. As compared to statistical copolymers, block copolymers may condense DNA more efficiently in their core resulting in smaller size complexes.

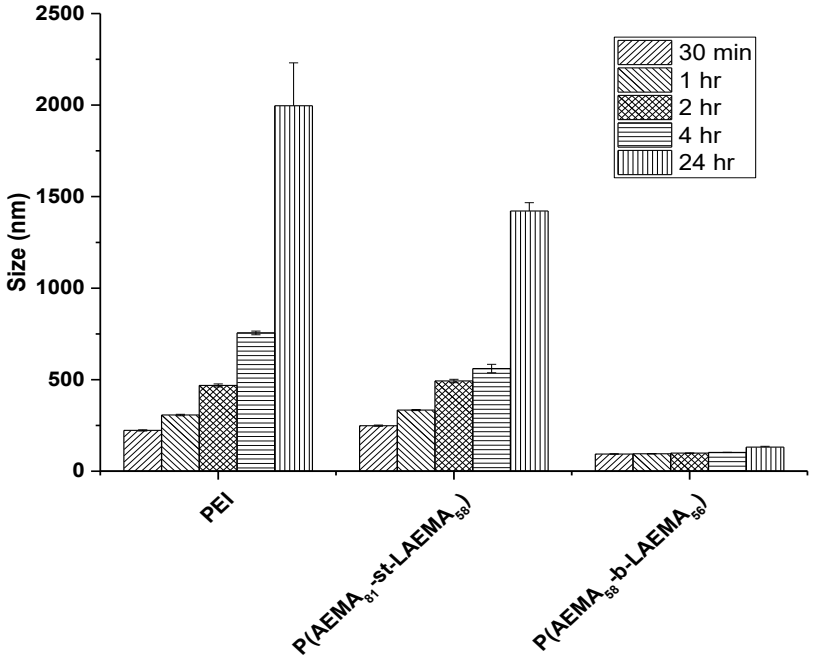

Figure 2.2: DLS analysis of the time dependent aggregation of polyplexes in media.

In addition, these polyplexes were much more stable than polyplexes derived from statistical copolymers. Size of polyplexes obtained from statistical copolymer, P(AEMA$_{81}$-*st*-LAEMA$_{58}$) and PEI increased up to micron size with time. However, polyplexes with block copolymer P(AEMA$_{58}$-*b*-LAEMA$_{56}$) were very stable and the size did not change over time **(Figure 2.2**). Size of polyplexes with all statistical copolymers increased after incubation in media at 22 °C for 2 h whereas polyplexes with block copolymer remained stable under similar condition (supporting **figure S 2.1**). Higher positive surface charge of statistical copolymer resulted in aggregation of polyplexes. For the block copolymers, the dense carbohydrate shells seem to play a major role in the stability of those polyplexes.

Modification of cationic polymers with various biocompatible moieties without affecting gene delivery efficacy has been reported [281-285]. For example, derivatization with polyethyleneglycol (PEGylation) is one the most common approaches for this purpose. PEGylation of cationic polymers is known to solve the problem of cytotoxicity, aggregation and non-specific protein binding *in vivo* [282, 286]. Several carbohydrates such as β-cyclodextrin and chitosan had been used for gene delivery purposes [281]. Furthermore, various polysaccharide backbones were modified with different cationic polymers to produce less toxic carbohydrate-based gene delivery vehicles with enhanced transfection efficiencies. Modifying backbones of arabinogalactan, dextran and pullulan with PEI, spermine or other cationic polymers has demonstrated that charge ratio and the nature of carbohydrate moiety play a major role in gene delivery efficacy. Linear and branched PEIs grafted with β-cyclodextrin showed reduced transfection efficiency and lower cytotoxicity along with increasing grafting density [287]. In addition to lower toxicity of cationic polymer, carbohydrate molecules can also be used as ligands for specific receptors. Lactose and galactose, for instance, were conjugated to the polymeric carrier for targeting specifically ASGPR of hepatocytes [288, 289]. There is still needed to discuss the effects of architecture and composition of carbohydrate on ASGPR mediated gene delivery into hepatocytes. The resulting polymers contain galactose as a pendant making it accessible for interaction with ASGPR of hepatocytes even when complexed with DNA. Hence gene delivery efficacy of these polymers was determined using β-galactosidase plasmid in ASGPR rich (HepG2 and Huh 7.5 cells) and ASGPR deficient (SK hep1 and HeLa cells) cells.

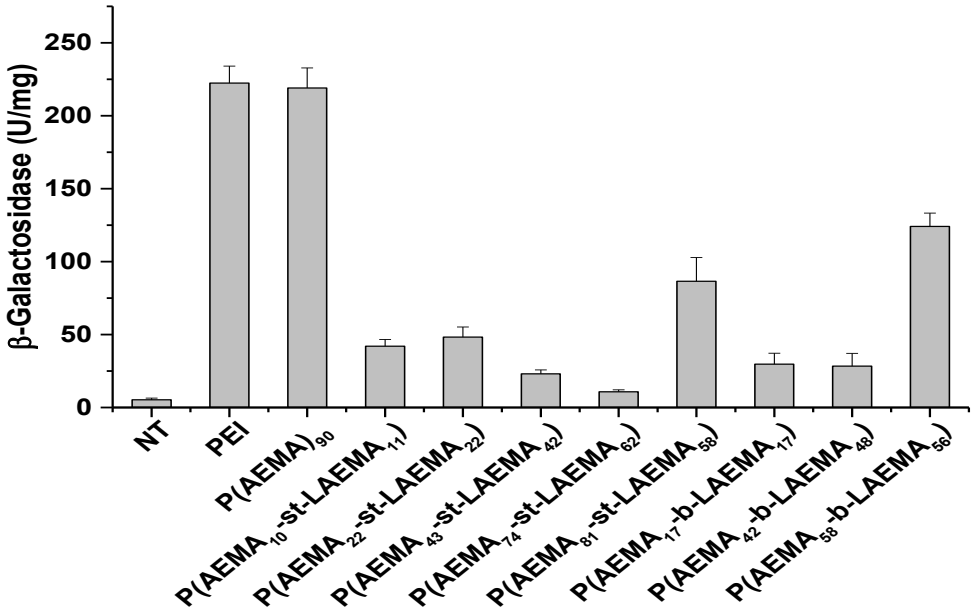

Figure 2.3. *β*-galactosidase activity after delivery of *β*-galactosidase plasmid by glycopolymers in Hep G2 cells in presence of 10% FBS. DNA amount is fixed to 1.2 μg in all experiments. Each value represents mean ± SD (n=3).

ASGPR is a c-type lectin whose main function is to remove desialylated serum proteins such as fibronectin [290]. ASGPR has carbohydrate recognition domain which can bind at least a single-terminal galactose or galactosamine residues and binding affinity increases with valence of sugar residues via phenomenon called cluster effect [291]. In both HepG2 and Huh7.5 cells, *β*-galactosidase plasmid transfection was found to be dependent on sizes, architectures and compositions of polymer (**Figure 2.3 -2.4**). Homopolymer, P(AEMA)$_{90}$, demonstrated the highest transfection which is equal or comparable to branched PEI (M_w=25kDa) at given plasmid dose. It should be noted that P(AEMA)$_{90}$ had higher LD_{50} values than branched PEI, however, it remained toxic to cells. Incorporation of carbohydrate units greatly decreased toxicity as well as transfection. As reported in a previous study [271], transfection efficiency of higher molecular weight polymer was higher than the corresponding lower molecular weight counterpart. For statistical copolymer, transfection efficiency is enhanced with increase in the cationic moieties. For example,

P(AEMA$_{81}$-*st*-LAEMA$_{58}$) expressed higher transfection than P(AEMA$_{74}$-*st*-LAEMA$_{62}$) although both of them have same molar masses. Similarly, block copolymer of higher molecular weight, P(AEMA$_{58}$-*b*-LAEMA$_{56}$) had high transfection efficiency than low molecular weight polymer P(AEMA$_{17}$-*b*-LAEMA$_{17}$). Like statistical copolymer, block copolymer having more cationic moiety P(AEMA$_{58}$-*b*-LAEMA$_{56}$) gave high transfection efficiency than copolymer having less cationic moiety P(AEMA$_{42}$-*b*-LAEMA$_{48}$) although molecular weight of them are very close and polyplexes of them are similar in terms of size and charge. This result emphasizes the importance of appropriate molecular weight and ratio between cationic and glucose monomer for efficient transfection. Block copolymer, P(AEMA$_{58}$-*b*-LAEMA$_{56}$) has higher transfection efficiency than the corresponding statistical copolymer of similar masses. It should be noted that block copolymer P(AEMA$_{58}$-*b*-LAEMA$_{56}$) showed greater transfection efficiency although it's polyplexes with plasmid had surface charge close to zero. Both HepG2 and Huh 7.5 cells are hepatocytes expressing ASGPR on their surface. Complexes with block copolymer contain galactose on outer shell that facilitates ASGPR mediated uptake of these particles. ASGPR can recognize and internalize the galactose terminal through receptor mediated endocytosis (see Scheme 3). ASGPR are present only on surface of mammalian hepatocytes.

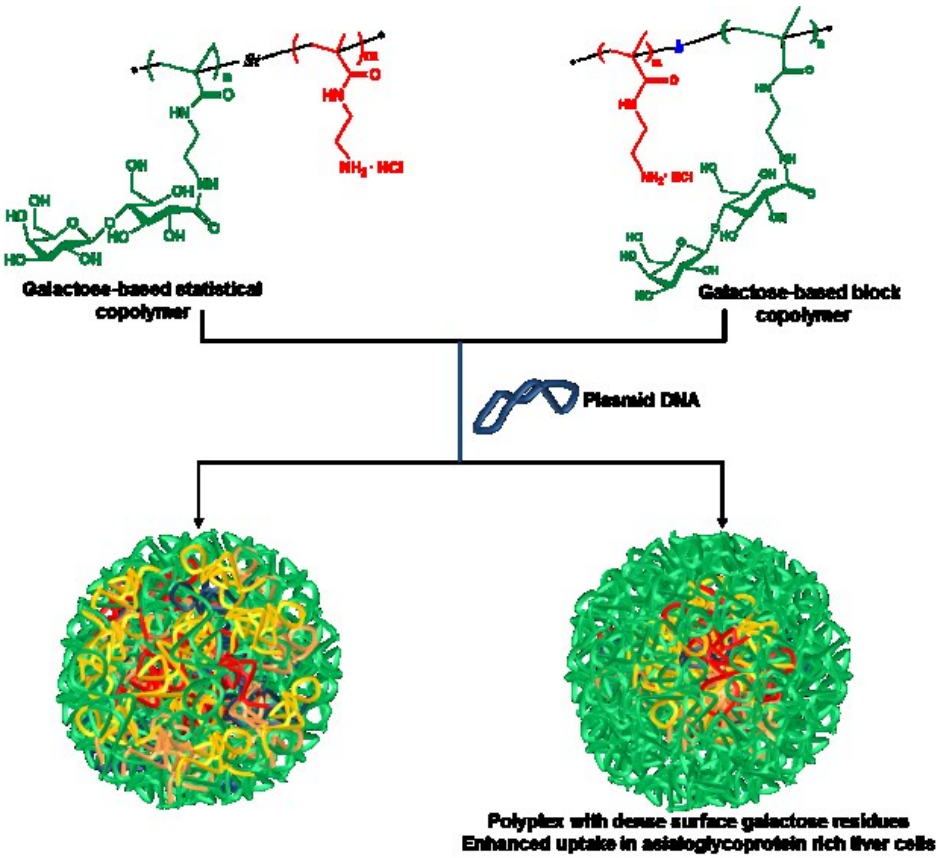

Scheme 3: Complexation of β-galactosidase plasmid with galactose based statistical and block copolymers. Block copolymer based polyplexes displaying higher surface galactose residues accounting for the enhanced uptake in asialoglycoprotein rich liver cells.

Furthermore, transfection efficiency of both statistical and block copolymers in HeLa cells and SK hep1 cells was negligible whereas PEI and $AEMA_{90}$ still exhibited high transfection in those cell lines (**Figure 2.5**). It is worth mentioning that HeLa and SK hep1 cells do not express ASGPRs on their surface. Although SK hep 1 is hepatocytes, ASGPR is absent on their surface and HeLa cell is derived from cervical cancer. Gene delivery efficacy of all polymers in HeLa cell is lower than in Hep G2 cells. Although PEI and $P(AEMA)_{90}$ showed some transfection, the efficiencies of block and statistical copolymers were insignificant.

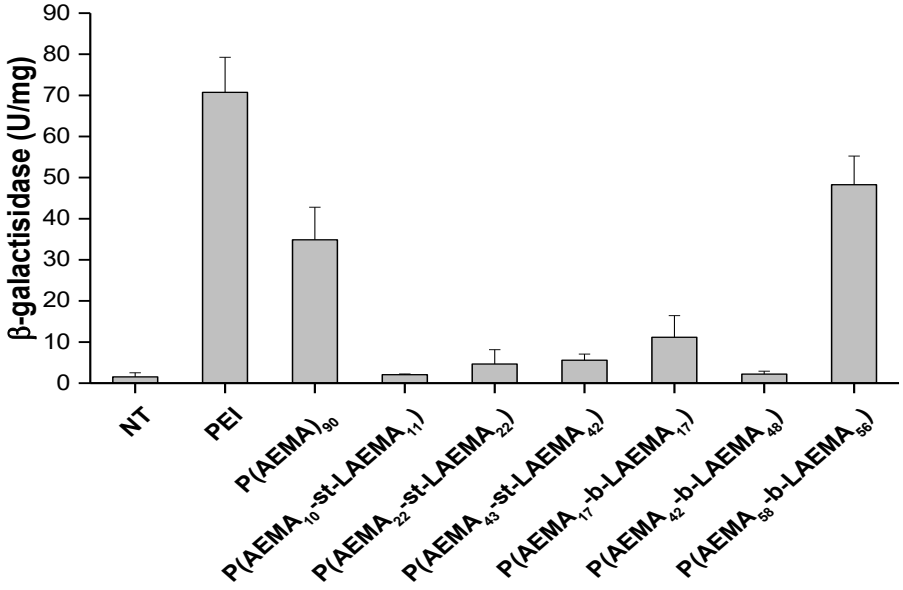

Figure 2.4. *β*-galactosidase activity after delivery of *β*-galactosidase plasmid by glycopolymers in Huh7.5 cells in presence of serum. Transfection was evaluated by *β*-galactosidase assay. DNA amount is fixed to 1.2 μg per well of 24 well plate in all experiments. Each value represents mean ± SD (n=3).

Uptake of polyplexes with PEI and $P(AEMA)_{90}$ may be driven by electrostatic interaction between polyplexes and cell membrane, therefore transfection efficiency is not hepatocytes specific. However, transfection efficiencies of block and statistical copolymers were negligible in HeLa cells which confirm that gene delivery efficacy of galactose containing statistical and block copolymer is hepatocytes specific. This observation is in support of finding by Wang *et al.*, where glycosylated poly (ethylene glycol) derivative-graft-polyethyleneimine exhibited reduced transfection in HeLa cells as compared to Hep G2 cells [292]. Importantly, transfection efficiency of block and statistical copolymer was significantly reduced while efficiency of PEI and $P(AEMA)_{90}$ remains intact in SK hep 1 cells. This proves ASGPR specificity of block and statistical copolymer for gene delivery. Polyplexes with $P(AEMA_{81}$-*st*-$LAEMA_{58})$ showed transfection in SK hep 1 cell to some extent which may be driven by its net positive charge. Gene

delivery efficiency of P(AEMA$_{58}$-*b*-LAEMA$_{56}$) which was highest among glycopolymer in both ASGPR expressing hepatocytes Hep G2 and Huh 7.5 cells was insignificant in ASGPR deficient hepatocyte SK hep 1 cells. Since net surface charge of polyplexes with P(AEMA$_{58}$-*b*-LAEMA$_{56}$) is near to neutral, electrostatic interaction may not be enough for uptake and ASGPR mediated endocytosis is not available in SK hep 1 cells. Hence P(AEMA$_{58}$-*b*-LAEMA$_{56}$) was unable to transfect SK hep 1 cells. These results suggested galactose containing copolymer promotes specific delivery of gene into hepatocytes which express ASGPR on surface.

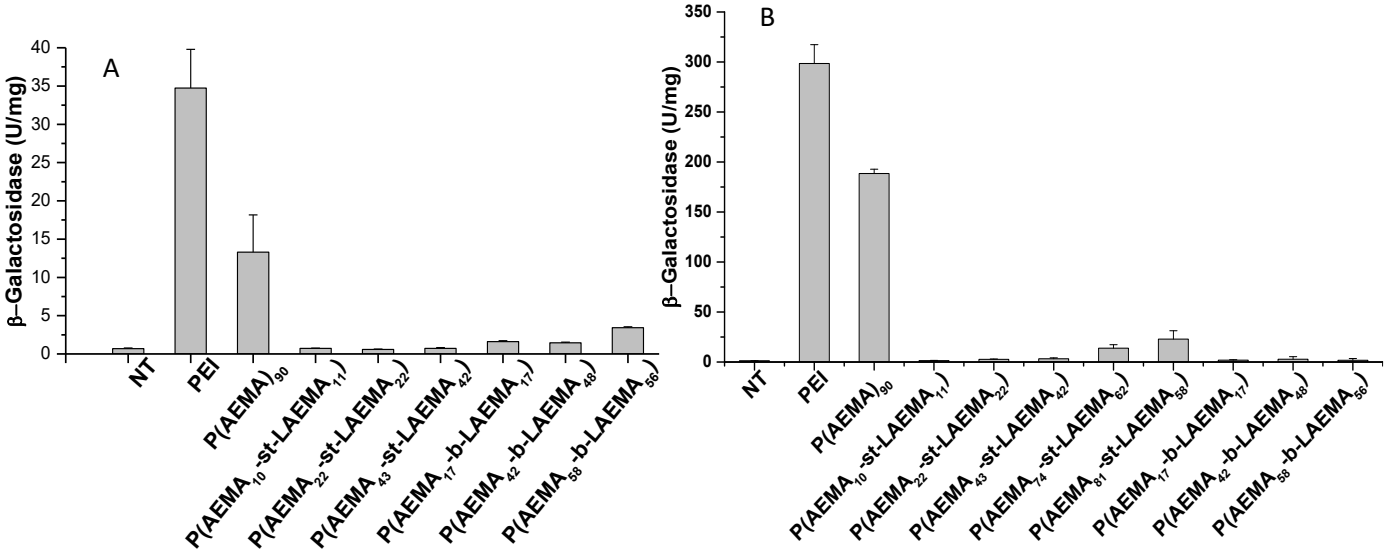

Figure 2.5. *β*-galactosidase activity after delivery of *β*-galactosidase plasmid by glycopolymers in HeLa (A) and SK hep 1 (B) cells. DNA amount is fixed to 1.2 µg in all experiments. Each value represents mean ± SD (n=3).

To further confirm that galactose based polyplexes were recognized by ASGPR of Hep G2 cells, competitive assay of transfection and uptake of polyplexes in presence of free asialofetuin was performed. Recognition and binding to ASGPR facilitate the receptor mediated endocytosis. Hep G2 cells were pretreated with asialofetuin for 1 h prior to treatment or together with polyplexes. Transfection efficiency of PEI and homopolymer remains same regardless of the presence of asialofetuin. In the case of block copolymer P(AEMA$_{58}$-*b*-LAEMA$_{56}$), transfection

efficiency was greatly reduced in presence of asialofetuin (**Figure 2.6**). Decrease in transfection is more pronounced when complexes and asialofetuin were treated together. This may be due to the high competition between asialofetuin and polyplexes towards ASGPR. In case of 1 hour pretreated with asialofetuin, ASGPR may internalize a portion of asialofetuin followed by recycle of ASGPR on surface of HepG2 cells. Nevertheless, a significance portion of ASGPR may be blocked by asialofetuin resulting in reduced transfection.

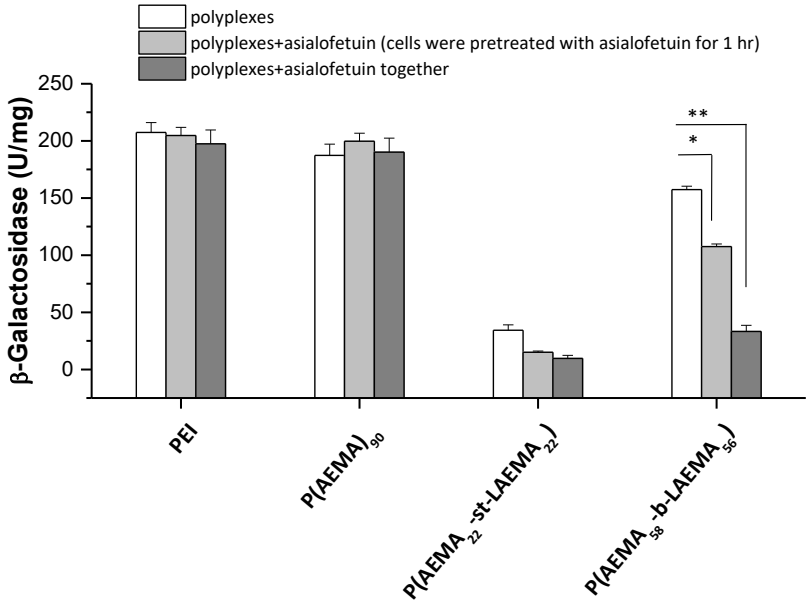

Figure 2.6. Effects of the presence of asialofetuin on transfection efficacy of polymers in their optimal polymer/DNA ratio in HepG2 cells. Asialofetuin was added to Hep G2 cells 1 hr prior treatment with polyplexes or together with polyplexes. DNA amount is fixed to 1.2 μg in all experiments. Each value represents mean ± SD (n=3). Statistical analysis was performed by analysis of variance. *($p < 0.003$) and **($p < 0.0005$) indicates significant difference when compared to polyplexes only.

However, asialofetuin treatment did not inhibit the transfection completely, which may be due to higher avidity of multiple galactose molecules on the surface to polyplexes. Lee *et al.* has demonstrated that binding affinity to ASGPR can be increased by multiple galactose molecules by so called cluster effect in which distance between galactose residues must be 15-25 Å [291].

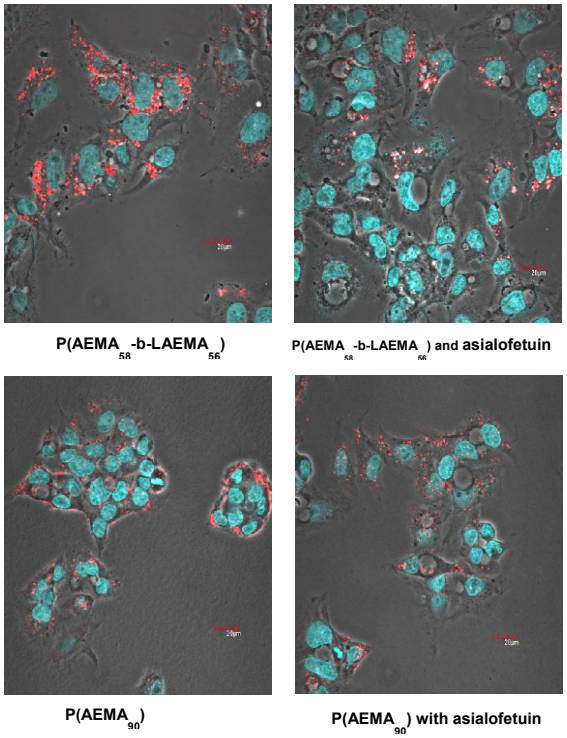

Figure 2.7. Study of polyplexes uptake in the presence and absence of asialofetuin using confocal microscope in Hep G2 cells. Upper images represent the uptake of Cy3-labelled plasmid using glycosylated block copolymer P(AEMA$_{58}$-*b*-LAEMA$_{56}$) and lower images using P(AEMA)$_{90}$ in absence and presence of asialofetuin.

In order to achieve gene expression, several barriers notably cellular uptake, endosomal escape and nuclear uptake must be overcome as any of these can significantly impact the transfection efficacy. In our design, uptake of polyplexes is mediated by the ASGPR which recognizes galactose residues of the copolymers and internalize them via receptor mediated endocytosis. Hence, changes in amount of ASGPR on cell surface will greatly affect the transfection efficiency. Here, we investigated the uptake of polyplexes containing Cy3-labeled plasmid using confocal microscopy and flow cytometer in the presence and absence of asialofetuin. Hep G2 cells were first treated with asialofetuin for 1 h followed by the addition of the polyplexes. Homopolymer P(AEMA)$_{90}$ showed similar extent of uptake regardless of pre-

treatment with asialofetuin. As expected, uptake of polyplexes with block copolymer P(AEMA$_{58}$-*b*-LAEMA$_{56}$) decreased significantly in the presence of asialofetuin (**Figure 2.7**).

ASGPR-mediated uptake of polyplexes with galactosylated copolymers in Hep G2 and SK Hep 1 cells was further confirmed by flow cytometry. Uptake of Cy3 labelled plasmid using homopolymer, statistical and block copolymer were studied in presence and absence of asialofetuin SK Hep1 cells and HepG2 cells. Flow cytometer analysis of percentage of positive cells supports observation that asialofetuin competitively inhibit uptake of polyplexes with galactose containing copolymers which supports observation from confocal microscopy images (**Figure 2.7**). Hep G2 cells were treated with free asialofetuin for 1 h followed by treatment with polyplexes of Cy3 labelled plasmid and polymers. Uptake of polyplexes was evaluated in terms of percentage of positive cell population by flow cytometry in FL2 channel. Positive cell population percentage was significantly reduced when treated with polyplexes with P(AEMA$_{58}$-*b*-LAEMA$_{56}$) and P(AEMA$_{43}$-*st*-LAEMA$_{42}$in presence of asialofetuin **(Figure 2.8**). On the other hand, asialofetuin treatment did not affect positive cell population when using PEI and homopolymer AEMA$_{90}$. Hence, uptake of polyplexes was found to be dependent on the ASGPR located on the surface of hepatocytes, which enables hepatocytes-specific targeting features in these copolymers. In HepG2 cells, although uptake of P(AEMA$_{43}$-*st*-LAEMA$_{42}$) is higher than of P(AEMA$_{58}$-*b*-LAEMA$_{56}$), transfection efficiency is low.

Although cellular uptake of polyplexes is first step, it may not be enough for successful transfection. Fate of internalized polyplexes will depend on their intracellular routing which determines transfection efficiency. Route of internalization depends on the type of delivery systems. In general, complexes bound to cell surface receptor enter cells via clarithrin mediated endocytosis and cationic complexes without any targeting ligands is guided through electrostatic

interaction with anionic cell surface, proteoglycans and pulled into cells via phagocytosis [90, 293]. According to Goncalvel et al., although polymer and plasmid polyplexes enter into Hep G2 cells via both clathrin dependent and independent pathways, clathrin dependent pathways is most productive for efficient gene transfection in Hep G2 cells [294].

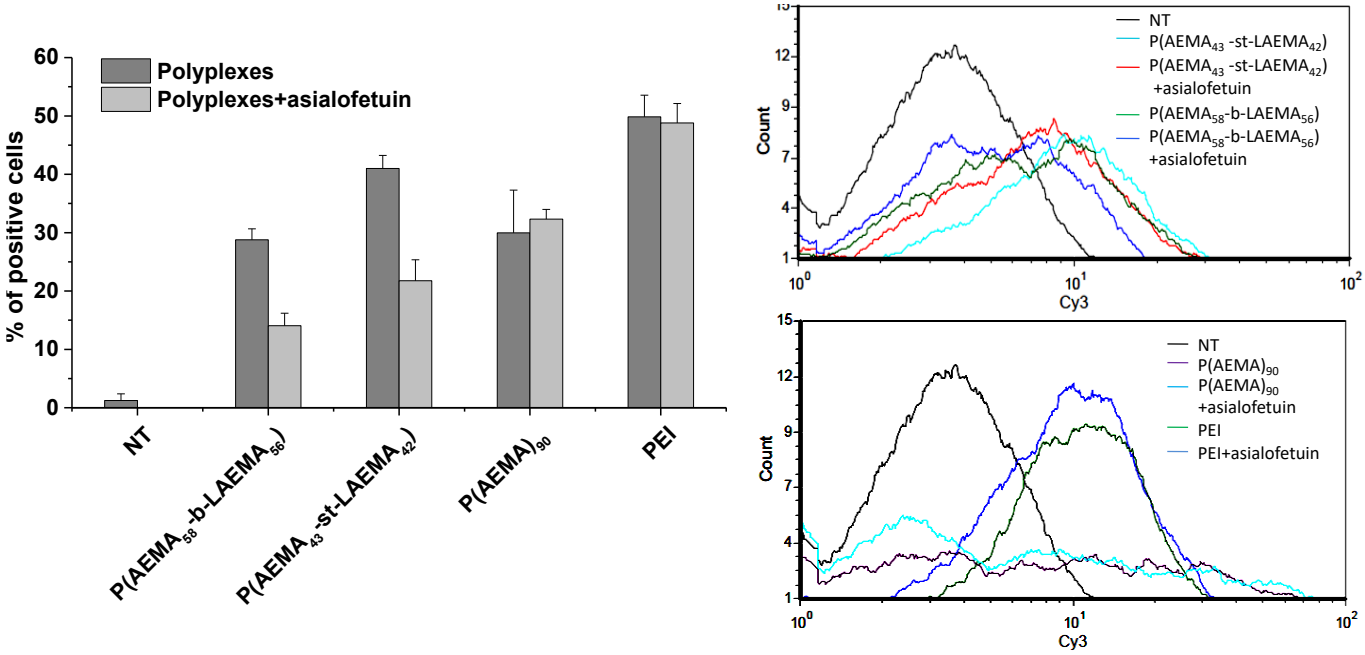

Figure 2.8. Uptake of polyplexes in the presence and absence of asialofetuin using flow cytometer in Hep G2 cells. For competitive assay, cells were incubated with asialofetuin for 1 h prior to adding polyplexes. Each value represents mean ± SD (n=3).

Surface charge of polyplexes with block copolymer P(AEMA$_{58}$-*b*-LAEMA$_{56}$) is close to neutral whereas with statistical copolymer P(AEMA$_{43}$-*st*-LAEMA$_{42}$) is positive. So, uptake of polyplexes with P(AEMA$_{58}$-*b*-LAEMA$_{56}$) is mainly via ASGPR mediated clathrin dependent pathways. Besides ASGPR mediated endocytosis, polyplexes with statistical copolymer can enter cell via nonspecific manner because of its net positive charge. Since clathrin dependent pathway is most effective for gene transfection in Hep G2 cells, P(AEMA$_{43}$-*st*-LAEMA$_{42}$) have lower transfection than P(AEMA$_{58}$-*b*-LAEMA$_{56}$) in spite of higher uptake. Another reason for lower

transfection efficiency of P(AEMA$_{43}$-*st*-LAEMA$_{42}$) in spite of high uptake may be due to its limited escape from endosomes. Nevertheless, precise role of architecture of polymer in gene transfection requires further investigation. Moreover, uptake of complexes with statistical and block copolymer was negligible as compared to homopolymer, P(AEMA)$_{90,}$ and PEI in SK Hep 1 cells (**Figure 2.9**) confirming the specificity of these copolymer towards ASGPR-expressing hepatocytes. Hence inability of block and statistical copolymer for transfection in SK Hep 1 cells (**Figure 2.5**) is because of insufficient uptake (**Figure 2.9**). These findings suggested that galactose moieties of the polymer are exposed on the surface of the polyplexes irrespective to the complexation with DNA, and can bind to the ASGPR of hepatocytes. This result also supports reduction of transfection in presence of asialofetuin (**Figure 2.6**) and confocal microscope image (**Figure 2.7**).

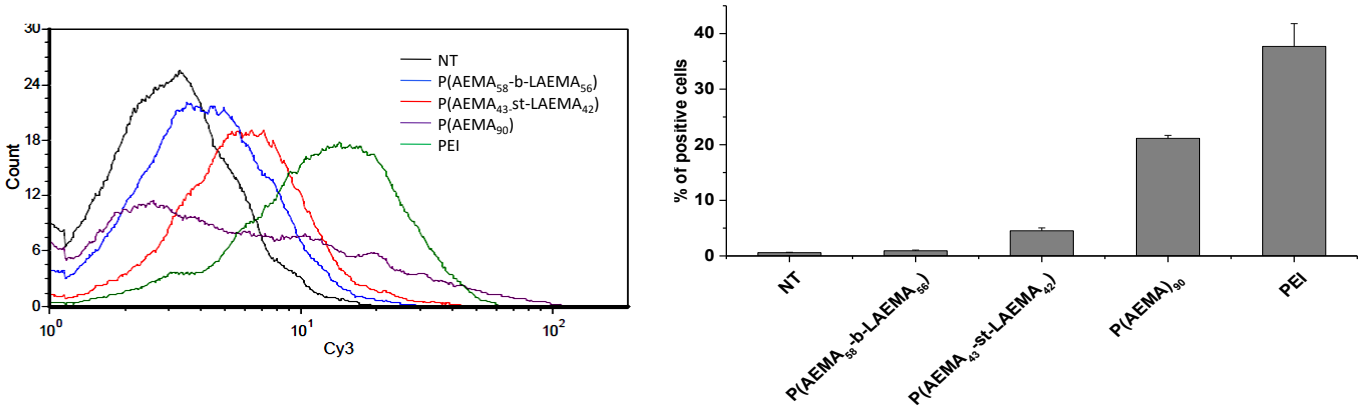

Figure 2.9. Flow cytometry analysis of uptake of polyplexes in SK hep 1. Cells were treated with the polyplexes of Cy3 labelled plasmid and polymers and uptake was quantitatively evaluated Histogram of SK hep 1 cells (top) and percentage of positive population (bottom) after incubation with polyplexes. Each value represents mean ± SD (n=3).

Several galactose-modified cationic lipids and polymers as non-viral vehicles for delivering hepatocytes-specific gene have been developed. ASGPR mediated endocytosis is central to the specificity of these vehicles towards hepatocytes. ASGPR is a c-type lectin whose main role is clearance of desialylated serum proteins, such as fibronectin [290] and all IgA2

allotypes [295]. ASGPR has carbohydrate recognition domain which can bind galactose or galactosamine residues, and affinity of ligands increases with the valance of sugar residues due to so called 'cluster effect' [291, 296]. Cluster effect depends on the distance between galactose residues and the optimum distance was 15-25Å [291, 297]. In this study, galactose containing block copolymer P(AEMA$_{58}$-*b*-LAEMA$_{56}$) showed high transfection efficiency into hepatoma cells **(Figures 2.3** and **2.4**). Moreover, observations of cellular uptake and effects of ASGPR on uptake (**Figures 2.7** and **2.8**) indicate that the galactose residues are exposed on the surface of polyplexes and the distances between residues are optimal.

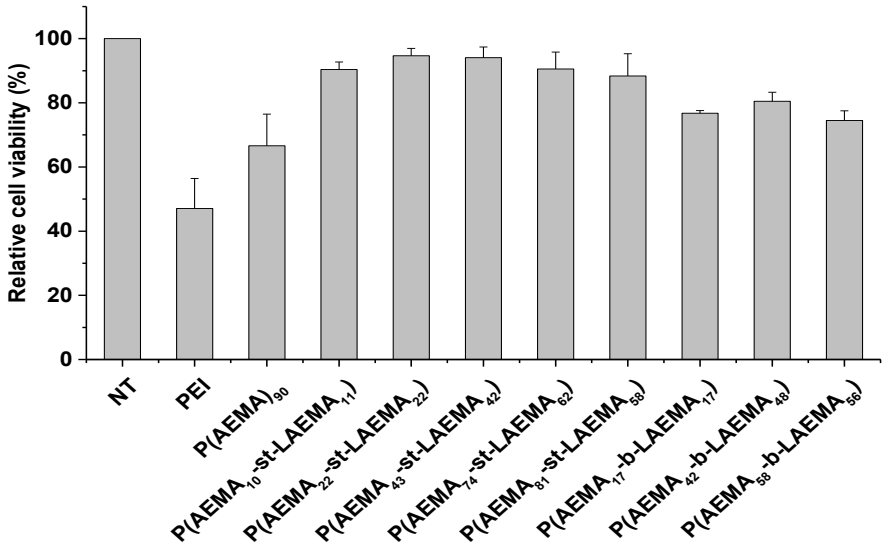

Figure 2.10. Post-transfection toxicity of polymer-based polyplexes at various polymers to plasmid ratios as measured by MTT assay in Hep G2 cells. Polymer to plasmid ratio and plasmid amount used for each polymer is similar to that used for transfection.

Post transfection toxicity assays of polyplexes revealed that PEI and cationic homopolymer exhibits strong cytotoxicity due to their higher positive charge density on their surfaces. However, both statistical and block glycopolymers were found to be non-toxic exhibiting more than 80% cell viability. Considering cytotoxicity, hepatocellular specificity and transfection efficiency, these galactose-based block copolymers are superior for gene delivery in hepatocytes.

2.4. Conclusions

We have synthesized novel cationic galactosylated glycopolymers for specific gene delivery to hepatocytes. In both HepG2 and Huh 7.5 cells, galactose containing block copolymer P($AEMA_{58}$-*b*-$LAEMA_{56}$) showed the highest transfection efficiency which is driven by the strong interactions of the galactose residues of the polyplexes with the over-expressed ASGPR of hepatocytes. The block copolymer architectures ensure a relatively high density of galactose residues on the surface in addition to increasing the stability of the polyplexes and hence making the system highly effective for gene delivery to hepatocytes. Due to the high stability of those block copolymer-based systems, they are suitable for *in vivo* application. Attenuation in transfection and uptake of galactose containing copolymer in the presence of asialofetuin confirm the hepatocytes selectivity of polymer. In addition, transfection efficiency of these polymers in ASGPR deficient cells is negligible. Finally, these glycopolymers are non-toxic and therefore are attractive for liver targeting gene delivery system. *In vivo* gene delivery efficacy of these polymers into liver is planned.

2.5. Acknowledgement

The authors gratefully acknowledge financial support from Alberta Innovates Health Solutions CRIO Program grant (AIHS 201201164, PK), the Natural Sciences and Engineering Research Council of Canada (NSERC), Discovery Grant program grant (RN, HZ) and Canadian Foundation for Innovation (CFI).

Chapter 3

Small Hydrophobe Substitution on Polyethylenimine for Plasmid DNA Delivery: Optimal Substitution is Critical for Effective Delivery

A version of this chapter was published in:

Bindu Thapa, Samarwadee Plianwong, Brad Rutherford, Remant Bahadur KC, Hasan Uludag, "Small Hydrophobe Substitution on Polyethylenimine for Plasmid DNA Delivery: Optimal Substitution is Critical for Effective Delivery", *Acta Biomaterialia*, 2016, 33, 213-224.

3.1. Introduction

Improved delivery systems are needed for intracellular delivery of difficult-to-deliver biologics such as polynucleotides. Cationic polymers have been developed as non-viral gene delivery agents due to their advantage of being safe, reproducible, and allowing facile chemistry for functionalization, as compared to their viral counterparts [249, 298, 299]. Cationic polymers can complex with anionic plasmid DNA (pDNA) via electrostatic interactions, and condense them into compact and nano-sized polyplexes, which provide sufficient protection from extracellular nucleases and enable effective cellular uptake [300]. To date, the clinical application of cationic polymers has been hampered by their low transfection efficiency and undesirable toxicity. In order to address this issue, cationic polymers have been modified with various substituents to improve gene delivery efficacy and compatibility [102, 301, 302]. Hydrophobic modification of cationic polymers with long lipid chains has been a common approach since grafted hydrophobic lipids improve the compatibility of condensed DNA polyplexes with cellular membranes and facilitate the endocytosis of the polyplexes [303]. Palmitic acid substitution on poly-L-Lysine (PLL), for example, has shown higher binding efficiency to pDNA and resulted in enhanced gene transfection as compared to unmodified PLL [304].

Among the cationic polymers, polyethylenimine (PEI) based polymers have become well-established for both *in vitro* and *in vivo* applications [281, 305]. PEIs display strong buffering property at acidic pH to escape endosomes via a process called 'proton sponge' activity [306]. Presence of abundant primary, secondary and tertiary amine groups makes it also possible to undertake hydrophobic modifications, while preserving its buffering capacity. While high molecular weight (MW) PEIs, and in particular branched 25 kDa PEI (25PEI), have emerged as broadly active gene delivery agents, they can cause severe cellular and systemic toxicities due to

high cationic charge density that destabilizes plasma and mitochondrial membranes [307]. Employing lower MW forms of PEI for gene delivery, on the other hand, is advantageous because of their low toxicities; these polymers display less interaction with plasma membranes and can be readily eliminated from the circulation *in vivo* [102, 308, 309]. Unfortunately, low MW PEIs are not also effective for gene delivery [102, 310], but it is possible to chemically functionalize them with hydrophobic groups to improve their efficiency [102, 311, 312]. Modification of 0.4 kDa linear PEI with cholesterol improved transgene expression when the modified polymer were formulated as a liposome [313]. Similarly, cholesterol-substituted 1.8 kDa PEI was a superior gene delivery agent than the native polymer [103]. Besides this multicyclic steroid, 1.8 kDa PEI were modified with long-chain dodecyl and hexadecyl moieties with significantly improved gene delivery results [104]. We also reported hydrophobic modification of low MW PEIs with aliphatic lipids of variable chain lengths and demonstrated improved gene delivery efficacy in different cell lines including primary cells [102, 314]. Among the lipids, unsaturated linoleic (C18) acid was found to be a superior lipid substituent for pDNA delivery [102]. However, hydrophobic modification of PEI and PEI-like polymers with long aliphatic chains and bulky multicyclic groups do not allow good control over grafting efficiency. Beyond a critical grafting amount, polymers become insoluble in aqueous systems and grafting efficiency is not well controlled due to bulky lipid substituents. Undertaking modification with smaller hydrophobic moieties may be advantageous in these aspects, but no information exists about using small hydrophobic moieties to convert low MW PEI into an effective transfection agent.

This study was designed to investigate the potential of a particular short chain hydrophobe, namely propionic acid (PrA), for grafting onto 1.2 kDa PEI (1.2PEI) in order to improve its pDNA delivery efficiency. Delivery of pDNA was explored in two models of breast cancer cells (MDA-

MB-231 and MCF-7 cells), due to urgent need to explore alternative treatments for cancer therapy. Since an optimal balance between the cationic charge (i.e., buffering capacity and pDNA binding) and hydrophobicity (i.e., cell membrane compatibility) is critical for enhanced cellular uptake and unpacking of complexes, extent of PrA substitution on PEI was varied, and physiochemical characteristics and transfection efficiency of the resultant polyplexes were investigated. Our goal was to convert the relatively non-toxic but ineffective polymer onto an effective pDNA delivery agent.

3.2. Materials and Methods

3.2.1. Materials

The 1.2PEI (M_n:1.1 kDa, M_w:1.2 kDa), 2PEI (2PEI; M_n: 1.8 kDa, M_w :2 kDa), 25PEI (M_n: 10 kDa, M_w: 25 kDa), dimethyl sulfoxide (DMSO), PrA, 1-ethyl-3-(3-dimethylaminopropyl) carbodiimide (EDC), N-hydroxysuccinimide (NHS), N,N-dimethyl-formamide (DMF), linoleyl chloride, chloroform ($CHCl_3$), methanol (MeOH) and diethylether, trypsin/EDTA solution, 3-(4,5-dimethylthiazol-2-yl)-2,5-diphenyltetrazolium bromide (MTT) were obtained from Sigma-Aldrich (St. Louis, MO). Hank's balanced salt solution (HBSS with phenol red) was purchased from Lonza (Walkersville, MD). Dulbecco's Modified Eagle's Medium (DMEM; low glucose with L-glutamine) and penicillin/streptomycin (10,000 U/ml and 10,000 µg/ml) solution were purchased from Life Technologies (Grand Island, NY). Fetal bovine serum (FBS) was from VWR (PAA, Ontario, Canada). Clear HBSS (phenol red free) was prepared in-house. UltraPure™ agarose was purchased from Invitrogen (Carlsbad, CA). The gWIZ and gWIZ-GFP plasmids were purchased from Aldevron (Fargo, ND). The scrambled control siRNA (C-siRNA) and FAM-siRNA was obtained from Ambion (Austin, TX).

3.2.2. Polymer Synthesis and Characterization

Hydrophobic modification of 1.2PEI and 2PEI using PrA was performed via *N*-acylation (**Figure 3.1A**). Briefly, PrA (3.34 mM in $CHCl_3$) was activated with EDC (5 mM in $CHCl_3$) for 30 min and then with NHS (5 mM in MeOH) at room temperature. The activated PrA solution was added dropwise to 1.2PEI or 2PEI solutions (3.34 mM in $CHCl_3$) under stirring and left stirring over night at room temperature. The crude product of PrA-grafted PEI (PEI-PrA) was precipitated (3X) in ice-cold diethylether and dried under vacuum for 48 hr. To prepare a lipid-substituted 1.2PEI, *N*-acylation of 1.2PEI was performed with the linoleyl chloride according to previously described procedure [102]. Briefly, linoleyl chloride was dissolved in DMF and added to 100 mg of PEI solution in 1 ml of DMSO. This mixture was allowed to react for 24 h at room temperature under nitrogen. Polymer was recovered by precipitating with excess of ethyl ether, and freeze dried. The composition of PEI-PrA and PEI-LAs (i.e., number of PrA/LA groups per 1.2PEI) was elucidated through ^{1}H-NMR spectroscopy (Bruker 300 MHz, Billerica, MA) using TMS as an internal standard in D_2O. Buffering capacity of PEI-PrAs was determined by acid-base titration as described earlier [315]. The polymer solution (1 mg/mL) was set at pH 10.0 and titrated with HCl (0.1M) up to pH 2.0. As a control 25PEI and 1.2PEI were titrated. Here buffering capacity of the polymers was defined as percentage of amines protonated from pH 7.4 to 5.1 and it was quantified with the protocol described earlier [316].

3.2.3. DNA Binding by Polymers

pDNA binding capacity of the polymers was elucidated by agarose gel retardation assay using 0.8% of agarose gel containing ethidium bromide (1 μg/mL). The stock polymer solution (1 μg/μL) was diluted in ddH_2O in polypropylene tubes to give final concentrations between 0 and

0.05 μg/μL (final volume of 22 μL). Subsequently, 2 μL of pDNA solution (gWIZ at 0.275 μg/μL) was added to each tube and gently vortexed to get complexes from 0 to 2.0 polymer: pDNA (w/w) ratios. The complexes were incubated for 30 min at room temperature and mixed with loading buffer (4 μL), loaded to agarose gel, electrophoresed for 45 min at 120 mV and pDNA bands were visualized under UV illumination (Alpha Imager EC). Binding capacity of the polymers was quantified and expressed as BC_{50} (polymer required for 50% pDNA binding) by the quantification of free pDNA in lanes.

3.2.4. Size and ξ-Potential of pDNA/Polymer Complexes

Hydrodynamic diameter (Z-average) and surface charge (ξ-potential) of polymer/pDNA complexes was studied in ddH_2O through dynamic light scattering (DLS) and electrophoretic light scattering (ELS) using Zetasizer Nano-ZS (Malvern, UK) equipped with He-Ne laser and operated at 10 mW. Freshly prepared complexes (polymer: pDNA = 2.5, 5.0, 10.0 w/w) were diluted to 1 mL ddH_2O for each measurement.

3.2.5. Cell Culture

Human breast cancer cells MDA-MB-231 and MCF-7 used as model cell lines were obtained from Dr. Michael Weinfeld (Department of Oncology, U. of Alberta) and Dr. Afsaneh Lavasanifar (Faculty of Pharmacy & Pharmaceutical Sciences, U. of Alberta), respectively. Cells were maintained in DMEM supplemented with 10% FBS, 100 unit/mL Penicillin, 100 μg/mL Streptomycin under a humidified atmosphere (95/5% air/CO_2) at 37 ºC. Cells were typically sub-cultured once a week using 1:10 dilution.

3.2.6. Cytotoxicity Assay

In vitro cytotoxicity of PEI-PrAs/pDNA complexes (2.5, 5.0, 7.5, 10.0, 15.0 and 20.0, w/w) was evaluated in MDA-MB-231 and MCF-7 cells using the MTT assay. Cells without any treatment were used as negative controls. Cells were seeded in 48-well plates at a density of 50,000 cells/well and allowed to attach for 24 hr (250 μL medium/well). The complexes were prepared in serum free DMEM and directly added to each well and incubated for 24 hr with complete culture medium under a humidified atmosphere (95/5% air/CO_2) at 37 ºC. The culture medium of each well was replaced with 250 μL of fresh medium after 24 hr and the cells were incubated for another 24 hr. The MTT reagent (5 mg/mL) was added to each well to give final concentration of 1 mg/mL and incubated for 1 hr. The medium was replaced with DMSO (200 μL) to dissolve formazan crystals and the optical density of the solution was measured in universal microplate reader (ELx; Bio-Tech Instrument, Inc.) at λ = 570 nm. The cell viabilities were expressed as a percentage of non-treated cells.

3.2.7. In-vitro Uptake of PEI-PrA/pDNA Complexes

The uptake of PEI-PrA/pDNA complexes was assessed in MDA-MB-231 and MCF-7 cells through flow cytometry and confocal microscopy using Cy^{TM3}-labelled pDNA (labeling following the protocol of the manufacturer). The cells were seeded in 24 well plate and grown overnight. The complexes with polymers and Cy^{TM3}-labelled pDNA of different composition, and with or without C-siRNA (see Results) were prepared. Then, cells were treated with these complexes. After 24 hours of treatment, cells were washed (3X) with HBSS, trypsinized and fixed with formaldehyde (300 μL, 3.5% in HBSS) and analyzed by flow cytometer. For confocal microscopy study, MDA-MB-231 cells were seeded on cover slips (15 mm diameter) inserted into 6 well-

plates and grown overnight (~50% confluences). Complexes were prepared as described above and were directly added to cells and incubated for 24 hr under a humidified atmosphere (95/5% air/CO_2) at 37 ºC. Cells were then washed (3X) with HBSS (pH 7.4) and fixed with 1 mL formaldehyde (3.75 % in HBSS) for 30 min and washed with ddH_2O. The cells nuclei were stained with 4,6-diamino-2-phenylindole (DAPI) and cytoplasm with wheat germ agglutinin (WGA), Oregon Green® 488 conjugate. Finally, the cover slips were mounted onto the slides and then it was observed under 60X 1.3 oil plan-apochromat lenses in Laser Scanning Confocal Microscopy (LSM710, Carl Zeiss AG, Oberkochen, Germany).

3.2.8. In vitro Transfection

Transfection efficiency of PEI-PrAs was investigated in MDA-MB-231 and MCF-7 cells through flow cytometry using gWIZ-GFP with a Green Fluorescent Protein (GFP) expression system under the CMV promoter. The 25PEI served as positive control and blank medium as the negative control during the transfections. Prior to each study, cells were seeded in 24 well-plates (50,000 cells/well) and allowed to attach overnight. The complexes of variable composition (mass ratios) with/without siRNAs was prepared in serum free DMEM (see Results), as described above. The complexes were directly added to each well and incubated for 24 hr under a humidified atmosphere (95/5% air/CO_2) at 37 ºC. The culture medium was replaced with fresh medium after 24 hr and then incubated for designed time period. The cells were then processed for flow cytometry; cells were washed (3X) with HBSS, trypsinized and fixed with formaldehyde (300 µL, 3.5% in HBSS). The GFP-positive population was quantified by Beckman Coulter QUANTA™ SC Flow Cytometer using FL1 channel (3000events/sample). The setting of the instrument was

calibrated for each run to obtain GFP expression of 1-2% for control samples (i.e., untreated cells). The mean fluorescence and the percentage of GFP positive cells were determined.

3.2.9. Statistics

The data were presented as mean ± standard deviation of three different replicates and analyzed for statistical significance by Student's two-tailed t-test (assuming equal variance).

3.3. Results and Discussion

3.3.1. Polymer Synthesis and Characterization

We designed a series of PEI-PrAs by grafting propionate onto 1.2PEI and explored their efficacy to deliver pDNA to MDA-MB-231 and MCF-7 breast cancer cells. Hydrophobic modification of PEIs via *N*-acylation is a straightforward method for synthesis of amphiphilic polymers, which can generate effective non-viral vectors [102]. The reaction conditions and resultant PEI-PrA polymers are summarized in **Figure 3.1**. As expected, PrA substitution onto 1.2PEI was increased with PrA: PEI feed ratio (**Figure 3.1B, C**). The ^{1}H-NMR spectrum of PEI-PrAs showed the characteristic proton resonance peaks of 1.2PEI (2.4 to 3.5 ppm) and PrA (1.05 and 2.15 ppm), indicating the desired modification (**Figure S3.1A**). The substitution efficacy was generally increased (up to ~70%) and then gradually decreased (~40%) with the feed ratios. The highest grafting was 1.6 PrA/polymer obtained from the feed ratio of 4.0 (PrA/PEI), which corresponded to 15.9% primary amine consumption, hence, leaving sufficient amines for nucleic acid binding. When long lipids were used as a substituent, amount of substitution ranged from 0.2 to 6.9 lipids per PEI with lipid: PEI amine feed ratios of 0.016 to 0.2 and as usual substitution per PEI increased with increase in the feed ratio [102, 317]. Higher substitutions of lipid per PEI might

be result of the using PEI of 2 kDa, which contains more amines for reaction than the 1.2PEI. Among these lipids, stearic acid substitution at highest the lipid: PEI amine ratio (0.2) was insoluble in water [317] . However, all polymers obtained from PrA conjugation were readily soluble in water in our hand.

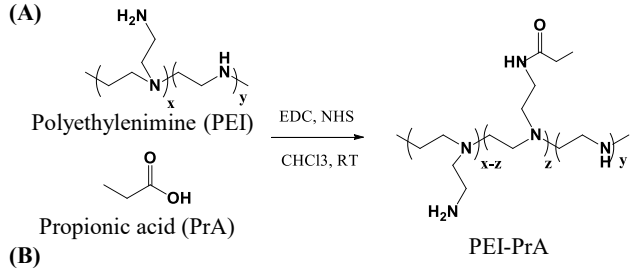

(B)

Polymer ID	Feed Ratio (mol/mol)	Calculated, NMR (mol/mol)
PEI-PrA0.5	**0.5**	**0.28**
PEI-PrA1.0	**1.0**	**0.76**
PEI-PrA2.0	**2.0**	**1.10**
PEI-PrA4.0	**4.0**	**1.6**

(C)

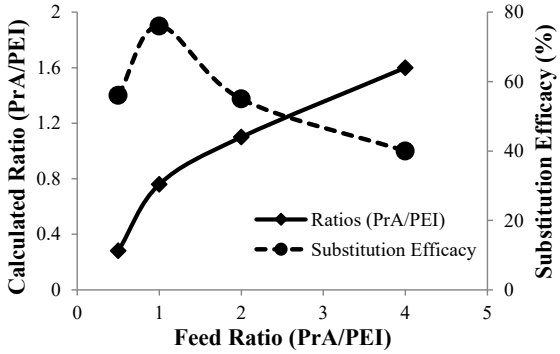

Figure 3.1. Synthesis and characterization of PEI-PrA polymers. Scheme for synthesis of PEI-PrA polymers (**A**), the obtained PrA substitutions (**B** and **C**) and substitution efficiency (**C**) as a function of PrA: polymer feed ratio. The number of PrA substituted was increased with feed ratio, but the substitution efficiency peaked at the feed ratios of 1.0.

3.3.2. Physicochemical Characterization of Polymers and Their Complexes

While chemical modification is intended to add beneficial features for gene delivery, *N*-acylation of PEIs could adversely affect critical features associated with successful gene delivery, such as buffer and DNA binding capacity. As expected, buffer capacity of the polymers was decreased from 31.7% (1.2PEI) to 24.8% (PEI-PrA1) upon PrA substitution as a function of modification (**Figure S3.1**), consistent with consumption of primary amines through *N*-acylation. The impact of PrA grafting was also observed in pDNA binding profiles (**Figure 3.2**).

The binding capacity of modified 1.2PEI was generally decreased with PrA substitution in proportion with the substitution amount (**Figure 3.2A**); the BC_{50} of 1.2PEI was increased from 0.25 (polymer/pDNA, w/w) with PrA substitution, reaching a maximal value of 0.59 (polymer/pDNA, w/w) with the highest substituted PEI-PrA (1.6 PrA/PEI). This was likely due to direct consequence of both primary amine consumption and steric hindrance arising from the PrA chains. This is a common phenomenon that we have been observing in aliphatic lipids substituted PEIs through *N*-acylation [102, 314, 318], and usually required polymer to nucleic acid ratios of >1.0 for complete binding. Although PrA substitution increased the BC_{50} values for pDNA, one can still use excess polymers for pDNA binding in order to realize the desired improved intracellular delivery.

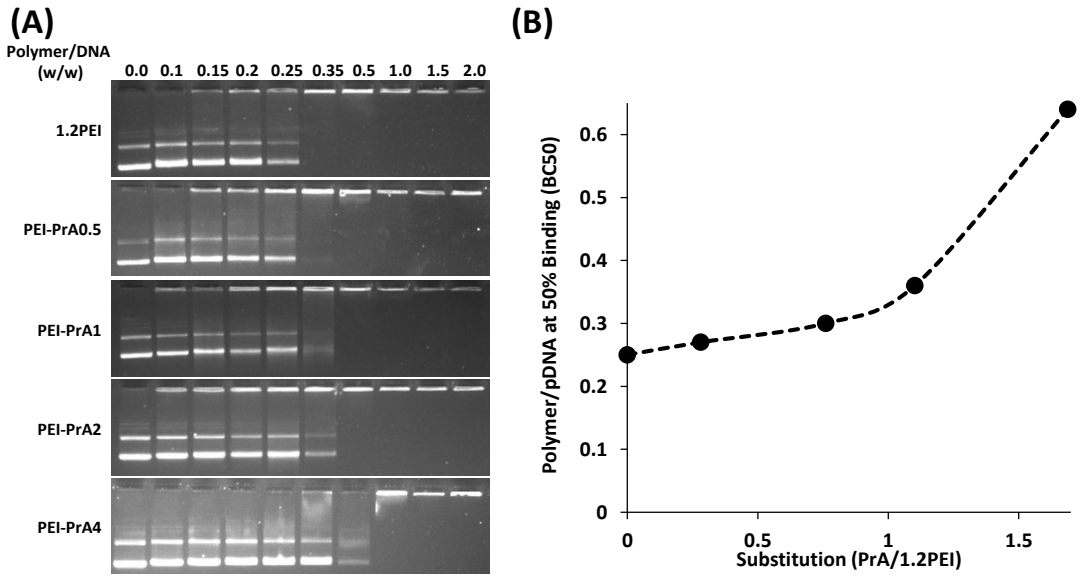

Figure 3.2. Agarose gel retardation assay of complexes of pDNA with native and PEI- PrAs at varying weight by weight ratios (**A**) and BC_{50} values (polymer: pDNA mass ratio to get 50 % of pDNA binding) as a function of PrA substitution per 1.2PEI (**B**). BC_{50} values were calculated using sigmoidal curve fits where % of pDNA binding with polymer obtained from gel electrophoresis, and plotted as a function of polymer: pDNA mass ratio. BC_{50} values increases as a function of PrA substitution, indicating reduced binding tendency of polymers with PrA substitution.

Hydrodynamic diameters and surface charges of polymer/pDNA complexes are additional parameters that may affect gene delivery efficacy [319, 320], as it is important to condense pDNA into cationic, nano-sized particles. All PEI-PrA polymers were able to condense pDNA into nanoparticles of 150 to 200 nm **(Figure 3.3).** The sizes of PEI-PrA/pDNA complexes at various polymer: pDNA ratios (2.5, 5.0 and 10, w/w) were similar irrespective of the PrA substitution level (**Figure 3.3**). These sizes were comparable to the size of native 1.2PEI/pDNA complexes.

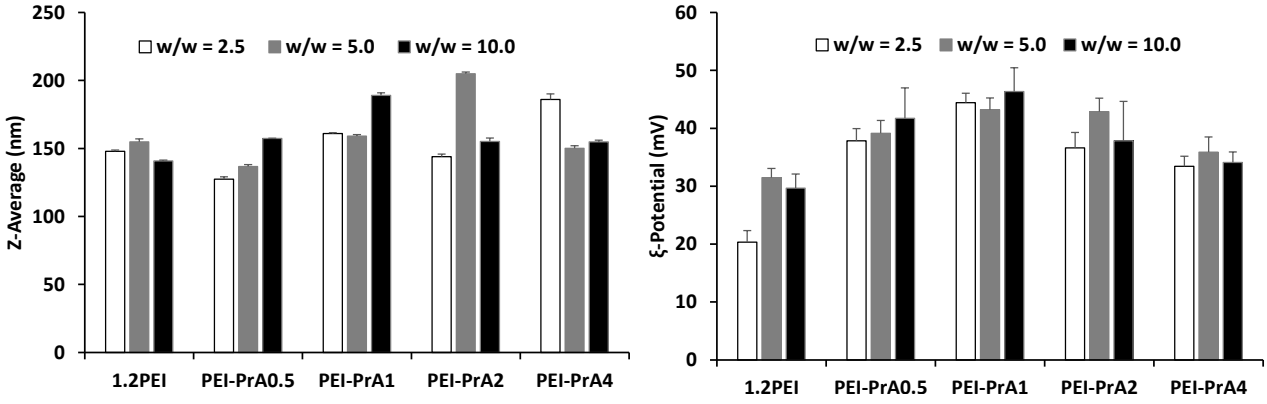

Figure 3.3. Hydrodynamic size (Z-average) and ξ-potential of polymer/pDNA complexes of polymer: nucleic acid ratios of 2.5, 5.0 and 10.0 (w/w). The PrA substitution did not significantly impact the hydrodynamic size but the ξ-potential was significantly altered as a function of PrA substitution. ξ-potential initially increased with PrA substitution and then decreased with high PrA substitution.

It is interesting to note that long lipid, linoleic acid (C16) substitutions on PEI significantly change the hydrodynamic size of complexes and importantly, the polymer: pDNA mass ratio used to form complexes had an impact on sizes as compared to extent of lipid substitution on polymer [314]. Unlike long lipids, modification with small hydrophobe may have less steric hindrances allowing the backbone of native 1.2PEI to undertake the necessary condensation process. Some studies showed that hydrophobic substitutions results in significant increase in particles size of

complexes due to aggregation of particles [321], presumably due to hydrophobic interactions under aqueous conditions. However, in another study, longer lipid-substitution on 2 kDa PEIs did not alter the size of complexes in a specific way [317]. The small hydrophobe PrA substitution also did not appear to affect the size of complexes indicating availability of enough amine content to condense pDNA. On the other hand, PrA grafting significantly increased the cationic charge of the complexes at the indicated polymer: pDNA ratios; the highest ζ-potential of PEI-PrA/pDNA complexes was +45 mV that was significantly higher than the 1.2PEI/pDNA complexes (+20 mV) (**Figure 3.3**). Interestingly, surface charge of polyplexes increased with low extent of PrA substitution and again decreased to levels consistent with the native 1.2PEI complexes with excess substitution. It is likely that while low PrA substitution enhanced the assembly of the complexes, the higher PrA substitution led to excessive consumption of amines and/or displayed steric hindrance to assembly.

3.3.3. Cytotoxicity of Modified Polymers and their Polyplexes

The MW dependent cytotoxicity of PEIs has been well recognized, which encouraged the use small MW PEIs as a template for gene carriers [322]. Complexes with pDNA and each polymer were prepared at different polymer to pDNA weight ratio and cytotoxicity was measured by the MTT assay. Modification of small MW PEIs with aliphatic lipids generally increases cellular toxicity of the resultant polymers due to enhanced polymer interaction with cells, as we have been observing in our studies [102, 314]. Consistent with this expectation, cytotoxicity of complexes with polymers PEI-PrA0.5 and PEI-PrA1 in MDA-MB-231 and MCF-7 cells was higher than 1.2PEI/pDNA complexes. However, these complexes still displayed better cell compatibility compared to 25PEI/pDNA complexes (**Figure 3.4**).

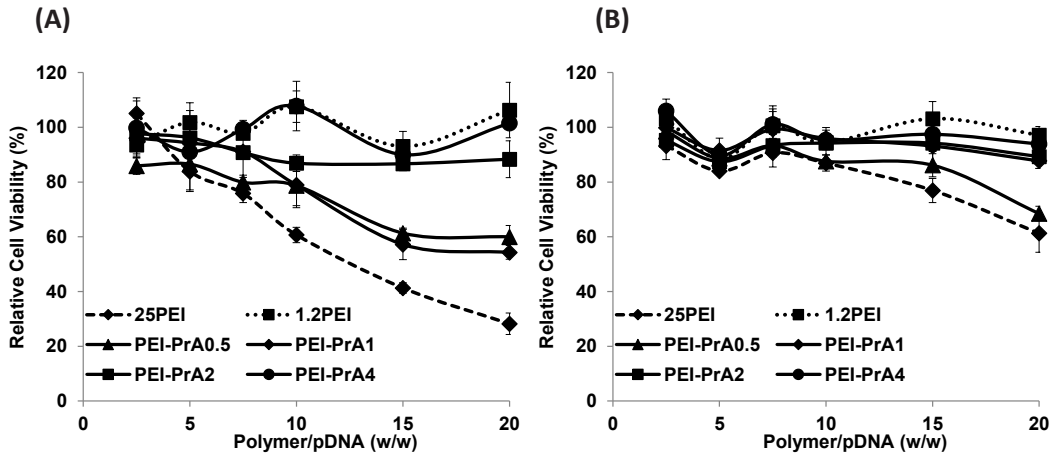

Figure 3.4. Cellular toxicity of polymer/pDNA complexes in MDA-MB-231 cells (**A**) and MCF-7 cells (**B**), as assessed by the MTT assay. Complexes with PEI-PrAs at lower substitution (PEI-PrA0.5 and PEI-PrA1) were more cytotoxic than complexes with 1.2PEI, but complexes with higher substitution (PEI-PrA4 and PEI-PrA2) gave similar toxicities to that of 1.2PEI.

Cholesterol, caprylic, myristic, palmitic, stearic, oleic and linoleic acid substituted 2PEI also showed lower cytotoxicity than 25PEI [102, 310]. As expected, increasing the polymer to pDNA weight ratio during complex preparations increased the cytotoxicity. At higher polymer to pDNA ratio, a significant amount of free polymer is expected to be present which represents the most cytotoxic component of the complexes. It is interesting to note that the complexes with high PrA substituted polymers, PEI-PrA2 and PEI-PrA4, did not induce any toxicity and this is in line with the surface charge of complexes form these polymers. PEI-PrA0.5/pDNA and PEI-PrA1/pDNA complexes displayed high ζ-potential than other polymers, which was presumably responsible for the observed cytotoxicity. These are likely more interactive complexes with the cells, leading to non-specific cytotoxicity. The toxicity similarities with these polymers in 2 different cell lines (MDA-MB-231 and MCF-7 cells) suggested a common, nonspecific mechanism such as cell membrane disruption. Cytotoxicity of polymers alone were tested in both cell lines in which concentration of polymers were equivalent to polyplexes of polymer to pDNA

weight ratio of 2.5 to 20. In contrast to toxic 25PEI, all PEI-PrA polymers were nontoxic even at high concentration (**Figure S3.2**).

3.3.4. Cellular Uptake of pDNA Complexes

One of the first key factors for effective non-viral gene delivery systems is the uptake of complexes. To further elucidate gene delivery efficacy, uptake of the complexes was determined using flow cytometry in MDA-MB-231 and MCF-7 cells using Cy^{TN3}-pDNA. Polymer complexes with Cy^{TN3}-pDNA were prepared at the ratio of 5 and 10 for flow cytometry analysis. Uptake of 25PEI complexes in MDA-MB-231 was equivalent to PEI-PrA1 complexes and more than other PEI-PrAs (**Figure 3.5A**). In case of MCF-7 cells, uptake of 25PEI complexes was higher than 1.2PEI complexes and its derivatives (**Figure 3.5C**). Interestingly, PEI-LA gave higher cellular uptake of complexes than the 25PEI in MDA-MB-231 cells, but the same did not apply for MCF-7 cells. Our previous study showed beneficial effect of long aliphatic lipid (LA- linoleic acid, CA-caprylic acid, MA-myristic acid) substitutions on 2 kDa PEI but only at relatively high substitutions. pDNA uptake was increased with increase in lipid substitution and correlation between pDNA uptake and lipid substitution was evident [102]. In this study, short hydrophobe substitution on 1.2PEI showed beneficial effect on the pDNA uptake but non-monotonic relation was obtained between pDNA uptake and PrA substitution: an optimal substitution was evident (with PEI-PrA1 having 0.76 PrA/PEI), after which a decrease in pDNA uptake was evident in both cell lines. PEI-PrA0.5 (0.28 PrA/PEI) and PEI-PrA2 (1.1 PrA/PEI) showed significantly higher uptake than parent 1.2PEI but the polymer with highest PrA substitution (PEI-PrA4: 1.6 PrA/PEI) was unable to deliver pDNA, reminiscent of 1.2PEI. The results were similar in the MCF-7 cells as well. pDNA delivery with PEI-PrA polymers were in line with the surface charge of the

polyplexes, where PEI-PrA1 complexes had the highest ζ-potential and the 1.2PEI with highest PrA substitution (PEI-PrA4) had the lowest ζ-potential complexes.

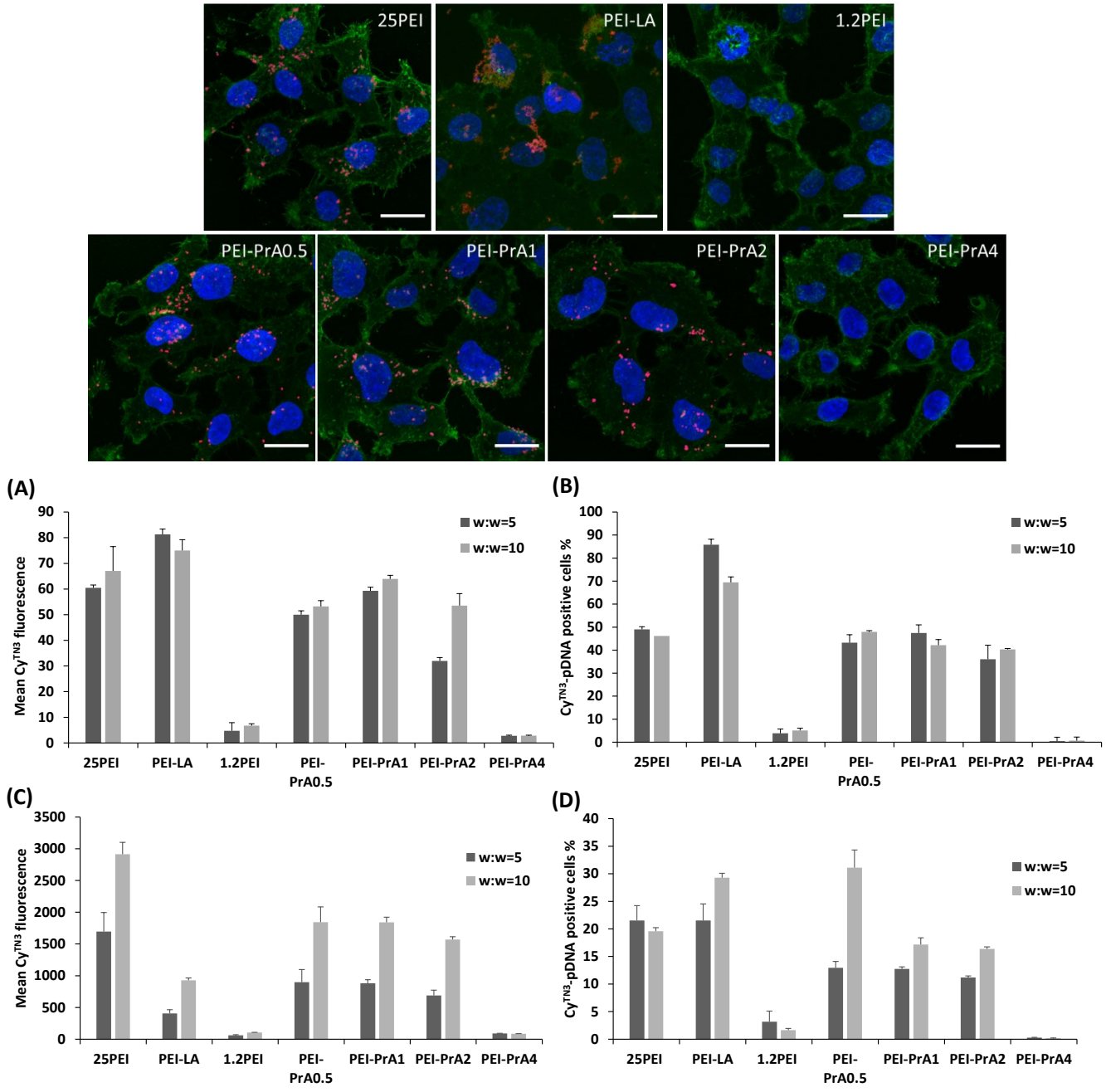

Figure 3.5. Confocal micrographs of MDA-MB-231 cells after 24 hr treatment with complexes of polymer and pDNA-Cy^{TM3} (red), w/w = 10. Note that lack of uptake with PEI-PrA4 polymer, unlike PEI-PrA1 that gave robust uptake. Cells were stained with WGA oregon green® 488 conjugate and nuclei are stained with DAPI (blue). Scale bar is 20 µm. pDNA uptake to MDA-MB-231 cells (**A** and **B**) and MCF-7 cells (**C** and **D**) with PEI-PrAs; measured by flow cytometry.

The uptake was determined by Cy^{TN3}-labeled pDNA and expressed as either mean pDNA uptake per cells (**A** and **C**) or as percentage of cells positive for pDNA (**B** and **D**). While small amount of PrA substitution helped pDNA delivery, excess PrA was detrimental for pDNA delivery.

Uptake of pDNA/polymer complexes was further studied by confocal microscopy. The confocal micrographs of MDA-MB-231 cells indicated distinct red fluorescent particles (i.e., Cy^{TN3}-labeled pDNA) around the nucleus of all cells, indicating internalization of complexes (**Figure 3.5**). The intensity and numbers of fluorescent particles in cells varied with the type of polymer used. Both 25PEI and PEI-PrA1 were able to deliver pDNA into MDA-MB-231 cells as revealed by red particles next to the nuclear membrane (**Figure S3.2**). Confocal microscopy also showed that pDNA complexes with PEI-PrA4 (highest PrA substitution) were not internalized as confocal microscopy image did not indicate any particles inside cells when using polymer indicated. While the hydrophobicity of PEI-PrA4 should be higher compared to PEI-PrA1 (hence displaying better membrane compatibility), the lower ζ-potential (equivalent to non-effective 1.2PEI) was likely the reason for reduced intracellular delivery of these complexes.

Finally, the effect of siRNA addition to pDNA/polymer complexes was investigated, since such siRNA addition may further enhance uptake of complexes [73]. For this purpose, complexes were prepared with or without control siRNA (CsiRNA) using PEI-PrA1 and uptake was assessed in MDA-MB-231 and MCF-7 cells by flow cytometer. Complexes with CsiRNA were prepared at different CsiRNA: pDNA ratio (from 0 to 2) using a polymer: nucleic acid (CsiRNA+pDNA) ratio of 5, which resulted in polymer: pDNA ratio from 5 to 15 (see **Figure 3.6**). As a control, complexes without CsiRNA but having an equivalent polymer: pDNA ratio were prepared. In MDA-MB-231 cells, addition C-siRNA at pDNA complexes with PEI-PrA1 was beneficial at polymer: pDNA ratio of 15 (where CsiRNA: pDNA ratio was 2), but no clear relation was evident in between

CsiRNA amount added and uptake efficiency (**Figure 3.6A** and **Figure S3.3A**). Complexes with equivalent amounts pDNA and PEI-PrA1 polymer (but without CsiRNA) also gave similar pDNA uptake, indicating that beneficial effect of CsiRNA addition could be duplicated by adjusting the polymer additive (**Figure 3.6B** and **Figure S3.3B**). While CsiRNA addition had detrimental effect on the uptake of pDNA complexes with 25PEI and same effect was observed with equal amount of pDNA and 25PEI.

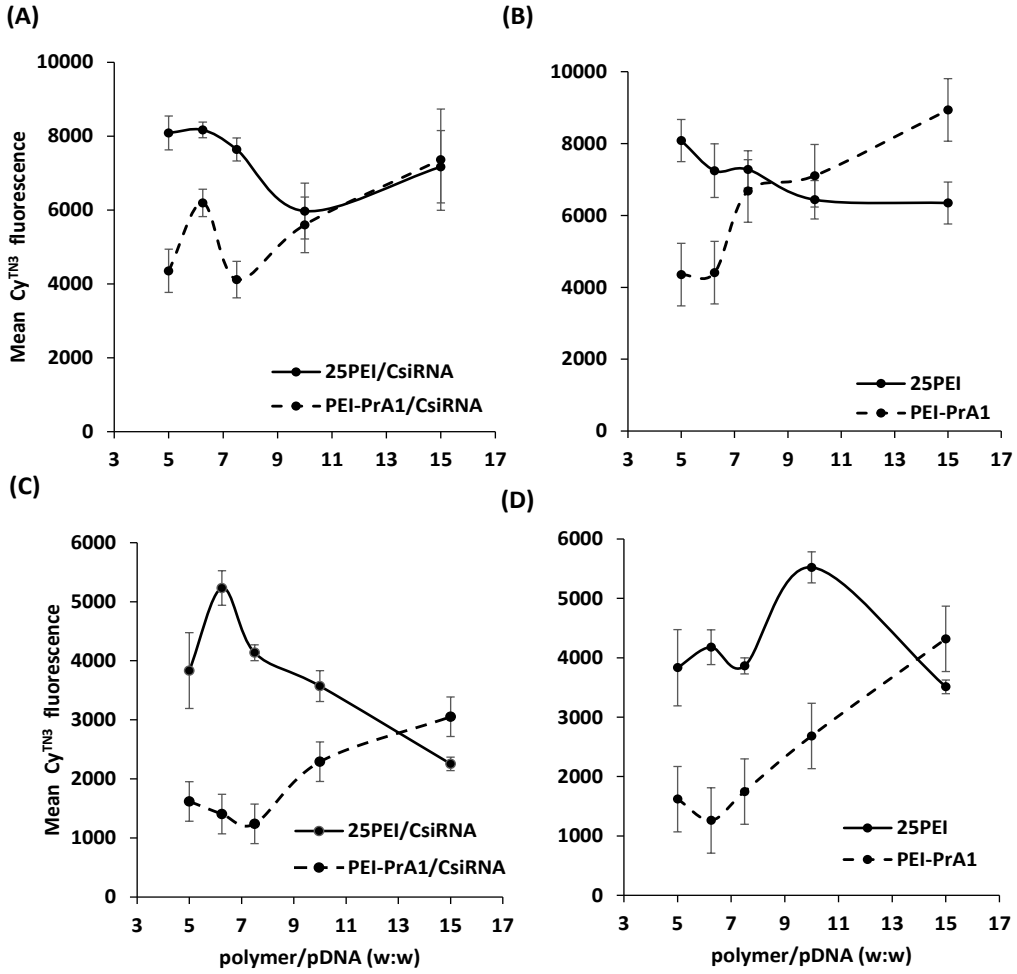

Figure 3.6. pDNA uptake in presence of siRNA. pDNA uptake in MDA-MB-231 cells (**A** and **B**) and MCF-7 (**C** and **D**) cells in the presence (**A** and **C**) and absence (**B** and **D**) of siRNA. Cy^{TN3}-labaled pDNA was complexed with the indicated polymers in the presence and absence of CsiRNA and uptake was determined after 24 hours as mean fluorescence of Cy^{TN3}-pDNA. Note that C-siRNA was not beneficial for increasing uptake, as increased polymer to pDNA ratio was sufficient to give similar uptake in the absence of CsiRNA.

These results clearly indicated that CsiRNA had no specific effect on the uptake of pDNA complexes in MDA-MB-231 cells. In MCF-7 cells, the CsiRNA additive to pDNA complexes with PEI-PrA1 also enhanced the uptake of complexes which was most prominent at the polymer: pDNA ratio of 15 (where CsiRNA: pDNA was 2:1); however, same results could be obtained with increasing polymer amount to match the equivalent complexes in the absence of CsiRNA (**Figure 3.6C, D**). Similar to the MDA-MB-231 cells, effect of siRNA on uptake of complexes with 25PEI was not evident in MCF-7 cells. Addition of C-siRNA to the 1.2PEI complexes did not improve the uptake of pDNA complexes neither (data not shown).

Beneficial effect of siRNA addition on uptake was shown in an independent study where the pDNA/siRNA/polymer (1/1/4 w/w/w) complexes showed higher uptake than pDNA/siRNA/polymer (1/0/2 w/w/w) [73]. However, the higher amount of polymer in the former complexes might have been the reason for higher uptake, since the appropriate control (i.e., complexes with equivalent amount of DNA and polymer) was missing. When the cationic polymers are used for complex formation, size of siRNA complexes is usually higher than with pDNA complexes [323]. Another study showed that the long winding pDNA and short rigid siRNA complexes with PEI with different hierarchical mechanisms [324]. It is possible that combined siRNA and pDNA polyplexes might have different polyplexes properties such as size and ζ-potential that might affect transfections [73]. In our hands, the addition is CsiRNA did not alter the sizes and ζ-potential of pDNA/PEI-PrA1 complexes **(Figure S3.4),** which might be the reason for the negligible effect of CsiRNA on pDNA complexes uptake.

3.3.5. Transfection Efficiency of Polymers

Modification of small MW PEIs with aliphatic lipids generally increases pDNA transfection efficacy due to improved cellular uptake [102, 314]. As expected, pDNA transfection efficacy (using GFP as a reporter gene) in breast cancer MDA-MB-231 and MCF-7 cells was significantly increased with PrA grafting on 1.2PEI while unmodified 1.2PEI was not effective at all (**Figure 3.7** and **Figure S3.5**).

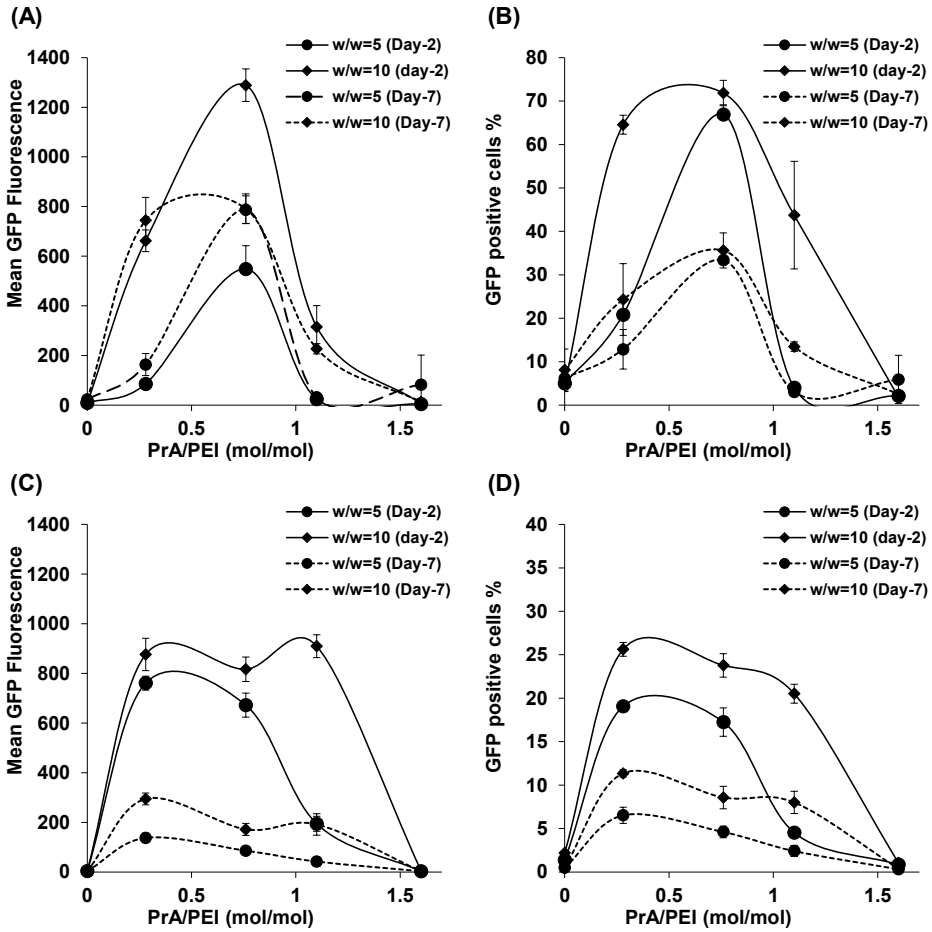

Figure 3.7. Transfection efficiency of PEI-PrA polymers. GFP expression in MDA-MB-231 (A, B) and MCF-7 (C, D) cells after treatment with PEI-PrA/pDNA complexes was evaluated on day 2 and day 7. Cells were analyzed through flow cytometry for GFP expression and data was expressed in mean fluorescence intensity (A, C) and percentage of GFP-positive population (B, D).

Interestingly, the relation between PrA substitution and transfection efficiency is not monotone which is in line with the surface charge and uptake of polyplexes with the respective polymers. The transfection efficiency was dependent on the cell type, where MDA-MB-231 cells displayed up to ~70% GFP-positive cells whereas MCF-7 cells gave only ~25% GFP-positive cells **(Figure 3.7B, D)**. As expected, transgene expression in both cell lines was dependent on polymer: pDNA ratio, as higher ratio gave better efficacy compared to lower ratio (10 vs. 5). The transfection levels were higher on day 2 and decreased after day 7, which is common with non-viral transfections. In MDA-MB-231 cells, the maximal transfection efficacy was obtained with PEI-PrA1 (0.76 PrA/PEI), whereas in MCF-7 cells, a wider range of PrA substitutions (0.3 to 1.1 PrA/PEI) displayed significant effect, which is supported by the cellular uptake of pDNA using respective polymers. The highest PrA substituted PEI (PEI-PrA4), consistent with cellular uptake results, did not yield any transfection efficiency. Such a drop in transfection efficiency was not observed with previous lipid-substituted PEIs, which typically displayed high transfection efficiency with higher lipid substitutions. Lower ζ-potential was one indication that increased PrA substitution might be detrimental for the overall charge of complexes by consuming cationic residues.

We prepared an equivalent line of polymers from 2 kDa PEI (2PEI) in order to confirm the observed PrA substitution effect with an independent series of polymers. Our results (summarized in **Figure S3.6**) with the 2PEI polymers indicated a similar trend; the ineffective 2PEI became an effective gene delivery agent after some PrA substitution, but high PrA substitution was again detrimental on transfection efficiency. Therefore, these two sets of results clearly emphasized that appropriate ratio of hydrophobic substituent to be critical for PEI-mediated transfection.

Improved transfection with hydrophobic modification may be due to increased lipophilicity resulting in better membrane compatibility and/or weaker interactions with pDNA, resulting in increased dissociation of complexes in the cytoplasm. An independent study also explored substitution of small hydropbobic moieties (acetate, butanoate and hexanoate) on 25PEI; Transfection efficiency was increased at low degree of substitution, where optimal modification was seen at ~25% acetylation, after which a reduction in transfection efficiency was noted [302]. In contrast, other investigators had shown that complete deacylation of linear PEIs (25, 22, 87 and 217 kDa) enhanced its transfection efficiency in A549 (human lung carcinoma) cells, supposedly by increasing the number of protonatable Ns, thereby increasing the binding affinity to pDNA [325]. However, branched 25PEI itself is a relatively effective transfection agent and it is not clear if the toxicity of this agent could be overcome by such a modification. Another group modified 2PEI with alkyl chains dodecyl and hexadecyl, which dramatically increased the transfection efficiency [104], but there was no modification with small hydrophobes was reported. Here we were able to modify 1.2PEI with small hydrophobe and find optimum degree of substitution for effective gene delivery. Our result suggested that using EDC/NHS conjugation method to substitute small hydrophobe where only primary amines of PEI are modified, substitution at the range of 0.3 to 1.1 small hydrophobe per PEI molecules enhances transfection, but the beneficial effects of PrA substitution reversed above these levels.

We then compared the transfection capacity of the most effective PEI-PrA1 and the broadly effective 25PEI. As before, unmodified 1.2PEI showed negligible efficacy in both cell lines (data not shown) whereas the efficacies of 25PEI and PEI-PrA1 were comparable at day 2 (**Figure 3.8**). While the transfection efficacy was decreased with time (**Figure 3.8, Figure S3.5**), the efficiency of PEI-PrA1 in MDA-MB-231 cells was higher than the 25PEI at day 7 and day 14, indicating

more stable transfection with PEI-PrA1. The transfection efficiency of PEI-PrA1 was comparable to 25PEI in MCF-7 cells at Day 2 and Day 7 **(Figure 3.8B)**. It should be noted that complexes with PEI-PrA1 polymer were less toxic than the complexes with 25PEI in both cell lines.

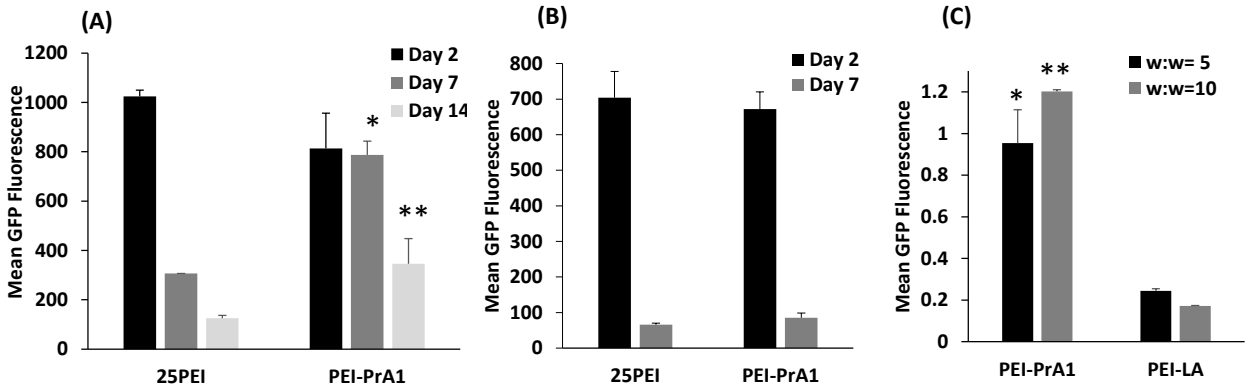

Figure 3.8: Comparison of transfection efficiency of PrA polymers with other polymers. GFP expression in MDA-MB-231 (**A**) and MCF-7 (**B**) cells at different time point after the treatment with polymer/pDNA (w/w =5) complexes. PrA grafting significantly increased the transgene expression in both cells lines and the efficacy was comparable with 25PEI (*P< 0.001 **P<0.05 Vs 25PEI (Day 7 and Day 14 respectively). (**C**) Comparison of GFP expression in MDA-MB-231 with PEI-PrA1 and PEI-LA. The complexes were formed at polymer:pDNA ratio of 5 and 10, and transfection efficiency was assessed after 2 days (*P< 0.05 **P<0.001 Vs PEI-LA (w:w = 5 and 10 respectively).

The transfection efficiency of PEI-PrA1 was also compared with linoleic acid (LA)-substituted 1.2PEI (PEI-LA), since LA was previously found to be the best performing lipid substituent on 2PEI [102]. In that study, unlike the PEI-PrAs here, no correlation was evident between transfection efficiency and degree of LA substitution, although transfection efficiency increased with high substitution level. The PEI-LA we used had 2.3LA per 1.2PEI and compared its transfection efficiency to PEI-PrA1 (**Figure 3.8C**). The transfection efficiency of PEI-PrA1 was higher than PEI-LA, suggesting that small hydrophobe PrA can effectively impart higher transfection efficiency than the longer lipid chains. Although cellular uptake with PEI-LA

complexes was higher than PEI-PrA1 complexes (see **Figure 3.5A**), lower transfection efficiency was observed in the former case. Increased lipophilicity (i.e., membrane compatibility) may be the reason for high uptake of particles with PEI-LA. At the same time, long lipids may facilitate stronger hydrophobic associations among lipids and form more compact particles [326], which may hinder dissociation of complexes in cytoplasm. This may not be the case for the short hydrophobes, which may explain their superior effectiveness. This observation suggested that balance of hydrophobicity is critical for enhanced transfection. Therefore, the chosen small hydrophobe could be a better option than the long aliphatic lipids, in addition convenience and better control during the substitution reactions.

We noted that an independent study performed with 25PEI noted a more beneficial effect of smaller hydrophobes; using β-galactosidase transfection in COS-7 cells, branched 25PEI modified with alanine gave superior performance than leucine (1C vs. 4C side chain) substitution [104]. Modification with amino acids can maintain total number of protonable Ns similar to unmodified 25PEI, which can maintain the DNA binding capacity. Teo *et al.* recently, reported hydrophobic modification of 1.8PEI with hydrophobic group of variable (and longer) chain lengths; methyl carboxytrimethylene carbonate (MTC)-ethyl, MTC-octyl and MTC-deodecyl [327]. Among the substituents, the shortest MTC-ethyl was found to be more effective than the longer chains, reportedly due to lower cellular uptake with the longer hydrophobic groups. Unfortunately, it is difficult to directly compare these results with PrA and LA substitutions on 1.2PEI reported here, since MTC incorporated between the 1.8PEI and alkyl chains might impact the physical properties of latter polymers unpredictably. In addition, modification with longer alkyls resulted in less cellular uptake of complexes, which was not in line with our results (PEI-LA gave superior uptake than PEI-PrA1 in MDA-MB-231). Unlike the conjugates created with

the MTC intermediate, Doody *et al.* modified 25PEI with hydrophobic acetyl (C2) butyl (C4) and hexyl (C6) moieties and suggested no clear correlation in between hydrocarbon length and transfection efficiency [302]. Because of the solubility problems, hydrocarbon length was limited in that study, so that longer lipids (i.e., LA) could not be substituted onto their PEIs and a comparison between very short substituents (e.g., acetyl) and aliphatic lipid substituents could not be compared in that study.

3.3.6. Effect of siRNA Additive on Transfection

We further explored the transfection efficiency of PEI-PrA1 by formulating additive polyplexes using CsiRNAs. Electrostatic interaction strength of pDNA and siRNA with cationic polymers is expected to be different due to difference in characteristics of the nucleic acids, including size, morphology, rigidity and charge [73]. Unlike long and flexible pDNA, siRNA is short and rigid, which may result in much lower strength of association with cationic polymers [320]. Hence addition of CsiRNA during complexation is believed to enhance the dissociation kinetics of complexes, which could facilitate non-viral transfection [318, 328]. To investigate effects of CsiRNA on transfection efficiency, we formulated 2 types of additive complexes: (i) complexes where polymer: pDNA ratio was fixed and CsiRNA amount was serially increased, and (ii) complexes where polymer:nucleic acid (pDNA+siRNA) ratio was fixed by increasing the polymer amount in proportion with CsiRNA, while keeping pDNA constant in both cases. Addition of CsiRNA in the former complexes where the polymer: pDNA ratio was fixed while increasing CsiRNA amount, was not beneficial in both cell lines. Transfection efficiency by both 25PEI and PEI-PrA1 decreased with increasing CsiRNA amount in these complexes (data not shown). Addition of CsiRNA without increasing polymer amount decreases cation: anion (polymer: pDNA+CsiRNA) ratio was expected to reduce the transfection efficiency due to

insufficient polymer to condense the available pDNA/CsiRNA. We then increased the polymer amount to ensure the same polymer: polynucleotide ratio (w/w=5) and assessed pDNA transfection **(Figure 3.9** and **Figure S3.7).**

In MDA-MB-231 cells, addition of CsiRNA to the complexes did not alter transfection efficiency as long as polymer: polynucleotide ratio was retained **(Figure 3.9A).** With complexes bearing an equivalent amount of polymer and pDNA (but without CsiRNA), transfection efficiency of PEI-PrA1 increased at increasing polymer/pDNA ratio but it dropped significantly at high polymer/pDNA ratio of 15 (**Figure 3.9B**). This may be due to toxicity of excessive polymer or decreases complex dissociation since uptake of these complexes were still high. Complexes with the same amount and pDNA and polymer (polymer/pDNA =15) but with CsiRNA (siRNA/pDNA=2) retained same level of transfection indicating beneficial role of CsiRNA in the complexes with high polymer/pDNA ratio. With MCF-7 cells, CsiRNA bearing complexes had increased transfection efficiency (**Figure 3.9C**), but the same response was obtained with an equivalent of polymer and pDNA complexes without the added CsiRNA **(Figure 3.9D).** Hence, addition of CsiRNA in pDNA transfection was not detrimental in both cell lines as long as polymer: polynucleotide ratio was maintained. Similar results were observed after day 7 of -transfection wherein transfection efficiency of PEI-PrA1 was higher than the 25PEI **(Figure S3.7).** Transfection efficiency in terms of percentage of GFP positive cells also showed a similar trend **(Figure S3.8** and **S3.9).** In addition, we found no significant change in the size and surface charge of polyplexes after addition of siRNA, as long as polymer: polynucleotide ratio was kept constant **(Figure S3.4).** The beneficial effect of siRNA in transgene expression was reported elsewhere [31]; DNA transfection efficiencies of both 25PEI and arginine-rich oligopeptide-grafted 25PEI

modified with polyethylene glycol with or without siRNA were studied. Beneficial effects of siRNA addition were noted in MCF-7 and MCF-7/Adr cells.

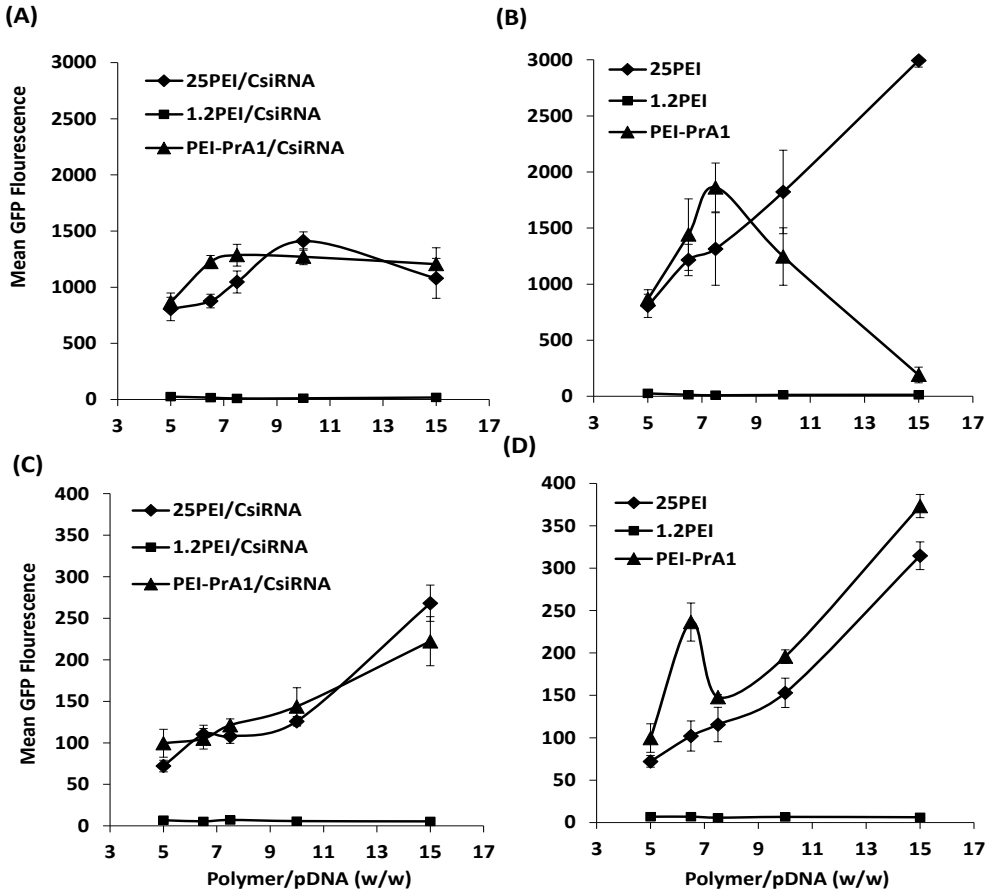

Figure 3.9. Effect of siRNA on pDNA transfection**.** Transgene expression in MDA-MB-231 (**A** and **B**) and MCF-7 (**C, D**) cells with (**A** and **C**) and without (**B** and **D**) CsiRNA additive (polymer: pDNA+siRNA ratio of 5) after 48 hours of transfection was evaluated. In MDA-MB-231 cells, adding CsiRNA did not alter the transfection efficiency (as long as polymer: polynucleotide ratio was constant, see **A**), while in MCF-7 cells, adding CsiRNA helped with transfection efficiency (see **C**) but the same effect was obtained with addition of equivalent amount of polymer in the absence of CsiRNA (see **D**).

In both cell lines, complexes DNA/siRNA/polymer (D/S/P) of weight ratio 1/2/3 and 1/1/2 resulted in higher transfection than by complexes without siRNA i.e. D/S/P of weight ratio 1/0/1

[73]. Yet, the polymer amount in former complexes, which showed high transfection, was higher than the latter complexes, and this effect was not specifically probed in that study. Our study showed equivalent amount of transfection can be obtained with simply increasing the polymer amount without CsiRNA. Similarly, another group studied effects of siRNA on GFP expression by PLL in HEK293 (kidney fibroblast) cells. GFP expression was higher with siRNA addition (PLL/pGFP/siRNA at cation: anion ratio of 2) vs. complexes without siRNA (PLL/pGFP of equivalent cation: anion ratio) [72]. It should be noted that to maintain the same cation: anion ratio, these two complexes had different amounts of polymer. In these studies, control experiments (transfection with equivalent polymer and DNA amounts in the absence of siRNA) were missing and enhanced transfection efficiency might have been simply due to this factor, as demonstrated in our study.

3.4. Conclusions

We successfully synthesized a small hydrophobe (PrA) modified 1.2 kDa PEI through *N*-acylation and validated the efficacy of resultant polymers for pDNA delivery in breast cancer cells. PrA grafting decreased pDNA binding and buffering capacity of the polymers, as well as increasing the toxicity to some extent. *In vitro* gene delivery efficacy of PEI-PrA to MDA-MB-231 and MCF-7 cells increased with degree of PrA substitution, but excess PrA (>1.2 PrA/PEI) was detrimental suggesting that an optimum ratio between the substituent and polyethylenimine backbone was critical. The transfection efficiency after PrA substitution was more effective than long chain lipid (linoleic acid) substitution on 1.2PEI, emphasizing importance of balancing hydrophobicity of polymer for optimum gene delivery. However, siRNA supplementation, unlike literature reports, did not have specific effect on the pDNA transfection efficiency, as long as

polymer amounts are adjusted in the formulations. Thus, integration of small hydrophobic groups into cationic PEIs is an effective approach for designing polymers for pDNA delivery and could prove useful in gene therapy approach for cancer.

3.5. Acknowledgements

This study was supported by an Operating Grant from the Canadian Institutes of Health Research (CIHR), a Discovery Grant from the Natural Sciences and Engineering Research Council of Canada (NSERC) and an Innovation Grant from the Canadian Breast Cancer Foundation (CBCF). We acknowledge the technical help provided by Dr. Vishwa Somayaji in generating the ^{1}H-NMR spectra and by Cezary Kucharski for general help with cell culture techniques. Bindu Thapa was supported by a studentship from NCPRM (NSERC CREATE Program for Regenerative Medicine, PI: G. Laroche, University of Laval, Quebec City, WC, Canada). Samarwadee Plianwong was supported by a studentship from Thailand Research Fund (TRF) through the Royal Golden Jubilee Ph.D. Program.

Chapter 4

Novel Targets for Sensitizing Breast Cancer Cells to TRAIL-Induced Apoptosis with siRNA Delivery

A version of this chapter was published in:

Bindu Thapa, Remant Bahadur KC, Hasan Uludag, "Novel targets for sensitizing breast cancer cells to TRAIL induced apoptosis with siRNA delivery", *International Journal of Cancer*, 2017, 142, 597-606.

4.1. Introduction

Resistance to apoptosis is one of the hallmarks of cancer [329]. Malignant cells develop resistance to apoptosis mainly by up-regulating anti-apoptotic proteins and/or diminishing pro-apoptosis signals. Facilitating apoptosis during therapy has a strong potential to eradicate cancer cells. Most conventional chemotherapy and radiotherapy regimens induce apoptosis via the intrinsic pathway that is p53-dependent [330]. However, p53 is functionally inactivated in some malignant cells as a result of mutation(s) or loss of expression, which makes these malignant cells display resistance to conventional therapies [331]. Alternatively, binding of death ligands to death receptors (DRs) triggers the extrinsic apoptosis pathway where p53 appears to be dispensable in most cases [332]. Tumor necrosis factor-related apoptosis-inducing ligand (TRAIL), in particular, has the potential to induce the extrinsic apoptosis pathway after binding to TRAIL-R1 (DR4) or TRAIL-R2 (DR5) on the surface of malignant cells [152].

TRAIL has a unique capacity to induce apoptosis in a variety of tumor cell lines, but not in most normal cells, providing a highly promising avenue for therapy in cancer.[116-118] Several clinical trials (Phase I and II) demonstrated that TRAIL and TRAIL receptor agonists are safe,[124, 129, 333] but unlike the preclinical results, TRAIL therapy tested so far failed to exert a robust anticancer activity in patients. Resistance to TRAIL has been shown to occur through defects at every level of the TRAIL signaling pathways, from ligand binding to cleavage of the effector caspases [152, 161]. Several inhibitory proteins such as cellular FLICE-inhibitory protein (cFLICE), anti-apoptotic Bcl-2 family members and XIAPs were overexpressed in malignant cells and have been associated with TRAIL resistance [124, 334]. Hence, TRAIL treatment along with inhibiting anti-apoptotic proteins could augment pro-apoptotic signaling. Several independent studies found that chemotherapeutics and inhibitors of anti-apoptotic proteins sensitized cells to

TRAIL-induced apoptosis [124, 152, 334]. However, systemic studies to determine key inhibitors of TRAIL in breast cancer cells have not been clearly established.

In this study, we took advantage of RNAi screening technology to identify key targets that regulate TRAIL-induced apoptosis in breast cancer cells. By using synthetic siRNA-mediated RNAi screening against 446 human apoptosis-related proteins, complementary protein targets to TRAIL induced apoptosis were identified and silenced to sensitize breast cancer cells to TRAIL treatment. For the delivery of siRNA, we employed non-viral cationic lipopolymers after grafting aliphatic lipids onto the low molecular weight (MW) polyethyleneimines (PEIs). Low MW PEIs are more biocompatible than conventional cationic biomolecules and could be cleared easier in body due to smaller size. To improve the stability of complexation with nucleic acids, we have been grafting aliphatic lipids onto PEI and such modifications enhanced the delivery efficacy via increased membrane interaction and intracellular uptake.[108, 110, 314] These lipopolymers effectively undertook siRNA delivery to breast cancer cells, including xenograft models in mouse [110]. Hence, this study pursued simultaneous induction of apoptosis by TRAIL and lipopolymer-mediated siRNA delivery against TRAIL-sensitizing targets for a superior anticancer activity in breast cancer cells.

4.2. Methods

4.2.1. Polymer Synthesis and Characterization

Chemical modification of low MW (0.6, 1.2 and 2 kDa) PEIs was performed via *N*-acylation using α-linoleoyl chloride (αLA) as a hydrophobic moiety as described earlier [335] (**Figure 4.1**). Structural composition of PEI-αLAs was elucidated through ^{1}H-NMR spectroscopy (Bruker 300MHz, Billerica, MA).

4.2.2. Cell Culture

Human breast cancer cells MDA-MB-231 and MCF-7, and normal breast cells MCF-10A were obtained from Dr. Judith Hugh (Department of Oncology, U. of Alberta). MDA-MB-231 and MCF-7 cells were maintained in Dulbecco's Modified Eagle's Medium supplemented with 10% FBS 100 unit/mL Penicillin, and 100 µg/mL Streptomycin. MCF-10A cells were maintained in DMEM: F12 (1:1) supplemented with 5% Horse Serum 100 unit/mL Penicillin, 100 µg/mL Streptomycin, Hydrocortisone (500 ng/mL), hEGF (20 ng/mL), Human Insulin (0.01 mg/mL) (Sigma-Aldrich, St. Louis, MO), and Cholera Toxin (100 ng/mL) (List Biological Laboratories, Campbell, CA). Human umbilical vein cells (HUVEC) were obtained from Dr. Janet Elliott (Department of Chemical and Material Engineering, U. of Alberta) and cultured in rat tail type I collagen coated flasks with endothelial growth medium-2 with manufacturer's growth factor BulletKit™ (Lonza), 10% FBS, 100 unit/mL Penicillin and 100 µg/mL Streptomycin. Human bone marrow stromal cells (hBMSC) were obtained and maintained as described previously [336].

4.2.3. Uptake of PEI-αLA/siRNA Complexes in Breast Cancer Cells

The cellular uptake of PEI-αLA/siRNA complexes was assessed in MDA-MB-231 through flow cytometry and confocal microscopy using FAM-labelled siRNA. For flow cytometry studies, cells were seeded (10^5 cells/mL) in 24 well plate and grown overnight. The polymer/FAM-siRNA complexes were prepared at room temperature by incubating polymer and siRNA (ratio 6, w/w) in the medium and then directly added to the cells in triplicate. After 24 h, cells were analyzed by flowcytometer as described earlier [337]. For confocal microscopy study, MDA-MB-231 cells were seeded (10^5 cells/mL) on cover slips (15 mm diameter) inserted into 24 well-plates and grown

overnight. Cells were treated with the complexes as described above. After 24 h cells were processed and observed under confocal microscope as described earlier [337].

4.2.4. siRNA Library Screening

siRNA library screenings were conducted by using siRNAs against 446 apoptosis-related genes (siGENOME Human Apoptosis siRNA Library; G-003905, GE Dharmacon). The desired cells (MDA-MB-231 and MCF-10A) were seeded in 96-well cell culture plates using a Perkin Elmer Janus Automated Workstation. After 24 h, 1.0 μM dilution plate sets were prepared from the 96-well 5.0 μM plates of the siRNA Library. Polymer solution was then added to the siRNA solutions (ratio 6, w/w) and allowed to complex for 30 min at room temperature. Then 10 μL of complexes was added to the cells (30 nM final siRNA concentration) in triplicate. When indicated, paired screens were conducted, where one screen received 20 μL of complete medium after 24 h of incubation, whereas the other screen received 20 μL of recombinant human TRAIL (Life Technologies, Grand Island, NY) solution to make a final concentration of 5 ng/mL TRAIL. Treated cells were then incubated for another 48 h, before the final evaluation of cell growth by 3-(4,5-dimethylthiazol-2-yl)-2,5-diphenyltetrazolium bromide (MTT) (Sigma-Aldrich, St. Louis, MO) assay. To ensure the efficiency of siRNA silencing using the selected delivery system, CDC20 silencing siRNA (Cat # HSC.RNAI.N001255.12.1, IDT) was used as positive control, which was the most powerful siRNA we identified from a siRNA library against cell cycle proteins.[338] In addition, we used 2 scrambled siRNAs as negative controls in our screens. The siRNAs from the library are 21 mer siRNAs, so that one negative control was a scrambled 21-mer siRNA (CsiRNA; Ambion, Cat# AM4635). The positive control, CDC20 siRNA was a dicer-

substrate 27-mer siRNA, so that the negative control siRNA for this reagent was a dicer-substrate scrambled 27 mer siRNA (Cat # DS NC1, IDT).

4.2.5. Validation of Identified siRNA Targets for Cell Growth Inhibition

Efficacy of identified targets was validated in MDA-MB-231 and MCF-7 cells by monitoring cell growth inhibition using the MTT assay. Cells were seeded (10^5 cells/mL) in 48-well plates and incubated for 24 h. The polymer/siRNA complexes were prepared as described earlier and directly added to the cells. The final siRNA concentration was 30 nM. A custom synthesized two sets of siRNAs targeting BCL2L12 (cat # HSS.RNAI.N001040668.12.2 and HSS.RNAI.N001040668.12.1, IDT), two sets siRNAs targeting SOD1 (cat# HSC.RNAI.N000454.12.1 and HSC.RNAI.N000454.12.2, IDT) and negative control scrambled siRNA were used. To determine synergistic effect with TRAIL, 20 µL of TRAIL solution was added to cells to give 5 ng/mL or 50 ng/mL TRAIL after 24 h of siRNA transfection. Treatment groups without TRAIL received 20 µL of complete medium. After 48 h of further incubation, MTT assay was proceed as described above.

4.2.6. Gene Silencing Measurement by Real-Time PCR

After treatment with polymer/siRNA complexes, gene knockdown at the mRNA level was assessed by real-time PCR (qPCR). Briefly, MDA-MB-231 and MCF-7 cells were seeded (10^5 cells/mL) in 6-well plates and allowed to grow overnight. Cells were then treated with polymer/siRNA complexes (ratio 6, w/w) at final siRNA concentration of 30 nM. Total RNA was isolated after 48 h of transfection using TRIzol (Invitrogen). Then, RNA was converted into cDNA using M-MLV reverse transcriptase (Invitrogen) according to manufacturer's instruction. The

qPCR was performed using 15 ng of each cDNA sample on StepOnePlus Real-time PCR system (Applied Biosystems, Foster City, CA, USA) with SYBR Green Mastermix containing ROX (MAF Center, University of Alberta, Edmonton, Canada). Two endogenous housekeeping gene, human GAPDH (Forward: 5'-TCA CTG TTC TCT CCC TCC GC-3'and Reverse: 5'-TAC GAC CAA ATC CGT TGA CTC C-3') and human β-actin (Forward: 5′-GCG AGA AGA TGA CCC AGA T-3′ and Reverse: 5′- CCA GTG GTA CGG CCA GA-3′), specific BCL2L12 primers (Forward: 5'-CCC GCC CCT ATG CCC TTT TT-3' and Reverse: 5'-ATA ACC GGC CCA GCG TAG AA-3') and SOD1 primers (Forward: 5'-GCA CAC TGG TGG TCC ATG AAA-3'and Reverse: 5'-TGG GCG ATC CCA ATT ACA CC-3') were used for amplification (all primers were obtained from IDT). Levels of mRNA for each gene were measured using the comparative threshold cycle method and presented as fold-change of the target relative to individual GAPDH and β-actin. In order to see effect of TRAIL on silencing of the targets, MDA-MB-231 cells were treated with polymer/siRNA complexes (ratio, 6 w/w) at final siRNA concentration 30 nM in paired treatment. After 24 h of transfection, one set received 50 μL of TRAIL to give a final concentration of 5 ng/mL and another set received 50 μL of complete medium. Total RNAs were extracted after 48 h of TRAIL treatment and qPCR was performed as described above. In addition, kinetics of siRNA silencing was observed in MDA-MB-231 cells by analyzing the mRNA levels of BCL2L12 and SOD1 by qPCR at different time points after siRNA treatment.

4.2.7. Analysis of Apoptotic Cell Population

Percentage of cells undergoing apoptosis was determined by using FITC-Annexin V and Propidium Iodide staining (BD Biosciences). MDA-MB-231 cells were seeded in the 12-well plate and treated with Polymer/siRNA complexes with or without TRAIL as described above. After 48

h of TRAIL treatment apoptosis was assessed by the FITC-Annexin V and Propidium Iodine staining kit following the manufacturer's protocol. Briefly, cells were collected using Accutase® digestion and washed with HBSS. Then, cells were washed with apoptosis binding buffer (1X) and, aliquots of about 1 x 10^5 cells diluted in 100 µL of 1X binding buffer were incubated with 2.5 µL of FITC-Annexin V and 2.5 µL of Propidium Iodide in dark for 15 min at room temperature. Then, cells were analyzed with flow cytometer within 30 min.

4.2.8. Caspase Activation Assays

Cells were seeded in 24-well plate and treated with polymer/siRNA complexes TRAIL as described above. After 24 h of TRAIL treatment, cells were lysed and cells extracts were collected. Total protein concentration in each extract was determined using the BCA Protein Assay (ThermoScientific, Waltham, MA) according to manufacturer's instruction. Caspase-3 and caspase-8 activity were determined using fluorogenic substrates, *N*-acetylaspartyl-glutamylvalinylaspartyl-7-amino-4-trifluoromethylcoumarin (Ac-DEVD-AFC) and *N*-acetylleusylglutamylthreonylaspartyl-7-amino-4-trifluromethylcoumarin (Ac-LETD-AFC), respectively, according to the manufacturer's instructions (Enzo Life Sciences, Farmingdale, NY). Caspase activity was expressed as increase of relative fluorescent units per hour and normalized with respect of total protein content.

4.2.9. Statistical Analysis

The data were presented as mean ± standard deviation of three different replicates and analyzed for statistical significance by Student's two-tailed t-test (assuming equal variance). A value of $p<0.05$ was considered significant. For siRNA library screening, relative cell growth was

calculated as a percentage of cell growth in non-treatment control group and statistical significance was calculated by student's two-tailed t-test and z score. The outliers were singled out by selecting the responses with -1.96 < z <1.96. z values were calculated by following equation,

$Z = \frac{xi-\mu}{s}$,

where xi is the percentage of the cell growth compared to non-treatment cells for each well, μ is the average and s is the standard deviation of all xi in the whole plate.

4.3. Results

4.3.1. Polymer Synthesis, Characterization and siRNA Delivery

For effective delivery of siRNAs into breast cancer cells, we prepared a series of polymers. In previous studies [108, 338], linoleic acid (C18) substituted PEIs were identified as the most promising carrier. To further optimize the siRNA carriers, we synthesized a small cationic lipopolymer library where 0.6, 1.2 and 2.0 kDa PEIs were substituted with αLA (**Figure 4.1A**). Modification of PEI with αLA was confirmed by the ^{1}H-NMR (**Figure S4.1**). A higher level of αLA was evident at higher lipid/polymer feed ratio during synthesis, but a similar level of substitution was obtained irrespective of the MW of the PEI (2-3 lipids/PEI). These polymers were screened for uptake of polymer/siRNA complexes in MDA-MB-231 cells using flow cytometry (**Figure 4.1B**). Hydrophobic modification significantly improved the siRNA uptake efficacy of the polymers to MDA-MB-231 cells that was most evident with PEI1.2 and PEI2.0 irrespective of the level of αLA substitution. Among the polymers, PEI1.2-αLA4 showed highest uptake as revealed by the mean fluorescence intensity from the flow cytometer analysis. The siRNA uptake efficacy of αLA derivatives of PEI1.2 and PEI2.0 was significantly higher than the PEI25, the broadly effective non-viral gene delivery carrier and commonly used as a transfecting agent.

Despite the differences in mean fluorescence intensity, percentage of FAM-siRNA positive population was similar for all groups, indicating uniform uptake of siRNA complexes among the cell population. Confocal micrograph images (**Figure 4.1C**) showed that FAM-siRNA complexes with PEI25 were relatively small, uniformly distributed in all cells, but with low fluorescence intensity in each cell. On the other hand, FAM-siRNA complexes with PEI1.2-αLA4 and PEI2-αLA4 were distributed to all cells but in clusters resulting higher mean fluorescence intensity at distinct spots. From this screening, PEI1.2-αLA4 was selected as the most effective siRNA carrier for further experiment.

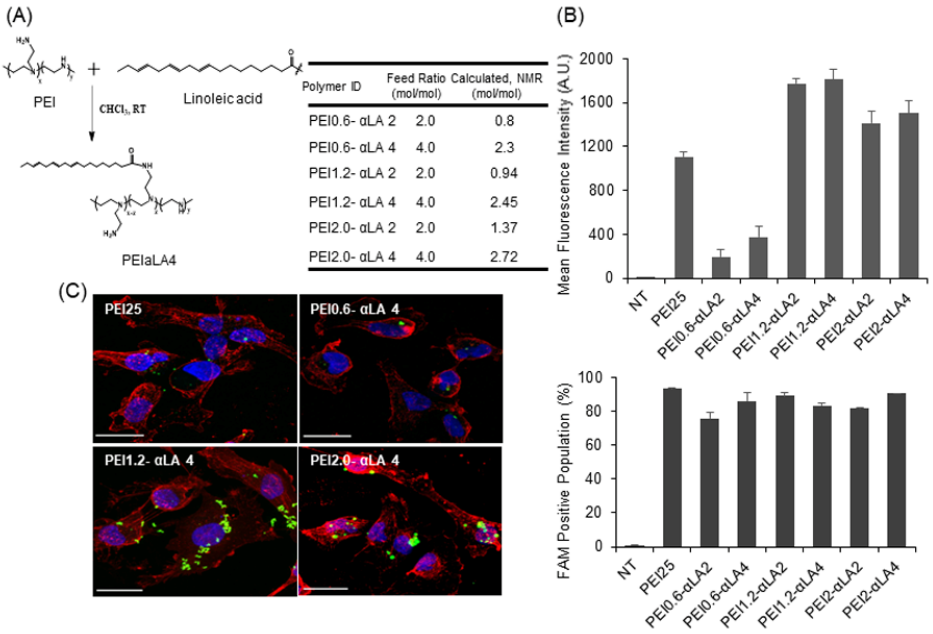

Figure 4.1: Synthesis of αLA-substituted PEIs and their siRNA uptake efficiency. Scheme for synthesis of αLA-substituted PEIs and the obtained αLA substitutions for individual polymers (**A**), flowcytometer analysis of polymer/FAM-siRNA uptake using in MDA-MB-231 cells (**B**) and confocal micrographs showing polymer/FAM-siRNA uptake using select αLA-substituted PEIs and PEI25 (**C**; scale bar is 20 μm). Complexes were prepared at the ratio of 6 (w/w) and MDA-MB-231 cells were analyzed by flow cytometry or confocal microscopy after 24 h of treatment. FAM-siRNA delivery efficiency of αLA substituted 1.2 kDa PEI was higher than PEI25 as revealed from confocal microscopy and flow cytometry.

4.3.2. Identifying Effective Targets by siRNA Library Screening

In order to identify targets whose silencing could enhance TRAIL-induced apoptosis, a library of 446 apoptosis-related siRNAs were screened for inhibition of MDA-MB-231 growth in the presence and absence of TRAIL. A siRNA against CDC20, a cell cycle protein whose silencing was most effective previously in inhibiting growth of MDA-MB-231 cells [338], served as a positive control. This siRNA provided more effective inhibition of cell growth than ~95% of the screened siRNAs (**Figure 4.2A, B and C**), still confirming its potency among the screened siRNAs. As compared to siRNAs' effects on MDA-MB-231 cells, most of the siRNAs in the library were unable to inhibit the growth of normal MCF-10A cells, although a few siRNAs also showed significant inhibition of growth in the latter cells (**Figure 4.2C**).

Using the relative cell growth <70% and the z-score <-1.96 as a cut-off, 23 siRNAs were found to inhibit the growth of MCF-10A cells on their own. Among them, only 3 siRNAs in the presence of TRAIL and 2 siRNAs in the presence/absence of TRAIL significantly inhibited growth of MDA-MB-231 cells, indicating a unique set of 18 siRNAs that are only effective in normal cells (and should be avoided). With the same cut-off criteria, only 14 siRNAs were found to inhibit growth of MDA-MB-231 cells. Importantly, only 2 of them were effective on MCF-10A cells, leaving 12 siRNA affecting only MDA-MB-231 cells, while 11 of them also showed significant growth inhibition in the presence of TRAIL in MDA-MB-231 cells. The critical targets which showed growth inhibition in the presence of TRAIL in MDA-MB-231 cells ($z < -1.96$) were shown in **Figure 4.2D**. A total 27 siRNAs were found to inhibit growth of MDA-MB-231 cells in the presence of TRAIL. Among them 5 siRNAs significantly inhibited MCF-10A cell growth (not desirable) and 11 of which retarded growth of MDA-MB-231 cells without TRAIL. Importantly, 16 of the 27 siRNAs sensitized the TRAIL induced cell death in MDA-MB-231 cells.

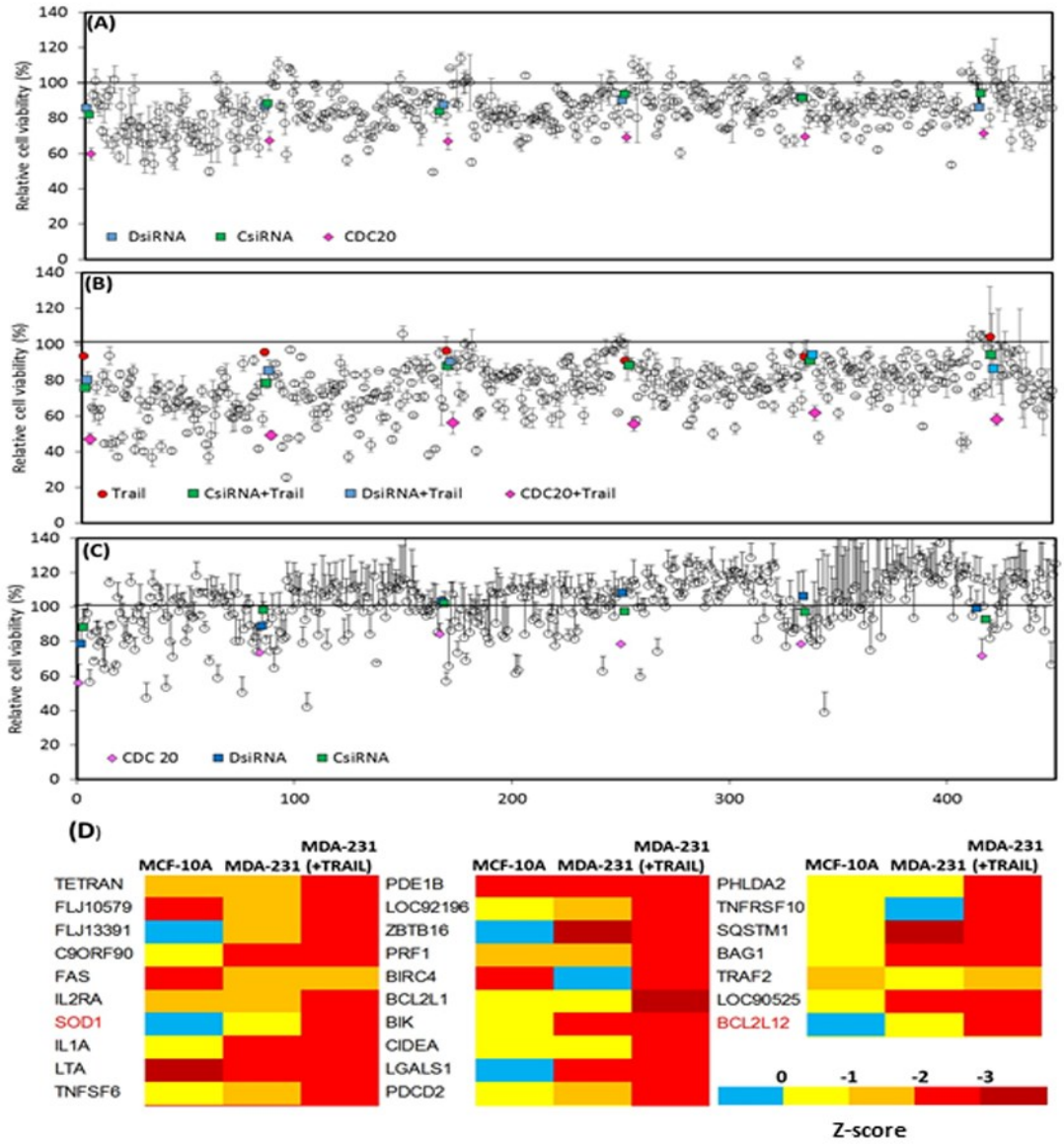

Figure 4.2: Target identification by siRNA library screening. siRNA library was screened in MDA-MB-231 cells with (**B**) or without (**A**) TRAIL (5 ng/mL) and in MCF-10A cells (**C**). The relative cell growth for treated cells was calculated as a percentage of cell growth of non-treated group. Final concentration of siRNA used for cell treatment was 30 nM. CDC20 siRNA was used as positive control and DsiRNA and CsiRNA were two scrambled control siRNAs. (**D**) Heat map for the siRNAs that induced significant cell death ($z < -1.96$) in MDA-MB-231 cells (with and without TRAIL) and MCF-10A cells. Many siRNAs including BCL2L12, SOD1, BCL2L2, FLJ13391 and LGALS1, showed significant cell death in the presence of TRAIL in MDA-MB-231 cells without showing significant effects in MCF-10 cells (without TRAIL).

Among the 16 siRNAs, some targets (e.g., TNFRSF10D, BCL2L1, TRAF2 and BIRC4) have been reported to be involved in TRAIL induced apoptosis. Functions of some of the identified targets (e.g., FLJ13391, PHLDA2) are not completely understood based on our literature search. Among these siRNAs, we selected relatively more potent BCL2L12 and SOD1 as 'leads', which sensitized the TRAIL induced cell death in MDA-MB-231 cells but did not affect growth of MCF-10A cells. We further validated the effects of these two targets on TRAIL-induced apoptosis in MDA-MB-231 cells.

4.3.3. Validation of Targets to Enhance TRAIL Induced Cell Death

In order to validate the involvement of BCL2L12 and SOD1 in TRAIL activity, the levels of targeted mRNAs were evaluated by qPCR after specific siRNA treatments. An independent set of siRNAs were secured from a different vendor, and MCF-7 cells were additionally used to explore siRNA efficacy with a different breast cancer cell model (**Figure 4.3A**). The BCL2L12 and SOD1 mRNA levels were significantly reduced after treatment with siRNAs for 48 h in both MDA-MB-231 and MCF-7 cells. The silencing appeared to be effective to the same extent in both MDA-MB-231 and MCF-7 cells at the siRNA concentration used (30 nM). In addition, we explored the effects of two additional siRNAs, each targeting BCL2L12 and SOD1 in both cell lines. These siRNAs were also able to silence the target mRNA (**Figure S4.2**). Then, we investigated the changes in the mRNA levels of BCL2L12 and SOD1 after treatment with combination of siRNA complexes and TRAIL in MDA-MB-231 cells. TRAIL was added after 24 h of siRNA complex treatment and mRNA levels were investigated after 48 h exposure to TRAIL. Silencing efficiency of TRAIL and siRNA complexes was equivalent to the single treatment with siRNA complexes, indicating no effect of TRAIL on silencing of the siRNA targets (**Figure 4.3B**).

We next analyzed the time-course of silencing of BCL2L12 and SOD1 after treatment with siRNA complexes (**Figure 4.3C and D**); maximum silencing of BCL2L12 and SOD1 were observed after day 2 of siRNA treatment and the levels of mRNA increased with time. BCL2L12 mRNA was significantly lower than the untreated group up to day 11 of siRNA treatment. However, SOD1 mRNA level was significantly lower that non-treated group up to day 8 of siRNA treatment.

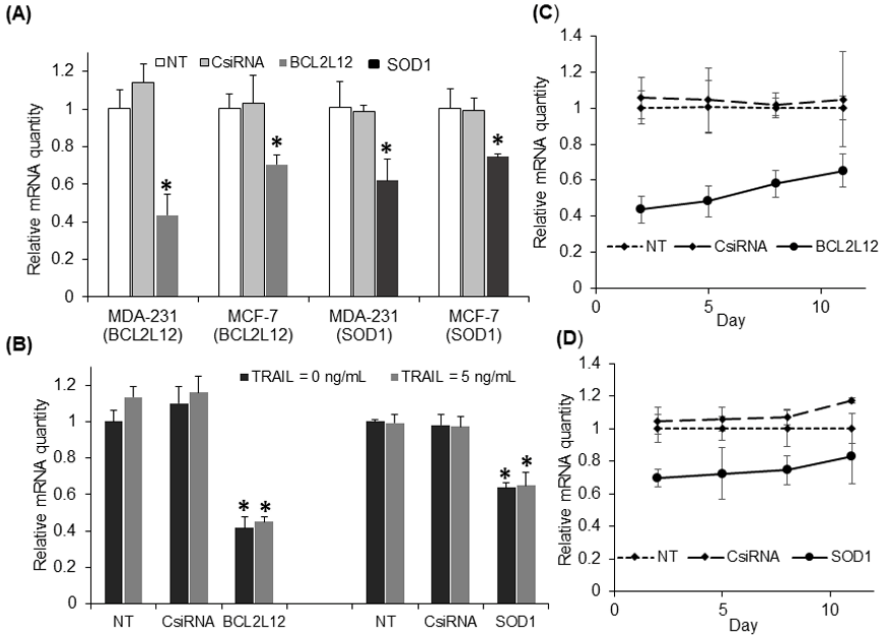

Figure 4.3: Analysis of siRNA silencing efficiency. Amount of mRNA was evaluated by qPCR in MDA-MB-231 and MCF-7 cells after 48 h of treatment with the indicated siRNAs (30 nM) (A). qPCR analysis of silencing effect of BCL2L12 and SOD1 siRNAs in MDA-MB-231 in absence/presence of TRAIL (B) and time course analysis of BCL2L12 and SOD1 mRNAs after specific siRNA (30 nM) treatments (C and D) in MDA-MB-231 cells. The relative quantity of mRNA transcripts was calculated relative to untreated cells using house-keeping genes GAPDH and β-actin as reference. After normalization, the results from the two reference genes were pooled together. *$p < 0.05$ compared with non-treated group.

The effect of the combination of siRNAs and TRAIL were evaluated on cell viabilities of MDA-MB-231 and MCF-7 cells. To optimize the dose of siRNA and TRAIL for synergistic

effects, two concentrations of siRNA (15 and 30 nM) were employed in the presence of TRAIL (0 to 100 ng/mL). TRAIL was added 24 h after siRNA complexes in these experiments, since this approach gave higher cell death than TRAIL treatment immediately after siRNA treatment (**Figure S4.3**). The MDA-MB-231 cells were responsive to TRAIL induced cell death where concentration-dependent cell death was observed at <20 ng/mL TRAIL (**Figure 4.4A** and **B**). Both siRNAs against BCL2L12 and SOD1 gave no significant cell death when used alone, but were able to enhance the cell death in the presence of TRAIL.

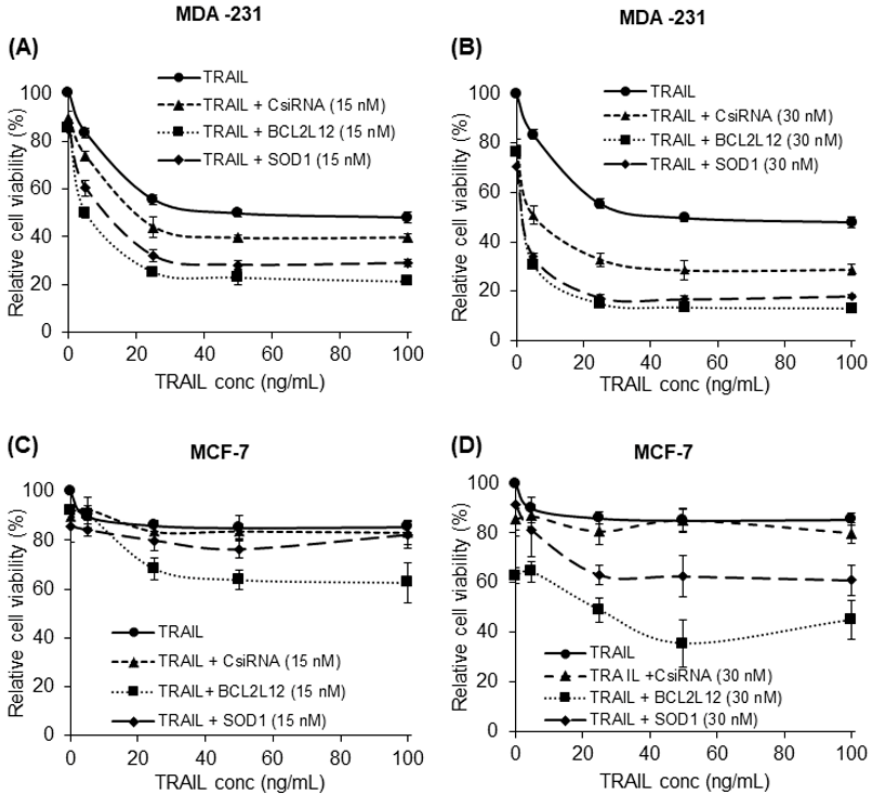

Figure 4.4: Inhibition of cell growth using siRNAs against BCL2L12 and SOD1 at 15 nM (**A** and **C**) and 30 nM (**B** and **D**) concentration with different concentration of TRAIL (0 to 100 ng/mL) in MDA-MB-231 (**A** and **B**) and MCF-7 (**C** and **D**) cells. Cells were first treated with siRNA complexes (24 h) and incubated with TRAIL for another 48 h.

The TRAIL response was significantly higher even at low concentrations (e.g., 5 ng/mL) with these siRNA treatments. On the other hand, MCF-7 cells showed an attenuated response to

TRAIL even at higher concentrations (**Figure 4.4C** and **D**), indicating a certain TRAIL resistance. The TRAIL effect on MCF-7 was increased with BCL2L12 and SOD1 siRNA treatments; siRNA silencing BCL2L12 resulted in significant effects with TRAIL at lower concentration (15 nM) whereas siRNAs silencing SOD1 was effective with TRAIL at higher concentration (30 nM) in MCF-7 cells. The siRNA silencing BCL2L12 had the ability to inhibit growth of MCF-7 cells at 30 nM without TRAIL and sensitized the TRAIL-mediated inhibition of growth (**Figure 4D**).

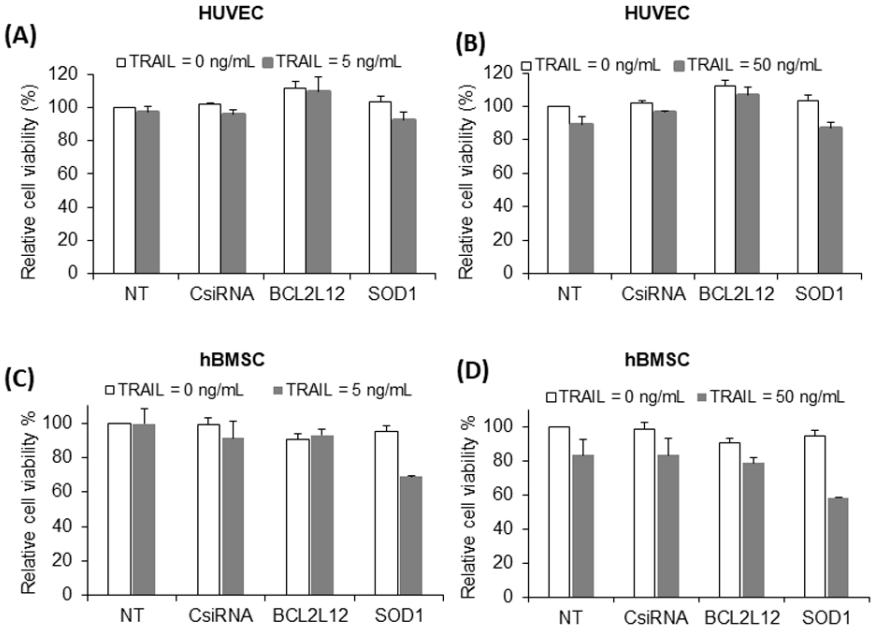

Figure 4.5: Effects of siRNA and TRAIL combinations in untransformed cells; HUVEC cells (**A** and **B**) and hBMSC (**C** and **D**). Concentration of siRNA used was 30 nM and TRAIL was 5 ng/mL (A and C) 50 ng/mL (B and D) which were optimal to retard growth of breast cancer cells; MDA-MB-231 and MCF-7 cells respectively.

Based on these results, 30 nM siRNA and 5 ng/mL TRAIL was considered optimal for MDA-MB-231 cells. Since no significant cell death was observed at 5 ng/mL TRAIL in MCF-7 cells (**Figure S4.4**), combination of 30 nM siRNA and 50 ng/mL TRAIL were considered optimal for these cells. The effects of these combinations were further evaluated in HUVEC and hBMSC. Both combinations of the siRNA and TRAIL that previously inhibited the growth of MDA-MB-

231 and MCF-7 had no effects on HUVEC cells **(Figure 4.5A** and **B**), and BCL2L12 and SOD1 siRNAs did not sensitize HUVEC cells to TRAIL induced cell death. In hBMSC cells, although 5 ng/mL of TRAIL did not retard growth, higher dose of TRAIL (50 ng/mL) inhibited cell growth to some extent (~20%). Both siRNAs at 30 nM did not affect growth of hBMSC growth significantly, but their combination with TRAIL had mixed response. Silencing BCL2L12 did not show any synergistic effect with TRAIL (5 or 50 ng/mL); while silencing SOD1 enhanced TRAIL (5 or 50 ng/mL) induced cell death in hBMSC (**Figure 4.5C** and **D**). The response of MDA-MB-231 and MCF-7 cells were similar to the above response (See **Figure S4.5**). In addition, a different set of siRNAs targeting BCL2L12 and SOD1 also sensitized the TRAIL-induced cell death in both MDA-MB-231 and MCF-7 cells (**Figure S4.6**). However, these siRNAs were less efficient than the previous set of siRNAs.

4.3.4. Apoptosis Induction and Caspase-3 Activation by TRAIL/siRNA Combination

Since MDA-MB-231 cells were more sensitive towards TRAIL-induced apoptosis, we further explored the ability of identified siRNAs to enhance TRAIL induced apoptosis in MDA-MB-231 cells (**Figure 4.6**). The percentage of early apoptotic population was small as compared to late apoptotic population in all treated groups (**Figure 4.6B**). TRAIL (5 ng/mL) alone did not induce a clear increase in apoptosis, based on the percentage of late apoptotic cells in TRAIL-treated cells (**Figure 4.6C**). Induction of apoptosis by siRNAs targeting BCL2L12 and SOD1 was not significantly higher than by control siRNA in the absence of TRAIL. On the other hand, combination of TRAIL and siRNA targeting BCL2L12 or SOD1 induced significant apoptosis; with the combination of TRAIL/BCL2L12 siRNAs, late apoptotic population was 71.1 ± 2.5% whereas the late apoptotic population was 61.3 ± 3.1% with the combination of TRAIL/SOD1 siRNAs.

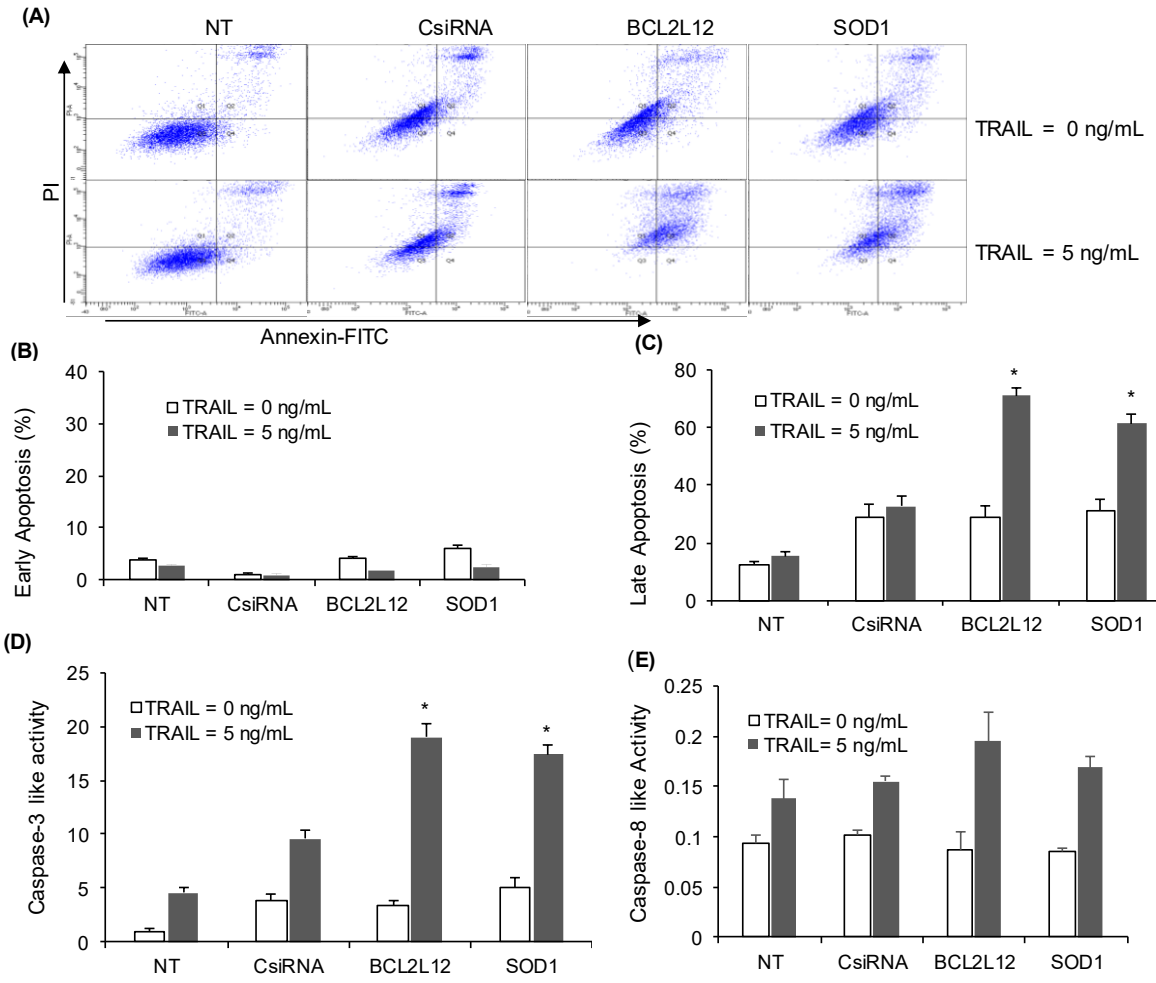

Figure 4.6: Annexin-FITC/PI apoptosis and caspases assay in MDA-MB-231 cells. MDA-MB-231 cells were treated with siRNAs (30 nM) targeting BCL2L12 and SOD1 followed by addition of 5 ng/mL TRAIL. After 48 h of TRAIL treatment apoptosis assay was conducted (A). Early apoptotic population (B) was the percentage of Annexin^{+}/PI^{-} population and late apoptotic population (C) was the percentage of Annexin^{+}/PI^{+} population. Percentage of apoptotic cells after treatment with combination of TRAIL and either siRNA was significantly higher than TRAIL and siRNAs alone. Effects of siRNA, TRAIL and their combination on the caspase-3 (D) and caspase-8 activity (E) in MDA-MB-231 cells. MDA-MB-231 cells were treated with siRNA (30 nM) targeting SOD1 and BCL2L12 for 24 hr, after which TRAIL was added (0 or 5 ng/mL) and caspase activities were determined after 24 h and expressed as increase of relative fluorescence units per hour and normalized with protein amount. Caspase-3 and caspase-8 activity were determined using fluorogenic substrates, *N*-acetylaspartyl-glutamylvalinylaspartyl-7-amino-4-

trifluoromethylcoumarin (Ac-DEVD-AFC) and *N*-acetylleusylglutamylthreonylaspartyl-7-amino-4-trifluromethylcoumarin (Ac-LETD-AFC), respectively. Caspase-3 was significantly increased after siRNA and TRAIL combination treatment. *$p < 0.05$ compared with CsiRNA and TRAIL.

In order to probe which caspases were activated to induce apoptosis, we investigated the level of caspase-3 and caspase-8 activation by the TRAIL and siRNAs in MDA-MB-231 cells (**Figure 4.6D** and **E**). As compared to non-treatment group, TRAIL (5 ng/mL) significantly induced the activation of caspase-3 and caspase-8, even though there was no apoptosis induction based on Annexin/PI staining. Silencing BCL2L12 and SOD1 siRNAs alone (in the absence of TRAIL) was unable to activate the caspase-3 and caspase-8. However, the combination of TRAIL and either BCL2L12 or SOD1 siRNA increased the caspase-3 activity by ~3-fold (**Figure 4.6D**). The caspase-8 activation by either of siRNA (BCL2L12 or SOD1), on the other hand, and the TRAIL combination was not significant than the control siRNA and TRAIL combination. Doing an assessment of caspase-8 activity at earlier time point (3 h vs 24 h as in **Figure 4.6E**) gave similar trends (**Figure S4.7**). Hence, siRNAs against BCL2L12 or SOD1 enhanced TRAIL induced apoptosis via synergistically activating caspase-3 in MDA-MB-231 cells. However, siRNA silencing BCL2L12 or SOD1 did not increase the caspase-8 activation.

4.4. Discussion

The siRNA approach has become a powerful tool for its specificity and efficiency to knock-down therapeutic targets [339-341]. However, safe and efficient delivery systems for siRNA are paramount for a functional effect. Lipid moieties such as linoleic and caprylic acids were used in our previous studies to substitute PEI amines, which converts the ineffective polymers into effective siRNA delivery agents via increasing the interaction with anionic cell membrane,

facilitating their cellular entry [110, 338]. Although we reported several polymers in the past for siRNA delivery to breast cancer cells [108, 110, 338], αLA substituted PEIs used in this study appear to be the most effective system to-date and they have been used here to identify targets for enhancing TRAIL sensitivity in breast cancer cells. TRAIL has been recognized as a potent agent to induce apoptosis in malignant cells, but the underlying determinants of TRAIL sensitivity are not clearly understood. Apoptosis-related proteins that regulate TRAIL-induced apoptosis could be important, as they could be used as predictive biomarkers of TRAIL sensitivity and/or provide additional targets for enhancing TRAIL-induced apoptosis. Similar to our siRNA library screenings in this study, an independent group also recently identified several positive and negative regulators of TRAIL action by using RNAi-based screen in MDA-MB-231 cell [206]. The reported screen included many kinases and anti-apoptotic proteins as negative regulator of TRAIL, but little overlap was evident between our results and the results in that study. Of the 16 genes selected as putative negative regulators of TRAIL in this independent study, only BCL2L1 was common with our results. Although the same type of cell was used for both studies, several significant differences were noted. First, we performed screening of human apoptosis-related siRNAs (446 genes), whereas the prior study was focused on human kinome (691 genes), phosphatome (320 genes) and 300 additional genes. Second, our selection of targets was based on the relative cell growth after 72 h after treatment, whereas the other study measured caspase-3/7 activation 1 hour after addition of TRAIL. Another important difference was the delivery system; while we used a polymeric carrier for siRNA delivery, that study employed a liposomal carrier (RNAiMax^{TM}) and it is possible that physiological differences could arise due to carrier effects on the cells. Another siRNA library screening of 510 genes (380 kinases, 20 genes of interest, 100 genes of unknown function and 10 genes that play a role in apoptosis and TRAIL-mediated signaling) was also

conducted to reveal regulators of TRAIL in HeLa cells [205]. Evaluation was based on cell viability after 48 h of siRNA treatment followed by 20 h TRAIL treatment, which is a similar strategy to our study. Since the siRNA targets and the cell line were significantly different from this study, none of the top 20 negative regulator of TRAIL matched the outcome of our screening.

Several well-established anti-apoptotic proteins including BCL2L1 (BCL-XL) and BIRC4 (XIAP) were identified in our hands as targets, whose silencing enhanced TRAIL-induced cell death, supporting the validity of the screening results. Another identified target, TNFRSF10D (tumor necrosis factor receptor superfamily member 10d) and TRAF2 were already known to play an inhibitory role in TRAIL-induced cell apoptosis [124],[342]. In addition to these targets, we reported two new targets, BCL2L12 and SOD1, for the first time to sensitize TRAIL induced apoptosis. BCL2L12 (for BCL2-like-12) is a proline-rich and BH2 domain-containing protein, which is known to inhibit effector caspase-3 and -7 [343, 344]. Two independent studies in glioblastoma showed that BCL2L12 inhibits caspase-7 via physical interaction [343] and caspase-3 via induction of the oncoprotein αβ-crystallin, which then interacts and inhibits caspase-3 [344]. Our study showed that BCL2L12 silencing did not increase the activation of caspase-3 by itself but synergistically activated caspase-3 in the presence of TRAIL. Although the role of BCL2L12 is well characterized in glioblastoma, its role in breast cancer is not completely understood and remains paradoxical. BCL2L12 was found highly expressed in low-stage breast cancer clinical samples [345]. Based on the gene expression analysis in breast cancer tissues, over-expression of BCL2L12 was speculated to lead to lower relapse or mortality rate [345] in contrast to its expected role as an anti-apoptotic protein. A shRNA mediated silencing of BCL2L12 resulted in acquired resistance to cisplatin in MDA-MB-231 cells [346]. Contrary to this result, siRNA mediated silencing of BCL2L12 sensitized MDA-MB-231 and MCF-7 cells to doxorubicin and cisplatin

induced apoptosis in a separate study [347], in line with its expected role as anti-apoptotic protein. In our study, silencing BCL2L12 sensitized MDA-MB-231 and MCF-7 cells to TRAIL-induced apoptosis, which was in line with the latter study.

Another target, SOD1 is well known to catalyze the conversion of superoxide ion (O_2^-) into H_2O_2 and O_2 to maintain low levels of reactive oxygen species (ROS) in lung adenocarcinoma cells [348]. Transformed cells have persistently higher levels of ROS than the non-transformed cells because of increased metabolic activity and the dysregulation of redox balance. Excessive amount of ROS results in oxidative damage to lipids, proteins and cellular DNA, and induces apoptosis [349]. Hence, transformed cells including breast cancer cells have typically elevated levels of SOD1 to maintain cellular ROS under a critical threshold and protect cells from the ROS damage [350]. Inhibition of SOD1 with small molecules had led to cell death in various cancer [351, 352], including breast cancer models *in vitro* [350]. In addition, many apoptotic stimuli up-regulate the SODs among the other pro-survival molecules which delays apoptosis [353]. Down-regulation of SOD1 using a small molecule was attempted to enhance TRAIL induced apoptosis; embelin sensitized the inflammatory breast cancer rSUM149 cells to TRAIL-induced apoptosis [354], but embelin is an inhibitor of XIAP as well so that its effect might have been mediated by both mechanisms. Although an siRNA against SOD1 were reported to inhibit growth of lung adenocarcinoma cells *in vitro* [348], a synergistic effect of SOD1 silencing with TRAIL has not been reported before.

We have also shown that the mechanism of increased apoptosis is a result of enhanced caspase-3 activation in MDA-MB-231 cells, which is a central event in apoptosis of malignant cells. However, MCF-7 cells are known to have lost the expression of capsase-3 [355] and, accordingly, we were not able to detect caspase-3 activity in the MCF-7 cells. However, significant

cell death was still observed in this cell type after treating with TRAIL and siRNA targeting BCL2L12 or SOD1. Indeed, TRAIL resistance in MCF-7 was reversed by silencing the BCL2L12 and SOD1. Several independent studies previously showed that despite the absence of caspase-3, MCF-7 can undergo apoptosis after induction of various stimuli [356, 357]. One study showed apoptosis induction in MCF-7 cells via sequential activation of caspases-9, -7 and -6 without involvement of caspase-3 [356]. In this study, we evaluated activation of caspase-3 using substrate DEVD, which is also a substrate for caspase-7. DEVDase activity was not significant in MCF-7 cells after treatment implying lack of involvement of caspase-7. However, another independent study showed apoptotic induction in MCF-7 cells after treatment with staurosporin via activation of caspase-6 independent of caspase-3 and -7 [358]. Further studies are needed to find out the specific mechanism associated with MCF-7 response with the proposed combination therapy.

4.5. Conclusions

In this study, we identified and explored two new targets, namely BCL2L12 and SOD1 to enhance TRAIL-induced apoptosis in breast cancer cells by screening human siRNA library using lipid-substituted PEI polymer as a non-viral siRNA carrier. The siRNA-mediated silencing of these targets was able to sensitize breast cancer cells a to cell death with minimum effects on the normal cells. These siRNA targets BCL2L12 and SOD1 enhanced the TRAIL-induced apoptosis via synergistically activating caspase-3 in MDA-MB-231 cells. Further studies to elucidate the mechanisms of these targets to regulate TRAIL-induced effects in MCF-7 are needed. Hence, the present study pointed out the importance of a combination therapy with the highly promising TRAIL protein and siRNAs targeting two specific apoptosis mediators to retard growth of breast cancer with minimal effect on normal cells.

4.6. Acknowledgements

This study was supported by an Operating Grant from an Alberta Innovates Health Solutions (AIHS) Bridge Fund, a Discovery Grant from the Natural Sciences and Engineering Research Council of Canada (NSERC) and an Innovation Grant from the Canadian Breast Cancer Foundation (CBCF). BT was supported by a studentship from NCPRM (NSERC CREATE Program for Regenerative Medicine PI: G. Laroche, University of Laval, Quebec City, Canada).

Chapter 5

Breathing New Life into TRAIL for Breast Cancer Therapy: Co-delivery of *pTRAIL* and Complementary siRNAs using Lipopolymers

A version of this chapter was submitted for publication as:

Bindu Thapa, Remant Bahadur KC, Mary Hitt, Afsaneh Lavasanifar, Olaf Kutsch, Dai - Wu Seol, Hasan Uludağ, "Breathing a new life into TRAIL: Co-delivery of TRAIL plasmid and complementary siRNA for breast cancer treatment."

5.1. Introduction

Tumor necrosis factor-related apoptosis-inducing ligand (TRAIL), a member of tumor necrosis factor (TNF) superfamily, has emerged as a promising cancer therapeutic since its discovery in 1995, because of its ability to induce apoptosis in a variety of transformed cells while sparing vital normal cells [115, 189]. TRAIL binds to the death receptors TRAIL-R1 and TRAIL-R2 and induces trimerization of death receptors, which is prerequisite for death induced signalling complex (DISC) formation and thereby to initiate apoptosis in activated cells. In apoptosis induction by death receptors, p53 appears to be dispensable, so that TRAIL therapy could be the most effective therapeutic approach for cancers with p53 mutation. TRAIL exerted potent tumor-suppressor activity after systemic administration in tumor-bearing mice without affecting normal tissues [189]. In order to translate the promising preclinical outcomes into the clinical realm, two approaches were taken for therapy, one based on recombinant human TRAIL protein and other based on TRAIL receptor agonistic antibodies [124]. These TRAIL therapies tested so far were safe and well tolerated in patients but, unfortunately, they failed to exert a robust anticancer activity [119, 124, 129, 137, 147]. The ineffectiveness of these therapies was attributed to (i) development of intrinsic or acquired resistant to TRAIL therapy [124, 359], (ii) poor pharmacokinetic profile of recombinant TRAIL proteins due to rapid renal clearance with short half-lives about 3-5 min in rodents and 23-31 min in nonhuman primates [180], and (iii) weak apoptosis induction by TRAIL receptor agonistic antibodies due to bivalent nature of antibodies which prevents trimerization [124]. Therefore, improved pharmacokinetics as well as increasing potency of TRAIL therapy is needed.

PEGylation of TRAIL [360], and fusion of TRAIL to polyhistidine (His) [361], Flag [232], human serum albumin [232], isoleucine zipper (iz) [230], and leucine zipper (LZ) [189], Fc portion

of human IgG [362] showed increased stability and extended half-life [119, 189, 362, 363]. However, His-TRAIL and Flag-TRAIL induced hepatotoxicity, which was not observed with native TRAIL [230, 361, 364] and PEGylation decreased the efficacy due to interference in TRAIL-R binding [200]. To this end, TRAIL gene therapy can overcome the fundamental pharmacokinetics limitations by allowing continuous *in situ* production for sustained presence of TRAIL at the tumor microenvironment [363]. Successful studies on viral TRAIL gene therapy [365, 366] were reported in recent studies, but the safety issues related to viral vectors (e.g., unpredictable immunogenicity and toxicity) are always a concern for their clinical translation [367-369]. Alternatively, several non-viral vectors (e.g., cationic polymers [370] dendrimers [371] peptides [372] and lipid nanoparticles [373] were used as gene delivery agents for TRAIL. The TRAIL gene used in these studies encoded a membrane bound full-length TRAIL isoform. After the discovery of homotrimeric structure of receptor binding domain of TRAIL (114-281 a.a.), a modified trimeric form of TRAIL was tested for anticancer activity [374, 375] and shown to be more potent in independent studies [189, 376]. Low potency of TRAIL to induce apoptosis, however, is a significant concern that cannot be readily solved with improved pharmacokinetics [124]. In order to address this issue, we had previously showed that silencing two proteins, Bcl2-like 12 (BCL2L12) and superoxide dismutase 1 (SOD1) using small interfering RNA (siRNA), sensitized the breast cancer to TRAIL-induced apoptosis [377]. Therefore, co-delivery of a trimeric TRAIL expressing plasmid (pTRAIL) and 'sensitizing siRNAs (BCL2L12 and SOD1) was proposed in this study to improve potency of TRAIL therapy.

Co-delivery of pDNA and siRNA can enable simultaneous knockdown of undesirable proteins with siRNA and forced expression of desirable proteins with pDNA in same cells [71]. In addition, this approach can synchronize the pharmacokinetics of bioactive agents and the targeted

cells are exposed to both therapeutics at a defined ratio, thereby optimizing the therapeutic outcomes. Co-delivery of different therapeutics into cancer cells at a desired ratio would be possible only with the appropriate biomaterial carrier which can accommodate both. The structural differences between the pDNA and the siRNA make identifying a single (common) carrier for co-delivery of both agents challenging. Functional pDNAs are long (>3000 base pairs) flexible molecules while siRNAs are short (<30 base pairs) rigid molecules. We have been tailoring cationic lipopolymers generated by grafting lipophilic ligands onto low molecular weight (0.6 to 1.8 kDa) polyethylenimines (PEIs) for delivery of nucleic acids. The resultant amphiphilic polymers are relatively non-toxic and possess high charge density suitable for polynucleotide interactions. The grafting of lipophilic molecules imparts significant lipophilic characteristic onto parent polymers without affecting their inherent features. Our past work identified distinct carriers that were suitable for either pDNA or siRNA delivery to a variety of adherent and suspension-growing cells, as well as preclinical tumor xenografts [337, 377]. In this study, we report cationic lipopolymers prepared by grafting aliphatic lipids onto PEI via thioester and amide bonding [378] and demonstrate their promise for co-delivery of pDNA and siRNA for TRAIL therapy in *in vitro* and *in vivo* breast cancer models.

5.2. Materials and Methods

5.2.1. Materials

Branched 1.2 kDa PEI (PEI1.2) was obtained from Polysciences, Inc. (Warrington, PA, USA) and used without further purification. (3-(4,5-Dimethylthiazol-2-yl)-2,5-diphenyltetrazolium bromide (MTT), human insulin, heparin and organic solvents were obtained from Sigma-Aldrich (St. Louis, MO). SYBR Green I was purchased from Cambrex BioScience

(Rockland, MD). The unlabeled scrambled siRNA (CsiRNA) and 5'-carboxyflourescein (FAM)-labeled scrambled siRNA (FAM-siRNA), BCL2L12 siRNA, SOD1 siRNA and all primers were obtained from Integrated DNA Technologies, Inc. (IDT; Coralville, IA). Cell culture medium, Dulbecco's Modified Eagle's Medium (DMEM)/F12, supplied with L-glutamine and 25 mM HEPES, and penicillin (10.000 U/mL)/streptomycin (10 mg/mL) were obtained from Invitrogen (Grand Island, NY). FB essence 100% US origin serum was obtained from VWR Life Science Paradigm (Radnor, PA). Cholera toxin was obtained from List Biological Laboratories (Campbell, CA). Annexin V-FITC Apoptosis Kit I was purchased from BD Biosciences (San Jose, CA). The preparation and characterization of trimeric secretable TRAIL encoding plasmid was described before [376]. TRAIL encoding plasmid construct contains the pCMVdw expression vector with TRAIL sequence (114 – 281 amino acids) fused with SEC(CV) sequence from human growth hormone (N-terminal 26 amino acids), furin-specific cleavage site (SARNRQKR) and isoleucine-zipper sequence (ILZ) (**Figure S5.1**). The gWIZ and gWIZ-GFP plasmids were obtained from Aldevron (Fargo, ND).

5.2.2. Cell culture

Human breast cancer cells MDA-MB-231, MCF-7 and MCF-10A were obtained from Dr. Judith Hugh (Department of Oncology, U. of Alberta) and SUM-149 and MB-MB-436 were obtained form Dr. Raymond Lai (Department of Laboratory Medicine and Pathology, U. of Alberta). GFP-positive MDA-MB-231 cells (MDA-MB-231-GFP$^+$) were obtained by retroviral transformation as described before [379]. MDA-MB-231, MCF-7, SUM-149 and MDA-MB-436 were maintained in DMEM/F12 supplemented with 10% FB essence, 100 unit/mL penicillin, and 100 μg/mL streptomycin. Human umbilical vein cells (HUVEC) were obtained from Dr. Janet

Elliott (Department of Chemical and Material Engineering, U. of Alberta) and cultured in rat tail type I collagen coated flasks with endothelial growth medium-2 with manufacturer's growth factor BulletKit™ (Lonza), 10% FBS, 100 unit/mL penicillin and 100 µg/mL streptomycin. MCF-10A cells were maintained in DMEM/F12 supplemented with 5% horse serum, 100 unit/mL penicillin, 100 mg/mL streptomycin, hydrocortisone (500 ng/mL), hEGF (20 ng/mL), human insulin (0.01 mg/mL) and cholera toxin (100 ng/mL). Human bone marrow stromal cells (hBMSC) were obtained and maintained as described earlier [336]. All the cell lines were authenticated by STR DNA profiling analysis at Genetic Analysis Facility, The Hospital for Sick Children (Toronto, ON).

5.2.3. Polymer synthesis, complex preparation and characterization

Hydrophobically-modified PEI were synthesized via *N*-acylation using carboxyl end-capped aliphatic lipids which was prepared by coupling α-Linoleoyl chloride (αLA) with mercaptopropionic acid (MPA) through thioester (-S-CO-) bonding (PEI-tαLA; **Figure 5.1**) as reported previously [378]. As a control group, PEI1.2 modified with αLA (PEI-αLA), LA (PEI-LA) and tLA (PEI-tLA) were prepared according to previous protocols [378]. The complexes (polymer/siRNA, polymer/pDNA or polymer/siRNA/pDNA) were prepared at room temperature by incubating the polymers with nucleic acids with a polymer: nucleic acid ratio of 5 (w/w) in nuclease free water for 30 min. Size of complexes and surface charge were measured using Zeta Nano-ZS (Malvern, UK). Dissociation of complexes were studied in the anionic environment of heparin by agarose gel retardation assay [378].

5.2.4. Uptake of polymer/siRNA/pDNA complexes

Cellular uptake of complexes (polymer/siRNA, polymer/pDNA or polymer/siRNA/pDNA) was assessed in MDA-MB-231 cells through flow cytometry and confocal microscopy using FAM-labelled siRNA and Cy3-labelled gWIZ (Cy3 labeling according to manufacturer's protocol). MDA-MB-231 cells were seeded (10^5 cells/mL) in 24 well plate and grown overnight. The complexes (polymer/FAM-siRNA, polymer/Cy3-gWIZ or polymer/FAM-siRNA/Cy3-gWIZ) were prepared at room temperature by incubating the polymers with nucleic acids with a polymer: nucleic acid ratio of 5 (w/w) in DMEM and then directly added to the cells. After 24 h of incubation, cells were analyzed by flow cytometry [337]. For confocal microscopy, MDA-MB-231 cells were treated, processed and observed under confocal microscope as described earlier [337].

5.2.5. DNA transfection and effect of siRNA

Transfection efficiency of the polymers was assessed in MDA-MB-231 cells through flow cytometry using GFP expressing plasmid (gWIZ-GFP). Cells were seeded (10^5 cells/mL) in 24 well plate and grown overnight. Polymer/gWIZ-GFP complexes (polymer: nucleic acid = 5, w/w) prepared in DMEM were added to the cells. In order to reveal the effect of siRNA on transfection efficiency, negative control scrambled siRNA (CsiRNA) was loaded into the complexes along with gWIZ-GFP plasmid. Briefly, gWIZ-GFP and CsiRNA were well-mixed in separate tubes at different ratios and then added to polymers solution (in DMEM) making the final polymer:nucleic acid ratio of 5 (w/w). After 30 min of incubation, complexes were added directly to the cells and GFP expression were analyzed by flow cytometry after 48 h of transfection as described earlier [337].

5.2.6. siRNA transfection and effects of pDNA

The siRNA transfection efficiency of the polymers was assessed by measuring the GFP silencing in MDA-MB-231-GFP$^+$ cells using flow cytometry and a GFP-specific siRNA (GFP-siRNA). Cells were seeded (10^5 cells/mL) in 24 well plate and grown overnight. Polymer/siRNA (GFP-siRNA or CsiRNA) complexes (polymer: nucleic acid = 5, w/w) prepared in serum free DMEM medium were directly added to the cells. To reveal the effect of DNA on transfection, gWIZ plasmid was loaded into the complexes along with GFP-siRNA. Briefly, gWIZ and GFP-siRNA were mixed at different ratios (w/w) in separate tubes and added to polymers solution in DMEM (final polymer: nucleic acid = 5, w/w) and incubated for 30 min at room temperature. The complexes were directly added to the cells. After 3 days of incubation, cells were processed for flow cytometry and GFP expression was analyzed and expressed as relative to group treated with the polymer/CsiRNA complexes.

5.2.7. Cell viability

Anticancer efficacy of pTRAIL, and BCL212 and SOD1 siRNA co-delivery was evaluated in breast cancer cell lines MDA-MB-231, MCF-7, SUM-149 and MDA-MB-436 cells, as well as normal HUVEC, hBMSC and MCF-10A cells by monitoring cell growth using the MTT assay. Cells were seeded (10^5 cells/mL) in 48-well plates and treated with polymer/pDNA/siRNA complexes as described earlier. Custom synthesized siRNAs targeting BCL2L12 (cat#HSS.RNAI.N001040668.12.2, IDT) and SOD1 (cat# HSC.RNAI.N000454.12.1, IDT), and pTRAIL were used for the formation of complexes [377]. The scrambled siRNA (CsiRNA) and gWIZ-GFP were used as negative controls for siRNAs and pTRAIL, respectively. In parallel, separate complexes containing either pTRAIL or siRNAs were prepared, and their efficiency was

compared to the complexes containing both the pTRAIL and siRNAs. After 72 h of incubation with complexes, cells were processed for the MTT assay as described earlier [377].

5.2.8. Gene silencing by real-time PCR

Gene knockdown of BCL2L12 and SOD1 as well as expression of TRAIL at the mRNA level in the cells (MDA-MB-231 and MCF-7) transfected with polymer/nucleic acid complexes was assessed by real-time PCR (qPCR) as described before [377]. Human endogenous housekeeping gene β-actin (Forward: 5′-GCG AGA AGA TGA CCC AGA T-3′ and Reverse: 5′-CCA GTG GTA CGG CCA GA-3′), specific BCL2L12 primers (Forward: 5'-CCC GCC CCT ATG CCC TTT TT-3' and Reverse: 5'-ATA ACC GGC CCA GCG TAG AA-3'), SOD1 primers (Forward: 5'-GTG TGA CTT TTT CAG AGT TGC T -3' and Reverse: 5' -AAG TCT GGC AAA ATA CAG GTC A -3') and TRAIL primers (Forward: 5'-ATT GTC TTC TCC AAA CTC CAA G-3' and Reverse: 5'-TGC TCA GGA ATG AAT GCC CAC-3') were used for amplification. Levels of mRNA for each gene were determined using the comparative threshold cycle method [380] and presented as fold-change relative to *β*-actin.

5.2.9. Analysis of apoptotic cell population and caspase-3 activity

MDA-MB-231 cells were seeded in 12-well plates and treated with complexes as described above. After 72 hr, induction of apoptosis was assessed by using FITC-Annexin V and Propidium Iodide staining according to the manufacturer's protocol. To elucidate apoptosis mechanism, caspase-3 activity in the cells was assayed after 48 h of transfection as described before [377]. Caspase-3 activity was expressed as increase in relative fluorescence units per hour and normalized with respect to total protein content (from BCA assay).

5.2.10. TRAIL secretion by ELISA

The secretion of TRAIL protein from MDA-MB-231 and MCF-7 cells after treatment with polymer/nucleic acid complexes was assayed through ELISA. The cells were seeded in 24-well plates (10^5 cells/mL) and transfected as described above. After 48 h of transfection, secreted TRAIL protein in the supernatants was determined by human TRAIL Duo set ELISA kit (R&D Systems; Minneapolis, MN) according to manufacturer's instructions.

5.2.11. Animal studies

All experiments were conducted in accordance with the pre-approved procedure by the Health Sciences Laboratory Animal Services (HSLAS), University of Alberta. To create breast cancer xenografts, 7-8 weeks old male ICR-Prkdc^{scid} mice (Taconic Farms; Seattle, WA) were kept in a bio-containment unit. Male mice were used because of availability. The main difference between male and female is the type of hormone present. Since triple negative breast cancer (MDA-MB-231) does not have any hormone receptor growth of MDA-MB-231 breast cancer xenograft does not depend on the hormone. Therefore, male mice can be used to evaluate the efficacy of pTRAIL and BCL2L12 siRNA co-delivery in reducing the tumor growth in *in vivo* model. Mice were anesthetized using isoflurane, shaved left flank (about 2X2 cm) and ~3 million MDA-MB-231 cells in Matrigel and PBS (1:1) were injected subcutaneously into shaved area. Tumor growth was monitored every 72-96 h and tumor volume was measured using a digital caliper. Once the tumor volume reached ≥ 50 mm^3 (length x $width^2$ x 0.5), 40 µl of pDNA/siRNA/polymer complexes (polymer: nucleic w/w ratio 5:1) were injected subcutaneously into tumor vicinity. Four injections were performed with 72-96 h apart with simultaneous

measurements of tumor volume. BCL2L12 siRNA was chosen for co-delivery with pTRAIL. The injected dose of siRNA was 6 μg/mouse while the dose of pTRAIL (3 μg/mouse) was lower than the typical 10 μg/mouse intratumoral dose used in other studies [381, 382]. Co-delivery of gWIZ-GFP (3 μg)/CsiRNA (6 μg) was used as control to evaluate the non-specific toxicity, if any, related to the delivery system and the nucleic acid. Co-delivery of pTRAIL (3 μg)/CsiRNA (6 μg) was performed to evaluate effect of pTRAIL only. About 72 h after the last injection, mice were euthanized, tumors were collected, weighted and stored in RNAlater in -20ºC until PCR analysis. Any mouse with large tumor volume (>1500 mm^3), necrotic spot or excessive weight loss (>20%) was euthanized for humane considerations.

5.2.12. Statistical analysis

The data were presented as mean ± standard deviation of three different replicates for all results except *in vivo* data. For comparison between two groups, the results were analyzed using Student's *t*-test. *In vivo* experiment represents mean ± standard deviation for groups with six to eight replicates and statistical significance was analyzed by one-way analysis of variance (ANOVA) followed by Tuckey's post hoc analysis for comparison between groups. A value of $p<0.05$ was considered significant.

5.3. Results

5.3.1. Polymer synthesis, characterization and transfection efficiency

We prepared a series of polymers by grafting unsaturated lipids α-LA and LA onto PEI1.2 via thioester bonding (**Figure 5.1A**) as described before [378] and explored their co-delivery efficiency into breast cancer cells. We were able to graft as much as 2.2 mol of lipid/mol PEI1.2.

As a control carrier, we chose the best performing polymers for pDNA and siRNA delivery from our previous studies, namely PEI-LA (LA/PEI = 2.5 mol/mol), PEI-tLA (tLA/PEI = 2.7 mol/mol) and PEI-αLA (αLA/PEI = 2.4 mol/mol) and explored their dual loading capacity (**Figure 5.1B**). These polymers showed a good capability to condense siRNA, pDNA or siRNA/pDNA mixtures into nanosized complexes, without any differences in size and charge density (Supplementary **Figure S5.2**). We monitored dual loading of nucleic acids into single complexes through flow cytometry. When the complexes were prepared separately with either Cy3-pDNA or FAM-siRNA, clear populations of corresponding fluorescence were confined to expected quadrant of the histogram in flow cytometry analysis.

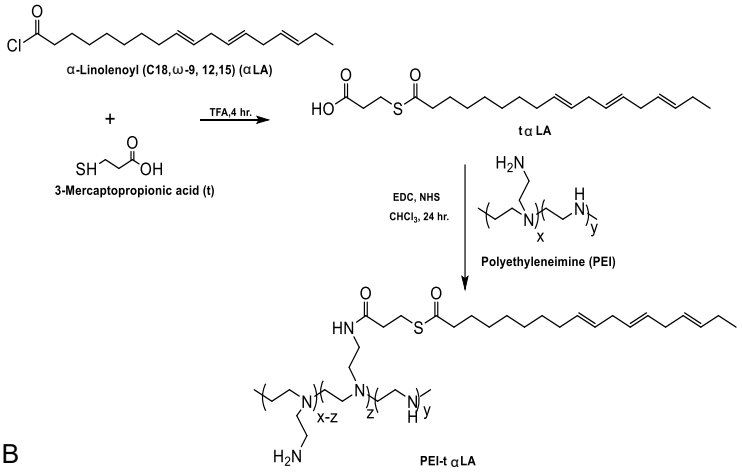

B

Polymer ID	PEI mol wt. (kDa)	Conjugated Lipid	Bonding Type	Feed Ratio Lipid/PEI(mol/mol)	Calculated fromNMR Lipid/PEI (mol/mol)
PEI1.2-LA	1.2	Linoleoyl	Amide	6.0	2.55
PEI1.2-αLA	1.2	α-Linolenoyl	Thioester	4.0	2.45
PEI1.2-tLA	1.2	Linoleoyl	Amide	6.0	2.77
PEI1.2-tαLA	1.2	α-Linolenoyl	Thioester	6.0	2.2

Figure 5.1. Synthesis of thioester linked lipopolymer. (A) Unsaturated aliphatic lipid αLA was coupled with 3-mercaptopropionic acid at room temperature via a thioester linkage. The modified αLA (tαLA) was then grafted onto PEI1.2 through an amide linkage to generate PEI-tαLA. (B) list of polymers and PEI to lipid substitution ratio.

The ternary complexes with Cy3-pDNA and FAM-siRNA were localized in the quadrant specific for double labeling, indicating co-loading of both pDNA and siRNA into the complexes (**Figure S5.3**). Dual (pDNA+siRNA) loading capability of the polymers was further confirmed by cellular uptake study in MDA-MB-231 cells (**Figure 5.2**). Flow cytometry showed that cells treated with individual nucleic acid (pDNA or siRNA) loaded complexes were localized in the quadrant of the corresponding fluorescence, whereas cells treated with the dual pDNA/siRNA complexes were localized in the quadrant associated with both fluorescence dyes, indicating efficient uptake of the ternary complexes. Broadly effective l-PEI40 was able to deliver pDNA into MDA-MB-231 cells, but not siRNA, unlike the prepared polymers.

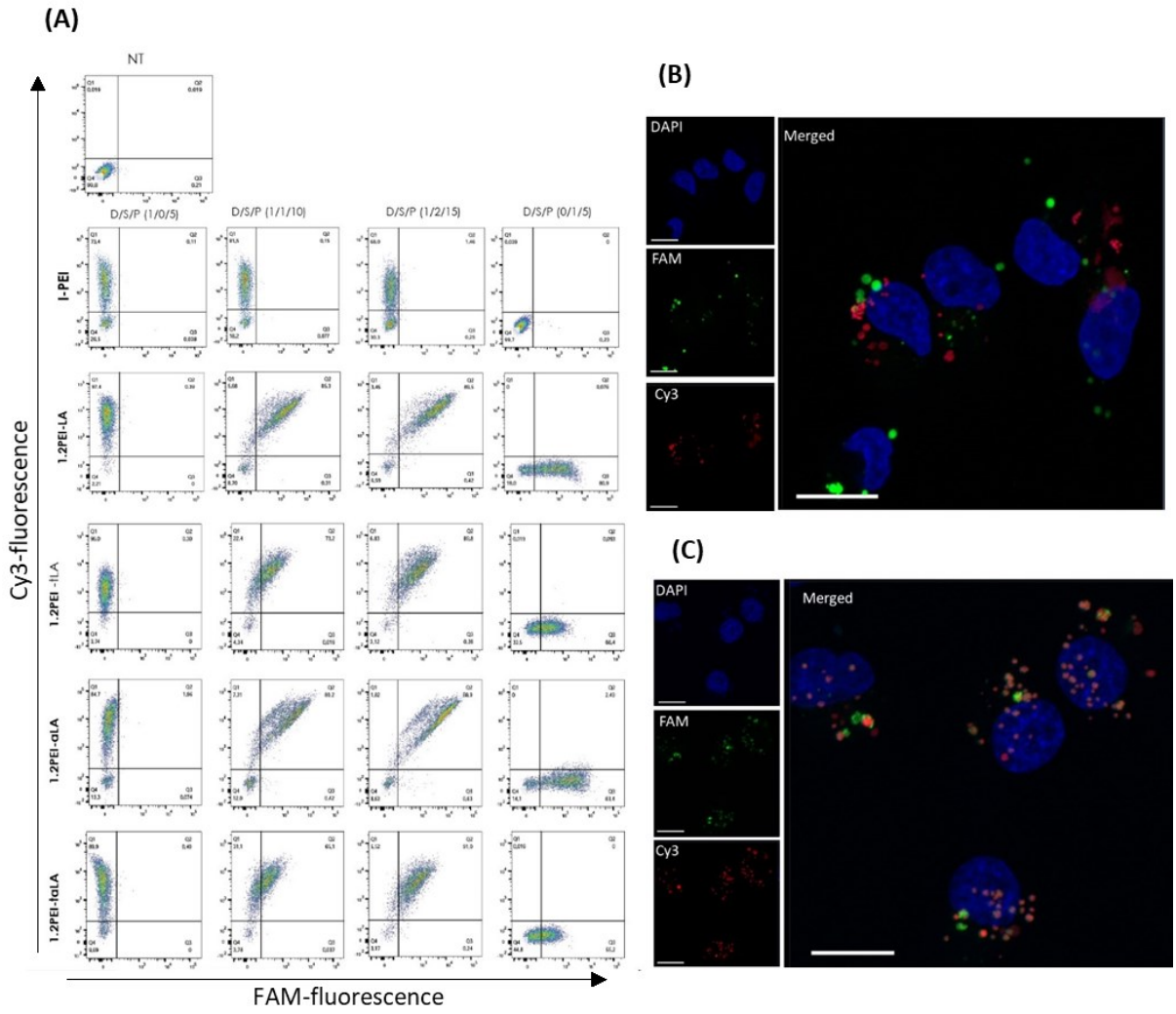

Figure 5.2. Uptake of pDNA and siRNA complexes. Cy3-pDNA and FAM-siRNA uptake in MDA-MB-231 cells was studied by flow cytometry (**A**) and confocal microscopy (**B** and **C**). For flow cytometry analysis, complexes of polymers were prepared with pDNA, siRNA or pDNA/siRNA mixture (different DNA:siRNA w/w ratios; D:pDNA, S:siRNA, P:polymer). All the polymers except l-PEI were able to co-deliver Cy3-pDNA and FAM-siRNA into MDA-MB-231 cells. For confocal microscopy, pDNA and siRNA complexes (with PEI1.2-tαLA) were visualized inside the cells by separate red and green dots, respectively. (**C**)When pDNA and siRNA were co-delivered in ternary complexes, co-localization of pDNA and siRNA was evident based on orange colored particles. Nucleus is stained with DAPI in **A** and **B** (scale bar = 20 μm).

Higher siRNA uptake was achieved by the polymers with amide bonding (PEI1.2-LA and PEI1.2-αLA) than the polymer with thioester bonding (PEI1.2-tLA and PEI1.2-tαLA) (**Figure 5.2A**). About 80% cells were FITC-siRNA positive with amide linked polymers while ~60% of cells were FITC-siRNA positive with thioester linked polymers. In case of Cy3-pDNA uptake, ~90% cells were Cy3-pDNA positive with all polymers. Interestingly, approximately 90% of cells were pDNA and siRNA positive with dual loaded complexes, indicating quite uniform uptake among the cell population (**Figure 5.2A**).

Confocal micrographs of MDA-MB-231 cells after co-delivery of pDNA and siRNA (**Figure 5.2C**) shows distinct particles that are mostly orange indicating the entrapment of both siRNA and pDNA in the same complexes. Unlike co-delivery, separate delivery of pDNA and siRNA complexes leads to distribution of distinct green (FAM-siRNA) and red (Cy3-pDNA) particles inside the cells. To measure the transfection efficiency of polymers, gWIZ-GFP complexes were formed with/without scrambled siRNA. The thioester linked polymers (PEI1.2-tLA and PEI1.2-tαLA) displayed higher transfection efficiency with/without siRNA than the amide linked polymers (PEI1.2-LA and PEI1.2-αLA) (**Figure 5.3A**), despite the amide linked polymer giving higher delivery of pDNA with/without siRNA as compared to thioester linked polymers (**Figure S5.4**). Therefore, the higher transfection efficiency of thioester–linked polymers is likely attributed to better dissociation of complexes to release the nucleic acid cargo (**Figure 5.3B**). The transfection efficiency of thioester polymers was increased with addition of siRNA (**Figure 5.3A**); as an example, as compared to pDNA/siRNA/polymer weight ratios of 1/0/5 (i.e., no siRNA), higher transfection was achieved in the presence of siRNA with weight ratios of 1/0.5/7.5, 1/1/10 and 1/2/15 (where the polymer/nucleic acid ratios were maintained at 5).

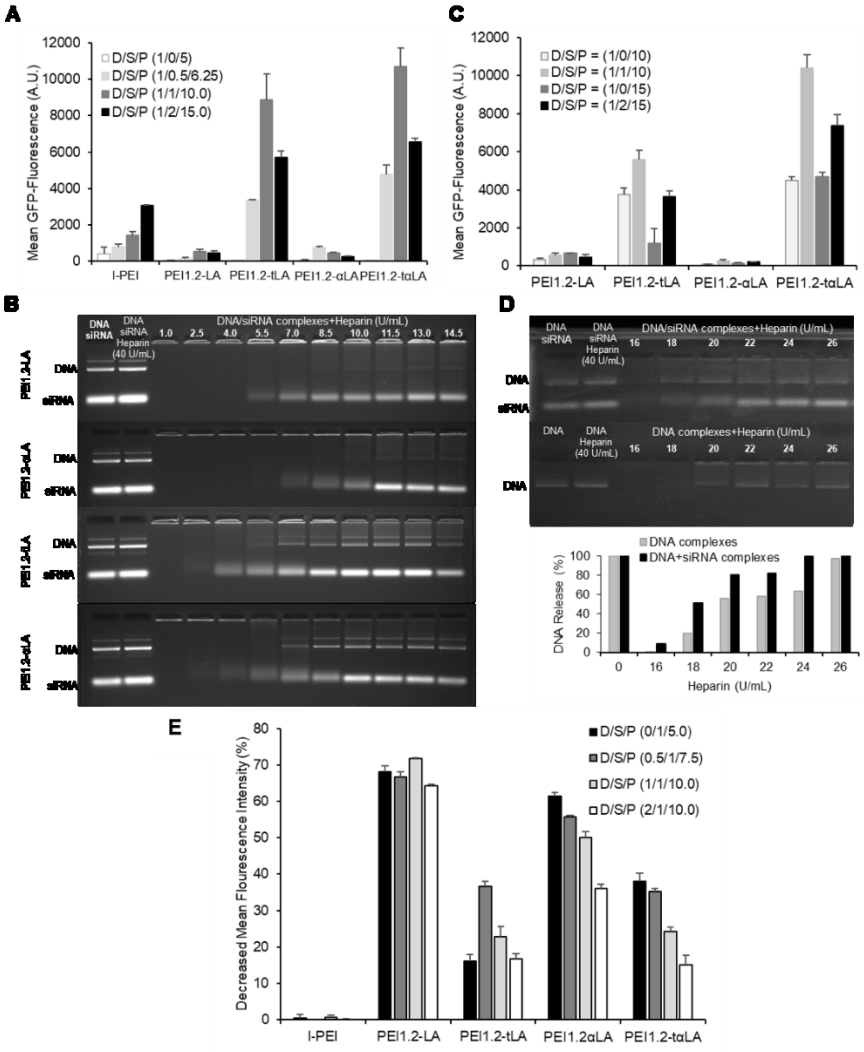

Figure 5.3: Transfection efficiency of polymers and dissociation of complexes. (**A**) DNA transfection efficiency of polymers in MDA-MB-231 cells based on GFP expression. DNA transfection efficiency of thioester linked polymers was higher than the amide linked polymers. (**B**) Heparin-induced dissociation of ternary complexes as analyzed by agarose gel retardation assay. Weight ratio of polymer to nucleic acid was 5 while pDNA to siRNA ratio was 1 for the dissociation study. Number above band represents the amount of heparin used in U/ml. (**C**) Effect of siRNA addition on pDNA transfection in MDA-MB-231 cells. Addition of siRNA increased the DNA transfection (**D**) Dissociation of complexes with/without siRNA by using heparin. Addition of siRNA increased the pDNA transfection efficiency which was attributed to better release of pDNA in the presence of siRNA. (**E**) siRNA silencing efficiency of polymers and effect of pDNA in siRNA transfection in MDA-MB-231-GFP$^+$ cells. All data were presented as mean ± SD where n=3 replicates.

Despite the significant increase in transfection efficacy after supplementing the complexes with siRNA, effect of siRNA on the uptake of PEI1.2-taLA/pDNA was minimal (**Figure S5.4**) and a heparin dissociation of PEI1.2-taLA/pDNA complexes showed faster release of pDNA when siRNA was added (**Figure 5.3D**). Therefore, the reason for higher pDNA transfection of ternary complexes (polymer/pDNA/siRNA) was because of better unpacking of the complexes due to addition of an extra anionic siRNA payload [378]. Transfection efficiency of polymers was generally increased with increasing polymer amount.

To further evaluate the net effect of siRNA addition, we also tested complexes with fixed ratio of polymer/pDNA (10 or 15) and with or without siRNA. Effect of siRNA on pDNA transfection was clear where the complexes with siRNA gave higher transfection than the complexes without siRNA (**Figure 5.3C**). Therefore, co-delivery of pDNA and siRNA may not only improve therapeutic response, but also enhanced transgene expression. We further evaluated the complexes with similar composition for siRNA silencing efficiency. Analogous to the use of scrambled siRNA in previous studies, blank gWIZ plasmid was used to assess the effect of pDNA on siRNA silencing efficiency. The silencing efficiency was expressed as a percentage of GFP fluorescence in MDA-MB-231-GFP^{+} cells by using GFP-specific siRNA. Unlike pDNA transfection, amide-linked polymers gave higher GFP silencing than thioester-linked polymers (**Figure 5.3E**). In general siRNA silencing efficiency of all polymers was decreased with the addition of pDNA. Indeed, same level of siRNA silencing was achieved when the siRNA amount was double than the pDNA amount with PEI1.2-tαLA. Since, PEI1.2-tαLA polymer facilitated high transgene expression and siRNA silencing efficiency with the optimal pDNA to siRNA ratio, this polymer was further explored for co-delivery of pTRAIL and its complementary siRNAs.

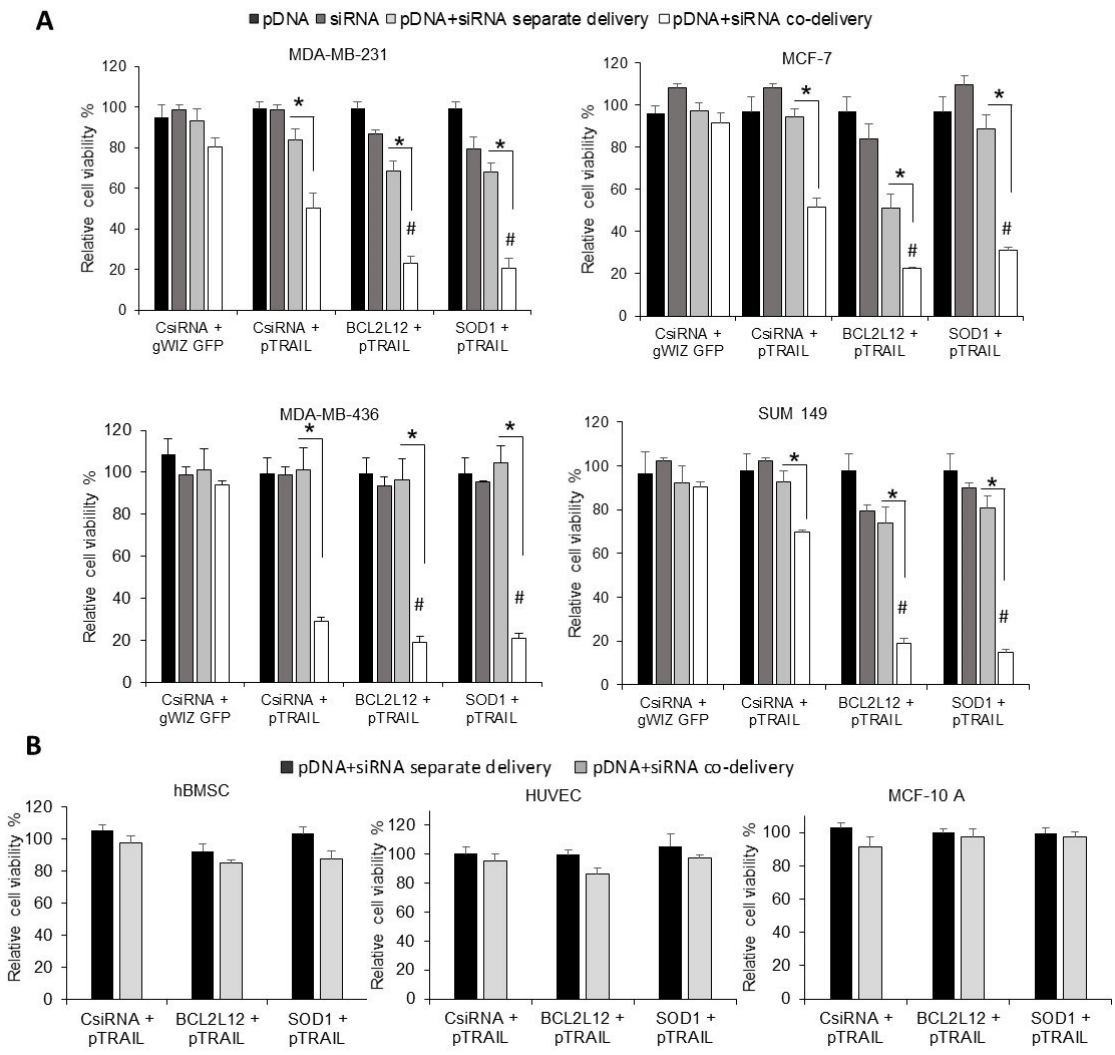

Figure 5.4. Effect of complexes on growth inhibition of breast cancer cells and effect on normal cells. (**A**) Cell viability in four separate breast cancer cells (MTT assay) after complex treatment. For MDA-MB-231, 30 nM of siRNA was used while 20 nM of siRNA was used for remaining cell lines. The siRNA:pTRAIL ratio was 4 (w/w) and polymer:nucleic acid ratio was 5 in all cases. The cell viability was expressed as a percentage of non-treated cells. # $p < 0.05$ compared with CsiRNA and pTRAIL co-delivery. *$p < 0.05$ compared with separate delivery of same amount of nucleic acids. In all cell lines, co-delivery resulted in higher cell death than separate delivery. (**B**) Toxicity of pTRAIL and siRNAs combinations in hBMSC, HUVEC and MCF-10A cells when delivered via separate complexes or together in the same complexes. The cell viability was expressed as a percentage of non-treated cells. None of formulation induced were toxic to these cells. All data were presented as mean ± SD where n=3 replicates.

5.3.2. Co-delivery of pTRAIL and siRNAs for induced cell death

The effects of pTRAIL treatment in combination with BCL2L12 and SOD1 siRNAs on growth inhibition of different breast cancer cells (MDA-MB-231, MCF-7, MDA-MB-436, SUM-149) are summarized in **Figure 5.4A**. The pTRAIL on its own (within indicated doses) was not effective in breast cancer cells, but when pTRAIL was co-delivered with CsiRNA, significant cell death was observed. The co-delivery of gWIZ-GFP/CsiRNA remained non-toxic, which indicated the enhanced cell death was due to secretion of TRAIL. When CsiRNA was replaced with BCL2L12 and SOD1 siRNAs, significantly enhanced cells death was observed in all cells as compared to pTRAIL/CsiRNA treatment. Responses to separate delivery of pTRAIL combination with CsiRNA or BCL2L12 or SOD1 siRNAs varied with cell lines. Separate delivery of pTRAIL and BCL2L12 resulted in higher cell death in MCF-7 cells than in other cells. More importantly, co-delivery of pTRAIL and BCL2L12 or SOD1 siRNAs within the same complex displayed significantly higher cell death than separate delivery of same dose of pTRAIL and siRNAs complexes (**Figure 5.4A**), giving synergism between therapeutic agents only in co-delivered formulations. All pTRAIL and siRNAs combinations, either co-delivered or separately-delivered, had minimal effect on normal (non-malignant) cells; hBMSC, HUVEC and MCF-10A cells, compared to the effect achieved in breast cancer cells under similar conditions (**Figure 5.4B**).

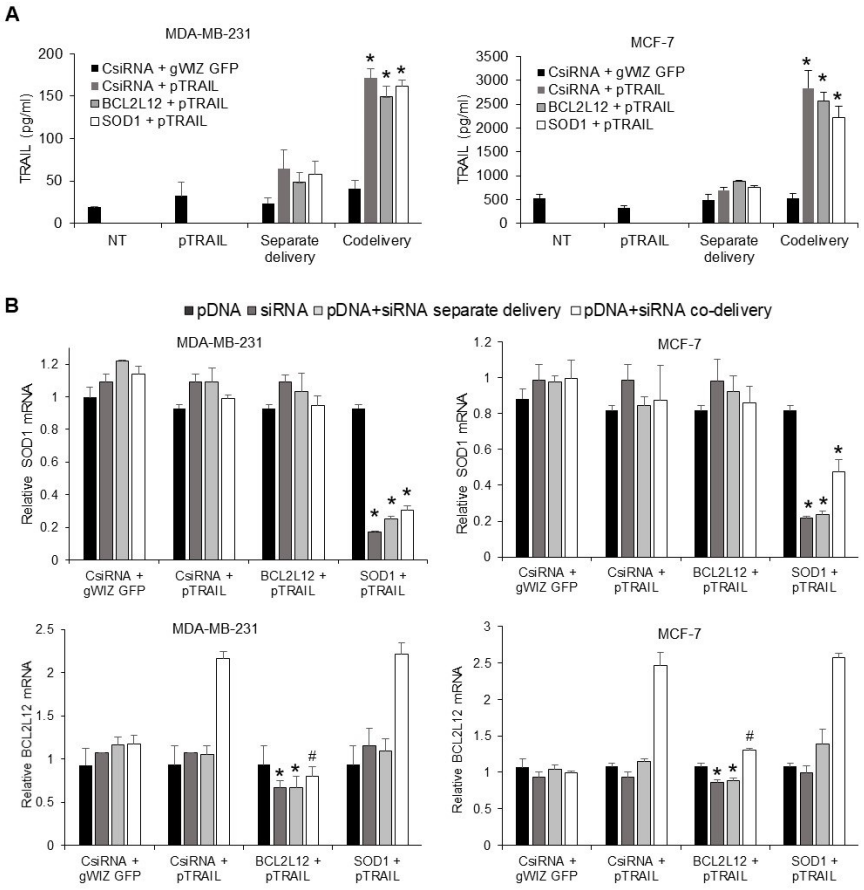

Figure 5.5. Analysis of TRAIL secretion and siRNA mediated silencing. (**A**) Secretion of TRAIL protein into cell culture supernatants of MDA-MB-231 and MCF-7 cells measured by ELISA. Addition of siRNA into the complexes increased the secretion of TRAIL protein. *$p < 0.05$ compared with pTRAIL alone or separate delivery of respective complexes. (**B**) Silencing of BCL2L12 and SOD1 in MDA-MB-231 and MCF-7 cells by qPCR analysis. The mRNA levels were normalized with respect to non-treated cells. *$p < 0.05$ compared with CsiRNA. $^{\#}p < 0.05$ compared with CsiRNA and pTRAIL co-delivery or SOD1 and pTRAIL co-delivery. All data were presented as mean ± SD where n=3 replicates.

5.3.3. Secretion of TRAIL protein and siRNA silencing in breast cancer cells

To confirm the underlying basis of cell killing following pTRAIL/siRNA delivery, TRAIL protein secretion and target silencing by BCL2L12 or SOD1 siRNAs were investigated. Co-delivery of pTRAIL and siRNAs resulted in higher TRAIL secretion than separate delivery in both

MDA-MB-231 and MCF-7 cells (**Figure 5.5**), similar to GFP expression results above. We observed higher TRAIL secretion in MCF-7 cells (~2500 pg/mL) compared to MDA-MB-231 cells (~200 pg/mL), in line with higher induction of TRAIL mRNA in the MCF-7 cells (**Figure S5.5**). The relative quantity of SOD1 mRNA after specific siRNA treatment either alone or in combination with pTRAIL (i.e., separate delivery vs. co-delivery) was significantly less than the CsiRNA treatment in both cell lines. SOD1 mRNA silencing after co-delivery of pTRAIL/SOD1 siRNA was not as effective as delivery of SOD1 siRNA alone in MDA-MB-231 (~17% vs. 30% silencing vs. non-treatment) and MCF-7 (~21% vs. 47% silencing vs. non-treatment). However, the BCL2L12 mRNA levels displayed a more complex behavior; BCL2L12 mRNA expression was increased upon pTRAIL/siRNA co-delivery (with CsiRNA or SOD1 siRNA), but the increase was attenuated with BCL2L12 siRNA inclusion in the complexes. The BCL2L12 silencing after pTRAIL/BCL2L12 co-delivery was found to be equivalent to CsiRNA treatment group, but the effect of BCL2L12 siRNA was manifested by preventing its increase above the levels found in non-treated cells.

5.3.4. Apoptosis and caspase-3 induction by pTRAIL and siRNA co-delivery

We further explored the effect of separate and co-delivery of pTRAIL and siRNAs on apoptosis induction (**Figure 5.6**). No significant apoptosis was observed with pTRAIL alone, nor by BCL2L12 or SOD1 siRNA as compared to CsiRNA with the chosen doses. Most of the cells in these groups were Annexin-FITC and PI negative (**Figure S5.6**) In line with **Figure 5.4,** co-delivery of pTRAIL/siRNAs (CsiRNA, BCL2L12 or SOD1) induced more apoptosis than the separate delivery. Co-delivery of pTRAIL and BCL2L12 or SOD1 siRNAs resulted in significantly higher levels of apoptosis (64.7% and 65.3%, respectively) in MDA-MB-231 cells

compared to co-delivery of pTRAIL/CsiRNA (44.6%**)**. Caspase-3 was also induced in MDA-MB-231 cells after co-delivery, consistent with activation of intrinsic apoptotic pathway (**Figure 5.6**).

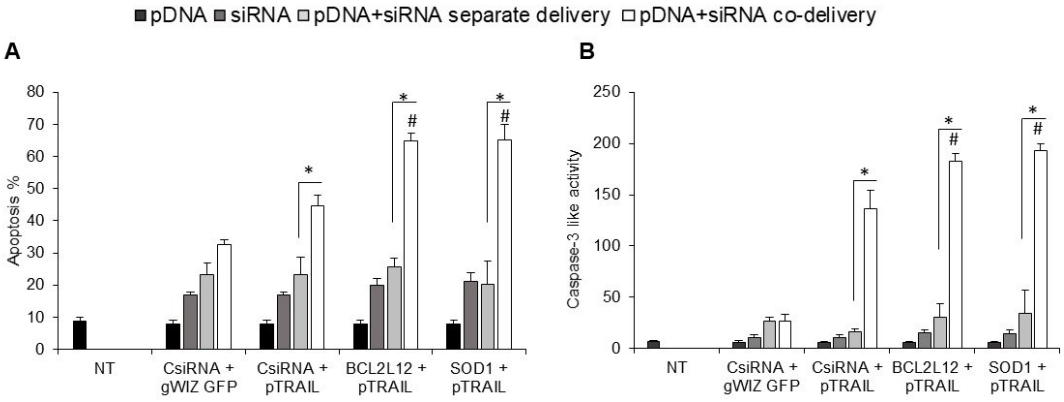

Figure 5.6. Apoptosis and caspase activation in MDA-MB-231 cells. Cells were treated with combination of pTRAIL and siRNAs (CsiRNA, BCL2L12 or SOD1 siRNAs) as a separate or co-delivery of complexes. Apoptosis (**A**) and caspase assays (**B**) were performed after 72 and 48 h of transfection, respectively. Apoptosis induction as well as caspase-3 activity was increased after co-delivery than separate delivery of complexes. *$p < 0.05$ compared to separate delivery of respective complexes. $^{\#}p< 0.05$ compared to CsiRNA and pTRAIL co-delivery. All data were presented as mean ± SD where n=3 replicates.

5.3.5. Antitumor activity of pTRAIL/BCL2L12 siRNA delivery *in vivo*

MDA-MB-231 xenografts were established in mice and treated with combinations of gWIZ-GFP/CsiRNA (as negative control), pTRAIL/CsiRNA (TRAIL therapy alone) and pTRAIL/BCL2L12 siRNA (TRAIL and specific siRNA therapy) at indicated time points in **Figure 5.7.** Co-delivery of gWIZ-GFP/CsiRNA did not affect the tumor growth (not significantly different from non-treated tumors). Co-delivery of pTRAIL/CsiRNA was effective in significantly reducing tumor volume only after day 11. Co-delivery of pTRAIL/BCL2L12 siRNA showed the most

potent response, giving significant tumor retardation compared to non-treatment group after day 4 and to gWIZ-GFP/CsiRNA co-delivery group after day 8 (**Figure 5.7A**).

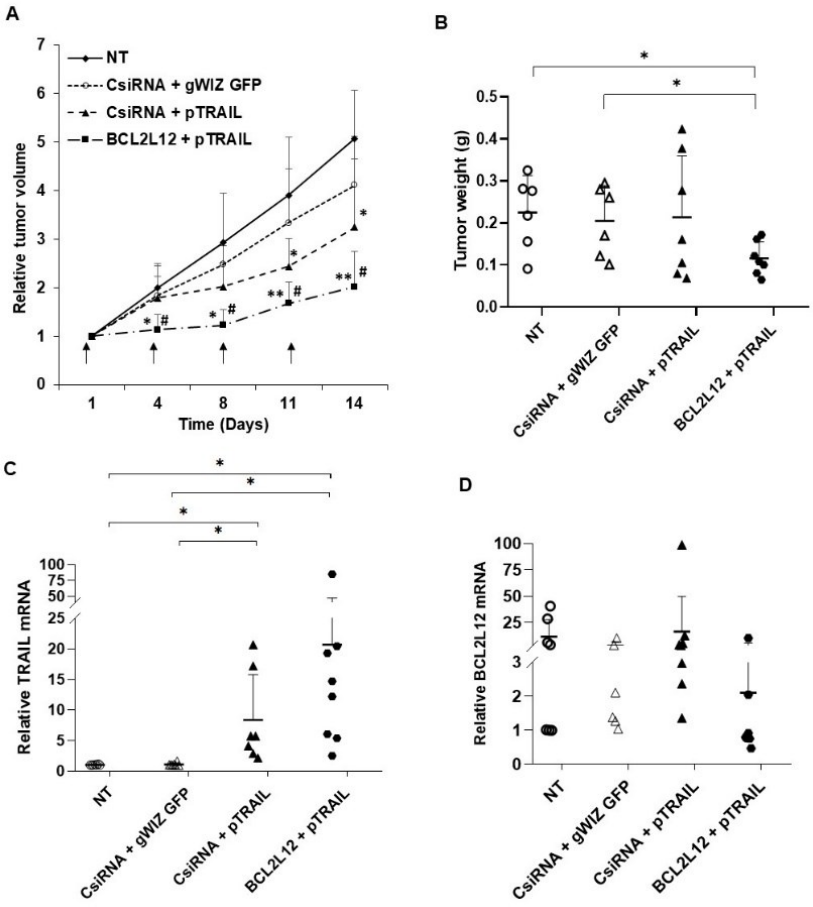

Figure 5.7. Tumor growth inhibition after nucleic acid co-delivery. Polymer/nucleic acid complexes were injected into the tumor vicinity. Data represent mean ± SD of n = 6-8 at each time point. (**A**) Relative tumor volumes (tumor volume at a time point/initial tumor volume) as a function of time. Black arrows indicate the time of injections. Only positive SD bars were shown for clarity. Both the pTRAIL/CsiRNA and pTRAIL/BCL2L12 retarded the tumor growth. Tumor volume after treatment of pTRAIL/CsiRNA was significantly less than untreated tumors after day 11 (*$p < 0.05$). Treatment with pTRAIL/BCL2L12 siRNA was more effective in reducing the tumor growth. Tumor volume was significantly lower that untreated and gWIZ-GFP/CsiRNA treatment groups (*$p<0.01$, **$p<0.001$ vs. NT and #$p<0.05$ vs. gWIZ-GFP/CsiRNA by ANOVA). (**B**) Wet weight of extracted tumors at the end of study also indicated the retardation of tumor growth by pTRAIL/BCL2L12 siRNA treatment (*$p<0.05$). (**C**) Level of TRAIL mRNA in both pTRAIL treatments was significantly higher than the control group (*$p < 0.05$). (**D**) The level of

BCL2L12 mRNA was lower in most of pTRAIL/BCL2L12 treatment but was not significant due to variation in mRNA level within group including untreated animals.

The tumor weights recovered at the end of the study were in line with measured changes in tumor volume, where the lowest tumor weight was observed with the pTRAIL/BCL2L12 siRNA treatment (**Figure 5.7B**). We also assessed TRAIL expression by quantification of mRNA through qPCR analysis; high TRAIL mRNA expression was evident in pTRAIL treatment group, which was significantly higher than the other groups (**Figure 5.7C**). Despite similar level of TRAIL mRNA, pTRAIL/CsiRNA was not as effective as pTRAIL/BCL2L12 siRNA in reducing the tumor volume, which further confirmed the role of BCL2L12 siRNA in sensitizing TRAIL. Although we were not able to see a significant silencing of BCL2L12 mRNA in pTRAIL/BCL2L12 treated group as compared to un-treated (due to high variations among samples in study groups) we observed low levels (<1) of BCL2L12 mRNA in most of the pTRAIL/BCL2L12 treated tumors (**Figure 5.7D**).

5.4. Discussion

To facilitate TRAIL therapy in a clinical setting, we explored the possibility of co-delivering pTRAIL to enhance *in situ* availability of the protein and siRNAs that sensitize malignant cells to TRAIL action both *in vitro* and *in vivo* models. Co-delivery of pDNA and siRNA is envisioned as a milestone approach for the treatment of drug-resistant cancers since it can trigger synergistic effects via complementary pathways which is greater than the sum of the constituent components. Many aggressive heterogeneous cancers where targeting individual signaling pathway have failed to block abnormal proliferation will benefit from this strategy [71]. Identification of ideal carrier that can accommodate nucleic acid combinations is always challenging due to variations in ionic charge density, size and stiffness of the constituent nucleic

acid molecules. Here, we designed specific cationic lipopolymers tailored by grafting aliphatic lipids via thioester bonding for this particular purpose. One can independently vary the polymeric backbone, the nature of hydrophobe and the linkage chemistry of these lipopolymers to make it suitable for co-delivery of nucleic acids. These polymers efficiently accommodated both pDNA (e.g. pTRAIL) and siRNAs (e.g. BCL2L12 and SOD1 siRNA) into single complexes.

In our previous study, using high-throughput screening, we identified siRNAs against BCL2L12 and SOD1 that sensitized breast cancer cells to TRAIL protein to induce apoptosis [377]. Therefore, we assessed the therapeutic potency of pTRAIL plasmid and siRNAs (silencing BCL2L12 and SOD1) to inhibit breast cancer growth in this study. We were able to enhance cell death in breast cancer cells via simultaneous induction of apoptosis with pTRAIL and inhibition of antiapoptotic proteins with specific siRNAs which further potentiated TRAIL action. More importantly, co-delivery of pTRAIL and BCL2L12 or SOD1 siRNAs elicited potent anticancer response than the separate delivery at similar doses. Better therapeutic outcome after co-delivery of these nucleic acid was because of (i) improved TRAIL expression due to additive actions of the supplemented siRNAs, and (ii) sensitization TRAIL action by co-delivered siRNAs (silencing BCL2L12 and SOD1). We previously showed that addition of extra polyanions (e.g., hyaluronic acid) enhanced the release of payload and resulted in higher transfection [378] and the siRNA in the current complexes also improved the dissociation (**Figure 5.3D**) efficacy of the complexes. In line with our findings, pDNA transfection was increased with siRNA when co-delivered with arginine-based PEI [73] and poly(L-lysine) with or without oligomeric sulfadiazine [72]. However, other non-viral delivery systems used to co-deliver pDNA and siRNA such as polymer coated gold nanoparticles [114] and PEI modified poly-(lactide-co-glycolic acid) nanoparticle [113] were unable to show beneficial effect of siRNA additive on transgene expression. To co-deliver pDNA

and siRNA by polymer coated gold nanoparticles and PEI modified poly-(lactide-co-glycolic acid) nanoparticles, layers of pDNA and siRNA were added on the surface of pre-made nanoparticles without affecting compactness of nanoparticles, so that presence of the second polyanion had no effect on transgene expression.

In addition to enhanced transgene expression, the BCL2L12 and SOD1 siRNAs sensitized the TRAIL action by facilitating apoptosis induction. BCL2L12 is known to inhibit the caspase-3/7 thereby impeding apoptosis. The other target, SOD1 maintains the levels of reactive oxygen species (ROS) under a critical threshold to protect cells from ROS damage. Therefore, silencing SOD1 is likely to increase ROS levels causing oxidative damage to cellular lipids, proteins and DNA, inducing apoptosis [349]. Therefore, co-delivery of pTRAIL and these siRNAs (silencing BCL2L12 and SOD1) generated higher apoptosis via increased caspase-3 activity in MDA-MB-231 cells, which was in line with our previous results where the delivery of BCL2L12 and SOD1 siRNAs with recombinant TRAIL protein substantially induced apoptosis [377]. Despite the absence of caspase-3, MCF-7 can undergo apoptosis via activation of caspase-6 independent of caspase-3/7 [358]. It was not surprising to see increased BCL2L12 expression (mRNA) upon pTRAIL treatment since it could facilitate survival of malignant cells in the face of TRAIL threat [353] but co-delivery of pTRAIL and BCL2L12 siRNA prevented the BCL2L12 mRNA induction. Up-regulation of the pro-survival transcription factor Nuclear Factor-κB (NF-κB) by TRAIL in different pancreatic cell lines is another example of TRAIL induced-survival response [383]. Although TRAIL protein has minimal effect on the normal cells, strategies to increase the TRAIL potency may increase the toxicity of TRAIL therapy. Fortunately, this was not the case in this study. Co-delivery of pTRAIL and BCL2L12 or SOD1 siRNAs did not induce any toxicity in non-transformed cells *in vitro.*

Co-delivery of pTRAIL and the specific siRNAs not only enhanced the TRAIL potency in TRAIL sensitive cells, but also reversed the TRAIL resistance. Among the cells lines used, MCF-7 was resistant to TRAIL therapy, which was attributed to the higher expression of decoy receptor TRAIL-R4 [384] and the defects in apoptosis pathway such as the lack of caspase-3, minimal caspase-8 expression and expression of higher anti-apoptotic proteins relative to pro-apoptotic protein [385]. Despite the resistance to TRAIL, co-delivery of pTRAIL and BCL2L12 or SOD1 siRNA to MCF-7 cells turned out to be as effective as TRAIL treatment in sensitive cells. TRAIL expression (at both mRNA and protein levels) was ~16-fold higher in MCF-7 cells compared to MDA-MB-231 cells, which could have caused the reversal of TRAIL resistance. Separate delivery of pTRAIL and BCL2L12 siRNA also resulted in significant cell death of MCF-7 cells, which was increased with co-delivery. Therefore, silencing BCL2L12 is another mechanism to reverse TRAIL resistance in MCF-7 cells.

In vivo results further confirmed the potency of pTRAIL and BCL2L12 siRNA co-delivery in retarding tumor growth in breast cancer xenograft model. We are aware of only two studies which evaluated non-viral delivery systems for co-delivery of pDNA and siRNA *in vivo* [113, 386]. One study explored PLGA nanoparticles to co-deliver SOX9 gene and anti-Cbfa-1 siRNA to stimulate chondrogenesis in human MSCs *in vivo* [113]. In that study, human MSCs were transfected *in vitro* and transfected cells were administered to mice, which did not rely on the efficacy of delivery systems under physiological conditions. Another study utilized surface-functionalized polymer microparticles for dual delivery of IL-10 targeted siRNA and pDNA vaccines to dendritic cells to modulate T-cell responses [386]. Since siRNA was encapsulated and pDNA was coated on the surface of microparticles, siRNA did not affect the transfection efficiency of pDNA. To our knowledge, this is the first *in vivo* study demonstrating co-delivery of pTRAIL

and BCL2L12 siRNA in breast cancer xenografts, reflecting the limited success of co-delivering pDNA and siRNA with a single carrier in the past. Most importantly, co-delivery enabled us to achieve tumor growth inhibition with low dose of pTRAIL (3 μg/mouse) as compared to typical 10 μg/mouse intratumoral dose used in other studies [381, 382]. Reducing the dose will be beneficial to attenuate the side effects when employed in clinics. Future studies to co-deliver the pTRAIL and BCL2L12 siRNA systemically will expand the scope of our proposed TRAIL therapy.

5.5. Conclusions

We describe ternary complexes of polymer/pDNA/siRNA that were more efficient than the binary complexes (polymer/pDNA and polymer/siRNA). Upon co-delivery of pTRAIL and BCL2L12 siRNA in an *in vivo* model, the growth of breast cancer tumor was significantly retarded which was the consequences of (i) increased *in situ* TRAIL protein secretion due to polyanionic siRNA, and (ii) sensitization of cells to TRAIL action by BCL2L12 silencing. The convergent action of these two mechanisms ultimately induced a stronger apoptotic effect and inhibited the anti-apoptotic response, resulting in a promising therapeutic activity in both *in vitro* and *in vivo* models. Hence, the dual mode of delivery with a single carrier may provide a novel framework for nucleic acid combination therapy to potentiate the anticancer activity of TRAIL.

5.6. Acknowledgements

The authors are grateful for the technical assistance of Mr. Cezary Kucharksi and Dr. Juliana Valencia Serna (Department of Chemical and Material Engineering) with the animal studies, Dr. Markian Bahniuk (Department of Chemical and Material Engineering) with plasmid

expansion and purification, and Janine Schmitke (Department of Chemical and Material Engineering) with gel electrophoresis. B.T. is supported by Alberta Innovates Graduate Studentship. This study was supported by an Operating Grant from the Canadian Institutes of Health Research (CIHR), and a Discovery Grant from the Natural Sciences and Engineering Research Council of Canada (NSERC).

Chapter 6

Modified mRNA delivery for TRAIL mediated cytotoxicity of breast cancer cells

A version of this chapter will be submitted for publication as:

Bindu Thapa, Remant KC, Uludag, Modified mRNA delivery for TRAIL mediated cytotoxicity of breast cancer cells.

6.1. Introduction

Gene therapy holds a great promise to treat acquired or genetic diseases. Both viral and non-viral vectors were used in delivery of gene-based medicines. Immunogenicity, potential of insertional mutagenesis and/or serious toxicities associated with viral vectors limit their use in a clinical setting. After decades of efforts, only a limited number of gene-based therapeutics with viral vectors, such as adenoviral vector encoding p53 and adeno-associated viral vector encoding lipoprotein lipase, were approved for human use [387, 388]. Alternatively, non-viral vectors such as nano-assembled complexes with cationic lipids, polymers and peptides are increasingly used to deliver plasmid DNA (pDNA) [238, 389, 390]. Low transfection efficiency and the potential of insertional mutagenesis are major concerns associated with the non-viral vectors. Nuclear transport of pDNA is a major hurdle for pDNA transfection which is especially critical in non-dividing or slow-dividing cells [391-393]. Recently, messenger RNA (mRNA) garnered significant attention for expressing therapeutic proteins to avoid the problem associated with the need for nuclear delivery of pDNA [394-396]. Unlike pDNA, mRNA does not require to be transferred into the nucleus and can be processed in the cytoplasm. Therefore, easier protein expression can be achieved especially in non-dividing and hard-to-transfect cells. The risk of permanent integration of pDNA into the genome can be excluded with the mRNA, since it has a relatively short half-life in cytoplasm (~7.1 h median half life) and usually degraded after translation [397, 398]. In addition, mRNA is devoid of immunogenic CpG motif which makes it less immunogenic, therefore, pDNA and vector induced immunogenicity may be avoidable [393]. The mRNA delivery is being increasing used to treat diseases caused by deficiencies of proteins [399-401].

In this study, we explored the use of mRNA to induce apoptosis in breast cancer cells by employing a trimeric tumor necrosis factor apoptosis inducing ligand (TRAIL) specific mRNA.

TRAIL, a member of tumor necrosis factor superfamily, has emerged as a promising cancer therapeutic because of its ability to induce apoptosis in variety of cancer cells while sparing the vital normal cells [115, 189]. Rapid clearance of systemically administered recombinant TRAIL protein via kidneys results in short serum half-life of only 3-5 min in rodents and 23-31 min in nonhuman primates. This is major problem in clinical use of TRAIL protein [180]. Delivery of mRNA can prolong the TRAIL exposure to tumor site which is achieved via sustained expression of TRAIL at site of action. To this end, we explored the effect of TRAIL secreting mRNA (mTRAIL) in breast cancer cells. We further investigated the possibility of modifying hard-to-transfect human bone marrow stromal cells (hBMSC) with mTRAIL, comparing the transfection efficiencies achieved with mRNA over pDNA. On one hand, we envision the possibility of using the mTRAIL modified hBMSC as a stand alone therapy to induce apoptosis in breast cancer cells. On the other hand, mTRAIL modified hBMSC could serve as a model to investigate the effects of mRNA modification of by-stander cells in the vicinity of breast cancer tumors.

As in other gene-based therapies, the major hurdle to translate advantage of mRNA use in clinics remains delivery into eukaryotic cells. After the delivery of mRNA using cationic lipid for first time [402], several synthetic delivery vehicles were reported for delivery of mRNA [395, 396, 403]. Several cationic carriers such as cationic lipids [404, 405] and cationic polymers e.g. poly(β-amino esters), triblock polymer containing cationic dimethylaminoethyl methacrylate [394, 406] have been used to deliver mRNA translating therapeutic as well as reporter proteins. We have been working on developing low molecular weight (MW 0.6 to 1.8 kDa) polyethyleneimine (PEI) lipopolymers (L-PEI) for nucleic acid delivery. These are uniquely designed non-viral vectors that display dual characteristics features essential for nucleic acid delivery; cationic charge to bind nucleic acid and lipophilicity to enhance cellular uptake [110, 207, 337, 407]. Inspired from our

previous studies on pDNA and siRNA delivery with these carriers, here, we explored L-PEI reagents for mRNA delivery for the first time and systemically evaluated the effect of mTRAIL over pTRAIL to induce apoptosis in breast cancer cells. We further investigated the kinetics of TRAIL protein secretion with mRNA in breast cancer cells and hBMSCs. Given the instability and rapid degradation of mRNA inside cytoplasm [398], we employed a chemically modified mRNA (modRNA) designed to express TRAIL based on modification with 3'-O-Me-m7G(5') ppp(5')G and replacing uridine with N1-methylpseudorudine. Such chemically modified mRNAs offer increased stability and better performance especially in an *in vivo* setting [408, 409].

6.2. Materials and Methods

6.2.1. Materials

Branched 1.2 kDa PEI (PEI1.2) was obtained from Polysciences, Inc. (Warrington, PA, USA) and used without further purification. (3-(4,5-Dimethylthiazol-2-yl)-2,5-diphenyltetrazolium bromide (MTT), and organic solvents were obtained from Sigma-Aldrich (St. Louis, MO). Cell culture medium, Dulbecco's Modified Eagle's Medium (DMEM)/F12, supplied with L-glutamine and 25 mM HEPES, and penicillin (10.000 U/mL)/streptomycin (10 mg/mL) were obtained from Invitrogen (Grand Island, NY). Fetal Bovine (FB) essence 100% US origin serum was obtained from VWR Life Science Paradigm (Radnor, PA). gWIZ-GFP plasmid (pGFP) was obtained from Aldevron (Fargo, ND) and TRAIL expressing plasmid (pTRAIL) was a generous gift from Prof. Dai-Wu Seol (College of Pharmacy, Chung-ang University, South Korea) and it was prepared and characterized as described before [376]. GFP expressing mRNA (mGFP) was obtained from Pharna (Houston, TX).

6.2.2. Cell culture

Human breast cancer cells MDA-MB-231 and MCF-7 were obtained from Dr. Judith Hugh (Department of Oncology, U. of Alberta) and SUM-149 was obtained form Dr. Raymond Lai (Department of Laboratory Medicine and Pathology, U. of Alberta). MDA-MB-231, MCF-7 and SUM-149 were maintained in DMEM/F12 supplemented with 10% FB essence, 100 unit/mL penicillin, and 100 µg/mL streptomycin. Human bone marrow stromal cells (hBMSC) were obtained and maintained as described earlier [336]. All the cell lines were authenticated by STR DNA profiling analysis at Genetic Analysis Facility, The Hospital for Sick Children (Toronto, ON).

6.2.3. In vitro synthesis of TRAIL bearing mRNA (mTRAIL)

mRNA was synthesized *in vitro* using T7 RNA polymerase-mediated transcription from a linearized DNA template, which incorporates the 5'and 3'UTRs and a poly-A tail as previously described [410]. RNA was purified using Ambion MEGA clear spin columns and then treated with Antarctic Phosphatase (New England Biolabs) for 30 min at 37°C to remove residual 5′-phosphates. Treated RNA was re-purified and quantified by Nanodrop (Thermo Scientific). After purification, modRNA was resuspended in 10 mM Tris HCl, 1 mM EDTA at 1µg/µl for use and stored at -80ºC. In mRNA, all uridine was fully replaced by N1-methylpseudouridine. Open reading frame sequence for human TRAIL modRNA is provided in the **Figure S6.1**.

6.2.4. Polymer synthesis, complex preparation and transfection efficiency

Lipid-modified PEIs were synthesized via *N*-acylation using carboxyl end-capped aliphatic lipids as reported previously [378]. Transfection efficiency of the polymers was assessed in breast

cancer cells and hBMSC through flow cytometry using GFP expressing plasmid (pGFP) and mRNA (mGFP). Cells were seeded in 48 well plate (10^5 cells/mL) and grown overnight. The complexes (polymer/mRNA, or polymer/pDNA were prepared at room temperature by incubating the polymers and nucleic acids with different polymer: nucleic acid w/w ratio in serum free DMEM for 30 min. After 30 min of incubation, complexes were added directly to the cells and GFP expression was analyzed by flow cytometry after 48 h post-transfection as described earlier [337].

6.2.5. Effect of mTRAIL/pTRAIL complexes and mTRAIL modified- hBMSCs on viability of breast cancer cells.

Cytotoxic efficacy of TRAIL-expressing DNA (pTRAIL) and mRNA (mTRAIL) was evaluated in breast cancer cell lines MDA-MB-231, MCF-7 and SUM-149 cells, as well as in normal hBMSC cells by monitoring cell viability using the MTT assay. Cells were seeded (10^5 cells/mL) in 48-well plates and treated with polymer/pDNA or polymer/mRNA complexes as described earlier. After 72 h of incubation with complexes, cells were processed for the MTT assay as described earlier [377]. Cytotoxic activity of mTRAIL modified hBMSC was studied by MTT after co-culturing modified hBMSC with SUM-149 cells. hBMSC were seeded in 48 well plate ($8x10^4$ cells/mL) and complexes of pTRAIL and mTRAIL with polymers were added. After 6 h or 24 h incubation with complexes, hBMSC were washed with HBSS (x3) and trypsinized. Then, fixed number of cells (10,000 or 5,000 cells) from each group were added to the 48-well plate containing SUM-149 cells. hBMSC transfected with GFP-expressing plasmid (pGFP) and mRNA (mGFP) was used as negative control to calculate non-specific toxicity of complexes. After 72 h of co-culture, MTT assay was performed to evaluate cell viability which was normalized with SUM-149 + non-treated hBMSC co-culture group.

6.2.6. Analysis caspase-3 activity

MDA-MB-231 and SUM-149 cells were seeded in 24-well plates and treated with complexes as described above. After 48 h of transfection in MDA-MB-231 and after 12 of transfection in SUM-149 cells, caspase-3 activity in the cells was assayed as described before [377]. Caspase-3 activity was expressed as increase in relative fluorescence units per hour and normalized with respect to total protein content (from BCA assay).

6.2.7. TRAIL secretion by ELISA

The secretion of TRAIL protein from MDA-MB-231, SUM-149 and hBMSC cells after treatment with polymer/nucleic acid complexes was assayed through ELISA. The cells were seeded in 48-well plates and transfected as described above. The supernatant was collected at different time points and amount of TRAIL protein in supernatant was determined by human TRAIL Duo set ELISA kit (R&D Systems; Minneapolis, MN) according to manufacturer's instructions.

6.2.8. Animal experiment

All experiments were conducted in accordance with the pre-approved procedure by the Health Sciences Laboratory Animal Services (HSLAS), University of Alberta. To create breast cancer xenografts, 12-14 weeks old female mice NOD.Cg.Prkdc(Scid)II2rg (from breeding facility of Dr. Lynne Postovit lab, University of Alberta) were kept in a bio-containment unit. All the mice were divided into three group; no treatment, mGFP treatment and mTRAIL treatment. Each group has 5 to 8 mice. Mice were anesthetized using isoflurane, shaved left flank (about 2X2 cm) and ~3 million SUM-149 cells in Matrigel and serum free DMEM (1:1) were injected subcutaneously into

shaved area. Tumor growth was monitored every 96 h and tumor volume was measured using a digital caliper using formula (length x width^2 x 0.5). Once the tumor was developed, 40 µl of mRNA/polymer complexes (w/w ratio 5:1) were injected subcutaneously into tumor vicinity. Four injections were performed with 96 h apart with simultaneous measurements of tumor volume. The first two injections were 5 µg and second two were 3 µg per animal. mGFP was used as control to evaluate the non-specific toxicity, if any, related to the delivery system and mRNA. After 48 h after last injection, mice were euthanized, tumors were collected and weighted. Any mouse with large tumor volume (>1500 mm^3), necrotic spot or excessive weight loss (>20%) was euthanized for humane considerations.

6.2.9. Statistical analysis

The data were presented as mean ± standard deviation of three different replicates. For comparison between two groups, the results were analyzed using Student's *t*-test. A value of $p<0.05$ was considered significant.

6.3. Results and Discussion

6.3.1. Synthesis of chemically modified mRNA expressing TRAIL

Increased translation of mRNA with less immunogenicity are key factors for therapeutic application of mRNA. Both viral and non-viral approaches can be used in RNA-based protein expression. RNA viruses such as Sendai virus can produce large amount of protein in cytoplasm [411]. However, problems associated with such viruses such as difficulty of production, poor control of gene expression, immunogenicity and toxicity limit their use. Therefore, we used synthetic modified mRNA (modRNA) in this study, which solves some of problem associated with

the viral approach. Therapeutic application of mRNA gained very little attention initially due to stability issues (short half-life in cytoplasm and quick degradation under *in vitro* storage)[397, 408, 412] and immunogenicity associated with mRNA. Later, several studies on modification and engineering of mRNA were performed to address these stability and immunogenicity problems [413-415]. In this study, we synthesized the modRNA harboring TRAIL coding sequences which contains 5' cap (3'-O-Me-m7G(5') ppp(5')G), 5' untranslated region (UTR), open reading frame (ORF), 3' UTR and 3' poly adenosine (polyA) tail. The 5' cap structure and the polyA tail not only increases stability but also *in situ* protein production by facilitating ribosome recruitment [415, 416]. To reduce the immune response to mTRAIL, uridine was replaced with N1-methlypseudouridine and 5' triphosphate was removed. The ORF contains the TRAIL coding sequences (amino acid 114 to 281). Since trimeric secretable TRAIL is more potent [202], isoleucine zipper and secretion signal and furin specific sequences were added to the TRAIL coding sequences.

6.3.2. Polymer synthesis and mRNA transfection efficiency

Since the first preclinical study of mRNA using liposomes in 1978 [417], significant progress has been made in clinical translation of mRNA through advances in mRNA manufacturing and delivery. Several cationic carriers such as cationic lipids [404, 405] and cationic polymers [394, 406] have been used to deliver mRNA translating therapeutic as well as reporter proteins. Among the cationic polymers, small molecular weight polythelyneimine (PEI) modified with the lipids could serve as a potential carrier for mRNA delivery because of biocompatibility, endosomal escape and efficient delivery of nucleic acids. We prepared a series of polymers by grafting unsaturated lipids α-LA and LA onto PEI1.2 via amide or thioester bond as described

before [378] and explored mRNA delivery efficiency. These polymers had already showed efficacy to deliver pDNA and siRNA [110, 207, 418]. The pDNA is usually several kilobase pairs long, the siRNA is only 21-23 base pairs while the mRNA is usually several hundreds to kilo base pairs long. Their distinctive structural and chemical characteristics are expected to affect their complex formation properties with synthesis carriers. However, requirements of delivery systems for pDNA, mRNA and siRNA have several similar elements, including protection from nuclease degradation, facilitating cellular uptake, rapid endosomal escape and intracellular release. Our previous study (see chapter 5, **Figure 5.3**) showed that amide linked polymers PEI1.2-LA (LA/PEI = 2.5 mol/mol) and PEI1.2-αLA (αLA/PEI = 2.4 mol/mol) were effective siRNA delivery agents and thioester-linked polymer PEI1.2-tLA (tLA/PEI = 2.7 mol/mol) and PEI1.2-tαLA (tαLA/PEI = 2.2 mol/mol) were effective pDNA transfection reagents. In addition, thioester-linked polymers were able to co-deliver both pDNA and siRNA in breast cancer cells.

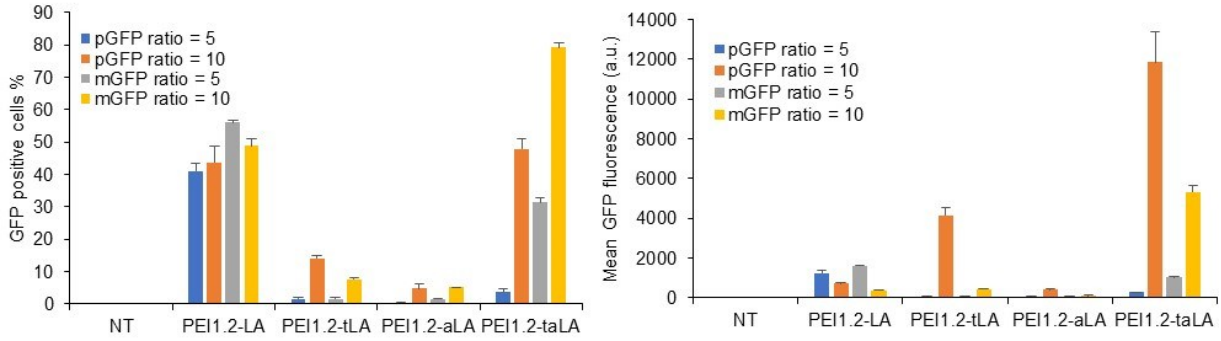

Figure 6.1: Polymer efficiency in MDA-MB-231 cells for mRNA delivery. Transfection efficiency was evaluated based on GFP expression after 48 h of transfection with the indicated polymer and mGFP complexes by using flow cytometry.

Therefore, we chose these polymers as potential mRNA delivery reagents based on these considerations. Complexes of polymer with pDNA or mRNA were prepared at weight ratio of 5 and 10 and added to MDA-MB-231 cells. Similar to pDNA (see chapter 5, **Figure 5.3**), thioester-

linked polymers PEI1.2-tLA and PEI1.2-tαLA gave higher mRNA transfection than the amide-linked polymers PEI1.2-LA and PEI1.2-αLA (**Figure 6.1**). Percentage of GFP-positive cells with polymer PEI1.2-LA was high for both pGFP and mGFP indicating uniform transfection of most cells, but the mean GFP fluorescence intensity was low for the mGFP.

Among these polymers, PEI1.2-tαLA resulted higher mean GFP fluorescence as well as percentage of GFP-positive cells. Transfection efficiency of PEI1.2-tαLA increased with increase in the polymer to nucleic acid ratio (w/w). At lower polymer to nucleic acid ratio (w/w = 5), mGFP resulted in higher transfection efficiency than the pGFP, while at higher polymer to nucleic acid ratio (w/w = 10), pGFP gave higher fluorescence intensity. However, percentage of GFP-positive cells were higher with the mGFP than the pGFP, indicating more uniform transfection with the mGFP. In our previous study (chapter 5, **Figure 5.2**), PEI1.2-tαLA was able to co-deliver pDNA and siRNA into the breast cancer cells. This study further confirmed the mRNA delivery efficiency by PEI1.2-tαLA suggesting a universal polymer for delivery of these types of nucleic acids regardless of size and structure. Similar to lipid modified PEIs in this study, PEI (2K) modified with a peptide [403], PEI (5K or 25 K) and poly(ethylene glycol) blends [419] were also successful to deliver mRNA.

6.3.3. Cytotoxicity of complexes in breast cancer cells

Since PEI1.2-tαLA gave higher mRNA and pDNA transfection efficiency, it was used to deliver mTRAIL. We first evaluated the mRNA delivery (mGFP and mTRAIL) in breast cancer cells; MCF-7, MDA-MB-231 and SUM-149 cells and compared it with the pDNA delivery (i.e., mGFP vs. pGFP [gWIZ-GFP] and mTRAIL vs. pTRAIL). GFP-expression was evaluated after 48 h of transfection and TRAIL-induced cytotoxicity was evaluated after 72 h of transfection.

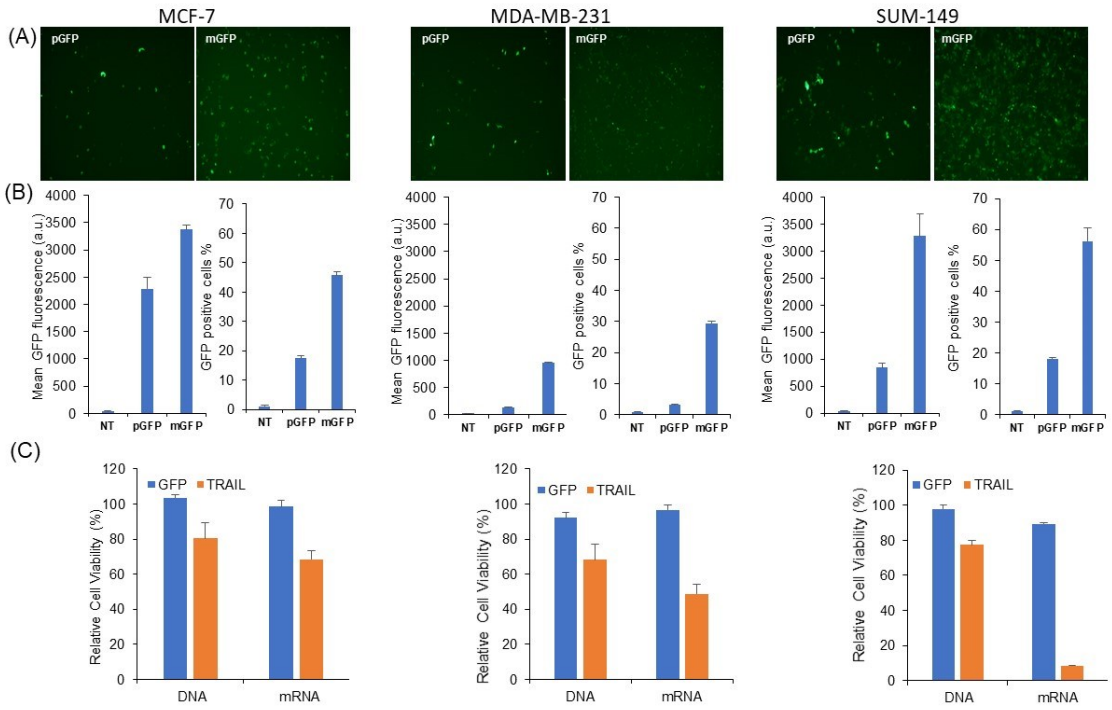

Figure 6.2: DNA and mRNA transfection in breast cancer cells. Breast cancer cells MCF-7, MDA-MB-231 and SUM-149 cells were transfected with mTRAIL and pTRAIL using PEI1.2-tαLA. pGFP and mGFP were used as control to evaluate non-specific toxicity of complexes. GFP expression after mGFP and pGFP expression were shown in fluorescence microscope image (A) and mean fluorescence intensity and GFP positive cells were evaluated using using flowcytometer (B). Cytotoxicity of control and mTRAIL and pTRAIL complexes were evaluated by MTT assay (C). Higher transfection was achieved with mRNA than pDNA as shown by both higher GFP expression with mGFP and higher cytotoxicity with mTRAIL.

PEI1.2tαLA resulted in higher mGFP transfection than the pGFP transfection at polymer to nucleic acid ratio of 5 in MDA-MB-231 cells, while mean GFP expression was higher with the pGFP transfection at ratio 10 (**Figure 6.1**). However, control complexes (polymer/pGFP) at ratio 10 was toxic (**Figure S6.2**). Therefore, polymer/nucleic acid ratio of 5 was used to study effect of mTRAIL. As compared to pGFP, mGFP resulted in higher GFP expression in all MCF-7, MDA-MB-231 and SUM-149 (**Figure 6.2A** and **B**) cells. Similarly, transfection of mTRAIL resulted in

higher cell death than the pTRAIL transfection. Among the cell lines, MCF-7 cells was known to be resistant to TRAIL, therefore it was not surprising that the cytotoxicity with either pTRAIL or mTRAIL was less in this cell line (**Figure 6.2C**). MDA-MB-231 and SUM-149 cells are known to be sensitive to TRAIL and therefore resulted in a higher cell death resulted as a consequence of pTRAIL treatment. SUM-149 cells were most responsive to mTRAIL resulting in almost 90% of cell death (**Figure 6.2C**). Based on the GFP expression, a higher mRNA transfection was also achieved in SUM-149 cells (~60% GFP-positive cells) than the MDA-MB-231 cells (~30% GFP positive cells), which might be one of the factors contributing higher cell death in SUM-149 cells.

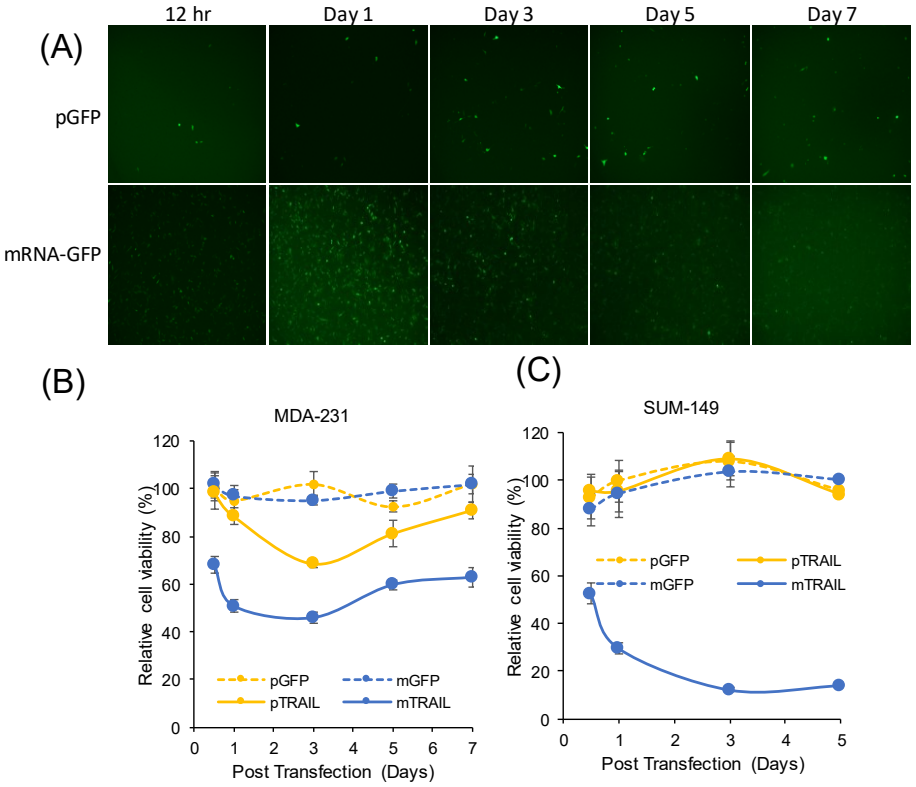

Figure 6.3: Time course analysis of mRNA (mGFP and mTRAIL) and pDNA (pGFP and pTRAIL) in MDA-MB-231 and SUM-149 cells. (A) Fluorescence microscope image showing GFP expression in MDA-MB-231 cells at different period of incubation with pGFP and mGFP complexes. Similarly, cytotoxicity of complexes at different time points of treatment was evaluated in MDA-MB-231 and (B) SUM-149 cells.

In contrast to pDNA or viral vectors, mRNAs do not need to enter the nucleus of cells for protein translation and, therefore, mRNAs can be immediately translated into proteins after cytoplasmic entry. Integration into the host genome is also avoided preventing risk of insertional mutations. Since exogenously delivered synthetic mRNA will be transiently present in cells due to physiological degradation, continuous overexpression of therapeutic protein can not be achieved with mRNA. To elucidate the effect of mRNA on the breast cancer cells over the time, we treated MDA-MB-231 and SUM-149 cells with mRNA (mGFP and mTRAIL), and protein expression and cytotoxic effect was evaluated and compared with pDNA delivery. As expected, GFP expression with mGFP was maximum at 24 h of transfection which was reduced over the time in MDA-MB-231 cells (**Figure 6.3A**). We could detect GFP expression up to day7 post-transfection. The GFP expression with pGFP reached a maximum at day 3. Similarly, the cytotoxic effect of mTRAIL started earlier than with the effect with pTRAIL in MDA-MB-231 cells (**Figure 6.3B**). Similar to previous results, complexes with pGFP and mGFP did not exert any cytotoxic effect on the cells. Effect of mTRAIL complexes started as early as 12 h of transfection, resulting in maximum cell death at 24 h of transfection while pTRAIL complexes began to kill cells at 24 h of transfection and reached maximum at 72 h. After 72 h, effects of both pTRAIL and mTRAIL complexes were reduced. At day 7 of post-transfection, effect of pTRAIL had almost disappeared, resulting only ~10% of cell death while the effect of mTRAIL was still evident with a higher cell death of ~40% at day 7. Similarly, effect of mTRAIL treatment had already appeared at 12 h of post-transfection in SUM-149 cells (**Figure 6.3C**) and continued to increase with time. Since cytotoxic effect of mTRAIL complexes in SUM-149 was so pronounced that cells can not recover even after 5 days of transfection. The pTRAIL complexes and control complexes (mGFP and pGFP) did not have any effect in SUM-149 cells.

6.3.4. Evaluation of TRAIL secretion and apoptosis induction

In order to confirm that the cell death obtained after mTRAIL transfection was due to translation and secretion of the TRAIL protein, we evaluated the TRAIL protein secretion at different time of transfection in MDA-MB-231 and SUM-149 cells. In MDA-MB-231 cells, TRAIL secretion was already evident at 12 h of mTRAIL transfection and reached maximum after 24 h, after which it started to deccrease (**Figure 6.4A**).

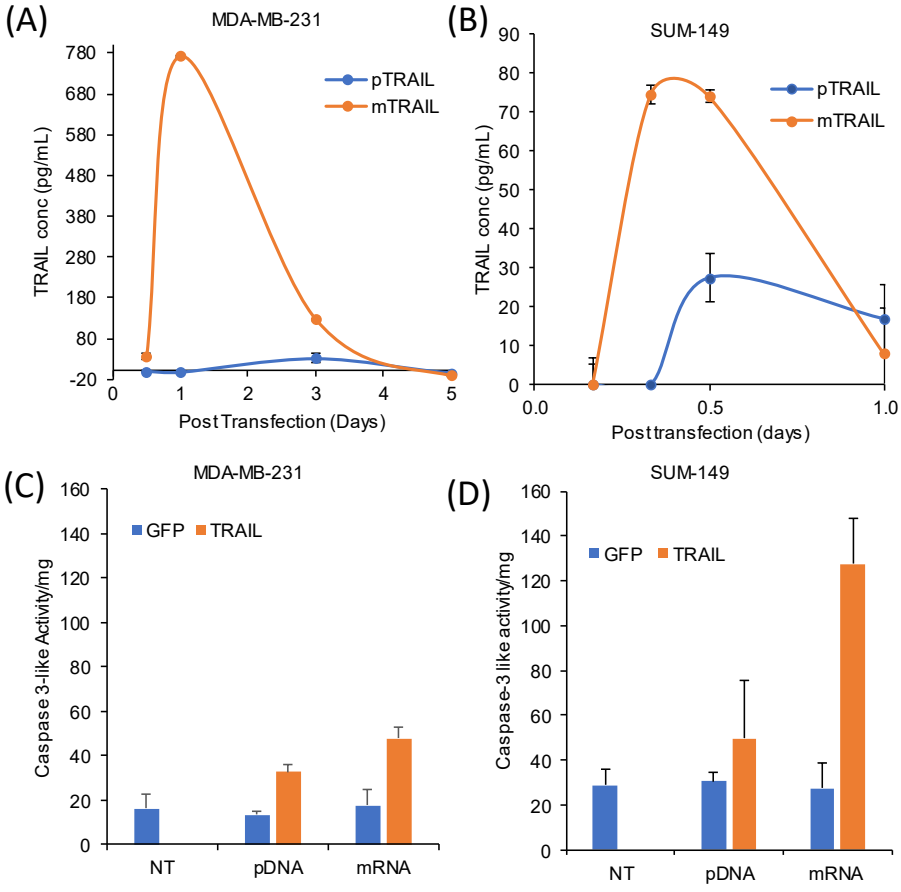

Figure 6.4: Secretion of TRAIL and caspase-3 activation after mTRAIL transfection. TRAIL secretion after pTRAIL and mTRAIL transfection in MDA-MB-231 and SUM-149 cells was determined by ELISA. mTRAIL resulted in higher TRAIL secretion than pTRAIL. To study mechanism of cell death, caspase -3 activity, a main caspase involved in apoptosis was evaluated in MDA-MB-231 and SUM-149 cells. Obviously, treatment with mTRAIL complexes resulted in higher caspase-3 activation resulting in higher apoptosis than with pTRAIL complexes.

The kinetics of TRAIL secretion with mTRAIL transfection matched closely to that of GFP expression with the mGFP transfection (in **Figure 6.3**). The mTRAIL transfection resulted in higher TRAIL secretion than the pTRAIL transfection in both MDA-MB-231 and SUM-149 cells. In MDA-MB-231 cells we were able to detect TRAIL secretion up to 72 h of mTRAIL transfection. In SUM-149 cells, however, TRAIL secretion after mTRAIL transfection was very low as compared to the MDA-MB-231 cells and duration of secretion was also transient; TRAIL secretion was close to zero at 24 h post-transfection (**Figure 6.4B**). After 24 h of mTRAIL transfection, ~70% of SUM-149 cells were dead leaving very few cells for TRAIL secretion, which explains the very low TRAIL concentration in the supernatant. Despite lower TRAIL secretion in SUM-149 cells than the MDA-MB-231 cells, effect on cell viability was very pronounced in SUM-149 cells, indicating enhanced sensitivity of this cell line to TRAIL induced cell death.

TRAIL is known to induce apoptosis in different cancer cell types. To confirm if the cell death was due to apoptosis induction, caspase-3 activity was evaluated. Apoptosis involved several types of caspases but capsase-3 is most commonly activated and is required for DNA fragmentation and typical morphological changes during apoptosis [355, 420]. Therefore, activation of caspase-3 was evaluated after treatment of cells with mTRAIL and pTRAIL complexes (**Figure 6.4C** and **D**). The caspase-3 activities after treatment with pGFP and mGFP complexes were similar to non-treatment group in both MDA-MB-231 and SUM-149 cells. As expected, mTRAIL complexes resulted in higher caspase-3 activation than the pTRAIL complexes. As compared to MDA-MB-231 cells, caspase-3 activation with mTRAIL complexes was higher in SUM-149 cells (**Figure 6.4D**), which may be the underlying basis for higher cell death in SUM-149 cells (**Figure 6.2C**).

6.3.5. Anticancer activity of hBMSC modified with mTRAIL

Rapid and efficient production of therapeutic proteins with mRNA provides an attractive option to transfect hard-to-transfect cells such as stem cells for cell-based therapies. As a proof of concept, we evaluated the modification of human bone marrow stromal cells (hBMSC) with mRNA using PEI1.2-tαLA. The hMBSC can differentiate into bone, cartilage and fat as well as play a role in differentiation of haematopoietic cells. They have the ability to migrate and incorporate within the connective tissue stroma of tumors [421-423]. First, we studied the mGFP transfection in hBMSC using PEI1.2-tαLA and optimized the amount of mRNA needed to achieve maximum transfection. The mGFP concentration of 0.5 µg/mL was optimal which showed highest GFP expression (**Figure 6.5A** and **B**). More than 80% cells were GFP-positive at higher mGFP concentrations. Increasing the amount of mGFP beyond 0.5 µg/mL reduced the GFP fluorescence, which might be indicative of toxicity. Transfection efficiency of PEI1.2-tαLA was higher than the commercial reagent Lipo 2K. Consistent with hard-to-transfect nature of hBMSC, GFP expression after pGFP transfection (~3%) using PEI1.2-tαLA was very little unlike the mGFP transfection (~65%). Differences on GFP expression after mGFP and pGFP expression was more prominent in hBMSC as compared to breast cancer cells (**Figure 6.5C**). Mean GFP fluorescence intensity was about 60 times higher with mGFP than pGFP transfection using PEI1.2-tαLA. Therefore, mRNA could be a very promising approach to induce therapeutic proteins in hBMSC and other mesenchymal stem cells as the basis of cell therapies.

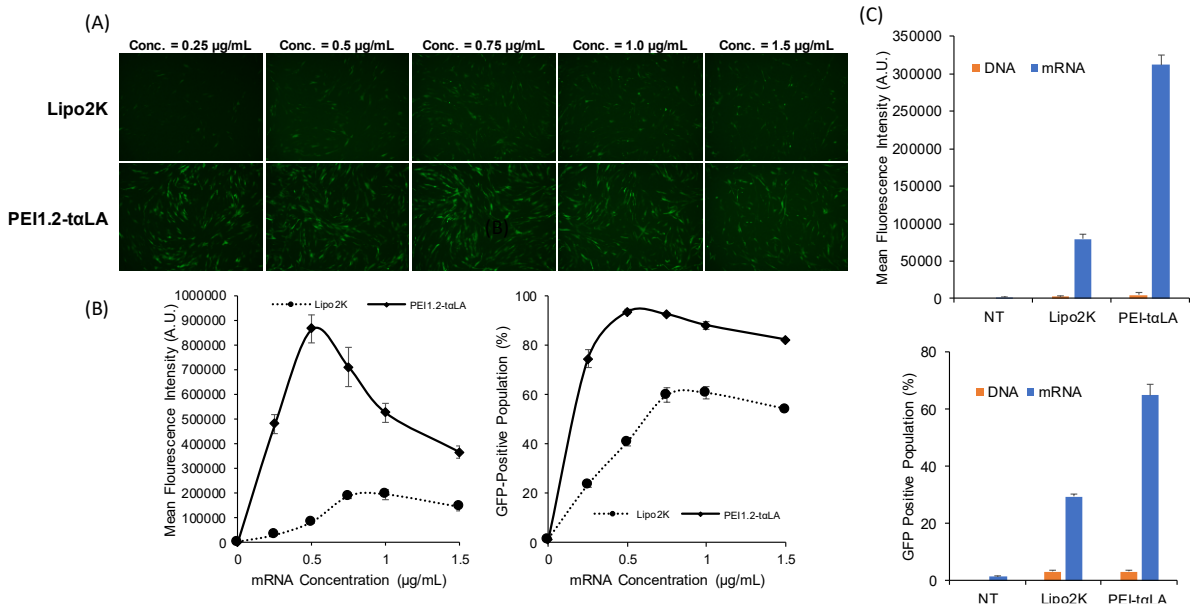

Figure 6.5: mGFP transfection in hMBSC. hBMSC was transfected with mGFP at different concentration using 1.2PEI-tαLA and Lipo 2K. Transfection efficiency was evaluated using fluorescence microscope (A) and flow cytometry (B). mGFP transfection was compared with pGFP transfection (C). Obviously, mGFP resulted in higher GFP expression than pGFP.

For cell-based therapy, cells need to be isolated from a host followed by modification *in vitro* before administration back to the host. The difficulty to transfect these cells and *in vitro* changes in cell phenotype as a result of prolonged culture on plasticware are important issues to tackle. It would be desirable to minimize the *in vitro* culture time and mRNA transfection could be advantageous in this context because of its relatively rapid translation. Here, we additionally explored the modification of hBMSC with mTRAIL and studied its effect on breast cancer cells. Similar to the GFP expression, higher concentrations of TRAIL protein were detected in the supernatant of hBMSC treated with mTRAIL complexes than the pTRAIL complexes (**Figure 6.6A**). With mTRAIL transfection, TRAIL secretion was higher after 6 h of transfection than 24 and 48 h of transfection confirming rapid protein translation with mRNA. While TRAIL secretion was negligible with pTRAIL transfection at 6 h, it slightly increased after 24 h. The modified

hBMSC were investigated for anti-cancer activity in breast cancer cells. After 6 h of transfection, hBMSC was trypsinized and fixed numbers of cells (10,000 or 5,000) were added to SUM-149 cells. Untreated hBMSC was also co-cultured with SUM-149 cells as a negative control. mTRAIL transfected hBMSC (mTRAIL-hBMSC) from different cell sources (I and II) effectively reduced the viability of the SUM-149 cells when co-cultured (**Figure 6.6B** and **D**). The cytotoxicity effect was proportional to the number of mTRAIL-hBMSC added. The pTRAIL, pGFP and mGFP transfected hMBSC did not have any effect on the viability of SUM-149 cells. In order to confirm the cell viability in co-culture of SUM-149 and mTRAIL-hBMSC is due to death of only SUM-149 cells, same number of hBMSCs (10,000) after 6 h of transfection were seeded and allowed to grow and cell viability was calculated using MTT assay. All transfections including the mTRAIL transfection were not toxic to hBMSC derived from both sources (**Figure 6.6C** and **E**), which confirms the cell death in SUM-149 cells in the absence of mTRAIL-hBMSC cell death. In a separate experiment, hBMSCs were transfected with the mTRAIL, pTRAIL and controls (pGFP and mGFP) and cell viability was evaluated after 72 h of transfection. All the complexes were non toxic to the hBMSC (**Figure S6.3**) which further confirms that mTRAIL complexes were non-toxic to hBMSCs. hBMSC grew uniformly with SUM-149 cells (**Figure 6.6F**). In all group except mTRAIL-hBMSC + SUM-149 cells, both SUM-149 cells (small round cells) and hBMSC (long and elongated cells; indicated by black arrow in **Figure 6.6F** proliferated effectively, forming a monolayer of cells. In contrast, most of the SUM-149 cells treated with mTRAIL-hBMSC were not viable visually while the hBMSC cells were intact (**Figure 6.6 F**).

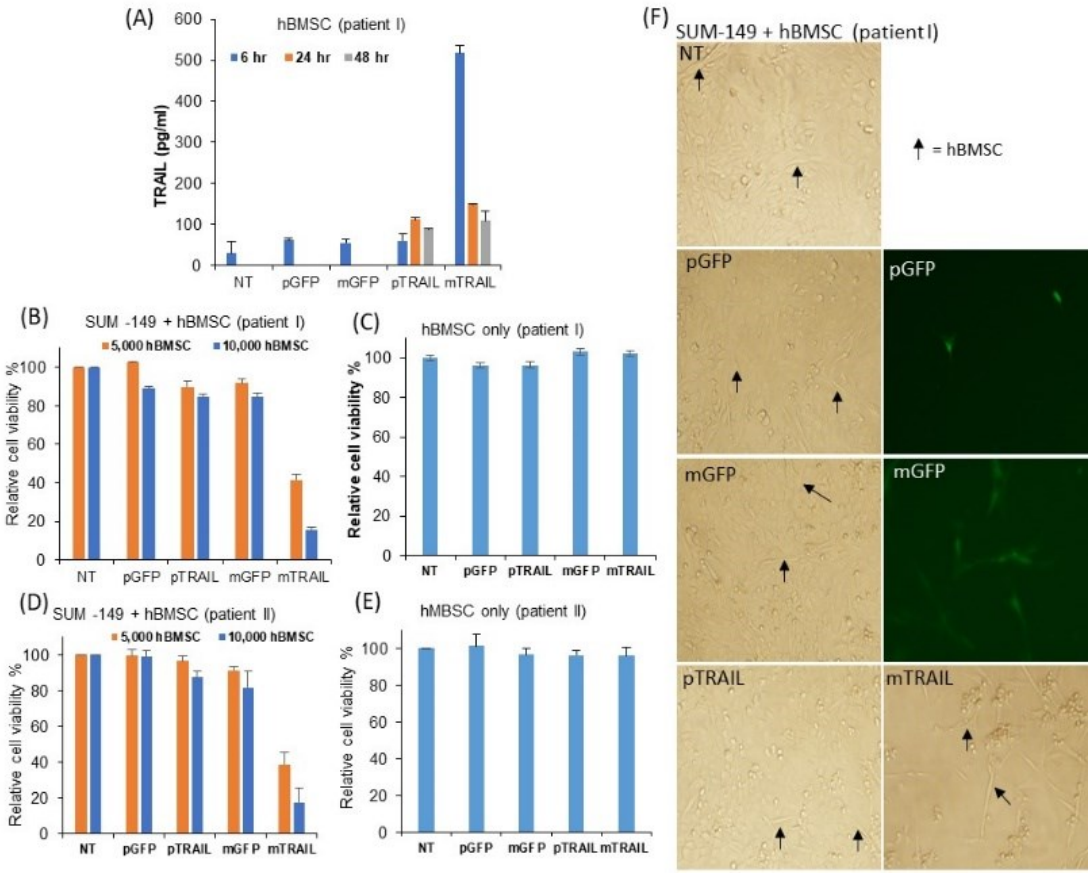

Figure 6.6: Cytotoxicity of mTRAIL modified hBMSC. hBMSC was modified with mTRAIL and pTRAIL and cytotoxicity activity of TRAIL modified hBMSC was evaluated. (A) TRAIL secretion by hBMSC after transfection with pTRAIL and mTRAIL. TRAIL secretion with mTRAIL was higher than with pTRAIL transfection reaching maximum as early as 6 h. After 6 h of transfection hBMSC was trypsinized and fixed number (10,000 or 5,000) cell per well were added to the SUM-149 cells. mTRAIL modified hBMSC from both patient I and II killed the SUM-149 cells (B and D) without killing hBMSCs (C and E). Cell death of SUM-149 cells without affecting hBMSC can be seen in the pictures (F) where black arrow pointed the hBMSCs.

The mTRAIL used in this study was designed to translate a soluble (not membrane-bound) TRAIL protein with a secretion signal. It is likely that the death of SUM-149 after co-culture with the mTRAIL-hBMSC might be due to the secretion of the soluble TRAIL proteins rather than the bystander effect of the TRAIL on hBMSC surface. However, the supernatant from the mTRAIL-

hBMSC after 24 h of transfection did not induce cell death on SUM-149 cells (**Figure S6.4**) which might be due to low TRAIL concentration after 24 h of transfection (**Figure 6.6A**). In this case, cell culture media had been changed after 6 h of transfection. TRAIL concentration was higher at 6 h of transfection but we were unable to evaluate effect to the supernatant at 6 h due to the presence of complexes in the supernatant.

6.3.5. Antitumor activity of mTRAIL *in vivo*

SUM-149 xenografts were established in mice and treated with mGFP/polymer complexes (as negative control) and mTRAIL/polymer complexes as indicated time points in **Figure 6.7A.**

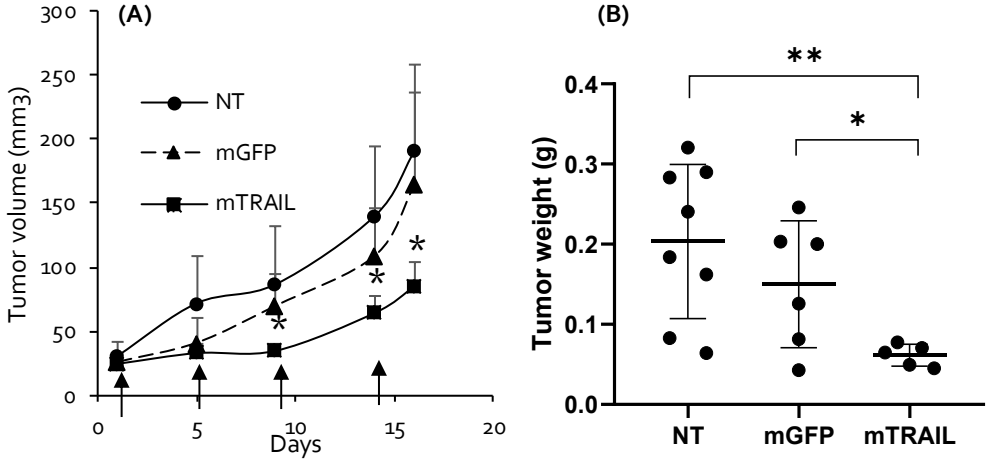

Figure 6.7. Tumor growth inhibition after polymer/mRNA complex treatment. Polymer/mRNA complexes were injected into the tumor vicinity. Data represent mean ± SD of n = 5-8 at each time point. (**A**) Tumor volumes as a function of time. Black arrows indicate the time of injections. Only positive SD bars were shown for clarity. Tumor volume after treatment of mTRAIL was significantly less than no treatment and mGFP treatment group after day 9 (*$p < 0.05$). (**B**) Wet weight of extracted tumors at the end of study also indicated the retardation of tumor growth by mTRAIL treatment (*$p<0.05$ **$p < 0.001$).

Injections were started with 5 µg of mRNA per mice. At day 5, there was no difference in tumor volume in between mGFP and mTRAIL treatment group. Therefore, dose of mRNA was reduced

to 3 μg of mRNA per mice to minimize the non-specific toxicity. Tumor growth in the mGFP group and no treatment group was not significantly different. Treatment with mTRAIL significantly reduced the tumor volume after day 9. The tumor weights recovered at the end of the study were in line with tumor volume, where the lowest tumor weight was observed with mTRAIL treatment (**Figure 6.7B**). TRAIL protein in the tumor and apoptosis in tumor need to be assessed.

6.4. Conclusions

In this study, we synthesized a synthetic modified mRNA harboring a TRAIL protein translation sequence that provided a soluble trimeric TRAIL protein. Lipid-modified small molecular weight PEIs linked with a thioester bond was superior to deliver mRNA (mGFP vs. pGFP) in breast cancer cells and hBMSC. Type of breast cancer cells used greatly determined the amount and duration of TRAIL expression after mTRAIL transfection. The mRNA transfection resulted in higher and faster protein expression (GFP and TRAIL) than the pDNA transfection in all cells used in this study. As a result, mTRAIL transfection resulted in higher apoptosis in breast cancer cells via enhanced caspase-3 activation. hBMSCs were successfully modified with mTRAIL which promises the use of hBMSC and other stem cells for cell-based therapies of cancer. Polymer/mTRAIL complex was effective to retard the SUM-149 xenograft in *in vivo* breast cancer model. However, transient expression of protein especially in hBMSCs with mRNA limits its use for conditions that require a prolonged protein expression.

6.5. Acknowledgement

B.T. is supported by Alberta Innovates Graduate Studentship. This study was supported by an Operating Grant from the Canadian Institutes of Health Research (CIHR), and a Discovery Grant from the Natural Sciences and Engineering Research Council of Canada (NSERC).

Chapter 7

General discussion, conclusion and future directions

7.1. General discussions and conclusions

The research work in this thesis explored the nucleic acids and their combinations for treatment of breast cancer. Nucleic acid-based therapy is presenting an alternative to traditional chemotherapy for treatment of cancer. The extensive crosstalk between signalling pathways, compensatory and neutralizing activities associated with cancer cells [5-11] have shifted the drug development paradigm towards nucleic acids for targeting specific pathways and proteins responsible for the disease. Nucleic acids can not enter the cells on their own and are easily degraded by serum endonucleases. Therefore, our goal in the first section (Chapters 2 and 3) was to design and develop polymeric nanocarriers for gene delivery. Careful engineering of polymers has enabled design of effective non-viral gene delivery agents in specified applications [267, 272]. Using RAFT polymerization, a library of the galactose containing glycopolymers were prepared. Several carbohydrates such as β-cyclodextrin and chitosan has been grafted with cationic molecules such as PEI and spermine to produce less toxic carbohydrate-based gene delivery vehicles [281, 287]. The gene delivery efficacy of these polymers was dependent on size, architecture and composition of carbohydrate moiety incorporated into the polymeric backbone (2-lactobionamidoethyl methacrylamide) and cationic molecule (2-aminoethylmethacrylamide). Most importantly, these polymers contain galactose as pendant which interacts with ASGPR of hepatocytes facilitating gene delivery specifically to hepatocyte cells. Block co-polymer containing galactose delivered gene into the ASGPR positive hepatocytes, while gene delivery efficacy in ASGPR deficient cells was negligible.

Several independent studies explored a wide range of cationic polymers including high molecular PEI, poly(L-lysine) and poly(amidoamines) for gene delivery [424]. Among them, PEIs were well established for both *in vitro* and *in vivo* applications. High molecular weight PEI,

particularly branched 25 kDa PEI is known to be efficient gene delivery vehicle. However, severe cellular and systemic toxicities associated with high cationic charge density of high molecular PEI limits its use. Low molecular weight PEI, on the other hand, is less toxic and can be readily eliminated from the body. Unfortunately, the low molecular PEI is not effective gene delivery agent, since it is generally believed to form unstable complexes unable to cross the cell membrane. Therefore, we modified low molecular weight PEI (1.2 to 2.0 kDa) with small hydrophobe, propionic acid (PrA) to improve its gene delivery efficacy. Modification of low molecular weigh PEI with aliphatic lipids of variable chain length was previously reported [102, 314], but PrA (C3) is significantly shorter than these lipids (>C8). We found that propionic acid substitution to 1.2 PEI converted it into effective pDNA transfecting reagent into breast cancer cells MDA-MB-231 and MCF-7. Transfection efficiency increased with degree of PrA substitution, but excess PrA was detrimental suggesting importance of optimal ratio between the substituent and PEI backbone. Molecular dynamics simulations revealed that optimum PrA substitution caused higher surface hydrophobicity and surface density, but higher PrA substitution caused deleterious effects on surface hydrophobicity and cationic charge [107]. We also observed higher surface charge and uptake of pDNA complexes of polymer with optimal PrA substitution which resulted in higher pDNA transfection. The excessive substitution decreased the surface charge as well as uptake of complexes. However, unlike literature reports, addition of siRNA to complexes did not increase pDNA transfection efficiency of PrA substituted 1.2 kDa PEI polymer. In addition, siRNA transfection efficiency of these polymers in breast cancer cells was negligible, clearly indicating the importance of cargo in delivery efficiency. Previous studies from our lab identified linoleic acid (C18) substituted PEIs as most promising siRNA carrier in breast cancer cells [108, 338]. To further optimize siRNA carrier, we substituted small molecular weight PEI with α-linoleic acid

(C18). We found 1.2PEI-αLA to be the most promising siRNA transfecting reagent in breast cancer cells MDA-MB-231 and MCF-7. Then, we synthesized a series of LA and αLA substituted 1.2PEI linked via thioester and amide bond. DNA transfection was higher with thioester linked lipopolymers while siRNA transfection was higher with amide linked lipopolymers. Thioester linked polymer (1.2PEI-tαLA) polymer successfully co-delivered both DNA and siRNA. In addition to DNA and siRNA, mRNA was also delivered by 1.2PEI-tαLA in breast cancer cells.

Using 1.2PEI-αLA, we performed siRNA library screening against 446 human apoptosis related proteins to identify novel regulator of TRAIL. TRAIL has a unique capacity to induce apoptosis in variety of cancer cells without affecting normal cells. Several Phase I and II clinical trials proved that TRAIL therapy tested so far was safe, but unlike the preclinical results, they failed to exert robust anticancer activity in patients [117, 124, 333]. We aimed to identify protein targets whose silencing will enhance the TRAIL induced apoptosis in breast cancer cells. One can identify sensitizer(s) of TRAIL therapy by exploring mechanistic insights into the apoptotic pathway. Instead, we used a high-throughput screening approach without a bias in the selection process. We performed human apoptosis related siRNA library screening in the presence or absence of TRAIL in MDA-MB-231 cells. Details of library screening were in Chapter 4. Control library screening was performed in normal breast cell MCF-10A to avoid targets that may affect normal cells. Two novel targets namely BCL2L12 and SOD1 were identified to enhance TRAIL-induced apoptosis in breast cancer cells without affecting normal cells. BCL2L12 is a proline-rich and BH2-domain containing protein which inhibits the effector caspase -3 and -7 [343, 344]. Other independent studies investigated the role of BCL2L12 in breast cancer cells with contradictory results to each other. One study showed that development of acquired resistant to cisplatin in MDA-MB-231 cells after BCL2L12 silencing [346] while in other study, silencing of BCL2L12

sensitized MDA-MB-231 and MCF-7 cells to doxorubicin and cisplatin induced apoptosis [347]. In line with the latter study, we confirmed the anti-apoptotic activity of BCL2L12 whose silencing sensitized MDA-MB-231 and MCF-7 against TRAIL induced apoptosis. Anti-apoptotic role of BCL2L12 was also confirmed in glioblastoma and a gold-based spherical nucleic acid nanoconjugate silencing BCL2L12 is currently in clinical trail for treatment of glioblastoma. [343, 344, 425].

Next, co-delivery of a TRAIL expressing plasmid (pTRAIL) and BCL2L12 siRNA was assessed *in vitro* and *in vivo* model. pTRAIL delivery can overcome the fundamental pharmacokinetics limitations associated with short-half of recombinant TRAIL protein (by allowing *in situ* synthesis of the protein) and BCL2L12 siRNA could further enhance the TRAIL induced apoptosis. Co-delivery of pTRAIL and BCL2L12 siRNA with 1.2PEI-tαLA polymer elicited potent anticancer activity in both *in vitro* and *in vivo* breast cancer model. This was attributed to (i) improved TRAIL expression due to additive actions of the supplemented siRNA and (ii) sensitization of TRAIL action by co-delivered BCL2L12 siRNA. In addition, BCL2L12 siRNA reversed the TRAIL resistance in MCF-7 cells. Since strategies to target individual signaling pathways may not be sufficient to block the abnormal proliferation due to cellular plasticity that tap into alternative pathways for vital cellular activities [6], inducing apoptosis with pTRAIL and simultaneous support with BCL2L12 silencing will be more effective to eradicate breast cancer.

Finally, we showed that delivery of mRNA expressing TRAIL (mTRAIL) resulted in enhanced cell death obtained by the pTRAIL treatment in breast cancer cells. Nuclear transport, one of the major hurdle of pDNA transfection can be avoided with the use of mRNA. Therefore, using mRNA derived therapeutic protein expression can be pursued in hard-to-transfect and slow

dividing cells. In this study, we not only achieved greater effect of mTRAIL therapy in breast cancer cells, but also modified hBMSC with mTRAIL in order to kill the breast cancer cells after co-culture as a result of TRAIL secretion by the hBMSC.

7.2. Future directions

Our ultimate goal remains the development of nucleic acid based combination therapy for treatment of breast cancer. I propose several areas of future explorations to improve nucleic acid based therapy of breast cancer.

- **Exploring new polymers for nucleic acid delivery**. We found that size of the lipid substituted, extent of lipid substitution and the type of bond between the lipid and PEI affect the transfection efficiency of pDNA or siRNA. LA substituted 1.2PEI with thioester bond resulted better pDNA transfection while the amide linkage showed better siRNA transfection into breast cancer cells. Besides thioester and amide bond, other linkers to connect PEI and lipid can be explored. We did not find the thioester polymer to be sensitive towards the glutathione, which is expected to cleave disulfide and thioester linkages in conjugates. Synthesis of lipid substituted PEIs with pH or glutathione-responsive conjugation is another avenue to explore. These smart polymers can exploit the elevated glutathione concentration in the intracellular compartment or lower pH at the tumor microenvironment to release payload inside tumor cells (assuming cleavable conjugates will facilitate better release of the nucleic acid cargo). Efficient vehicles are as important as therapeutic nucleic acid combinations to achieve the therapeutic benefit from co-delivery of nucleic acid. Thioester-linked lipid substituted PEI delivered both pDNA and siRNA into breast cancer cells. Addition of siRNA enhanced the pDNA transfection but pDNA failed to show beneficial effect on

siRNA transfection. Therefore, we can explore developing polymers for co-delivery of nucleic acid where the loaded nucleic acid will enhance each other's transfection efficiency, amplifying the synergistic activity.

- ***In vivo* characterization of nucleic acid delivery system**. We performed subcutaneous injection of complexes into the tumor vicinity as a preliminary study to determine effect of complexes *in vivo*. There is an obvious need for evaluation of physicochemical state of the complexes after systemic administration (IV or IP). In addition, bio-distribution, pharmacokinetics and toxicity of polymer/nucleic acid complexes need to be studied in detail. The proof-of-principle studies reported here were mainly focussed on therapeutic efficacy. The suggested studies will give better idea how often complexes should be injected and the tolerable doses. If tumor targeting of the complexes are limited, designing tumor targeted complexes by modifying PEI polymers with cancer specific ligands is the next step towards delivering nucleic acid specifically to cancer.

- **Evaluation of safety and efficacy of TRAIL and complementary therapeutic targets in *vivo*.** Several independent studies showed the modification of TRAIL with polyhistidine tag and antibody-crosslinked Flag improved the apoptosis induction but they also induce apoptosis in human hepatocytes *in vitro* [230, 361]. This observation has not been validated *in vivo*, to the best of our knowledge. In this study, we reported that siRNAs silencing BCL2L12 and SOD1 not only sensitized TRAIL-induced apoptosis in breast cancer cells but also reversed the TRAIL resistance in MCF-7 cells. The possibility of increasing toxicity while potentiating actions of TRAIL therapy should not be overlooked. TRAIL combination

with BCL2L12 and SOD1 siRNAs were non toxic in select normal cell, hMBSC and HUVEC cells. Safety of these therapeutic combinations should be further evaluated *in vivo.* Further, efficacy to these therapeutics combinations should be evaluated in more clinically relevant breast cancer model such as orthotopic breast cancer model or preferably patient-derived xenograft model.

- **Modification of tumor homing stem cells with TRAIL expressing mRNA and elevated antitumor activity *in vivo*.** The main technical problems associated with clinical translation of stem cell-based therapy are difficulty to transfect stem cells, and loss of phenotypic features due to prolonged culturing *in vitro*. It would be desirable to minimize the *in vitro* culture time in between the isolation and administration of the cells back to body. In this context, mRNA transfection is advantageous because of its relatively rapid translation and high transfection efficiency as compared or pDNA. As a proof of concept, we modified the hBMSC with mTRAIL, which killed the SUM-149 cells very efficiently when co-cultured. Anticancer activity of mTRAIL modified mesenchymal stem cells should be investigated further. This may avoid direct administration of complexes into the body, and may limit associated toxicities.

References

[1] Kay MA, Woo SL. Gene therapy for metabolic disorders. Trends Genet. 1994;10:253-7.

[2] Isner JM. Myocardial gene therapy. Nature. 2002;415:234-9.

[3] Baekelandt V, De Strooper B, Nuttin B, Debyser Z. Gene therapeutic strategies for neurodegenerative diseases. Curr Opin Mol Ther. 2000;2:540-54.

[4] Bunnell BA, Morgan RA. Gene therapy for infectious diseases. Clin Microbiol Rev. 1998;11:42-56.

[5] Papp B, Pal C, Hurst LD. Metabolic network analysis of the causes and evolution of enzyme dispensability in yeast. Nature. 2004;429:661-4.

[6] Smalley KS, Haass NK, Brafford PA, Lioni M, Flaherty KT, Herlyn M. Multiple signaling pathways must be targeted to overcome drug resistance in cell lines derived from melanoma metastases. Mol Cancer Ther. 2006;5:1136-44.

[7] Pilpel Y, Sudarsanam P, Church GM. Identifying regulatory networks by combinatorial analysis of promoter elements. Nat Genet. 2001;29:153-9.

[8] Muller R. Crosstalk of oncogenic and prostanoid signaling pathways. J Cancer Res Clin Oncol. 2004;130:429-44.

[9] Sergina NV, Rausch M, Wang D, Blair J, Hann B, Shokat KM, et al. Escape from HER-family tyrosine kinase inhibitor therapy by the kinase-inactive HER3. Nature. 2007;445:437-41.

[10] Overall CM, Kleifeld O. Tumour microenvironment - opinion: validating matrix metalloproteinases as drug targets and anti-targets for cancer therapy. Nat Rev Cancer. 2006;6:227-39.

[11] Bahadur KCR, Xu P. Multicompartment intracellular self-expanding nanogel for targeted delivery of drug cocktail. Adv Mater. 2012;24:6479-83.

[12] Kitano H. A robustness-based approach to systems-oriented drug design. Nat Rev Drug Discov. 2007;6:202-10.

[13] Dancey JE, Chen HX. Strategies for optimizing combinations of molecularly targeted anticancer agents. Nat Rev Drug Discov. 2006;5:649-59.

[14] Kaelin WG, Jr. The concept of synthetic lethality in the context of anticancer therapy. Nat Rev Cancer. 2005;5:689-98.

[15] Keith CT, Borisy AA, Stockwell BR. Multicomponent therapeutics for networked systems. Nat Rev Drug Discov. 2005;4:71-8.

[16] Chou TC. Theoretical basis, experimental design, and computerized simulation of synergism and antagonism in drug combination studies. Pharmacol Rev. 2006;58:621-81.
[17] Johnson MD, MacDougall C, Ostrosky-Zeichner L, Perfect JR, Rex JH. Combination antifungal therapy. Antimicrob Agents Chemother. 2004;48:693-715.
[18] Peterson JJ, Novick SJ. Nonlinear blending: a useful general concept for the assessment of combination drug synergy. J Recept Signal Transduct Res. 2007;27:125-46.
[19] Cokol M, Chua HN, Tasan M, Mutlu B, Weinstein ZB, Suzuki Y, et al. Systematic exploration of synergistic drug pairs. Mol Syst Biol. 2011;7:544.
[20] Nelander S, Wang W, Nilsson B, She QB, Pratilas C, Rosen N, et al. Models from experiments: combinatorial drug perturbations of cancer cells. Mol Syst Biol. 2008;4:216.
[21] Jansen G, Lee AY, Epp E, Fredette A, Surprenant J, Harcus D, et al. Chemogenomic profiling predicts antifungal synergies. Mol Syst Biol. 2009;5:338.
[22] Lehar J, Krueger AS, Avery W, Heilbut AM, Johansen LM, Price ER, et al. Synergistic drug combinations tend to improve therapeutically relevant selectivity. Nat Biotechnol. 2009;27:659-66.
[23] Owens CM, Mawhinney C, Grenier JM, Altmeyer R, Lee MS, Borisy AA, et al. Chemical combinations elucidate pathway interactions and regulation relevant to Hepatitis C replication. Mol Syst Biol. 2010;6:375.
[24] Jia J, Zhu F, Ma X, Cao Z, Li Y, Chen YZ. Mechanisms of drug combinations: interaction and network perspectives. Nat Rev Drug Discov. 2009;8:111-28.
[25] Greco F, Vicent MJ. Combination therapy: opportunities and challenges for polymer-drug conjugates as anticancer nanomedicines. Adv Drug Deliv Rev. 2009;61:1203-13.
[26] Li J, Wang Y, Zhu Y, Oupicky D. Recent advances in delivery of drug-nucleic acid combinations for cancer treatment. J Control Release. 2013;172:589-600.
[27] Janat-Amsbury MM, Yockman JW, Lee M, Kern S, Furgeson DY, Bikram M, et al. Combination of local, nonviral IL12 gene therapy and systemic paclitaxel treatment in a metastatic breast cancer model. Mol Ther. 2004;9:829-36.
[28] Berry DA, Cronin KA, Plevritis SK, Fryback DG, Clarke L, Zelen M, et al. Effect of screening and adjuvant therapy on mortality from breast cancer. N Engl J Med. 2005;353:1784-92.
[29] Akram M, Iqbal M, Daniyal M, Khan AU. Awareness and current knowledge of breast cancer. Biol Res. 2017;50:33.

[30] Pusztai L, Mazouni C, Anderson K, Wu Y, Symmans WF. Molecular classification of breast cancer: limitations and potential. Oncologist. 2006;11:868-77.
[31] Loibl S, Gianni L. HER2-positive breast cancer. Lancet. 2017;389:2415-29.
[32] Vogel CL, Cobleigh MA, Tripathy D, Gutheil JC, Harris LN, Fehrenbacher L, et al. Efficacy and safety of trastuzumab as a single agent in first-line treatment of HER2-overexpressing metastatic breast cancer. J Clin Oncol. 2002;20:719-26.
[33] Dent R, Trudeau M, Pritchard KI, Hanna WM, Kahn HK, Sawka CA, et al. Triple-negative breast cancer: clinical features and patterns of recurrence. Clin Cancer Res. 2007;13:4429-34.
[34] Hon JD, Singh B, Sahin A, Du G, Wang J, Wang VY, et al. Breast cancer molecular subtypes: from TNBC to QNBC. Am J Cancer Res. 2016;6:1864-72.
[35] Karam A. Update on breast cancer surgery approaches. Curr Opin Obstet Gynecol. 2013;25:74-80.
[36] Keskin G, Gumus AB. Turkish hysterectomy and mastectomy patients - depression, body image, sexual problems and spouse relationships. Asian Pac J Cancer Prev. 2011;12:425-32.
[37] Hall EJ, Brenner DJ. Cancer risks from diagnostic radiology. Br J Radiol. 2008;81:362-78.
[38] Hassan MS, Ansari J, Spooner D, Hussain SA. Chemotherapy for breast cancer (Review). Oncol Rep. 2010;24:1121-31.
[39] Smalley KS, Herlyn M. Targeting intracellular signaling pathways as a novel strategy in melanoma therapeutics. Ann N Y Acad Sci. 2005;1059:16-25.
[40] Aliabadi HM, Mahdipoor P, Kucharsky C, Chan N, Uludag H. Effect of siRNA pre-Exposure on Subsequent Response to siRNA Therapy. Pharm Res. 2015;32:3813-26.
[41] Bharadwaj U, Marin-Muller C, Li M, Chen C, Yao Q. Mesothelin confers pancreatic cancer cell resistance to TNF-alpha-induced apoptosis through Akt/PI3K/NF-kappaB activation and IL-6/Mcl-1 overexpression. Mol Cancer. 2011;10:106.
[42] Buchholz TA, Davis DW, McConkey DJ, Symmans WF, Valero V, Jhingran A, et al. Chemotherapy-induced apoptosis and Bcl-2 levels correlate with breast cancer response to chemotherapy. Cancer J. 2003;9:33-41.
[43] Sekine I, Shimizu C, Nishio K, Saijo N, Tamura T. A literature review of molecular markers predictive of clinical response to cytotoxic chemotherapy in patients with breast cancer. Int J Clin Oncol. 2009;14:112-9.

[44] Kanwar RK, Cheung CH, Chang JY, Kanwar JR. Recent advances in anti-survivin treatments for cancer. Curr Med Chem. 2010;17:1509-15.
[45] Wagle N, Emery C, Berger MF, Davis MJ, Sawyer A, Pochanard P, et al. Dissecting therapeutic resistance to RAF inhibition in melanoma by tumor genomic profiling. J Clin Oncol. 2011;29:3085-96.
[46] Aliabadi HM, Landry B, Sun C, Tang T, Uludag H. Supramolecular assemblies in functional siRNA delivery: where do we stand? Biomaterials. 2012;33:2546-69.
[47] Shin JY, Chung YS, Kang B, Jiang HL, Yu DY, Han K, et al. Co-delivery of LETM1 and CTMP synergistically inhibits tumor growth in H-ras12V liver cancer model mice. Cancer Gene Ther. 2013;20:186-94.
[48] Lee SJ, Yook S, Yhee JY, Yoon HY, Kim MG, Ku SH, et al. Co-delivery of VEGF and Bcl-2 dual-targeted siRNA polymer using a single nanoparticle for synergistic anti-cancer effects in vivo. J Control Release. 2015;220:631-41.
[49] Lee SH, Mok H, Jo S, Hong CA, Park TG. Dual gene targeted multimeric siRNA for combinatorial gene silencing. Biomaterials. 2011;32:2359-68.
[50] Pan Y, Zhang L, Zhang X, Liu R. Synergistic effects of eukaryotic co-expression plasmid-based STAT3-specific siRNA and LKB1 on ovarian cancer in vitro and in vivo. Oncol Rep. 2015;33:774-82.
[51] Li L, Yu C, Ren J, Ye S, Ou W, Wang Y, et al. Synergistic effects of eukaryotic coexpression plasmid carrying LKB1 and FUS1 genes on lung cancer in vitro and in vivo. J Cancer Res Clin Oncol. 2014;140:895-907.
[52] Deng WG, Kawashima H, Wu G, Jayachandran G, Xu K, Minna JD, et al. Synergistic tumor suppression by coexpression of FUS1 and p53 is associated with down-regulation of murine double minute-2 and activation of the apoptotic protease-activating factor 1-dependent apoptotic pathway in human non-small cell lung cancer cells. Cancer Res. 2007;67:709-17.
[53] Han L, Zhang AL, Xu P, Yue X, Yang Y, Wang GX, et al. Combination gene therapy with PTEN and EGFR siRNA suppresses U251 malignant glioma cell growth in vitro and in vivo. Med Oncol. 2010;27:843-52.
[54] Kasinski AL, Kelnar K, Stahlhut C, Orellana E, Zhao J, Shimer E, et al. A combinatorial microRNA therapeutics approach to suppressing non-small cell lung cancer. Oncogene. 2015;34:3547-55.

[55] Tai W, Qin B, Cheng K. Inhibition of breast cancer cell growth and invasiveness by dual silencing of HER-2 and VEGF. Mol Pharm. 2010;7:543-56.
[56] Liu K, Chen H, You Q, Shi H, Wang Z. The siRNA cocktail targeting VEGF and HER2 inhibition on the proliferation and induced apoptosis of gastric cancer cell. Mol Cell Biochem. 2014;386:117-24.
[57] Wu YY, Chen L, Wang GL, Zhang YX, Zhou JM, He S, et al. Inhibition of hepatocellular carcinoma growth and angiogenesis by dual silencing of NET-1 and VEGF. J Mol Histol. 2013;44:433-45.
[58] Doan CC, Le LT, Hoang SN, Do SM, Le DV. Simultaneous silencing of VEGF and KSP by siRNA cocktail inhibits proliferation and induces apoptosis of hepatocellular carcinoma Hep3B cells. Biol Res. 2014;47:70.
[59] Peng W, Chen J, Qin Y, Yang Z, Zhu YY. Long double-stranded multiplex siRNAs for dual genes silencing. Nucleic Acid Ther. 2013;23:281-8.
[60] Kaulfuss S, Burfeind P, Gaedcke J, Scharf JG. Dual silencing of insulin-like growth factor-I receptor and epidermal growth factor receptor in colorectal cancer cells is associated with decreased proliferation and enhanced apoptosis. Mol Cancer Ther. 2009;8:821-33.
[61] Yuan YL, Zhou XH, Song J, Qiu XP, Li J, Ye LF. Dual silencing of type 1 insulin-like growth factor and epidermal growth factor receptors to induce apoptosis of nasopharyngeal cancer cells. J Laryngol Otol. 2008;122:952-60.
[62] Chen SH, Chen XH, Wang Y, Kosai K, Finegold MJ, Rich SS, et al. Combination gene therapy for liver metastasis of colon carcinoma in vivo. Proc Natl Acad Sci U S A. 1995;92:2577-81.
[63] Chen SH, Kosai K, Xu B, Pham-Nguyen K, Contant C, Finegold MJ, et al. Combination suicide and cytokine gene therapy for hepatic metastases of colon carcinoma: sustained antitumor immunity prolongs animal survival. Cancer Res. 1996;56:3758-62.
[64] Kim SH, Carew JF, Kooby DA, Shields J, Entwisle C, Patel S, et al. Combination gene therapy using multiple immunomodulatory genes transferred by a defective infectious single-cycle herpes virus in squamous cell cancer. Cancer Gene Ther. 2000;7:1279-85.
[65] Oshikawa K, Shi F, Rakhmilevich AL, Sondel PM, Mahvi DM, Yang NS. Synergistic inhibition of tumor growth in a murine mammary adenocarcinoma model by combinational gene

therapy using IL-12, pro-IL-18, and IL-1beta converting enzyme cDNA. Proc Natl Acad Sci U S A. 1999;96:13351-6.
[66] Shibata MA, Morimoto J, Shibata E, Otsuki Y. Combination therapy with short interfering RNA vectors against VEGF-C and VEGF-A suppresses lymph node and lung metastasis in a mouse immunocompetent mammary cancer model. Cancer Gene Ther. 2008;15:776-86.
[67] Schaffert D, Wagner E. Gene therapy progress and prospects: synthetic polymer-based systems. Gene Ther. 2008;15:1131-8.
[68] Scholz C, Wagner E. Therapeutic plasmid DNA versus siRNA delivery: common and different tasks for synthetic carriers. J Control Release. 2012;161:554-65.
[69] Lachelt U, Wagner E. Nucleic Acid Therapeutics Using Polyplexes: A Journey of 50 Years (and Beyond). Chem Rev. 2015;115:11043-78.
[70] Zhang J, Li X, Huang L. Non-viral nanocarriers for siRNA delivery in breast cancer. J Control Release. 2014;190:440-50.
[71] K CR, Thapa B, Valencia-Serna J, Aliabadi HM, Uludag H. Nucleic acid combinations: A new frontier for cancer treatment. J Control Release. 2017;256:153-69.
[72] Chang Kang H, Bae YH. Co-delivery of small interfering RNA and plasmid DNA using a polymeric vector incorporating endosomolytic oligomeric sulfonamide. Biomaterials. 2011;32:4914-24.
[73] Lu S, Morris VB, Labhasetwar V. Codelivery of DNA and siRNA via arginine-rich PEI-based polyplexes. Mol Pharm. 2015;12:621-9.
[74] Mok H, Lee SH, Park JW, Park TG. Multimeric small interfering ribonucleic acid for highly efficient sequence-specific gene silencing. Nat Mater. 2010;9:272-8.
[75] Perche F, Torchilin VP. Recent trends in multifunctional liposomal nanocarriers for enhanced tumor targeting. J Drug Deliv. 2013;2013:705265.
[76] Allen TM, Cullis PR. Liposomal drug delivery systems: from concept to clinical applications. Adv Drug Deliv Rev. 2013;65:36-48.
[77] Zelphati O, Szoka FC, Jr. Mechanism of oligonucleotide release from cationic liposomes. Proc Natl Acad Sci U S A. 1996;93:11493-8.
[78] Kane RC, Farrell AT, Saber H, Tang S, Williams G, Jee JM, et al. Sorafenib for the treatment of advanced renal cell carcinoma. Clin Cancer Res. 2006;12:7271-8.

[79] Hashida M, Kawakami S, Yamashita F. Lipid carrier systems for targeted drug and gene delivery. Chem Pharm Bull (Tokyo). 2005;53:871-80.
[80] Navarro G, Sawant RR, Biswas S, Essex S, Tros de Ilarduya C, Torchilin VP. P-glycoprotein silencing with siRNA delivered by DOPE-modified PEI overcomes doxorubicin resistance in breast cancer cells. Nanomedicine (Lond). 2012;7:65-78.
[81] Chang RS, Suh MS, Kim S, Shim G, Lee S, Han SS, et al. Cationic drug-derived nanoparticles for multifunctional delivery of anticancer siRNA. Biomaterials. 2011;32:9785-95.
[82] Biswas S, Deshpande PP, Navarro G, Dodwadkar NS, Torchilin VP. Lipid modified triblock PAMAM-based nanocarriers for siRNA drug co-delivery. Biomaterials. 2013;34:1289-301.
[83] Ruponen M, Honkakoski P, Tammi M, Urtti A. Cell-surface glycosaminoglycans inhibit cation-mediated gene transfer. J Gene Med. 2004;6:405-14.
[84] Rhinn H, Largeau C, Bigey P, Kuen RL, Richard M, Scherman D, et al. How to make siRNA lipoplexes efficient? Add a DNA cargo. Biochim Biophys Acta. 2009;1790:219-30.
[85] Sun TM, Du JZ, Yao YD, Mao CQ, Dou S, Huang SY, et al. Simultaneous delivery of siRNA and paclitaxel via a "two-in-one" micelleplex promotes synergistic tumor suppression. ACS Nano. 2011;5:1483-94.
[86] Xiong XB, Lavasanifar A. Traceable multifunctional micellar nanocarriers for cancer-targeted co-delivery of MDR-1 siRNA and doxorubicin. ACS Nano. 2011;5:5202-13.
[87] Patil YB, Swaminathan SK, Sadhukha T, Ma L, Panyam J. The use of nanoparticle-mediated targeted gene silencing and drug delivery to overcome tumor drug resistance. Biomaterials. 2010;31:358-65.
[88] Wang Y, Gao S, Ye WH, Yoon HS, Yang YY. Co-delivery of drugs and DNA from cationic core-shell nanoparticles self-assembled from a biodegradable copolymer. Nat Mater. 2006;5:791-6.
[89] Sun TM, Du JZ, Yan LF, Mao HQ, Wang J. Self-assembled biodegradable micellar nanoparticles of amphiphilic and cationic block copolymer for siRNA delivery. Biomaterials. 2008;29:4348-55.
[90] Mintzer MA, Simanek EE. Nonviral vectors for gene delivery. Chem Rev. 2009;109:259-302.
[91] Putnam D. Polymers for gene delivery across length scales. Nat Mater. 2006;5:439-51.

[92] Kim E, Jung Y, Choi H, Yang J, Suh JS, Huh YM, et al. Prostate cancer cell death produced by the co-delivery of Bcl-xL shRNA and doxorubicin using an aptamer-conjugated polyplex. Biomaterials. 2010;31:4592-9.
[93] Zhu C, Jung S, Luo S, Meng F, Zhu X, Park TG, et al. Co-delivery of siRNA and paclitaxel into cancer cells by biodegradable cationic micelles based on PDMAEMA-PCL-PDMAEMA triblock copolymers. Biomaterials. 2010;31:2408-16.
[94] Dufes C, Uchegbu IF, Schatzlein AG. Dendrimers in gene delivery. Adv Drug Deliv Rev. 2005;57:2177-202.
[95] Kaneshiro TL, Wang X, Lu ZR. Synthesis, characterization, and gene delivery of poly-L-lysine octa(3-aminopropyl)silsesquioxane dendrimers: nanoglobular drug carriers with precisely defined molecular architectures. Mol Pharm. 2007;4:759-68.
[96] Kaneshiro TL, Lu ZR. Targeted intracellular codelivery of chemotherapeutics and nucleic acid with a well-defined dendrimer-based nanoglobular carrier. Biomaterials. 2009;30:5660-6.
[97] Liu XX, Rocchi P, Qu FQ, Zheng SQ, Liang ZC, Gleave M, et al. PAMAM dendrimers mediate siRNA delivery to target Hsp27 and produce potent antiproliferative effects on prostate cancer cells. ChemMedChem. 2009;4:1302-10.
[98] Kim C, Shah BP, Subramaniam P, Lee KB. Synergistic induction of apoptosis in brain cancer cells by targeted codelivery of siRNA and anticancer drugs. Mol Pharm. 2011;8:1955-61.
[99] Cao N, Cheng D, Zou S, Ai H, Gao J, Shuai X. The synergistic effect of hierarchical assemblies of siRNA and chemotherapeutic drugs co-delivered into hepatic cancer cells. Biomaterials. 2011;32:2222-32.
[100] Burnett JC, Rossi JJ, Tiemann K. Current progress of siRNA/shRNA therapeutics in clinical trials. Biotechnol J. 2011;6:1130-46.
[101] Fan H, Hu QD, Xu FJ, Liang WQ, Tang GP, Yang WT. In vivo treatment of tumors using host-guest conjugated nanoparticles functionalized with doxorubicin and therapeutic gene pTRAIL. Biomaterials. 2012;33:1428-36.
[102] Neamnark A, Suwantong O, Bahadur RK, Hsu CY, Supaphol P, Uludag H. Aliphatic lipid substitution on 2 kDa polyethylenimine improves plasmid delivery and transgene expression. Mol Pharm. 2009;6:1798-815.
[103] Han S, Mahato RI, Kim SW. Water-soluble lipopolymer for gene delivery. Bioconjug Chem. 2001;12:337-45.

[104] Thomas M, Klibanov AM. Enhancing polyethylenimine's delivery of plasmid DNA into mammalian cells. Proc Natl Acad Sci U S A. 2002;99:14640-5.
[105] Remant Bahadur KC CKaHU. Additive nanocomplexes of cationic lipopolymers for improved non-viral gene delivery to mesenchymal stem cells. 2015.
[106] Hsu CY, Uludag H. Cellular uptake pathways of lipid-modified cationic polymers in gene delivery to primary cells. Biomaterials. 2012;33:7834-48.
[107] Meneksedag-Erol D, Kc RB, Tang T, Uludag H. A Delicate Balance When Substituting a Small Hydrophobe onto Low Molecular Weight Polyethylenimine to Improve Its Nucleic Acid Delivery Efficiency. ACS Appl Mater Interfaces. 2015;7:24822-32.
[108] Aliabadi HM, Mahdipoor P, Uludag H. Polymeric delivery of siRNA for dual silencing of Mcl-1 and P-glycoprotein and apoptosis induction in drug-resistant breast cancer cells. Cancer Gene Ther. 2013;20:169-77.
[109] Parmar MB, Arteaga Ballesteros BE, Fu T, K CR, Montazeri Aliabadi H, Hugh JC, et al. Multiple siRNA delivery against cell cycle and anti-apoptosis proteins using lipid-substituted polyethylenimine in triple-negative breast cancer and nonmalignant cells. J Biomed Mater Res A. 2016.
[110] Aliabadi HM, Maranchuk R, Kucharski C, Mahdipoor P, Hugh J, Uludag H. Effective response of doxorubicin-sensitive and -resistant breast cancer cells to combinational siRNA therapy. J Control Release. 2013;172:219-28.
[111] Han SE, Kang H, Shim GY, Kim SJ, Choi HG, Kim J, et al. Cationic derivatives of biocompatible hyaluronic acids for delivery of siRNA and antisense oligonucleotides. J Drug Target. 2009;17:123-32.
[112] Talekar M, Trivedi M, Shah P, Ouyang Q, Oka A, Gandham S, et al. Combination wt-p53 and MicroRNA-125b Transfection in a Genetically Engineered Lung Cancer Model Using Dual CD44/EGFR-targeting Nanoparticles. Mol Ther. 2016;24:759-69.
[113] Jeon SY, Park JS, Yang HN, Woo DG, Park KH. Co-delivery of SOX9 genes and anti-Cbfa-1 siRNA coated onto PLGA nanoparticles for chondrogenesis of human MSCs. Biomaterials. 2012;33:4413-23.
[114] Bishop CJ, Tzeng SY, Green JJ. Degradable polymer-coated gold nanoparticles for co-delivery of DNA and siRNA. Acta Biomater. 2015;11:393-403.

[115] Wiley SR, Schooley K, Smolak PJ, Din WS, Huang CP, Nicholl JK, et al. Identification and characterization of a new member of the TNF family that induces apoptosis. Immunity. 1995;3:673-82.
[116] Wang S, El-Deiry WS. TRAIL and apoptosis induction by TNF-family death receptors. Oncogene. 2003;22:8628-33.
[117] Ashkenazi A, Pai RC, Fong S, Leung S, Lawrence DA, Marsters SA, et al. Safety and antitumor activity of recombinant soluble Apo2 ligand. J Clin Invest. 1999;104:155-62.
[118] MacFarlane M. TRAIL-induced signalling and apoptosis. Toxicol Lett. 2003;139:89-97.
[119] Stuckey DW, Shah K. TRAIL on trial: preclinical advances in cancer therapy. Trends Mol Med. 2013;19:685-94.
[120] Linkermann A, Green DR. Necroptosis. N Engl J Med. 2014;370:455-65.
[121] Sun L, Wang H, Wang Z, He S, Chen S, Liao D, et al. Mixed lineage kinase domain-like protein mediates necrosis signaling downstream of RIP3 kinase. Cell. 2012;148:213-27.
[122] Cai Z, Jitkaew S, Zhao J, Chiang HC, Choksi S, Liu J, et al. Plasma membrane translocation of trimerized MLKL protein is required for TNF-induced necroptosis. Nat Cell Biol. 2014;16:55-65.
[123] Pan G, Ni J, Wei YF, Yu G, Gentz R, Dixit VM. An antagonist decoy receptor and a death domain-containing receptor for TRAIL. Science. 1997;277:815-8.
[124] Lemke J, von Karstedt S, Zinngrebe J, Walczak H. Getting TRAIL back on track for cancer therapy. Cell Death Differ. 2014;21:1350-64.
[125] Marsters SA, Sheridan JP, Pitti RM, Huang A, Skubatch M, Baldwin D, et al. A novel receptor for Apo2L/TRAIL contains a truncated death domain. Curr Biol. 1997;7:1003-6.
[126] Merino D, Lalaoui N, Morizot A, Schneider P, Solary E, Micheau O. Differential inhibition of TRAIL-mediated DR5-DISC formation by decoy receptors 1 and 2. Mol Cell Biol. 2006;26:7046-55.
[127] Morizot A, Merino D, Lalaoui N, Jacquemin G, Granci V, Iessi E, et al. Chemotherapy overcomes TRAIL-R4-mediated TRAIL resistance at the DISC level. Cell Death Differ. 2011;18:700-11.
[128] Park C, Moon DO, Ryu CH, Choi B, Lee W, Kim GY, et al. Beta-sitosterol sensitizes MDA-MB-231 cells to TRAIL-induced apoptosis. Acta Pharmacol Sin. 2008;29:341-8.

[129] Herbst RS, Eckhardt SG, Kurzrock R, Ebbinghaus S, O'Dwyer PJ, Gordon MS, et al. Phase I dose-escalation study of recombinant human Apo2L/TRAIL, a dual proapoptotic receptor agonist, in patients with advanced cancer. J Clin Oncol. 2010;28:2839-46.
[130] Hotte SJ, Hirte HW, Chen EX, Siu LL, Le LH, Corey A, et al. A phase 1 study of mapatumumab (fully human monoclonal antibody to TRAIL-R1) in patients with advanced solid malignancies. Clin Cancer Res. 2008;14:3450-5.
[131] Forero-Torres A, Shah J, Wood T, Posey J, Carlisle R, Copigneaux C, et al. Phase I trial of weekly tigatuzumab, an agonistic humanized monoclonal antibody targeting death receptor 5 (DR5). Cancer Biother Radiopharm. 2010;25:13-9.
[132] Camidge DR. Apomab: an agonist monoclonal antibody directed against Death Receptor 5/TRAIL-Receptor 2 for use in the treatment of solid tumors. Expert Opin Biol Ther. 2008;8:1167-76.
[133] Younes A, Vose JM, Zelenetz AD, Smith MR, Burris HA, Ansell SM, et al. A Phase 1b/2 trial of mapatumumab in patients with relapsed/refractory non-Hodgkin's lymphoma. Br J Cancer. 2010;103:1783-7.
[134] Soria JC, Mark Z, Zatloukal P, Szima B, Albert I, Juhasz E, et al. Randomized phase II study of dulanermin in combination with paclitaxel, carboplatin, and bevacizumab in advanced non-small-cell lung cancer. J Clin Oncol. 2011;29:4442-51.
[135] Wainberg ZA, Messersmith WA, Peddi PF, Kapp AV, Ashkenazi A, Royer-Joo S, et al. A phase 1B study of dulanermin in combination with modified FOLFOX6 plus bevacizumab in patients with metastatic colorectal cancer. Clin Colorectal Cancer. 2013;12:248-54.
[136] Soria JC, Smit E, Khayat D, Besse B, Yang X, Hsu CP, et al. Phase 1b study of dulanermin (recombinant human Apo2L/TRAIL) in combination with paclitaxel, carboplatin, and bevacizumab in patients with advanced non-squamous non-small-cell lung cancer. J Clin Oncol. 2010;28:1527-33.
[137] Tolcher AW, Mita M, Meropol NJ, von Mehren M, Patnaik A, Padavic K, et al. Phase I pharmacokinetic and biologic correlative study of mapatumumab, a fully human monoclonal antibody with agonist activity to tumor necrosis factor-related apoptosis-inducing ligand receptor-1. J Clin Oncol. 2007;25:1390-5.

[138] Mom CH, Verweij J, Oldenhuis CN, Gietema JA, Fox NL, Miceli R, et al. Mapatumumab, a fully human agonistic monoclonal antibody that targets TRAIL-R1, in combination with gemcitabine and cisplatin: a phase I study. Clin Cancer Res. 2009;15:5584-90.
[139] von Pawel J, Harvey JH, Spigel DR, Dediu M, Reck M, Cebotaru CL, et al. Phase II trial of mapatumumab, a fully human agonist monoclonal antibody to tumor necrosis factor-related apoptosis-inducing ligand receptor 1 (TRAIL-R1), in combination with paclitaxel and carboplatin in patients with advanced non-small-cell lung cancer. Clin Lung Cancer. 2014;15:188-96 e2.
[140] Trarbach T, Moehler M, Heinemann V, Kohne CH, Przyborek M, Schulz C, et al. Phase II trial of mapatumumab, a fully human agonistic monoclonal antibody that targets and activates the tumour necrosis factor apoptosis-inducing ligand receptor-1 (TRAIL-R1), in patients with refractory colorectal cancer. Br J Cancer. 2010;102:506-12.
[141] Herbst RS, Kurzrock R, Hong DS, Valdivieso M, Hsu CP, Goyal L, et al. A first-in-human study of conatumumab in adult patients with advanced solid tumors. Clin Cancer Res. 2010;16:5883-91.
[142] Paz-Ares L, Balint B, de Boer RH, van Meerbeeck JP, Wierzbicki R, De Souza P, et al. A randomized phase 2 study of paclitaxel and carboplatin with or without conatumumab for first-line treatment of advanced non-small-cell lung cancer. J Thorac Oncol. 2013;8:329-37.
[143] Kindler HL, Richards DA, Garbo LE, Garon EB, Stephenson JJ, Jr., Rocha-Lima CM, et al. A randomized, placebo-controlled phase 2 study of ganitumab (AMG 479) or conatumumab (AMG 655) in combination with gemcitabine in patients with metastatic pancreatic cancer. Ann Oncol. 2012;23:2834-42.
[144] Plummer R, Attard G, Pacey S, Li L, Razak A, Perrett R, et al. Phase 1 and pharmacokinetic study of lexatumumab in patients with advanced cancers. Clin Cancer Res. 2007;13:6187-94.
[145] Wakelee HA, Patnaik A, Sikic BI, Mita M, Fox NL, Miceli R, et al. Phase I and pharmacokinetic study of lexatumumab (HGS-ETR2) given every 2 weeks in patients with advanced solid tumors. Ann Oncol. 2010;21:376-81.
[146] Merchant MS, Geller JI, Baird K, Chou AJ, Galli S, Charles A, et al. Phase I trial and pharmacokinetic study of lexatumumab in pediatric patients with solid tumors. J Clin Oncol. 2012;30:4141-7.
[147] Forero-Torres A, Infante JR, Waterhouse D, Wong L, Vickers S, Arrowsmith E, et al. Phase 2, multicenter, open-label study of tigatuzumab (CS-1008), a humanized monoclonal antibody

targeting death receptor 5, in combination with gemcitabine in chemotherapy-naive patients with unresectable or metastatic pancreatic cancer. Cancer Med. 2013;2:925-32.
[148] Reck M, Krzakowski M, Chmielowska E, Sebastian M, Hadler D, Fox T, et al. A randomized, double-blind, placebo-controlled phase 2 study of tigatuzumab (CS-1008) in combination with carboplatin/paclitaxel in patients with chemotherapy-naive metastatic/unresectable non-small cell lung cancer. Lung Cancer. 2013;82:441-8.
[149] Rocha Lima CM, Bayraktar S, Flores AM, MacIntyre J, Montero A, Baranda JC, et al. Phase Ib study of drozitumab combined with first-line mFOLFOX6 plus bevacizumab in patients with metastatic colorectal cancer. Cancer Invest. 2012;30:727-31.
[150] Camidge DR, Herbst RS, Gordon MS, Eckhardt SG, Kurzrock R, Durbin B, et al. A phase I safety and pharmacokinetic study of the death receptor 5 agonistic antibody PRO95780 in patients with advanced malignancies. Clin Cancer Res. 2010;16:1256-63.
[151] Sharma S, de Vries EG, Infante JR, Oldenhuis CN, Gietema JA, Yang L, et al. Safety, pharmacokinetics, and pharmacodynamics of the DR5 antibody LBY135 alone and in combination with capecitabine in patients with advanced solid tumors. Invest New Drugs. 2014;32:135-44.
[152] Rahman M, Pumphrey JG, Lipkowitz S. The TRAIL to targeted therapy of breast cancer. Adv Cancer Res. 2009;103:43-73.
[153] Singh TR, Shankar S, Chen X, Asim M, Srivastava RK. Synergistic interactions of chemotherapeutic drugs and tumor necrosis factor-related apoptosis-inducing ligand/Apo-2 ligand on apoptosis and on regression of breast carcinoma in vivo. Cancer Res. 2003;63:5390-400.
[154] Keane MM, Rubinstein Y, Cuello M, Ettenberg SA, Banerjee P, Nau MM, et al. Inhibition of NF-kappaB activity enhances TRAIL mediated apoptosis in breast cancer cell lines. Breast Cancer Res Treat. 2000;64:211-9.
[155] Rahman M, Davis SR, Pumphrey JG, Bao J, Nau MM, Meltzer PS, et al. TRAIL induces apoptosis in triple-negative breast cancer cells with a mesenchymal phenotype. Breast Cancer Res Treat. 2009;113:217-30.
[156] Zhang L, Fang B. Mechanisms of resistance to TRAIL-induced apoptosis in cancer. Cancer Gene Ther. 2005;12:228-37.
[157] Sheikh MS, Huang Y, Fernandez-Salas EA, El-Deiry WS, Friess H, Amundson S, et al. The antiapoptotic decoy receptor TRID/TRAIL-R3 is a p53-regulated DNA damage-inducible gene that is overexpressed in primary tumors of the gastrointestinal tract. Oncogene. 1999;18:4153-9.

[158] Ganten TM, Sykora J, Koschny R, Batke E, Aulmann S, Mansmann U, et al. Prognostic significance of tumour necrosis factor-related apoptosis-inducing ligand (TRAIL) receptor expression in patients with breast cancer. J Mol Med (Berl). 2009;87:995-1007.
[159] Kim K, Fisher MJ, Xu SQ, el-Deiry WS. Molecular determinants of response to TRAIL in killing of normal and cancer cells. Clin Cancer Res. 2000;6:335-46.
[160] Lincz LF, Yeh TX, Spencer A. TRAIL-induced eradication of primary tumour cells from multiple myeloma patient bone marrows is not related to TRAIL receptor expression or prior chemotherapy. Leukemia. 2001;15:1650-7.
[161] Maksimovic-Ivanic D, Stosic-Grujicic S, Nicoletti F, Mijatovic S. Resistance to TRAIL and how to surmount it. Immunol Res. 2012;52:157-68.
[162] Krueger A, Schmitz I, Baumann S, Krammer PH, Kirchhoff S. Cellular FLICE-inhibitory protein splice variants inhibit different steps of caspase-8 activation at the CD95 death-inducing signaling complex. J Biol Chem. 2001;276:20633-40.
[163] Golks A, Brenner D, Fritsch C, Krammer PH, Lavrik IN. c-FLIPR, a new regulator of death receptor-induced apoptosis. J Biol Chem. 2005;280:14507-13.
[164] Micheau O, Thome M, Schneider P, Holler N, Tschopp J, Nicholson DW, et al. The long form of FLIP is an activator of caspase-8 at the Fas death-inducing signaling complex. J Biol Chem. 2002;277:45162-71.
[165] Micheau O, Lens S, Gaide O, Alevizopoulos K, Tschopp J. NF-kappaB signals induce the expression of c-FLIP. Mol Cell Biol. 2001;21:5299-305.
[166] Siegmund D, Hadwiger P, Pfizenmaier K, Vornlocher HP, Wajant H. Selective inhibition of FLICE-like inhibitory protein expression with small interfering RNA oligonucleotides is sufficient to sensitize tumor cells for TRAIL-induced apoptosis. Mol Med. 2002;8:725-32.
[167] Irmler M, Thome M, Hahne M, Schneider P, Hofmann K, Steiner V, et al. Inhibition of death receptor signals by cellular FLIP. Nature. 1997;388:190-5.
[168] Chawla-Sarkar M, Bae SI, Reu FJ, Jacobs BS, Lindner DJ, Borden EC. Downregulation of Bcl-2, FLIP or IAPs (XIAP and survivin) by siRNAs sensitizes resistant melanoma cells to Apo2L/TRAIL-induced apoptosis. Cell Death Differ. 2004;11:915-23.
[169] Zhang YP, Kong QH, Huang Y, Wang GL, Chang KJ. Inhibition of c-FLIP by RNAi enhances sensitivity of the human osteogenic sarcoma cell line U2OS to TRAIL-induced apoptosis. Asian Pac J Cancer Prev. 2015;16:2251-6.

[170] Ganten TM, Koschny R, Haas TL, Sykora J, Li-Weber M, Herzer K, et al. Proteasome inhibition sensitizes hepatocellular carcinoma cells, but not human hepatocytes, to TRAIL. Hepatology. 2005;42:588-97.
[171] Placzek WJ, Wei J, Kitada S, Zhai D, Reed JC, Pellecchia M. A survey of the anti-apoptotic Bcl-2 subfamily expression in cancer types provides a platform to predict the efficacy of Bcl-2 antagonists in cancer therapy. Cell Death Dis. 2010;1:e40.
[172] Altieri DC. Survivin, versatile modulation of cell division and apoptosis in cancer. Oncogene. 2003;22:8581-9.
[173] van Dijk M, Halpin-McCormick A, Sessler T, Samali A, Szegezdi E. Resistance to TRAIL in non-transformed cells is due to multiple redundant pathways. Cell Death Dis. 2013;4:e702.
[174] Sheridan JP, Marsters SA, Pitti RM, Gurney A, Skubatch M, Baldwin D, et al. Control of TRAIL-induced apoptosis by a family of signaling and decoy receptors. Science. 1997;277:818-21.
[175] Degli-Esposti MA, Smolak PJ, Walczak H, Waugh J, Huang CP, DuBose RF, et al. Cloning and characterization of TRAIL-R3, a novel member of the emerging TRAIL receptor family. J Exp Med. 1997;186:1165-70.
[176] Zhang XD, Franco A, Myers K, Gray C, Nguyen T, Hersey P. Relation of TNF-related apoptosis-inducing ligand (TRAIL) receptor and FLICE-inhibitory protein expression to TRAIL-induced apoptosis of melanoma. Cancer Res. 1999;59:2747-53.
[177] Morioka S, Omori E, Kajino T, Kajino-Sakamoto R, Matsumoto K, Ninomiya-Tsuji J. TAK1 kinase determines TRAIL sensitivity by modulating reactive oxygen species and cIAP. Oncogene. 2009;28:2257-65.
[178] Xiang H, Nguyen CB, Kelley SK, Dybdal N, Escandon E. Tissue distribution, stability, and pharmacokinetics of Apo2 ligand/tumor necrosis factor-related apoptosis-inducing ligand in human colon carcinoma COLO205 tumor-bearing nude mice. Drug Metab Dispos. 2004;32:1230-8.
[179] Lim SM, Kim TH, Jiang HH, Park CW, Lee S, Chen X, et al. Improved biological half-life and anti-tumor activity of TNF-related apoptosis-inducing ligand (TRAIL) using PEG-exposed nanoparticles. Biomaterials. 2011;32:3538-46.
[180] Kelley SK, Harris LA, Xie D, Deforge L, Totpal K, Bussiere J, et al. Preclinical studies to predict the disposition of Apo2L/tumor necrosis factor-related apoptosis-inducing ligand in

humans: characterization of in vivo efficacy, pharmacokinetics, and safety. J Pharmacol Exp Ther. 2001;299:31-8.
[181] Li F, Guo Y, Han L, Duan Y, Fang F, Niu S, et al. In vitro and in vivo growth inhibition of drug-resistant ovarian carcinoma cells using a combination of cisplatin and a TRAIL-encoding retrovirus. Oncol Lett. 2012;4:1254-8.
[182] Sayers TJ, Murphy WJ. Combining proteasome inhibition with TNF-related apoptosis-inducing ligand (Apo2L/TRAIL) for cancer therapy. Cancer Immunol Immunother. 2006;55:76-84.
[183] Bangert A, Cristofanon S, Eckhardt I, Abhari BA, Kolodziej S, Hacker S, et al. Histone deacetylase inhibitors sensitize glioblastoma cells to TRAIL-induced apoptosis by c-myc-mediated downregulation of cFLIP. Oncogene. 2012;31:4677-88.
[184] Lemke J, von Karstedt S, Abd El Hay M, Conti A, Arce F, Montinaro A, et al. Selective CDK9 inhibition overcomes TRAIL resistance by concomitant suppression of cFlip and Mcl-1. Cell Death Differ. 2014;21:491-502.
[185] Fulda S, Wick W, Weller M, Debatin KM. Smac agonists sensitize for Apo2L/TRAIL- or anticancer drug-induced apoptosis and induce regression of malignant glioma in vivo. Nat Med. 2002;8:808-15.
[186] Li L, Thomas RM, Suzuki H, De Brabander JK, Wang X, Harran PG. A small molecule Smac mimic potentiates TRAIL- and TNFalpha-mediated cell death. Science. 2004;305:1471-4.
[187] Huang S, Sinicrope FA. BH3 mimetic ABT-737 potentiates TRAIL-mediated apoptotic signaling by unsequestering Bim and Bak in human pancreatic cancer cells. Cancer Res. 2008;68:2944-51.
[188] Wang G, Zhan Y, Wang H, Li W. ABT-263 sensitizes TRAIL-resistant hepatocarcinoma cells by downregulating the Bcl-2 family of anti-apoptotic protein. Cancer Chemother Pharmacol. 2012;69:799-805.
[189] Walczak H, Miller RE, Ariail K, Gliniak B, Griffith TS, Kubin M, et al. Tumoricidal activity of tumor necrosis factor-related apoptosis-inducing ligand in vivo. Nat Med. 1999;5:157-63.
[190] Seki N, Toh U, Sayers TJ, Fujii T, Miyagi M, Akagi Y, et al. Bortezomib sensitizes human esophageal squamous cell carcinoma cells to TRAIL-mediated apoptosis via activation of both extrinsic and intrinsic apoptosis pathways. Mol Cancer Ther. 2010;9:1842-51.

[191] Jane EP, Premkumar DR, Pollack IF. Bortezomib sensitizes malignant human glioma cells to TRAIL, mediated by inhibition of the NF-{kappa}B signaling pathway. Mol Cancer Ther. 2011;10:198-208.
[192] Song JH, Kandasamy K, Kraft AS. ABT-737 induces expression of the death receptor 5 and sensitizes human cancer cells to TRAIL-induced apoptosis. J Biol Chem. 2008;283:25003-13.
[193] Karikari CA, Roy I, Tryggestad E, Feldmann G, Pinilla C, Welsh K, et al. Targeting the apoptotic machinery in pancreatic cancers using small-molecule antagonists of the X-linked inhibitor of apoptosis protein. Mol Cancer Ther. 2007;6:957-66.
[194] Fakler M, Loeder S, Vogler M, Schneider K, Jeremias I, Debatin KM, et al. Small molecule XIAP inhibitors cooperate with TRAIL to induce apoptosis in childhood acute leukemia cells and overcome Bcl-2-mediated resistance. Blood. 2009;113:1710-22.
[195] Hao JH, Yu M, Liu FT, Newland AC, Jia L. Bcl-2 inhibitors sensitize tumor necrosis factor-related apoptosis-inducing ligand-induced apoptosis by uncoupling of mitochondrial respiration in human leukemic CEM cells. Cancer Res. 2004;64:3607-16.
[196] Sayers TJ, Brooks AD, Koh CY, Ma W, Seki N, Raziuddin A, et al. The proteasome inhibitor PS-341 sensitizes neoplastic cells to TRAIL-mediated apoptosis by reducing levels of c-FLIP. Blood. 2003;102:303-10.
[197] Perlstein B, Finniss SA, Miller C, Okhrimenko H, Kazimirsky G, Cazacu S, et al. TRAIL conjugated to nanoparticles exhibits increased anti-tumor activities in glioma cells and glioma stem cells in vitro and in vivo. Neuro Oncol. 2013;15:29-40.
[198] Kim H, Jeong D, Kang HE, Lee KC, Na K. A sulfate polysaccharide/TNF-related apoptosis-inducing ligand (TRAIL) complex for the long-term delivery of TRAIL in poly(lactic-co-glycolic acid) (PLGA) microspheres. J Pharm Pharmacol. 2013;65:11-21.
[199] Shah K, Tung CH, Yang K, Weissleder R, Breakefield XO. Inducible release of TRAIL fusion proteins from a proapoptotic form for tumor therapy. Cancer Res. 2004;64:3236-42.
[200] Kim TH, Jo YG, Jiang HH, Lim SM, Youn YS, Lee S, et al. PEG-transferrin conjugated TRAIL (TNF-related apoptosis-inducing ligand) for therapeutic tumor targeting. J Control Release. 2012;162:422-8.
[201] Liu S, Guo Y, Huang R, Li J, Huang S, Kuang Y, et al. Gene and doxorubicin co-delivery system for targeting therapy of glioma. Biomaterials. 2012;33:4907-16.

[202] Kim CY, Jeong M, Mushiake H, Kim BM, Kim WB, Ko JP, et al. Cancer gene therapy using a novel secretable trimeric TRAIL. Gene Ther. 2006;13:330-8.
[203] Griffith TS, Anderson RD, Davidson BL, Williams RD, Ratliff TL. Adenoviral-mediated transfer of the TNF-related apoptosis-inducing ligand/Apo-2 ligand gene induces tumor cell apoptosis. J Immunol. 2000;165:2886-94.
[204] Mohr A, Henderson G, Dudus L, Herr I, Kuerschner T, Debatin KM, et al. AAV-encoded expression of TRAIL in experimental human colorectal cancer leads to tumor regression. Gene Ther. 2004;11:534-43.
[205] Aza-Blanc P, Cooper CL, Wagner K, Batalov S, Deveraux QL, Cooke MP. Identification of modulators of TRAIL-induced apoptosis via RNAi-based phenotypic screening. Mol Cell. 2003;12:627-37.
[206] Garimella SV, Gehlhaus K, Dine JL, Pitt JJ, Grandin M, Chakka S, et al. Identification of novel molecular regulators of tumor necrosis factor-related apoptosis-inducing ligand (TRAIL)-induced apoptosis in breast cancer cells by RNAi screening. Breast Cancer Res. 2014;16:R41.
[207] Thapa B, Bahadur Kc R, Uludag H. Novel targets for sensitizing breast cancer cells to TRAIL-induced apoptosis with siRNA delivery. Int J Cancer. 2018;142:597-606.
[208] Wang W, Zhang M, Sun W, Yang S, Su Y, Zhang H, et al. Reduction of decoy receptor 3 enhances TRAIL-mediated apoptosis in pancreatic cancer. PLoS One. 2013;8:e74272.
[209] Brooks AD, Sayers TJ. Reduction of the antiapoptotic protein cFLIP enhances the susceptibility of human renal cancer cells to TRAIL apoptosis. Cancer Immunol Immunother. 2005;54:499-505.
[210] Spee B, Jonkers MD, Arends B, Rutteman GR, Rothuizen J, Penning LC. Specific down-regulation of XIAP with RNA interference enhances the sensitivity of canine tumor cell-lines to TRAIL and doxorubicin. Mol Cancer. 2006;5:34.
[211] Park S, Shim SM, Nam SH, Andera L, Suh N, Kim I. CGP74514A enhances TRAIL-induced apoptosis in breast cancer cells by reducing X-linked inhibitor of apoptosis protein. Anticancer Res. 2014;34:3557-62.
[212] Nakao K, Hamasaki K, Ichikawa T, Arima K, Eguchi K, Ishii N. Survivin downregulation by siRNA sensitizes human hepatoma cells to TRAIL-induced apoptosis. Oncol Rep. 2006;16:389-92.

[213] Chen W, Wang X, Zhuang J, Zhang L, Lin Y. Induction of death receptor 5 and suppression of survivin contribute to sensitization of TRAIL-induced cytotoxicity by quercetin in non-small cell lung cancer cells. Carcinogenesis. 2007;28:2114-21.
[214] Jeong JK, Moon MH, Seo JS, Seol JW, Park SY, Lee YJ. Hypoxia inducing factor-1alpha regulates tumor necrosis factor-related apoptosis-inducing ligand sensitivity in tumor cells exposed to hypoxia. Biochem Biophys Res Commun. 2010;399:379-83.
[215] Harashima N, Takenaga K, Akimoto M, Harada M. HIF-2alpha dictates the susceptibility of pancreatic cancer cells to TRAIL by regulating survivin expression. Oncotarget. 2017;8:42887-900.
[216] Hayashi KT, S.; Piras, V.; Timota, M.; Selvarajoo, K. systems biology strategy reveals PKCδ is key for sensitizing TRAIL-resistant human fibrosarcoma. Frontiers in Immunology. 2015;5:9.
[217] Garimella SV, Rocca A, Lipkowitz S. WEE1 inhibition sensitizes basal breast cancer cells to TRAIL-induced apoptosis. Mol Cancer Res. 2012;10:75-85.
[218] Tseng HY, Chen LH, Ye Y, Tay KH, Jiang CC, Guo ST, et al. The melanoma-associated antigen MAGE-D2 suppresses TRAIL receptor 2 and protects against TRAIL-induced apoptosis in human melanoma cells. Carcinogenesis. 2012;33:1871-81.
[219] Zhuang H, Jiang W, Cheng W, Qian K, Dong W, Cao L, et al. Down-regulation of HSP27 sensitizes TRAIL-resistant tumor cell to TRAIL-induced apoptosis. Lung Cancer. 2010;68:27-38.
[220] Hayashi K, Tabata S, Piras V, Tomita M, Selvarajoo K. Systems Biology Strategy Reveals PKCdelta is Key for Sensitizing TRAIL-Resistant Human Fibrosarcoma. Front Immunol. 2014;5:659.
[221] Kim MJ, Kim HB, Bae JH, Lee JW, Park SJ, Kim DW, et al. Sensitization of human K562 leukemic cells to TRAIL-induced apoptosis by inhibiting the DNA-PKcs/Akt-mediated cell survival pathway. Biochem Pharmacol. 2009;78:573-82.
[222] Wan Z, Pan H, Liu S, Zhu J, Qi W, Fu K, et al. Downregulation of SNAIL sensitizes hepatocellular carcinoma cells to TRAIL-induced apoptosis by regulating the NF-kappaB pathway. Oncol Rep. 2015;33:1560-6.
[223] Sanlioglu AD, Karacay B, Koksal IT, Griffith TS, Sanlioglu S. DcR2 (TRAIL-R4) siRNA and adenovirus delivery of TRAIL (Ad5hTRAIL) break down in vitro tumorigenic potential of prostate carcinoma cells. Cancer Gene Ther. 2007;14:976-84.

[224] Weyhenmeyer BC, Noonan J, Wurstle ML, Lincoln FA, Johnston G, Rehm M, et al. Predicting the cell death responsiveness and sensitization of glioma cells to TRAIL and temozolomide. Oncotarget. 2016;7:61295-311.
[225] Park SJ, Kim MJ, Kim HB, Kang CD, Kim SH. Sensitization of imatinib-resistant CML cells to TRAIL-induced apoptosis is mediated through down-regulation of Bcr-Abl as well as c-FLIP. Biochem J. 2009;420:73-81.
[226] Duiker EW, Dijkers EC, Lambers Heerspink H, de Jong S, van der Zee AG, Jager PL, et al. Development of a radioiodinated apoptosis-inducing ligand, rhTRAIL, and a radiolabelled agonist TRAIL receptor antibody for clinical imaging studies. Br J Pharmacol. 2012;165:2203-12.
[227] Schneider P. Production of recombinant TRAIL and TRAIL receptor: Fc chimeric proteins. Methods Enzymol. 2000;322:325-45.
[228] Pitti RM, Marsters SA, Ruppert S, Donahue CJ, Moore A, Ashkenazi A. Induction of apoptosis by Apo-2 ligand, a new member of the tumor necrosis factor cytokine family. J Biol Chem. 1996;271:12687-90.
[229] Berg D, Lehne M, Muller N, Siegmund D, Munkel S, Sebald W, et al. Enforced covalent trimerization increases the activity of the TNF ligand family members TRAIL and CD95L. Cell Death Differ. 2007;14:2021-34.
[230] Ganten TM, Koschny R, Sykora J, Schulze-Bergkamen H, Buchler P, Haas TL, et al. Preclinical differentiation between apparently safe and potentially hepatotoxic applications of TRAIL either alone or in combination with chemotherapeutic drugs. Clin Cancer Res. 2006;12:2640-6.
[231] de Miguel D, Lemke J, Anel A, Walczak H, Martinez-Lostao L. Onto better TRAILs for cancer treatment. Cell Death Differ. 2016;23:733-47.
[232] Muller N, Schneider B, Pfizenmaier K, Wajant H. Superior serum half life of albumin tagged TNF ligands. Biochem Biophys Res Commun. 2010;396:793-9.
[233] Kim TH, Youn YS, Jiang HH, Lee S, Chen X, Lee KC. PEGylated TNF-related apoptosis-inducing ligand (TRAIL) analogues: pharmacokinetics and antitumor effects. Bioconjug Chem. 2011;22:1631-7.
[234] Li R, Yang H, Jia D, Nie Q, Cai H, Fan Q, et al. Fusion to an albumin-binding domain with a high affinity for albumin extends the circulatory half-life and enhances the in vivo antitumor effects of human TRAIL. J Control Release. 2016;228:96-106.

[235] De Miguel D, Gallego-Lleyda A, Anel A, Martinez-Lostao L. Liposome-bound TRAIL induces superior DR5 clustering and enhanced DISC recruitment in histiocytic lymphoma U937 cells. Leuk Res. 2015;39:657-66.
[236] Seifert O, Pollak N, Nusser A, Steiniger F, Ruger R, Pfizenmaier K, et al. Immuno-LipoTRAIL: Targeted delivery of TRAIL-functionalized liposomal nanoparticles. Bioconjug Chem. 2014;25:879-87.
[237] Bae S, Ma K, Kim TH, Lee ES, Oh KT, Park ES, et al. Doxorubicin-loaded human serum albumin nanoparticles surface-modified with TNF-related apoptosis-inducing ligand and transferrin for targeting multiple tumor types. Biomaterials. 2012;33:1536-46.
[238] Sun X, Pang Z, Ye H, Qiu B, Guo L, Li J, et al. Co-delivery of pEGFP-hTRAIL and paclitaxel to brain glioma mediated by an angiopep-conjugated liposome. Biomaterials. 2012;33:916-24.
[239] Zheng L, Weilun Z, Minghong J, Yaxi Z, Shilian L, Yanxin L, et al. Adeno-associated virus-mediated doxycycline-regulatable TRAIL expression suppresses growth of human breast carcinoma in nude mice. BMC Cancer. 2012;12:153.
[240] Zhang H, Sui A, Wang Z, Liu S, Yao R. Adenovirus-mediated TRAIL expression and downregulation of Bcl-2 expression suppresses non-small cell lung cancer growth in vitro and in vivo. Int J Mol Med. 2012;30:358-64.
[241] Grisendi G, Spano C, D'Souza N, Rasini V, Veronesi E, Prapa M, et al. Mesenchymal progenitors expressing TRAIL induce apoptosis in sarcomas. Stem Cells. 2015;33:859-69.
[242] Grisendi G, Bussolari R, Cafarelli L, Petak I, Rasini V, Veronesi E, et al. Adipose-derived mesenchymal stem cells as stable source of tumor necrosis factor-related apoptosis-inducing ligand delivery for cancer therapy. Cancer Res. 2010;70:3718-29.
[243] Lathrop MJ, Sage EK, Macura SL, Brooks EM, Cruz F, Bonenfant NR, et al. Antitumor effects of TRAIL-expressing mesenchymal stromal cells in a mouse xenograft model of human mesothelioma. Cancer Gene Ther. 2015;22:44-54.
[244] Kim SM, Lim JY, Park SI, Jeong CH, Oh JH, Jeong M, et al. Gene therapy using TRAIL-secreting human umbilical cord blood-derived mesenchymal stem cells against intracranial glioma. Cancer Res. 2008;68:9614-23.

[245] Yan C, Yang M, Li Z, Li S, Hu X, Fan D, et al. Suppression of orthotopically implanted hepatocarcinoma in mice by umbilical cord-derived mesenchymal stem cells with sTRAIL gene expression driven by AFP promoter. Biomaterials. 2014;35:3035-43.
[246] Kaczorowski A, Hammer K, Liu L, Villhauer S, Nwaeburu C, Fan P, et al. Delivery of improved oncolytic adenoviruses by mesenchymal stromal cells for elimination of tumorigenic pancreatic cancer cells. Oncotarget. 2016;7:9046-59.
[247] Hu YL, Huang B, Zhang TY, Miao PH, Tang GP, Tabata Y, et al. Mesenchymal stem cells as a novel carrier for targeted delivery of gene in cancer therapy based on nonviral transfection. Mol Pharm. 2012;9:2698-709.
[248] Tang XJ, Lu JT, Tu HJ, Huang KM, Fu R, Cao G, et al. TRAIL-engineered bone marrow-derived mesenchymal stem cells: TRAIL expression and cytotoxic effects on C6 glioma cells. Anticancer Res. 2014;34:729-34.
[249] Pack DW, Hoffman AS, Pun S, Stayton PS. Design and development of polymers for gene delivery. Nature reviews Drug discovery. 2005;4:581-93.
[250] Niidome T, Urakawa M, Sato H, Takahara Y, Anai T, Hatakayama T, et al. Gene transfer into hepatoma cells mediated by galactose-modified alpha-helical peptides. Biomaterials. 2000;21:1811-9.
[251] Arangoa MA, Duzgunes N, Tros de Ilarduya C. Increased receptor-mediated gene delivery to the liver by protamine-enhanced-asialofetuin-lipoplexes. Gene Ther. 2003;10:5-14.
[252] Zanta MA, Boussif O, Adib A, Behr JP. In vitro gene delivery to hepatocytes with galactosylated polyethylenimine. Bioconjug Chem. 1997;8:839-44.
[253] Kawakami S, Sato A, Nishikawa M, Yamashita F, Hashida M. Mannose receptor-mediated gene transfer into macrophages using novel mannosylated cationic liposomes. Gene Ther. 2000;7:292-9.
[254] Mansouri S, Cuie Y, Winnik F, Shi Q, Lavigne P, Benderdour M, et al. Characterization of folate-chitosan-DNA nanoparticles for gene therapy. Biomaterials. 2006;27:2060-5.
[255] Jeong JH, Lee M, Kim WJ, Yockman JW, Park TG, Kim YH, et al. Anti-GAD antibody targeted non-viral gene delivery to islet beta cells. J Control Release. 2005;107:562-70.
[256] Hashida M, Nishikawa M, Yamashita F, Takakura Y. Cell-specific delivery of genes with glycosylated carriers. Adv Drug Deliv Rev. 2001;52:187-96.

[257] Singh GK, Siahpush M, Altekruse SF. Time trends in liver cancer mortality, incidence, and risk factors by unemployment level and race/ethnicity, United States, 1969-2011. J Community Health. 2013;38:926-40.
[258] Bosch FX, Ribes J, Diaz M, Cleries R. Primary liver cancer: worldwide incidence and trends. Gastroenterology. 2004;127:S5-S16.
[259] Gerolami R, Uch R, Brechot C, Mannoni P, Bagnis C. Gene therapy of hepatocarcinoma: a long way from the concept to the therapeutical impact. Cancer Gene Ther. 2003;10:649-60.
[260] Singh M, Ariatti M. Targeted gene delivery into HepG2 cells using complexes containing DNA, cationized asialoorosomucoid and activated cationic liposomes. J Control Release. 2003;92:383-94.
[261] Peng DJ, Sun J, Wang YZ, Tian J, Zhang YH, Noteborn MH, et al. Inhibition of hepatocarcinoma by systemic delivery of Apoptin gene via the hepatic asialoglycoprotein receptor. Cancer Gene Ther. 2007;14:66-73.
[262] Khorev O, Stokmaier D, Schwardt O, Cutting B, Ernst B. Trivalent, Gal/GalNAc-containing ligands designed for the asialoglycoprotein receptor. Bioorg Med Chem 2008;16:5216-31.
[263] Ahmed M, Jawanda M, Ishihara K, Narain R. Impact of the nature, size and chain topologies of carbohydrate-phosphorylcholine polymeric gene delivery systems. Biomaterials. 2012;33:7858-70.
[264] Ahmed M, Deng Z, Liu S, Lafrenie R, Kumar A, Narain R. Cationic glyconanoparticles: their complexation with DNA, cellular uptake, and transfection efficiencies. Bioconjug Chem. 2009;20:2169-76.
[265] Ahmed M, Narain R. The effect of molecular weight, compositions and lectin type on the properties of hyperbranched glycopolymers as non-viral gene delivery systems. Biomaterials. 2012;33:3990-4001.
[266] Strand SP, Issa MM, Christensen BE, Varum KM, Artursson P. Tailoring of chitosans for gene delivery: novel self-branched glycosylated chitosan oligomers with improved functional properties. Biomacromolecules. 2008;9:3268-76.
[267] Liu Y, Reineke TM. Poly(glycoamidoamine)s for gene delivery. structural effects on cellular internalization, buffering capacity, and gene expression. Bioconjug Chem. 2007;18:19-30.

[268] Deng Z, Bouchekif H, Babooram K, Housni A, Choytun N, Narain R. Facile synthesis of controlled-structure primary amine-based methacrylamide polymers via the reversible addition-fragmentation chain transfer process. J Polym Sci, Part A: Polym Chem 2008;46:4984–96.
[269] Deng Z, Ahmed M, Narain R. Novel well-defined glycopolymers synthesized via the reversible addition fragmentation chain transfer process in aqueous media. Poly Sci Part A Polym Chem 2009;47:614-27.
[270] Deng Z, Li S, Jiang X, Narain R. Well-defined galactose-containing multifunctional copolymers and glyconanoparticles for biomolecular recognition processes. Macromolecules 2009;42:6393-405.
[271] Ahmed M, Narain R. The effect of polymer architecture, composition, and molecular weight on the properties of glycopolymer-based non-viral gene delivery systems. Biomaterials. 2011;32:5279-90.
[272] Srinivasachari S, Liu Y, Prevette LE, Reineke TM. Effects of trehalose click polymer length on pDNA complex stability and delivery efficacy. Biomaterials. 2007;28:2885-98.
[273] Lam JK, Ma Y, Armes SP, Lewis AL, Baldwin T, Stolnik S. Phosphorylcholine-polycation diblock copolymers as synthetic vectors for gene delivery. J Control Release. 2004;100:293-312.
[274] Uchida H, Miyata K, Oba M, Ishii T, Suma T, Itaka K, et al. Odd-even effect of repeating aminoethylene units in the side chain of N-substituted polyaspartamides on gene transfection profiles. J Am Chem Soc 2011;133:15524-32.
[275] Synatschke CV, Schallon A, Jerome V, Freitag R, Muller AH. Influence of polymer architecture and molecular weight of poly(2-(dimethylamino)ethyl methacrylate) polycations on transfection efficiency and cell viability in gene delivery. Biomacromolecules. 2011;12:4247-55.
[276] Ahmed M, Bhuchar N, Ishihara K, Narain R. Well-controlled cationic water-soluble phospholipid polymer-DNA nanocomplexes for gene delivery. Bioconjug Chem. 2011;22:1228-38.
[277] Bhuchar N, Deng Z, Ishihara K, Narain R. Detailed study of the reversible addition fragmentation chain transfer polymerization and co-polymerization of 2-methacryloyloxyethyl phosphorylcholine. Polym Chem. 2011;2:632-9.
[278] Boyer C, Bulmus V, Davis PT, Ladmiral V, Liu J, Perrier S. Bioapplications of RAFT Polymerization. Chem Rev 2009;109:5402-36.

[279] Popielarski SR, Mishra S, Davis ME. Structural effects of carbohydrate-containing polycations on gene delivery. 3. Cyclodextrin type and functionalization. Bioconjug Chem. 2003;14:672-8.
[280] Hwang SJ, Bellocq NC, Davis ME. Effects of structure of beta-cyclodextrin-containing polymers on gene delivery. Bioconjug Chem. 2001;12:280-90.
[281] Park TG, Jeong JH, Kim SW. Current status of polymeric gene delivery systems. Adv Drug Deliv Rev. 2006;58:467-86.
[282] Lee M, Kim SW. Polyethylene glycol-conjugated copolymers for plasmid DNA delivery. Pharm Res 2005;22:1-10.
[283] Petersen H, Fechner PM, Martin AL, Kunath K, Stolnik S, Roberts CJ, et al. Polyethylenimine-graft-poly(ethylene glycol) copolymers: influence of copolymer block structure on DNA complexation and biological activities as gene delivery system. Bioconjug Chem. 2002;13:845-54.
[284] Boussif O, Delair T, Brua C, Veron L, Pavirani A, Kolbe HV. Synthesis of polyallylamine derivatives and their use as gene transfer vectors in vitro. Bioconjug Chem. 1999;10:877-83.
[285] Le Bon B, Van Craynest N, Boussif O, Vierling P. Polycationic diblock and random polyethylene glycol- or tris(hydroxymethyl)methyl-grafted (co)telomers for gene transfer: synthesis and evaluation of their in vitro transfection efficiency. Bioconjug Chem. 2002;13:1292-301.
[286] Harada-Shiba M, Yamauchi K, Harada A, Takamisawa I, Shimokado K, Kataoka K. Polyion complex micelles as vectors in gene therapy--pharmacokinetics and in vivo gene transfer. Gene Ther. 2002;9:407-14.
[287] Pun SH, Bellocq NC, Liu A, Jensen G, Machemer T, Quijano E, et al. Cyclodextrin-modified polyethylenimine polymers for gene delivery. Bioconjug Chem. 2004;15:831-40.
[288] Midoux P, Mendes C, Legrand A, Raimond J, Mayer R, Monsigny M, et al. Specific gene transfer mediated by lactosylated poly-L-lysine into hepatoma cells. Nucleic Acids Res 1993;21:871-8.
[289] Hashida M, Takemura S, Nishikawa M, Takakura Y. Targeted delivery of plasmid DNA complexed with galactosylated poly(L-lysine). J Control Release. 1998;53:301-10.

[290] Rotundo RF, Rebres RA, McKeown-Longo PJ, Blumenstock FA, Saba TM. Circulating cellular fibronectin may be a natural ligand for the hepatic asialoglycoprotein receptor: possible pathway for fibronectin deposition and turnover in the rat liver. Hepatology. 1998;28:475-85.
[291] Lee RT, Lin P, Lee YC. New synthetic cluster ligands for galactose/N-acetylgalactosamine-specific lectin of mammalian liver. Biochemistry. 1984;23:4255-61.
[292] Wang Y, Su J, Cai W, Lu P, Yuan L, Jin T, et al. Hepatocyte-targeting gene transfer mediated by galactosylated poly(ethylene glycol)-graft-polyethylenimine derivative. Drug Des Devel Ther. 2013;7:211-21.
[293] Kopatz I, Remy JS, Behr JP. A model for non-viral gene delivery: through syndecan adhesion molecules and powered by actin. J Gene Med. 2004;6:769-76.
[294] Goncalves C, Mennesson E, Fuchs R, Gorvel JP, Midoux P, Pichon C. Macropinocytosis of polyplexes and recycling of plasmid via the clathrin-dependent pathway impair the transfection efficiency of human hepatocarcinoma cells. Mol Ther. 2004;10:373-85.
[295] Rifai A, Fadden K, Morrison SL, Chintalacharuvu KR. The N-glycans determine the differential blood clearance and hepatic uptake of human immunoglobulin (Ig)A1 and IgA2 isotypes. J Exp Med. 2000;191:2171-82.
[296] Lee YC, Townsend RR, Hardy MR, Lonngren J, Arnarp J, Haraldsson M, et al. Binding of synthetic oligosaccharides to the hepatic Gal/GalNAc lectin. Dependence on fine structural features. J Biol Chem 1983;258:199-202.
[297] Biessen EA, Beuting DM, Roelen HC, van de Marel GA, van Boom JH, van Berkel TJ. Synthesis of cluster galactosides with high affinity for the hepatic asialoglycoprotein receptor. J Med Chem 1995;38:1538-46.
[298] Morille M, Passirani C, Vonarbourg A, Clavreul A, Benoit JP. Progress in developing cationic vectors for non-viral systemic gene therapy against cancer. Biomaterials. 2008;29:3477-96.
[299] Li S, Huang L. Nonviral gene therapy: promises and challenges. Gene therapy. 2000;7:31-4.
[300] Zonghua Liua, Ziyong Zhanga, Changren Zhoua, Yanpeng Jiaoa. Hydrophobic modifications of cationic polymers for gene delivery. Progress in Polymer Science. 2010;35:1144-62.

[301] J.H. Jeong, S.W. Kim, Park TG. Molecular design of functional polymers for gene therapy. Prog Polym Sci. 2007;32 1239-74.
[302] Doody AM, Korley JN, Dang KP, Zawaneh PN, Putnam D. Characterizing the structure/function parameter space of hydrocarbon-conjugated branched polyethylenimine for DNA delivery in vitro. Journal of controlled release : official journal of the Controlled Release Society. 2006;116:227-37.
[303] Alshamsan A, Haddadi A, Incani V, Samuel J, Lavasanifar A, Uludag H. Formulation and delivery of siRNA by oleic acid and stearic acid modified polyethylenimine. Mol Pharm. 2009;6:121-33.
[304] Incani V, Tunis E, Clements BA, Olson C, Kucharski C, Lavasanifar A, et al. Palmitic acid substitution on cationic polymers for effective delivery of plasmid DNA to bone marrow stromal cells. J Biomed Mater Res A. 2007;81:493-504.
[305] Kircheis R, Wightman L, Wagner E. Design and gene delivery activity of modified polyethylenimines. Advanced drug delivery reviews. 2001;53:341-58.
[306] Gabrielson NP, Pack DW. Efficient polyethylenimine-mediated gene delivery proceeds via a caveolar pathway in HeLa cells. Journal of controlled release : official journal of the Controlled Release Society. 2009;136:54-61.
[307] Moghimi SM, Symonds P, Murray JC, Hunter AC, Debska G, Szewczyk A. A two-stage poly(ethylenimine)-mediated cytotoxicity: implications for gene transfer/therapy. Mol Ther. 2005;11:990-5.
[308] Ryser HJ. A membrane effect of basic polymers dependent on molecular size. Nature. 1967;215:934-6.
[309] Seymour LW, Duncan R, Strohalm J, Kopecek J. Effect of molecular weight (Mw) of N-(2-hydroxypropyl)methacrylamide copolymers on body distribution and rate of excretion after subcutaneous, intraperitoneal, and intravenous administration to rats. J Biomed Mater Res. 1987;21:1341-58.
[310] Bajaj A, Kondaiah P, Bhattacharya S. Synthesis and gene transfection efficacies of PEI-cholesterol-based lipopolymers. Bioconjugate chemistry. 2008;19:1640-51.
[311] Hsu CY, Hendzel M, Uludag H. Improved transfection efficiency of an aliphatic lipid substituted 2 kDa polyethylenimine is attributed to enhanced nuclear association and uptake in rat bone marrow stromal cell. The journal of gene medicine. 2011;13:46-59.

[312] Zheng M, Zhong Y, Meng F, Peng R, Zhong Z. Lipoic acid modified low molecular weight polyethylenimine mediates nontoxic and highly potent in vitro gene transfection. Mol Pharm. 2011;8:2434-43.
[313] Furgeson DY, Cohen RN, Mahato RI, Kim SW. Novel water insoluble lipoparticulates for gene delivery. Pharmaceutical research. 2002;19:382-90.
[314] Bahadur KC, Landry B, Aliabadi HM, Lavasanifar A, Uludag H. Lipid substitution on low molecular weight (0.6-2.0 kDa) polyethylenimine leads to a higher zeta potential of plasmid DNA and enhances transgene expression. Acta Biomater. 2011;7:2209-17.
[315] K.C. RB, Uludag H. A Comparative Evaluation of Disulfide-Linked and Hydrophobically-Modified PEI for Plasmid Delivery. Journal of Biomaterials Science. 2011;22:873-92.
[316] Zhong Z, Feijen J, Lok MC, Hennink WE, Christensen LV, Yockman JW, et al. Low molecular weight linear polyethylenimine-b-poly(ethylene glycol)-b-polyethylenimine triblock copolymers: synthesis, characterization, and in vitro gene transfer properties. Biomacromolecules. 2005;6:3440-8.
[317] Aliabadi HM, Landry B, Bahadur RK, Neamnark A, Suwantong O, Uludag H. Impact of lipid substitution on assembly and delivery of siRNA by cationic polymers. Macromol Biosci. 2011;11:662-72.
[318] Remant Bahadur KC CKaHU. Additive nanocomplexes of cationic lipopolymers for improved non-viral gene delivery to mesenchymal stem cells. J Mater Chem B. 2015;3:10.
[319] Kizzire K, Khargharia S, Rice KG. High-affinity PEGylated polyacridine peptide polyplexes mediate potent in vivo gene expression. Gene therapy. 2013;20:407-16.
[320] Bolcato-Bellemin AL, Bonnet ME, Creusat G, Erbacher P, Behr JP. Sticky overhangs enhance siRNA-mediated gene silencing. Proc Natl Acad Sci U S A. 2007;104:16050-5.
[321] Gabrielson NP, Pack DW. Acetylation of polyethylenimine enhances gene delivery via weakened polymer/DNA interactions. Biomacromolecules. 2006;7:2427-35.
[322] Lv H, Zhang S, Wang B, Cui S, Yan J. Toxicity of cationic lipids and cationic polymers in gene delivery. Journal of controlled release : official journal of the Controlled Release Society. 2006;114:100-9.
[323] Gary DJ, Puri N, Won YY. Polymer-based siRNA delivery: perspectives on the fundamental and phenomenological distinctions from polymer-based DNA delivery. Journal of controlled release : official journal of the Controlled Release Society. 2007;121:64-73.

[324] Zheng M, Pavan GM, Neeb M, Schaper AK, Danani A, Klebe G, et al. Targeting the blind spot of polycationic nanocarrier-based siRNA delivery. ACS Nano. 2012;6:9447-54.
[325] Thomas M, Lu JJ, Ge Q, Zhang C, Chen J, Klibanov AM. Full deacylation of polyethylenimine dramatically boosts its gene delivery efficiency and specificity to mouse lung. Proc Natl Acad Sci U S A. 2005;102:5679-84.
[326] Sun C, Tang T, Uludag H. A molecular dynamics simulation study on the effect of lipid substitution on polyethylenimine mediated siRNA complexation. Biomaterials. 2013;34:2822-33.
[327] Teo PY, Yang C, Hedrick JL, Engler AC, Coady DJ, Ghaem-Maghami S, et al. Hydrophobic modification of low molecular weight polyethylenimine for improved gene transfection. Biomaterials. 2013;34:7971-9.
[328] Schaffer DV, Fidelman NA, Dan N, Lauffenburger DA. Vector unpacking as a potential barrier for receptor-mediated polyplex gene delivery. Biotechnology and bioengineering. 2000;67:598-606.
[329] Hanahan D, Weinberg RA. Hallmarks of cancer: the next generation. Cell. 2011;144:646-74.
[330] Lowe SW, Bodis S, McClatchey A, Remington L, Ruley HE, Fisher DE, et al. p53 status and the efficacy of cancer therapy in vivo. Science. 1994;266:807-10.
[331] Whibley C, Pharoah PD, Hollstein M. p53 polymorphisms: cancer implications. Nat Rev Cancer. 2009;9:95-107.
[332] O'Connor L, Harris AW, Strasser A. CD95 (Fas/APO-1) and p53 signal apoptosis independently in diverse cell types. Cancer Res. 2000;60:1217-20.
[333] Yerbes R, Palacios C, Lopez-Rivas A. The therapeutic potential of TRAIL receptor signalling in cancer cells. Clin Transl Oncol. 2011;13:839-47.
[334] Refaat A, Abd-Rabou A, Reda A. TRAIL combinations: The new 'trail' for cancer therapy (Review). Oncol Lett. 2014;7:1327-32.
[335] Valencia-Serna J, Chevallier P, Kc RB, Laroche G, Uludag H. Fibronectin-modified surfaces for evaluating the influence of cell adhesion on sensitivity of leukemic cells to siRNA nanoparticles. Nanomedicine (Lond). 2016;11:1123-38.
[336] Wang Y, Mostafa NZ, Hsu CY, Rose L, Kucharki C, Yan J, et al. Modification of human BMSC with nanoparticles of polymeric biomaterials and plasmid DNA for BMP-2 secretion. J Surg Res. 2013;183:8-17.

[337] Thapa B, Plianwong S, Remant Bahadur KC, Rutherford B, Uludag H. Small hydrophobe substitution on polyethylenimine for plasmid DNA delivery: Optimal substitution is critical for effective delivery. Acta Biomater. 2016;33:213-24.
[338] Parmar MB, Aliabadi HM, Mahdipoor P, Kucharski C, Maranchuk R, Hugh JC, et al. Targeting Cell Cycle Proteins in Breast Cancer Cells with siRNA by Using Lipid-Substituted Polyethylenimines. Front Bioeng Biotechnol. 2015;3:14.
[339] McManus MT, Sharp PA. Gene silencing in mammals by small interfering RNAs. Nat Rev Genet. 2002;3:737-47.
[340] Kim DH, Rossi JJ. Strategies for silencing human disease using RNA interference. Nat Rev Genet. 2007;8:173-84.
[341] Lam JK, Chow MY, Zhang Y, Leung SW. siRNA Versus miRNA as Therapeutics for Gene Silencing. Mol Ther Nucleic Acids. 2015;4:e252.
[342] Karl I, Jossberger-Werner M, Schmidt N, Horn S, Goebeler M, Leverkus M, et al. TRAF2 inhibits TRAIL- and CD95L-induced apoptosis and necroptosis. Cell Death Dis. 2014;5:e1444.
[343] Stegh AH, Kim H, Bachoo RM, Forloney KL, Zhang J, Schulze H, et al. Bcl2L12 inhibits post-mitochondrial apoptosis signaling in glioblastoma. Genes Dev. 2007;21:98-111.
[344] Stegh AH, Kesari S, Mahoney JE, Jenq HT, Forloney KL, Protopopov A, et al. Bcl2L12-mediated inhibition of effector caspase-3 and caspase-7 via distinct mechanisms in glioblastoma. Proc Natl Acad Sci U S A. 2008;105:10703-8.
[345] Thomadaki H, Talieri M, Scorilas A. Prognostic value of the apoptosis related genes BCL2 and BCL2L12 in breast cancer. Cancer Lett. 2007;247:48-55.
[346] Hong Y, Yang J, Wu W, Wang W, Kong X, Wang Y, et al. Knockdown of BCL2L12 leads to cisplatin resistance in MDA-MB-231 breast cancer cells. Biochim Biophys Acta. 2008;1782:649-57.
[347] Lee MT, Ho SM, Tarapore P, Chung I, Leung YK. Estrogen receptor beta isoform 5 confers sensitivity of breast cancer cell lines to chemotherapeutic agent-induced apoptosis through interaction with Bcl2L12. Neoplasia. 2013;15:1262-71.
[348] Somwar R, Erdjument-Bromage H, Larsson E, Shum D, Lockwood WW, Yang G, et al. Superoxide dismutase 1 (SOD1) is a target for a small molecule identified in a screen for inhibitors of the growth of lung adenocarcinoma cell lines. Proc Natl Acad Sci U S A. 2011;108:16375-80.

[349] Bouayed J, Bohn T. Exogenous antioxidants--Double-edged swords in cellular redox state: Health beneficial effects at physiologic doses versus deleterious effects at high doses. Oxid Med Cell Longev. 2010;3:228-37.
[350] Papa L, Manfredi G, Germain D. SOD1, an unexpected novel target for cancer therapy. Genes Cancer. 2014;5:15-21.
[351] Huang P, Feng L, Oldham EA, Keating MJ, Plunkett W. Superoxide dismutase as a target for the selective killing of cancer cells. Nature. 2000;407:390-5.
[352] Glasauer A, Sena LA, Diebold LP, Mazar AP, Chandel NS. Targeting SOD1 reduces experimental non-small-cell lung cancer. J Clin Invest. 2014;124:117-28.
[353] Liu JW, Chandra D, Rudd MD, Butler AP, Pallotta V, Brown D, et al. Induction of prosurvival molecules by apoptotic stimuli: involvement of FOXO3a and ROS. Oncogene. 2005;24:2020-31.
[354] Allensworth JL, Aird KM, Aldrich AJ, Batinic-Haberle I, Devi GR. XIAP inhibition and generation of reactive oxygen species enhances TRAIL sensitivity in inflammatory breast cancer cells. Mol Cancer Ther. 2012;11:1518-27.
[355] Janicke RU, Sprengart ML, Wati MR, Porter AG. Caspase-3 is required for DNA fragmentation and morphological changes associated with apoptosis. J Biol Chem. 1998;273:9357-60.
[356] Liang Y, Yan C, Schor NF. Apoptosis in the absence of caspase 3. Oncogene. 2001;20:6570-8.
[357] Eck-Enriquez K, Kiefer TL, Spriggs LL, Hill SM. Pathways through which a regimen of melatonin and retinoic acid induces apoptosis in MCF-7 human breast cancer cells. Breast Cancer Res Treat. 2000;61:229-39.
[358] Mooney LM, Al-Sakkaf KA, Brown BL, Dobson PR. Apoptotic mechanisms in T47D and MCF-7 human breast cancer cells. Br J Cancer. 2002;87:909-17.
[359] Todaro M, Lombardo Y, Francipane MG, Alea MP, Cammareri P, Iovino F, et al. Apoptosis resistance in epithelial tumors is mediated by tumor-cell-derived interleukin-4. Cell Death Differ. 2008;15:762-72.
[360] Chae SY, Kim TH, Park K, Jin CH, Son S, Lee S, et al. Improved antitumor activity and tumor targeting of NH(2)-terminal-specific PEGylated tumor necrosis factor-related apoptosis-inducing ligand. Mol Cancer Ther. 2010;9:1719-29.

[361] Jo M, Kim TH, Seol DW, Esplen JE, Dorko K, Billiar TR, et al. Apoptosis induced in normal human hepatocytes by tumor necrosis factor-related apoptosis-inducing ligand. Nat Med. 2000;6:564-7.
[362] Wang H, Davis JS, Wu X. Immunoglobulin Fc domain fusion to TRAIL significantly prolongs its plasma half-life and enhances its antitumor activity. Mol Cancer Ther. 2014;13:643-50.
[363] Wu X, Wang S, Li M, Wang A, Zhou Y, Li P, et al. Nanocarriers for TRAIL delivery: driving TRAIL back on track for cancer therapy. Nanoscale. 2017;9:13879-904.
[364] Lawrence D, Shahrokh Z, Marsters S, Achilles K, Shih D, Mounho B, et al. Differential hepatocyte toxicity of recombinant Apo2L/TRAIL versions. Nat Med. 2001;7:383-5.
[365] Dong F, Wang L, Davis JJ, Hu W, Zhang L, Guo W, et al. Eliminating established tumor in nu/nu nude mice by a tumor necrosis factor-alpha-related apoptosis-inducing ligand-armed oncolytic adenovirus. Clin Cancer Res. 2006;12:5224-30.
[366] Kock N, Kasmieh R, Weissleder R, Shah K. Tumor therapy mediated by lentiviral expression of shBcl-2 and S-TRAIL. Neoplasia. 2007;9:435-42.
[367] Kim SM, Woo JS, Jeong CH, Ryu CH, Jang JD, Jeun SS. Potential application of temozolomide in mesenchymal stem cell-based TRAIL gene therapy against malignant glioma. Stem Cells Transl Med. 2014;3:172-82.
[368] Jing HX, Duan de J, Zhou H, Hu QM, Lei TC. Adiposederived mesenchymal stem cellfacilitated TRAIL expression in melanoma treatment in vitro. Mol Med Rep. 2016;14:195-201.
[369] Mohr A, Albarenque SM, Deedigan L, Yu R, Reidy M, Fulda S, et al. Targeting of XIAP combined with systemic mesenchymal stem cell-mediated delivery of sTRAIL ligand inhibits metastatic growth of pancreatic carcinoma cells. Stem Cells. 2010;28:2109-20.
[370] Li J, Gu B, Meng Q, Yan Z, Gao H, Chen X, et al. The use of myristic acid as a ligand of polyethylenimine/DNA nanoparticles for targeted gene therapy of glioblastoma. Nanotechnology. 2011;22:435101.
[371] Huang S, Li J, Han L, Liu S, Ma H, Huang R, et al. Dual targeting effect of Angiopep-2-modified, DNA-loaded nanoparticles for glioma. Biomaterials. 2011;32:6832-8.
[372] Mangipudi SS, Canine BF, Wang Y, Hatefi A. Development of a genetically engineered biomimetic vector for targeted gene transfer to breast cancer cells. Mol Pharm. 2009;6:1100-9.

[373] Luo C, Miao L, Zhao Y, Musetti S, Wang Y, Shi K, et al. A novel cationic lipid with intrinsic antitumor activity to facilitate gene therapy of TRAIL DNA. Biomaterials. 2016;102:239-48.
[374] Cha SS, Kim MS, Choi YH, Sung BJ, Shin NK, Shin HC, et al. 2.8 A resolution crystal structure of human TRAIL, a cytokine with selective antitumor activity. Immunity. 1999;11:253-61.
[375] Hymowitz SG, Christinger HW, Fuh G, Ultsch M, O'Connell M, Kelley RF, et al. Triggering cell death: the crystal structure of Apo2L/TRAIL in a complex with death receptor 5. Mol Cell. 1999;4:563-71.
[376] Kim MH, Billiar TR, Seol DW. The secretable form of trimeric TRAIL, a potent inducer of apoptosis. Biochem Biophys Res Commun. 2004;321:930-5.
[377] Thapa B, KC R, Uludag H. Novel targets for sensitizing breast cancer cells to TRAIL-induced apoptosis with siRNA delivery. Int J Cancer. 2018;142:597-606.
[378] KC RB, Kucharski C, Uludag H. Additive nanocomplexes of cationic lipopolymers for improved non-viral gene delivery to mesenchymal stem cells. J Mater Chem B. 2015;3:3972-82.
[379] Akhtar LN, Qin H, Muldowney MT, Yanagisawa LL, Kutsch O, Clements JE, et al. Suppressor of cytokine signaling 3 inhibits antiviral IFN-beta signaling to enhance HIV-1 replication in macrophages. J Immunol. 2010;185:2393-404.
[380] Livak KJ, Schmittgen TD. Analysis of relative gene expression data using real-time quantitative PCR and the 2(-Delta Delta C(T)) Method. Methods. 2001;25:402-8.
[381] Miao L, Zhang K, Qiao C, Jin X, Zheng C, Yang B, et al. Antitumor effect of human TRAIL on adenoid cystic carcinoma using magnetic nanoparticle-mediated gene expression. Nanomedicine. 2013;9:141-50.
[382] Wu X, Hui KM. Induction of potent TRAIL-mediated tumoricidal activity by hFLEX/Furin/TRAIL recombinant DNA construct. Mol Ther. 2004;9:674-81.
[383] Braeuer SJ, Buneker C, Mohr A, Zwacka RM. Constitutively activated nuclear factor-kappaB, but not induced NF-kappaB, leads to TRAIL resistance by up-regulation of X-linked inhibitor of apoptosis protein in human cancer cells. Mol Cancer Res. 2006;4:715-28.
[384] Sanlioglu AD, Dirice E, Aydin C, Erin N, Koksoy S, Sanlioglu S. Surface TRAIL decoy receptor-4 expression is correlated with TRAIL resistance in MCF7 breast cancer cells. BMC Cancer. 2005;5:54.

[385] Zhang Y, Zhang B. TRAIL resistance of breast cancer cells is associated with constitutive endocytosis of death receptors 4 and 5. Mol Cancer Res. 2008;6:1861-71.
[386] Singh A, Nie H, Ghosn B, Qin H, Kwak LW, Roy K. Efficient modulation of T-cell response by dual-mode, single-carrier delivery of cytokine-targeted siRNA and DNA vaccine to antigen-presenting cells. Mol Ther. 2008;16:2011-21.
[387] Wilson JM. Gendicine: the first commercial gene therapy product. Hum Gene Ther. 2005;16:1014-5.
[388] Yla-Herttuala S. Endgame: glybera finally recommended for approval as the first gene therapy drug in the European union. Mol Ther. 2012;20:1831-2.
[389] Li JF, Huang Y, Chen RL, Lee HJ. Induction of apoptosis by gene transfer of human TRAIL mediated by arginine-rich intracellular delivery peptides. Anticancer Res. 2010;30:2193-202.
[390] Tzeng SY, Wilson DR, Hansen SK, Quinones-Hinojosa A, Green JJ. Polymeric nanoparticle-based delivery of TRAIL DNA for cancer-specific killing. Bioeng Transl Med. 2016;1:149-59.
[391] Zabner J, Fasbender AJ, Moninger T, Poellinger KA, Welsh MJ. Cellular and molecular barriers to gene transfer by a cationic lipid. J Biol Chem. 1995;270:18997-9007.
[392] Brunner S, Sauer T, Carotta S, Cotten M, Saltik M, Wagner E. Cell cycle dependence of gene transfer by lipoplex, polyplex and recombinant adenovirus. Gene Ther. 2000;7:401-7.
[393] Yamamoto A, Kormann M, Rosenecker J, Rudolph C. Current prospects for mRNA gene delivery. Eur J Pharm Biopharm. 2009;71:484-9.
[394] Kaczmarek JC, Kauffman KJ, Fenton OS, Sadtler K, Patel AK, Heartlein MW, et al. Optimization of a Degradable Polymer-Lipid Nanoparticle for Potent Systemic Delivery of mRNA to the Lung Endothelium and Immune Cells. Nano Lett. 2018;18:6449-54.
[395] Rejman J, Tavernier G, Bavarsad N, Demeester J, De Smedt SC. mRNA transfection of cervical carcinoma and mesenchymal stem cells mediated by cationic carriers. J Control Release. 2010;147:385-91.
[396] Zou S, Scarfo K, Nantz MH, Hecker JG. Lipid-mediated delivery of RNA is more efficient than delivery of DNA in non-dividing cells. Int J Pharm. 2010;389:232-43.
[397] Sharova LV, Sharov AA, Nedorezov T, Piao Y, Shaik N, Ko MS. Database for mRNA half-life of 19 977 genes obtained by DNA microarray analysis of pluripotent and differentiating mouse embryonic stem cells. DNA Res. 2009;16:45-58.

[398] Chen CY, Ezzeddine N, Shyu AB. Messenger RNA half-life measurements in mammalian cells. Methods Enzymol. 2008;448:335-57.
[399] Kowalski PS, Rudra A, Miao L, Anderson DG. Delivering the Messenger: Advances in Technologies for Therapeutic mRNA Delivery. Mol Ther. 2019;27:710-28.
[400] Trepotec Z, Lichtenegger E, Plank C, Aneja MK, Rudolph C. Delivery of mRNA Therapeutics for the Treatment of Hepatic Diseases. Mol Ther. 2019;27:794-802.
[401] Kwon H, Kim M, Seo Y, Moon YS, Lee HJ, Lee K, et al. Emergence of synthetic mRNA: In vitro synthesis of mRNA and its applications in regenerative medicine. Biomaterials. 2018;156:172-93.
[402] Malone RW, Felgner PL, Verma IM. Cationic liposome-mediated RNA transfection. Proc Natl Acad Sci U S A. 1989;86:6077-81.
[403] Bettinger T, Carlisle RC, Read ML, Ogris M, Seymour LW. Peptide-mediated RNA delivery: a novel approach for enhanced transfection of primary and post-mitotic cells. Nucleic Acids Res. 2001;29:3882-91.
[404] Kauffman KJ, Mir FF, Jhunjhunwala S, Kaczmarek JC, Hurtado JE, Yang JH, et al. Efficacy and immunogenicity of unmodified and pseudouridine-modified mRNA delivered systemically with lipid nanoparticles in vivo. Biomaterials. 2016;109:78-87.
[405] Kauffman KJ, Dorkin JR, Yang JH, Heartlein MW, DeRosa F, Mir FF, et al. Optimization of Lipid Nanoparticle Formulations for mRNA Delivery in Vivo with Fractional Factorial and Definitive Screening Designs. Nano Lett. 2015;15:7300-6.
[406] Cheng C, Convertine AJ, Stayton PS, Bryers JD. Multifunctional triblock copolymers for intracellular messenger RNA delivery. Biomaterials. 2012;33:6868-76.
[407] Rose L, Mahdipoor P, Kucharski C, Uludag H. Pharmacokinetics and transgene expression of implanted polyethylenimine-based pDNA complexes. Biomater Sci. 2014;2:833-42.
[408] Ferizi M, Leonhardt C, Meggle C, Aneja MK, Rudolph C, Plank C, et al. Stability analysis of chemically modified mRNA using micropattern-based single-cell arrays. Lab Chip. 2015;15:3561-71.
[409] Youn H, Chung JK. Modified mRNA as an alternative to plasmid DNA (pDNA) for transcript replacement and vaccination therapy. Expert Opin Biol Ther. 2015;15:1337-48.
[410] Richner JM, Himansu S, Dowd KA, Butler SL, Salazar V, Fox JM, et al. Modified mRNA Vaccines Protect against Zika Virus Infection. Cell. 2017;169:176.

[411] Nakanishi M, Otsu M. Development of Sendai virus vectors and their potential applications in gene therapy and regenerative medicine. Curr Gene Ther. 2012;12:410-6.
[412] t Hoen PA, Hirsch M, de Meijer EJ, de Menezes RX, van Ommen GJ, den Dunnen JT. mRNA degradation controls differentiation state-dependent differences in transcript and splice variant abundance. Nucleic Acids Res. 2011;39:556-66.
[413] Stepinski J, Waddell C, Stolarski R, Darzynkiewicz E, Rhoads RE. Synthesis and properties of mRNAs containing the novel "anti-reverse" cap analogs 7-methyl(3'-O-methyl)GpppG and 7-methyl (3'-deoxy)GpppG. RNA. 2001;7:1486-95.
[414] Eberhardt W, Doller A, Akool el S, Pfeilschifter J. Modulation of mRNA stability as a novel therapeutic approach. Pharmacol Ther. 2007;114:56-73.
[415] Oh S, Kessler JA. Design, Assembly, Production, and Transfection of Synthetic Modified mRNA. Methods. 2018;133:29-43.
[416] Gallie DR. The cap and poly(A) tail function synergistically to regulate mRNA translational efficiency. Genes Dev. 1991;5:2108-16.
[417] Dimitriadis GJ. Translation of rabbit globin mRNA introduced by liposomes into mouse lymphocytes. Nature. 1978;274:923-4.
[418] KC RB, Kucharski C, Uludag H. Additive nanocomplexes of cationic lipopolymers for improved non-viral gene delivery to mesenchymal stem cells. J Mater Chem B. 2015;3:11.
[419] Debus H, Baumhof P, Probst J, Kissel T. Delivery of messenger RNA using poly(ethylene imine)-poly(ethylene glycol)-copolymer blends for polyplex formation: biophysical characterization and in vitro transfection properties. J Control Release. 2010;148:334-43.
[420] Zheng TS, Schlosser SF, Dao T, Hingorani R, Crispe IN, Boyer JL, et al. Caspase-3 controls both cytoplasmic and nuclear events associated with Fas-mediated apoptosis in vivo. Proc Natl Acad Sci U S A. 1998;95:13618-23.
[421] Menon LG, Picinich S, Koneru R, Gao H, Lin SY, Koneru M, et al. Differential gene expression associated with migration of mesenchymal stem cells to conditioned medium from tumor cells or bone marrow cells. Stem Cells. 2007;25:520-8.
[422] Xin H, Kanehira M, Mizuguchi H, Hayakawa T, Kikuchi T, Nukiwa T, et al. Targeted delivery of CX3CL1 to multiple lung tumors by mesenchymal stem cells. Stem Cells. 2007;25:1618-26.

[423] Nakamizo A, Marini F, Amano T, Khan A, Studeny M, Gumin J, et al. Human bone marrow-derived mesenchymal stem cells in the treatment of gliomas. Cancer Res. 2005;65:3307-18.
[424] De Smedt SC, Demeester J, Hennink WE. Cationic polymer based gene delivery systems. Pharm Res. 2000;17:113-26.
[425] Kumthekar P, Rademaker A, Ko C, Dixit K, Schwartz MA, Sonabend AM, et al. A phase 0 first-in-human study using NU-0129: A gold base spherical nucleic acid (SNA) nanoconjugate targeting BCL2L12 in recurrent glioblastoma patients. Journal of Clinical Oncology. 2019;37:3012-.
[426] Petrocca F, Altschuler G, Tan SM, Mendillo ML, Yan H, Jerry DJ, et al. A genome-wide siRNA screen identifies proteasome addiction as a vulnerability of basal-like triple-negative breast cancer cells. Cancer Cell. 2013;24:182-96.
[427] Mendes-Pereira AM, Sims D, Dexter T, Fenwick K, Assiotis I, Kozarewa I, et al. Genome-wide functional screen identifies a compendium of genes affecting sensitivity to tamoxifen. Proc Natl Acad Sci U S A. 2012;109:2730-5.
[428] Parmar MB, Meenakshi Sundaram DN, Kaur H, KC RB, Maranchuk R, Aliabadi HM, et al. Combinational siRNA delivery using hyaluronic acid modified amphiphilic polyplexes against cell cycle and phosphatase proteins to inhibit growth and migration of triple-negative breast cancer cells (Manuscript submitted for publication). 2017.
[429] Parmar MB, Aliabadi HM, Mahdipoor P, Kucharski C, Maranchuk R, Hugh JC, et al. Targeting cell cycle proteins in breast cancer cells with siRNA by using lipid-substituted polyethylenimines. Frontiers in Biotechnology & Bioengineering 2015;3:14.
[430] Jia J, Zhu F, Ma X, Cao Z, Cao ZW, Li Y, et al. Mechanisms of drug combinations: interaction and network perspectives. Nat Rev Drug Discov. 2009;8:111-28.
[431] Hsu CY, Uludag H. A simple and rapid nonviral approach to efficiently transfect primary tissue-derived cells using polyethylenimine. Nat Protoc. 2012;7:935-45.
[432] Meenakshi Sundaram DN, Kucharski C, Parmar MB, Kc RB, Uludag H. Polymeric Delivery of siRNA against Integrin-beta1 (CD29) to Reduce Attachment and Migration of Breast Cancer Cells. Macromol Biosci. 2017;17.
[433] Izumisawa T, Hattori Y, Date M, Toma K, Maitani Y. Cell line-dependent internalization pathways determine DNA transfection efficiency of decaarginine-PEG-lipid. Int J Pharm. 2011;404:264-70.

[434] Douglas KL, Piccirillo CA, Tabrizian M. Cell line-dependent internalization pathways and intracellular trafficking determine transfection efficiency of nanoparticle vectors. Eur J Pharm Biopharm. 2008;68:676-87.
[435] Birmingham A, Selfors LM, Forster T, Wrobel D, Kennedy CJ, Shanks E, et al. Statistical methods for analysis of high-throughput RNA interference screens. Nat Methods. 2009;6:569-75.

Appendix A : supplementary information of chapter 2

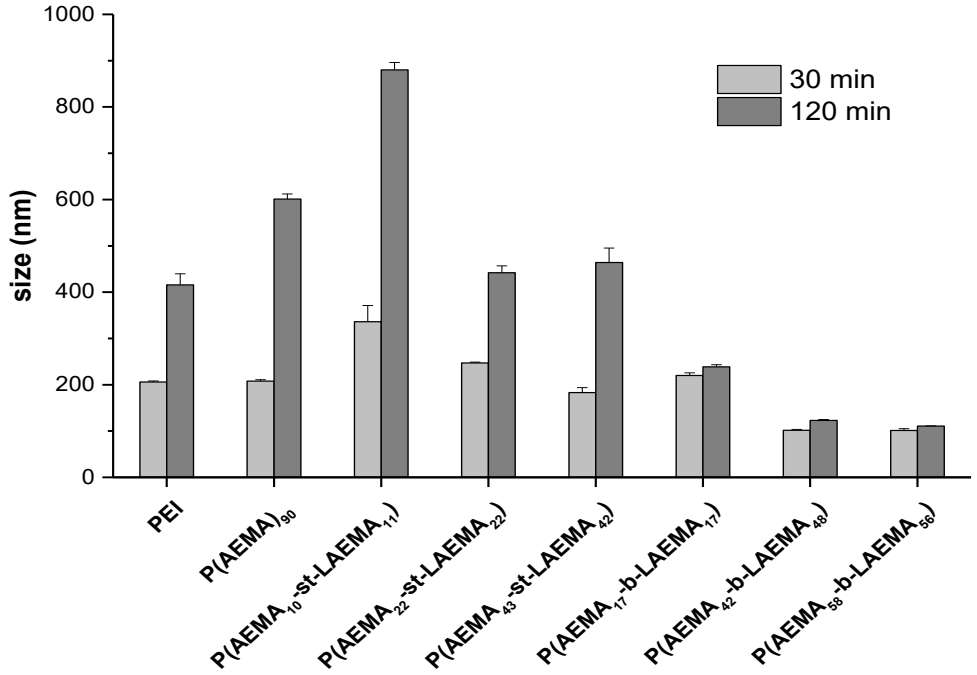

Figure S2.1: DLS analysis of aggregation of polyplexes in medium. Polyplexes of PEI, homopolymer and statistical copolymers were aggregated after incubation in medium whereas polyplexes of block copolymer remains stable.

Table S2.1: N/P ratio of polyplexes of each polymer. N/P is optimized for all polymers

Polymer composition	**N/P**
Homopolymer	
$P(AEMA_{90})$	10
Statistical copolymers	
$P(AEMA_{10}\text{-st-}LAEMA_{11})$	49
$P(AEMA_{22}\text{-st-}LAEMA_{22})$	52
$P(AEMA_{43}\text{-st-}LAEMA_{42})$	53
$P(AEMA_{74}\text{-st-}LAEMA_{62})$	61
$P(AEMA_{81}\text{-st-}LAEMA_{58})$	65
Block copolymers	
$P(AEMA_{17}\text{-b-}LAEMA_{17})$	52
$P(AEMA_{42}\text{-b-}LAEMA_{48})$	48

P(AEMA$_{58}$-b-LAEMA$_{56}$)	54
PEI	20

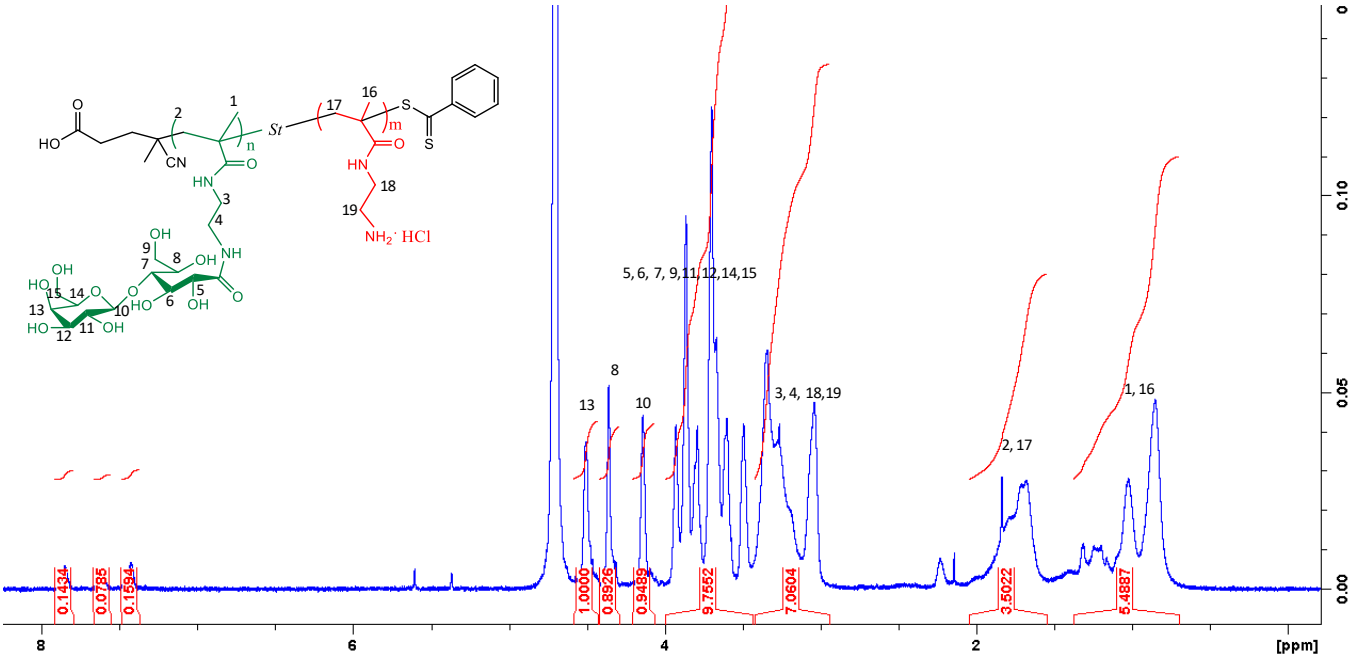

Figure S2.2: 1H NMR of statistical copolymer P(AEMA$_{10}$-st-LAEMA$_{11}$)

Appendix B: supplementary informations for chapter 3

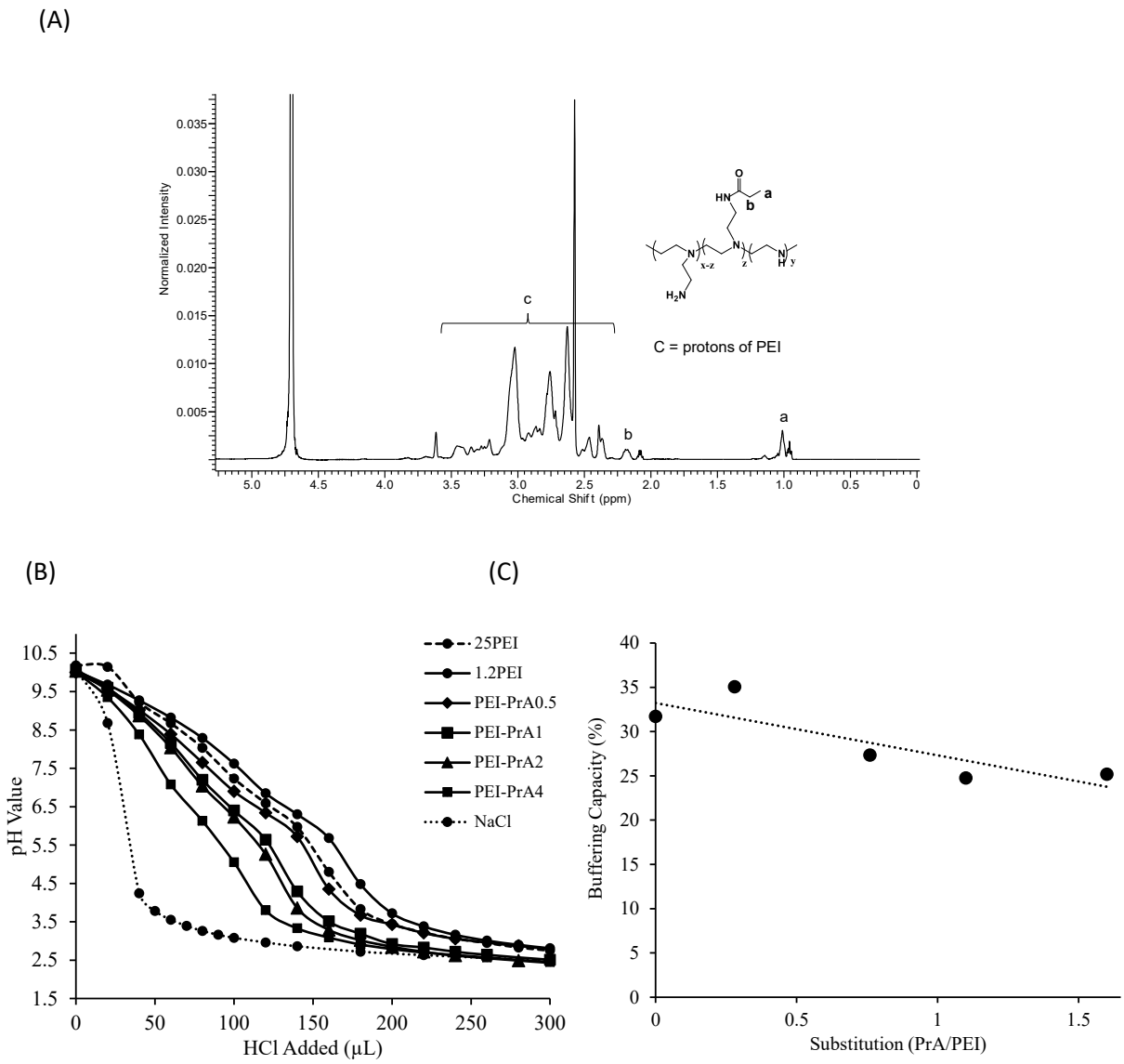

Figure S3.1. NMR spectrum of PEI-PrA polymer (A). Acid-base titration of polymers using 0.1 M HCl ((B) and quantification of buffering capacity (C).

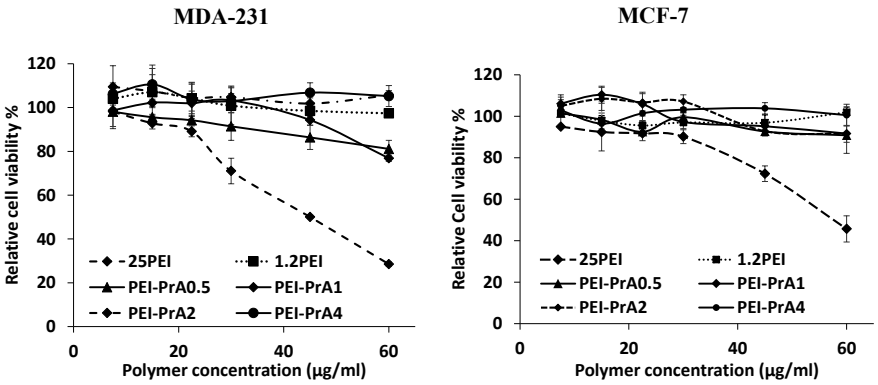

Figure S3.2. Cytotoxicity of polymers in MDA-231 and MCF-7 cells. In contrast to 25PEI, PEI-PrA polymers were not toxic in the experimental range studied. Concentration of polymers used were equivalent to polyplexes of polymer to pDNA weight ratio 2.5 to 20.

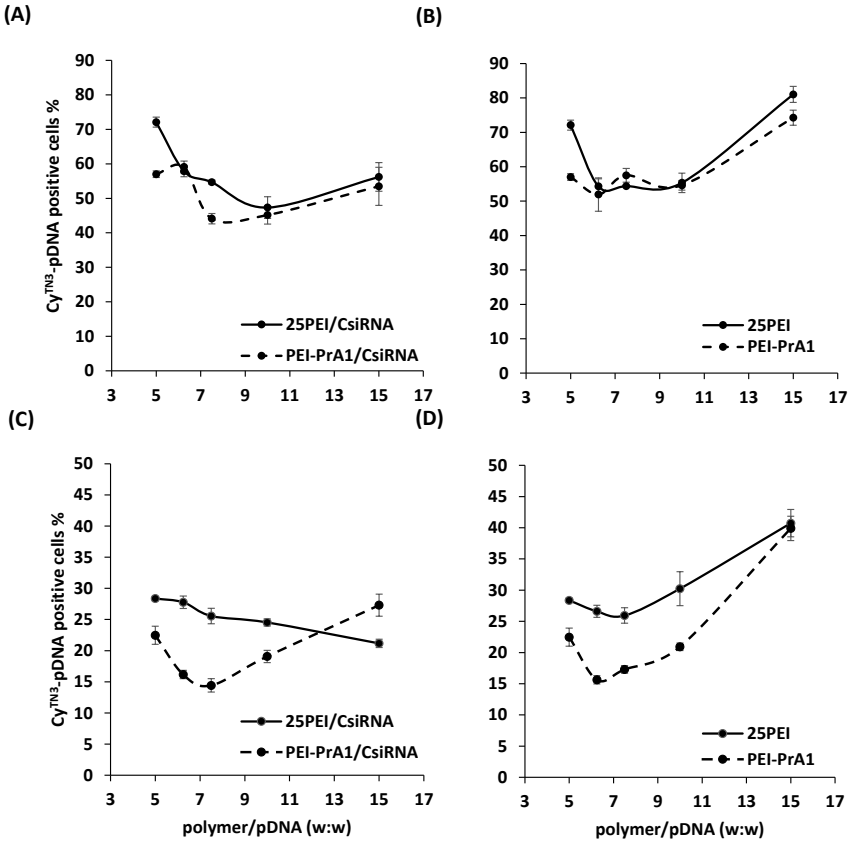

Figure S3.3. pDNA uptake as indicated by percentage of Cy3-positive cells in MDA-MB-231 cells in the presence (**A** and **B**) and absence (**C** and **D**) of siRNA. Cy3-labaled pDNA was compelexed with the indicated polymers in the presence and absence of C-siRNA and uptake was determined after 24 hours. Note that siRNA was not beneficial for increasing uptake, as increased polymer ratio was sufficient to give similar uptake in the absence of siRNA.

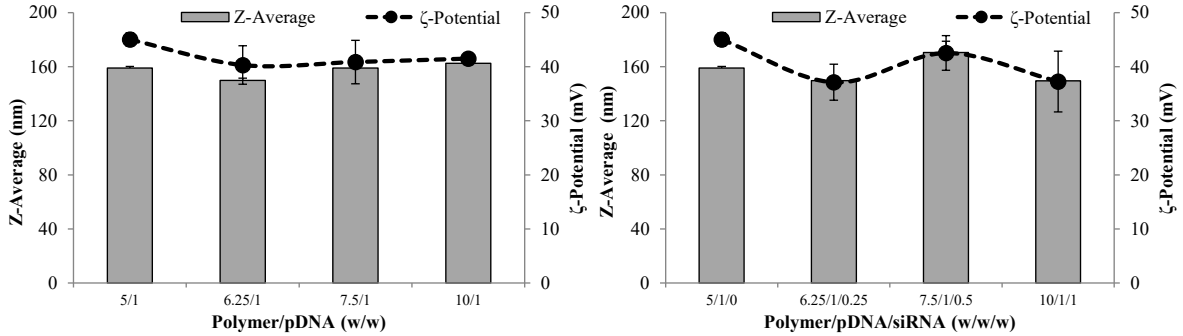

Figure S3.4. Size and zeta potential of dual complexes of DNA and siRNA with polymer PEI-PrA1.

(A) MDA-231 cells

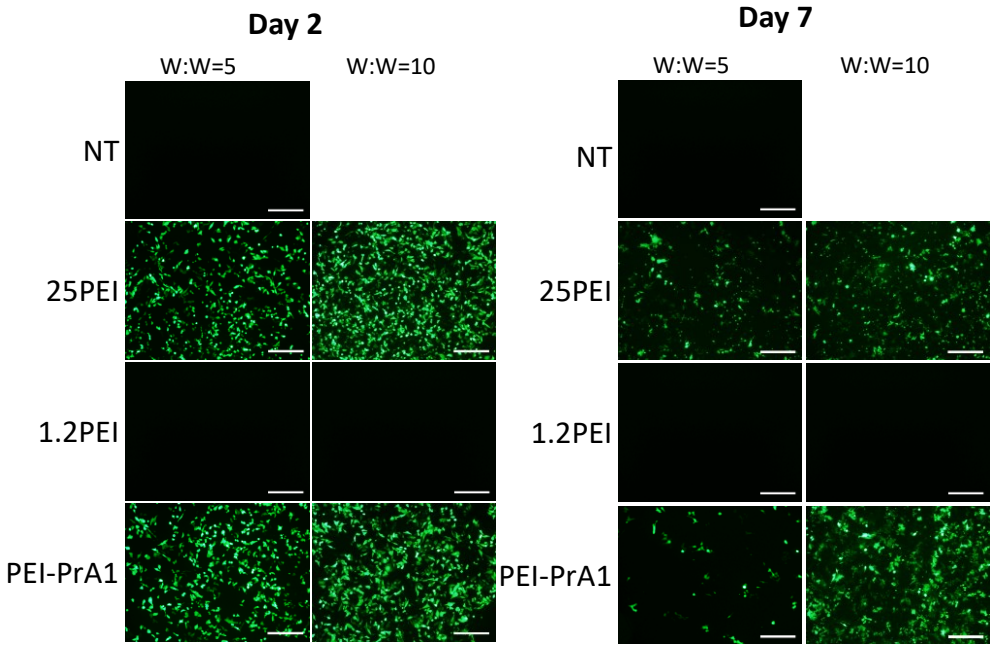

(B) MCF-7 cells

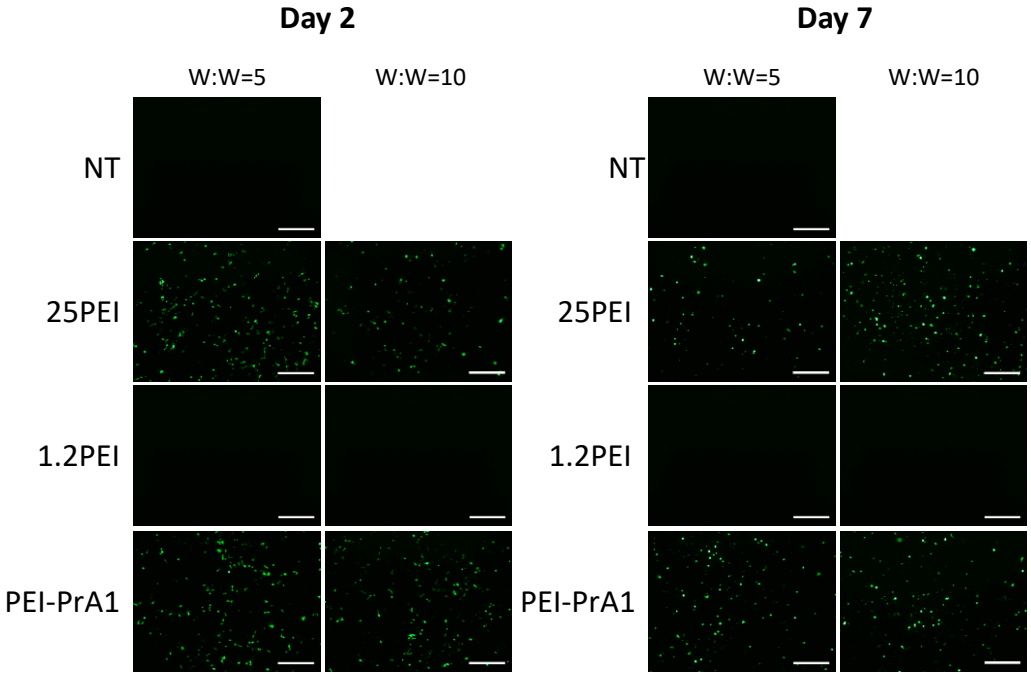

Figure S3.5. Microscopic image of MDA-MB-231 (A) and MCF-7 (B) cells showing GFP expression at different time of transfection, (scale bar 400 µm).

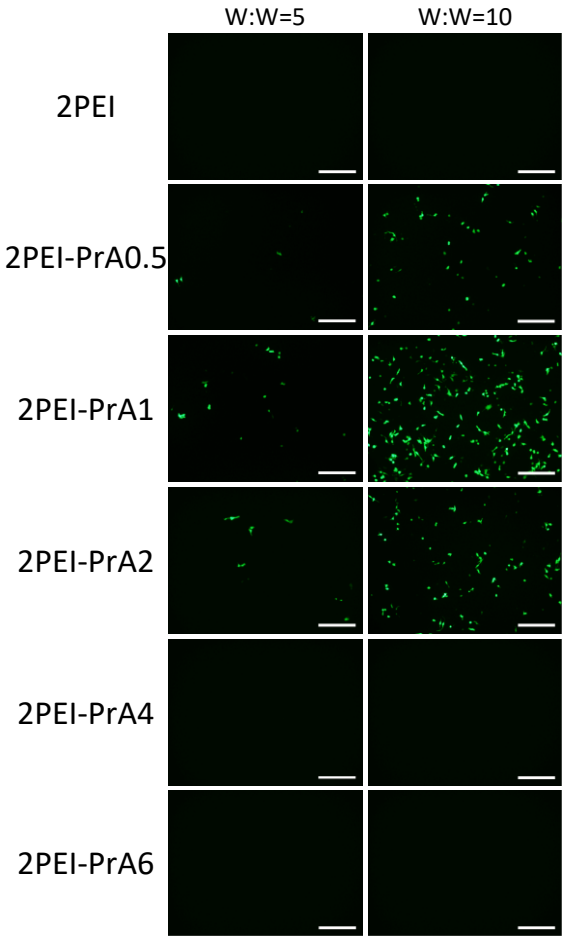

Figure S3.6. Microscopic image of MDA-231 cells showing GFP plasmid transfection using PrA modified 2PEI at polymer/pDNA ratio of 5 and 10. Similar to modification with 1.2PEI, 2PEI was modified with different amount of PrAs (the numbers indicate feed ratios). As in 1.2PEI, PrA substitution on 2PEI also showed beneficial effect for pDNA transfection at low substitution (best performance with 2PEI-PRA1, where the 2PEI:PrA feed ratio was 1:1 mol/mol again). However, higher PrA substitution was detrimental, (scale bar 400 μm).

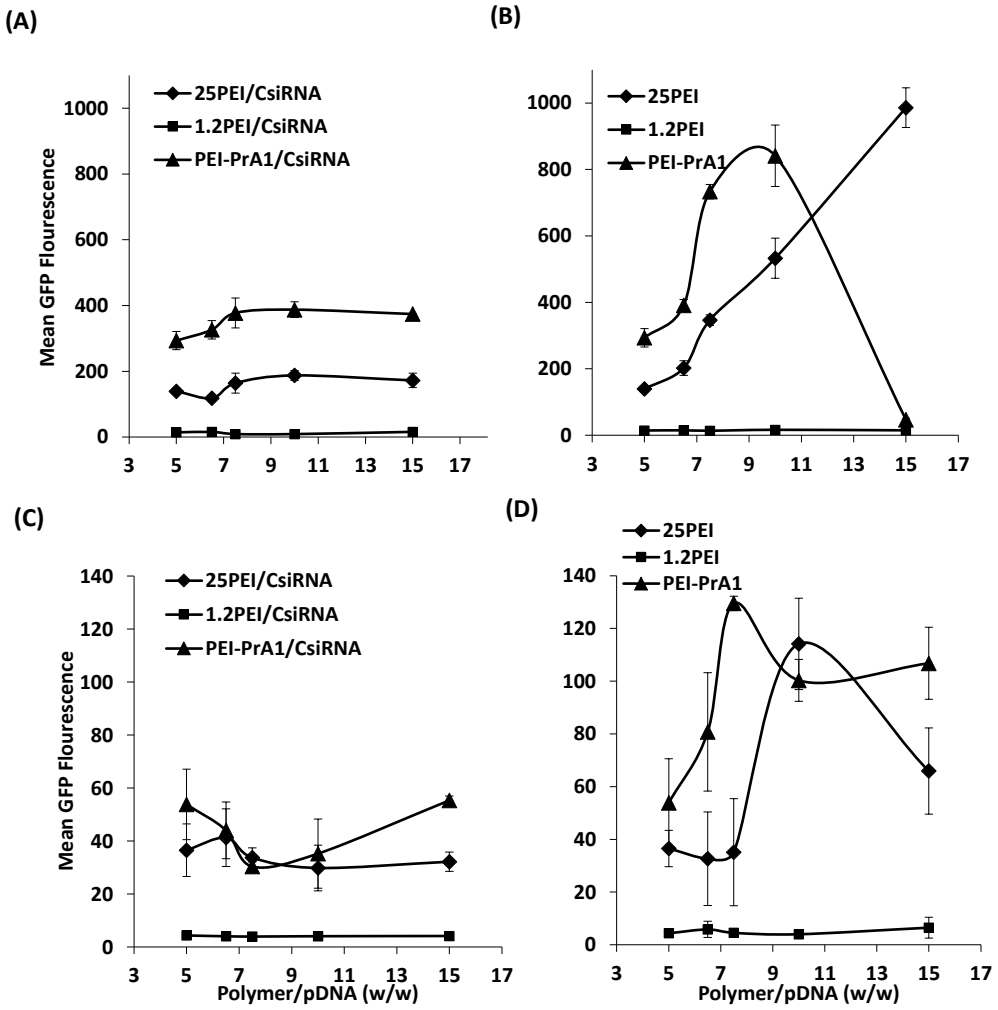

Figure S3.7. Transgene expression in MDA-MB-231 (**A** and **B**) and MCF-7 (**C, D**) cells with (**A** and **C**) and without (**B** and **D**) siRNA additive (polymer:pDNA+siRNA ratio of 5) after 7 days of transfection. In MDA-MB-231 cells, adding siRNA did not alter the transfection efficiency (as long as polymer:nucleic acid ratio was constant, see **A**), while in MCF-7 cells, adding siRNA slightly increased transfection efficiency (see **C**) but the same effect was obtained with addition of equivalent amount of polymer in the absence of siRNA (see **D**).

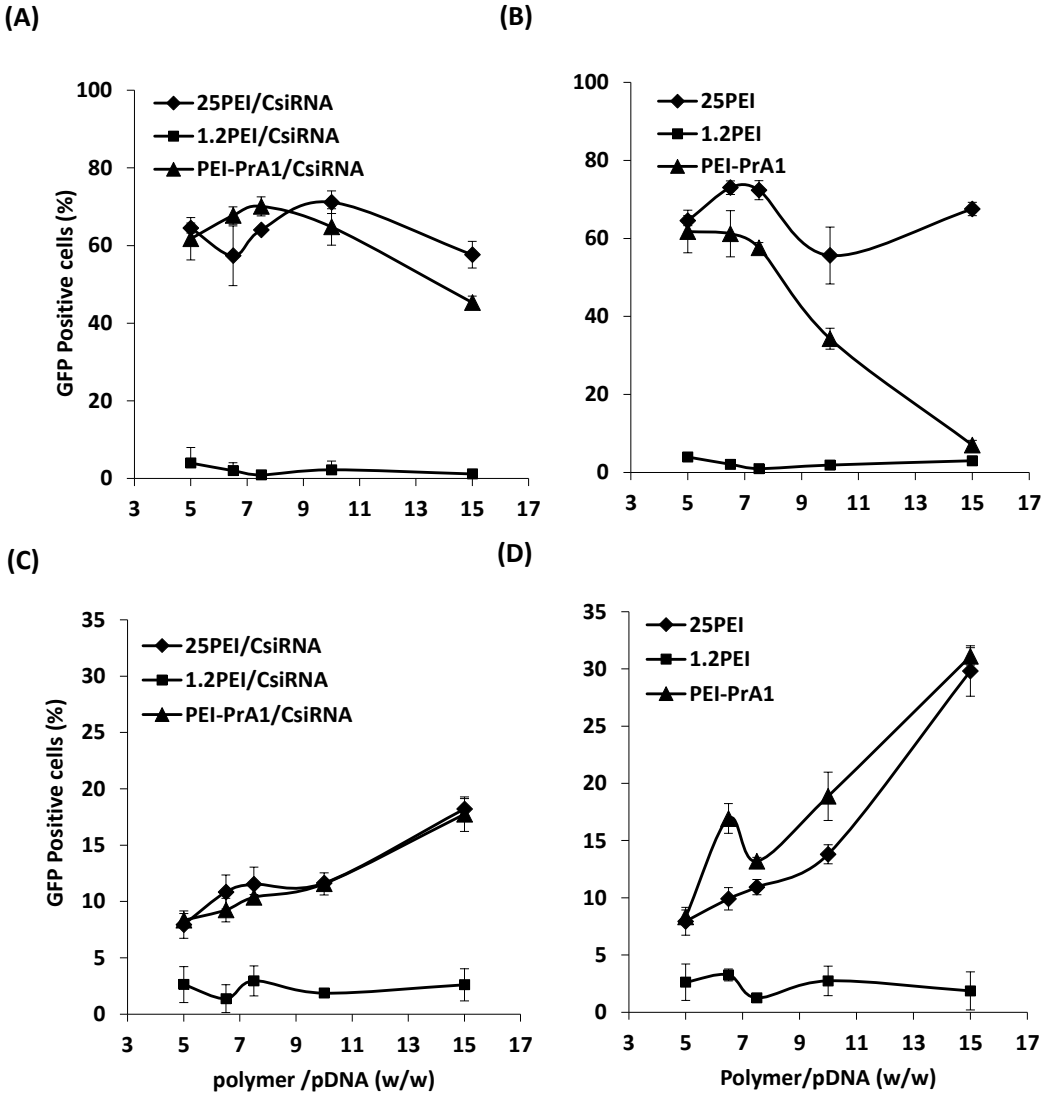

Figure S3.8. Transgene expression showing percentage of GFP positive population in MDA-MB-231 (**A** and **B**) and MCF-7 (**C, D**) cells with (**A** and **C**) and without (**B** and **D**) siRNA additive (polymer:pDNA+siRNA ratio of 5) after 2 days of transfection.

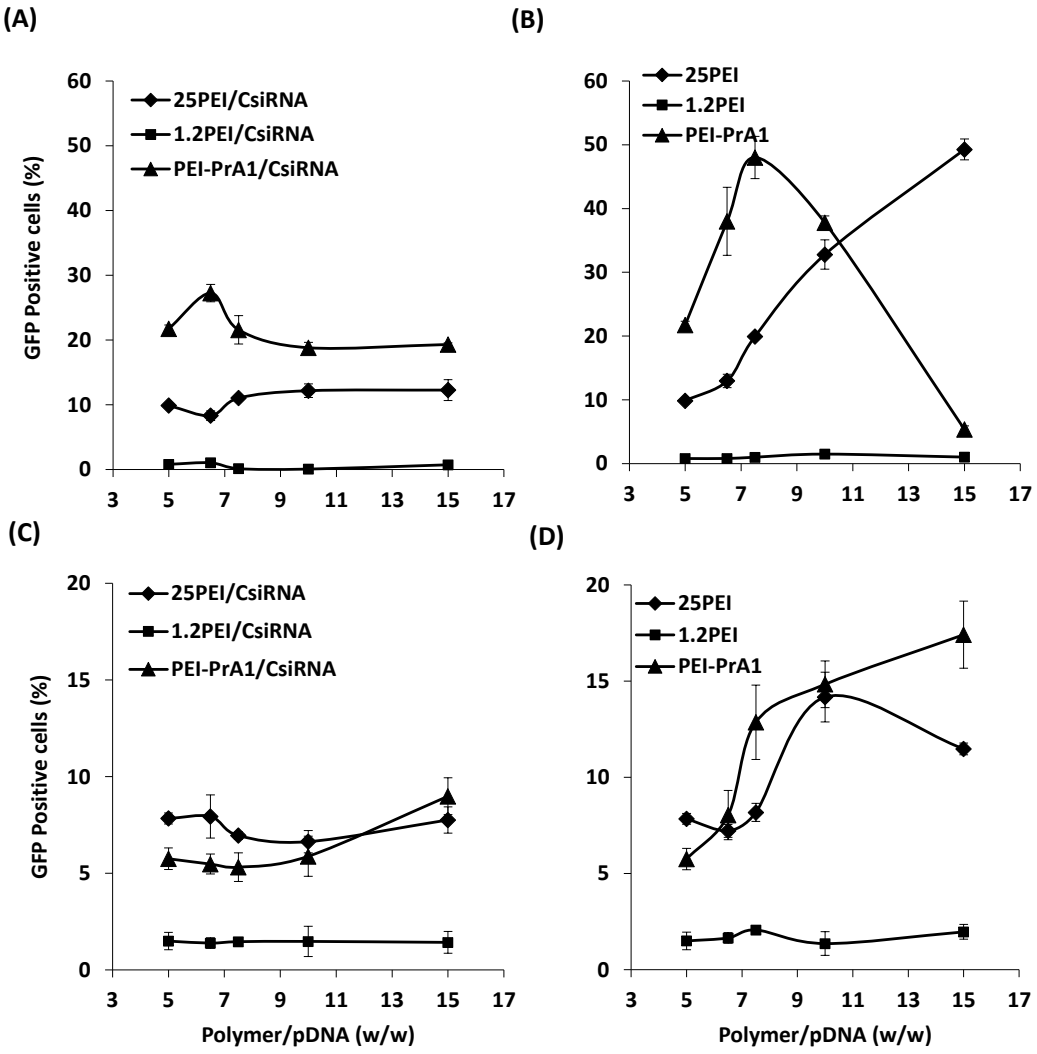

Figure S3.9. Transgene expression showing percentage of GFP positive population in MDA-MB-231 (**A** and **B**) and MCF-7 (**C, D**) cells with (**A** and **C**) and without (**B** and **D**) siRNA additive (polymer:pDNA+siRNA ratio of 5) after 7 days of transfection.

Appendix C: supplementary information for chapter 4

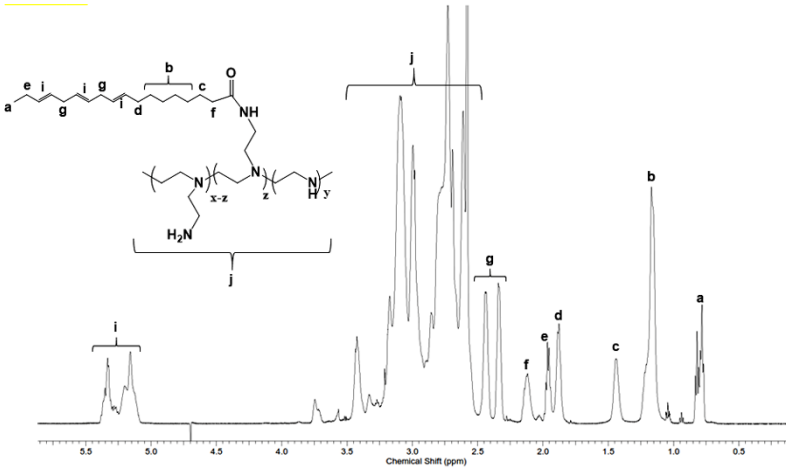

Figure S4.1: ^{1}H-NMR spectrum of PEI-αLA polymer.

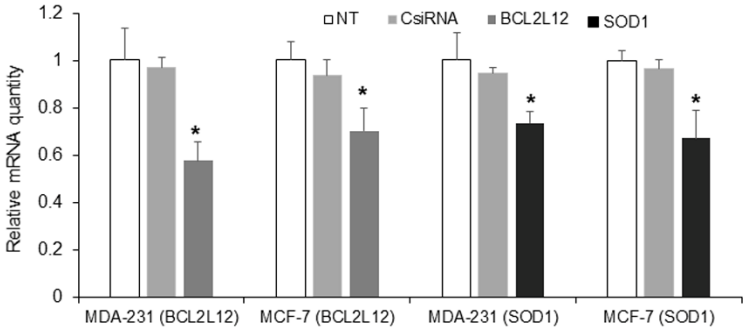

Figure S4.2: Analysis of mRNA by qPCR in MDA-MB-231 and MCF-7 cells after 48 h of treatment with the second sets of siRNA targeting BCL2L12 (Cat # HSS.RNAI.N001040668.12.1, IDT) and SOD1 (cat#HSC.RNAI.N000454.12.2, IDT) (30 nM) in MDA-MB-231 and MCF-7 cells. The relative quantity of mRNA transcripts was calculated relative to untreated cells using house-keeping genes GAPDH and β-actin as reference. After normalization, the results from the two reference genes were pooled together. *$p < 0.05$ compared with non-treated group.

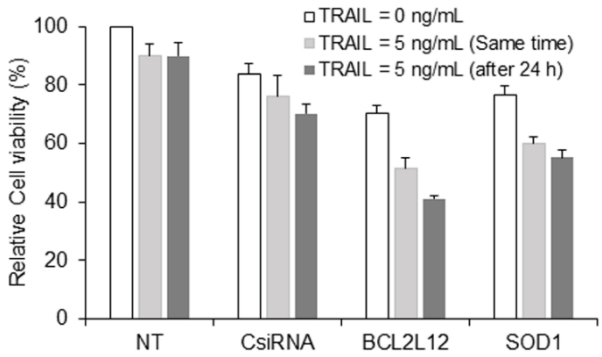

Figure S4.3: Comparison of cell viability of MDA-MB-231 cells after siRNA complexes and TRAIL treatment. Cells were treated with TRAIL immediately or 24 h after addition of siRNA complexes. Higher cell death was observed when TRAIL was added after 24 h treatment with siRNA complexes.

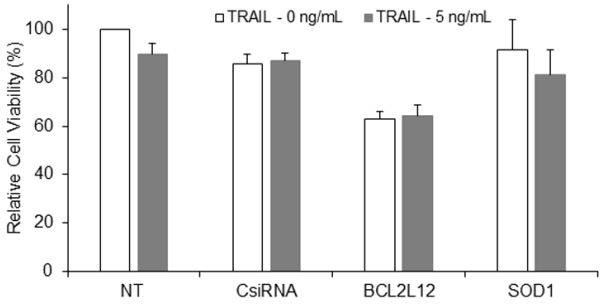

Figure S4.4: Effect of siRNA (30 nM) and TRAIL (5 ng/mL) combination in MCF-7 cells. No significant change in cell viability was observed at this concentration of TRAIL.

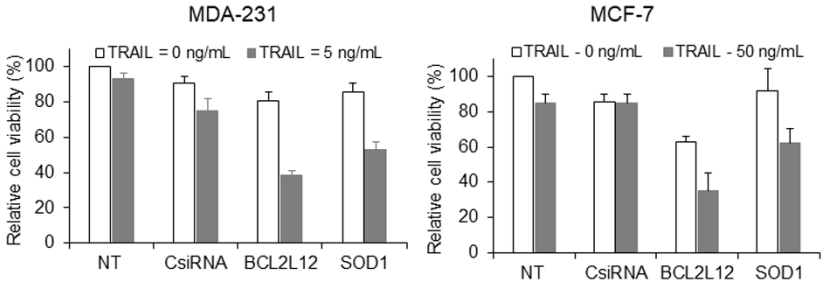

Figure S4.5: Effect of siRNA (30 nM) and TRAIL (5 ng/mL) combination in MDA-MB-231 cells and siRNA (30 nM) and TRAIL (50 ng/mL) in MCF-7 cells. These combinations were considered optimal to sensitize TRAIL induced cell death in these cells.

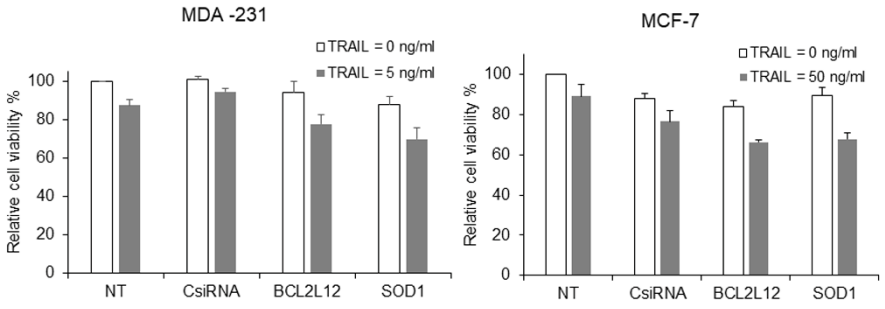

Figure S4.6: Effects of second sets of siRNA targeting BCL2L12 (Cat # HSS.RNAI.N001040668.12.1, IDT) and SOD1 (cat#HSC.RNAI.N000454.12.2, IDT). Dose of each siRNA was 30 nM in both cell lines while TRAIL concentration was 5 ng/ml in MDA-MB-231 and 50 ng/ml in MCF-7 cells.

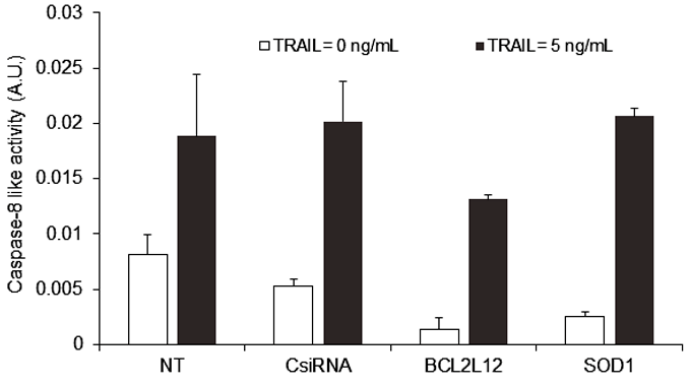

Figure S4.7: Effects of siRNA, TRAIL and their combination on the caspase-8 activity in MDA-MB-231 cells. MDA-MB-231 cells were treated with siRNA (30 nM) targeting SOD1 and BCL2L12 with or without TRAIL (5 ng/mL) and caspase-8 activity was determined 3 h after TRAIL treatment. Effects of siRNAs on the activation of caspase-8 was not significant.

Appendix D: supporing information for chapter 5

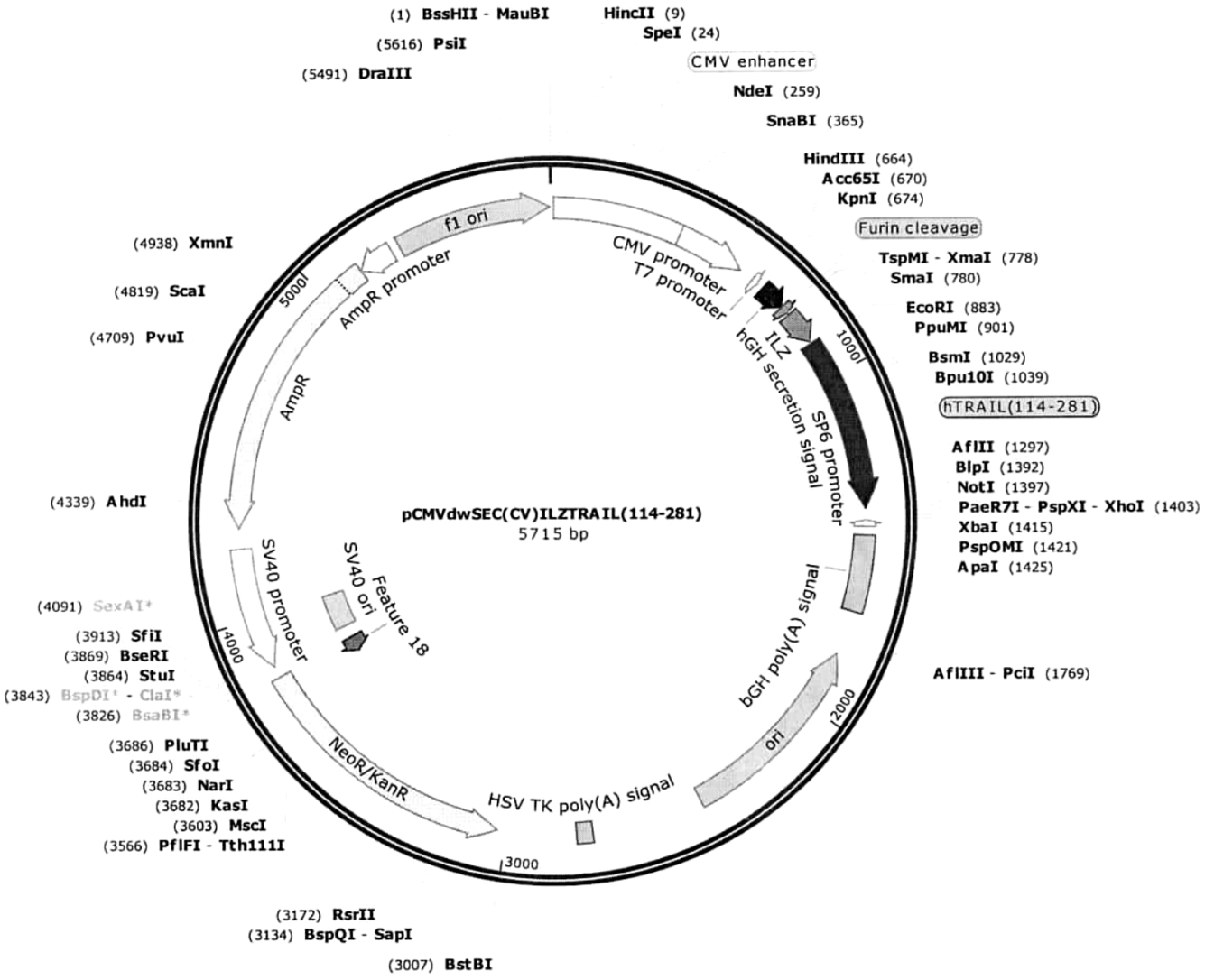

Figure S5.1: Full sequence map for TRAIL encoding plasmid (pCMVdwSEC(CV)ILZTRAIL(114-281).

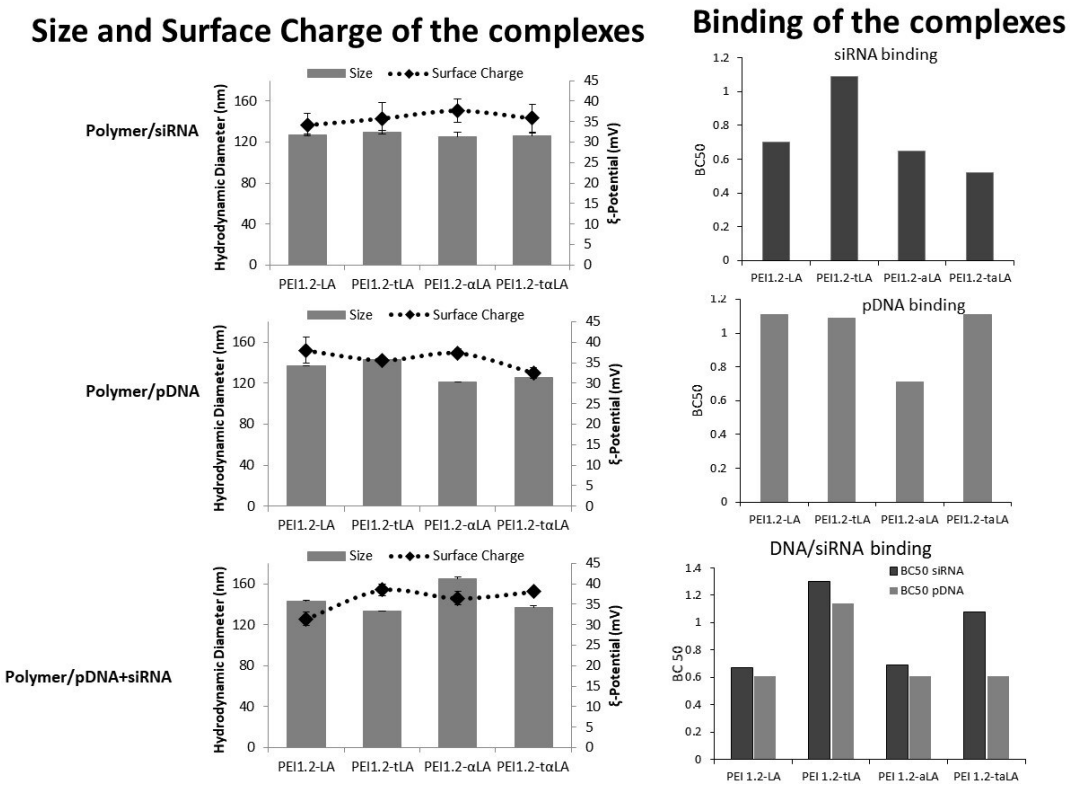

Figure S5.2: Physical characterization of the complexes with pDNA or siRNA or pDNA/siRNA combination. Size and surface charge of complexes did not change with type of nucleic acid used.

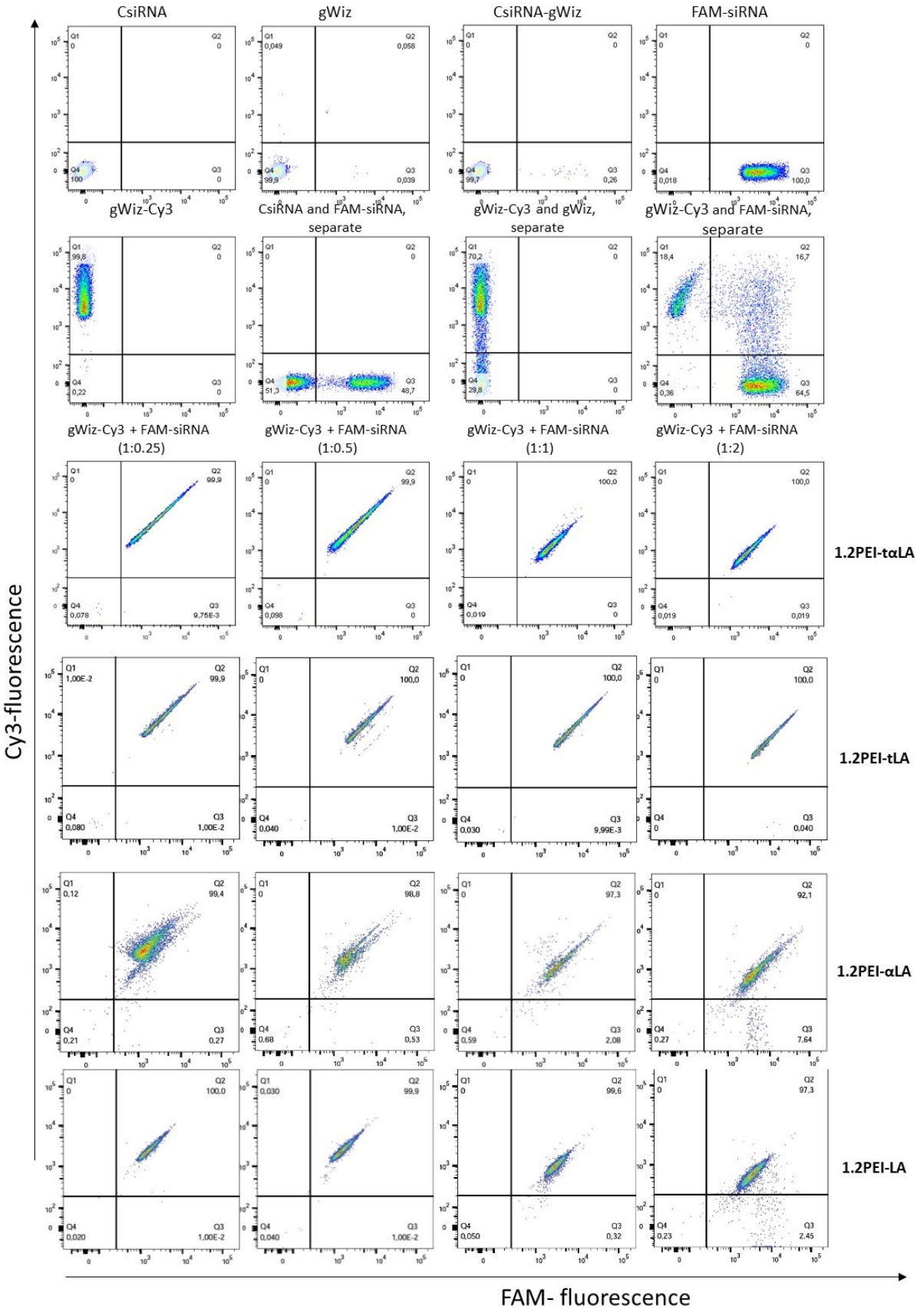
CsiRNA
gWiz
CsiRNA-gWiz
FAM-siRNA
gWiz-Cy3
CsiRNA and FAM-siRNA, separate
gWiz-Cy3 and gWiz, separate
gWiz-Cy3 and FAM-siRNA, separate
gWiz-Cy3 + FAM-siRNA (1:0.25)
gWiz-Cy3 + FAM-siRNA (1:0.5)
gWiz-Cy3 + FAM-siRNA (1:1)
gWiz-Cy3 + FAM-siRNA (1:2)
1.2PEI-tαLA
1.2PEI-tLA
1.2PEI-αLA
1.2PEI-LA
Cy3-fluorescence
FAM- fluorescence

Figure S5.3: Flow cytometry study of complexes with Cy3 labelled pDNA and FAM labelled siRNA. Unlabelled CsiRNA and gWIZ plasmid is used as control.

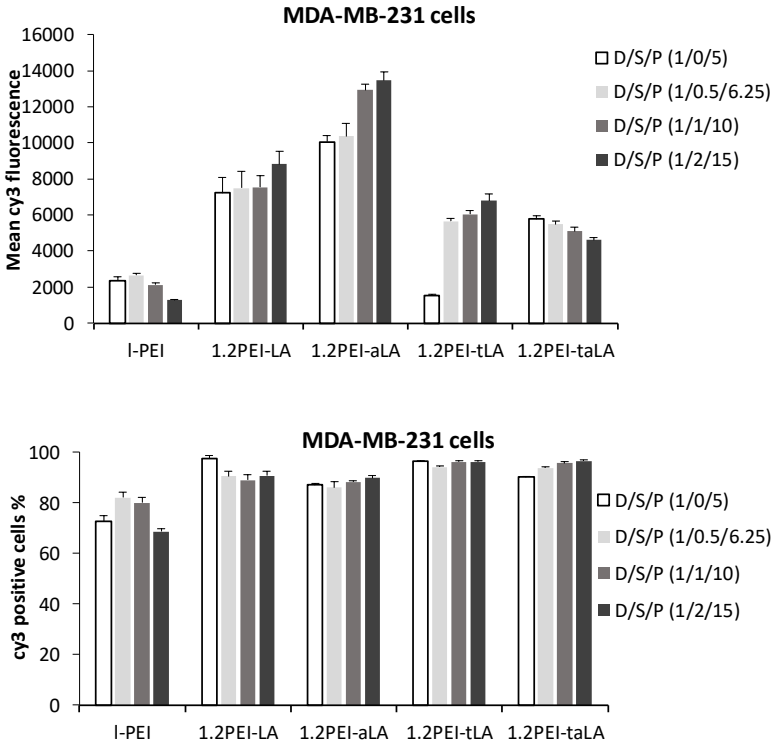

Figure S5.4: Uptake of DNA and polymer complexes and effect of siRNA. Cy3-labelled DNA used to observe uptake of particles in MDA-MB-231 cells.

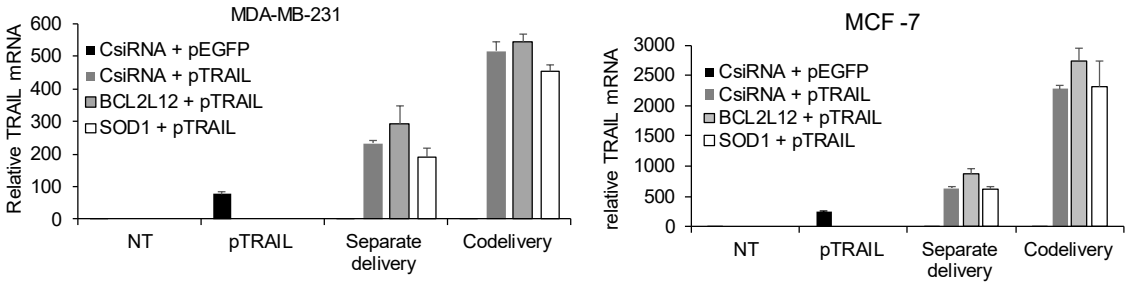

Figure S5.5: TRAIL mRNA expression after treatment with complexes in MDA-MB-231 and MCF-7 cells.

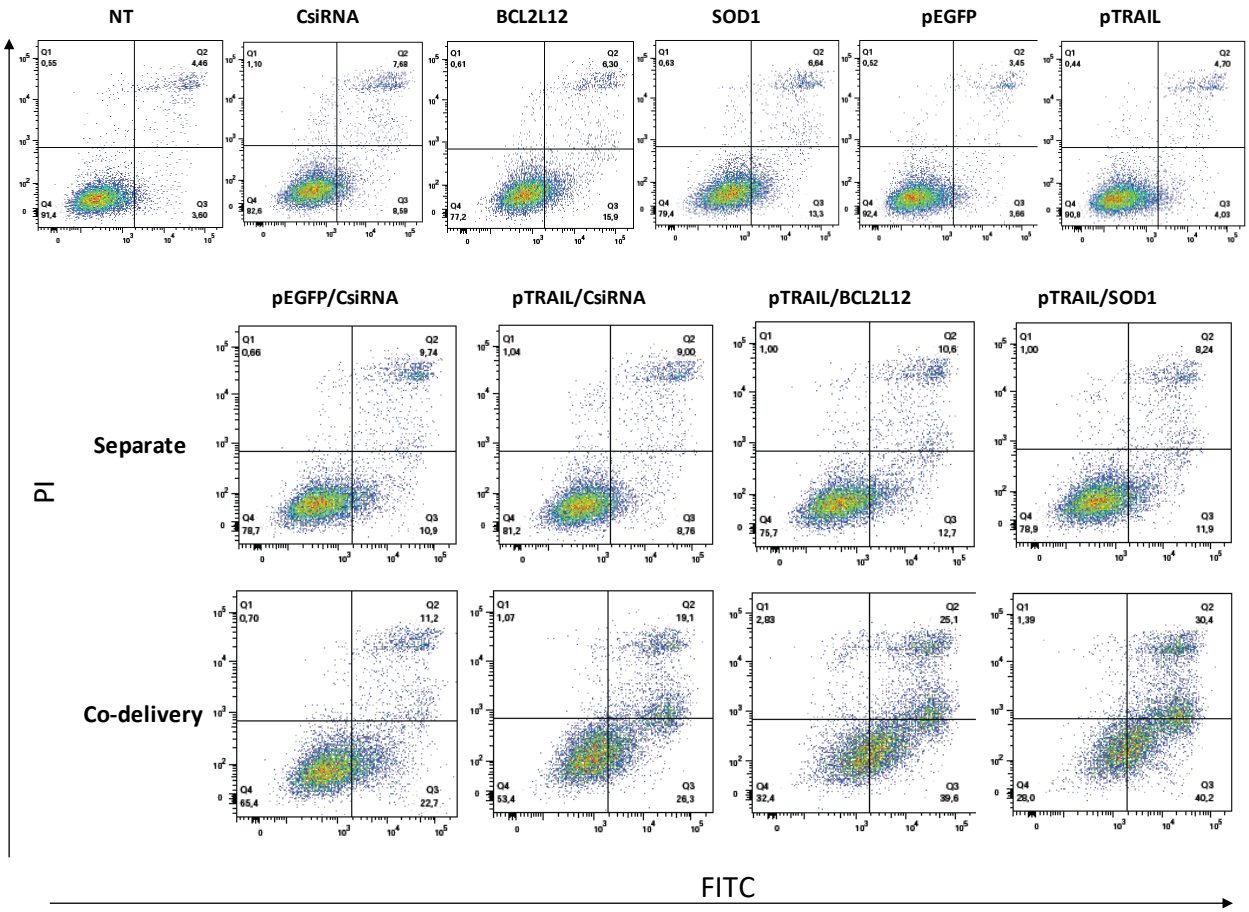

Figure S5.6: Annexin-FITC/PI apoptosis assay in MDA-MB-231 cells. Cells were treated with combination of TRAIL plasmid and siRNAs (BCL2L12 or SOD1) and apoptosis assay was performed after 72 h of transfection.

Appendix E: Supporing informations for chapter 6

ATGGCTACAGGCTCCCGGACGTCCCTGCTCCTGGCTTTTGGCCTGCTCTGCCTGCCCT
GGCTTCAAGAGGGCAGTGCCTCCGCTCGGAACAGGCAGAAGCGCCCCGGGAGAATG
AAGCAGATCGAGGACAAAATTGAGGAAATCCTGTCCAAGATTTACCACATCGAGAA
CGAGATCGCCCGGATTAAGAAACTCATTGGCGAGAGGGAATTCGTGAGAGAAAGAG
GTCCTCAGAGAGTAGCAGCTCACATAACTGGGACCAGAGGAAGAAGCAACACATTG
TCTTCTCCAAACTCCAAGAATGAAAAGGCTCTGGGCCGCAAAATAAACTCCTGGGA
ATCATCAAGGAGTGGGCATTCATTCCTGAGCAACTTGCACTTGAGGAATGGTGAACT
GGTCATCCATGAAAAAGGGTTTTACTACATCTATTCCCAAACATACTTTCGATTTCA
GGAGGAAATAAAAGAAAACACAAAGAACGACAAACAAATGGTCCAATATATTTAC
AAATACACAAGTTATCCTGACCCTATATTGTTGATGAAAAGTGCTAGAAATAGTTGT
TGGTCTAAAGATGCAGAATATGGACTCTATTCCATCTATCAAGGGGGAATATTTGAG
CTTAAGGAAAATGACAGAATTTTTGTTTCTGTAACAAATGAGCACTTGATAGACATG
GACCATGAAGCCAGTTTTTTCGGGGCCTTTTTAGTTGGCTAA

Figure S6.1. Open reading frame sequence for construction of TRAIL modRNA

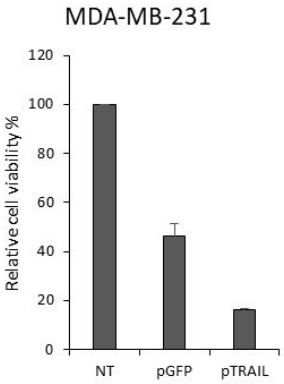

Figure S6.2: Toxicity of complexes in MDA-MB-231 cells at polymer: pDNA weight ratio of 10.

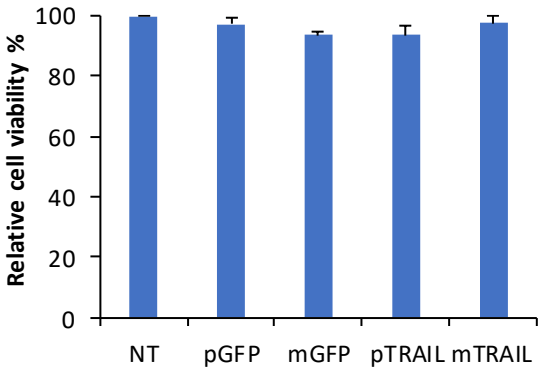

Figure S6.3: Toxicity of complexes in hBMSC after 72 h of transfection.

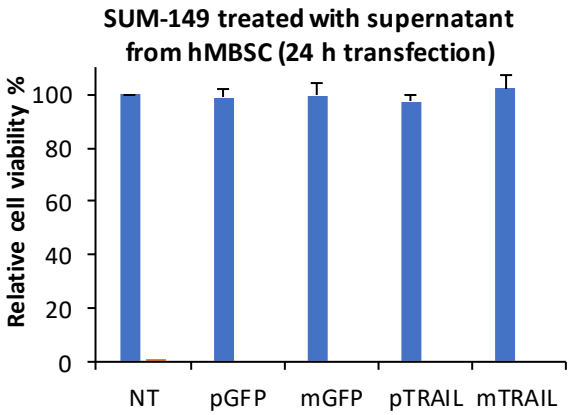

Figure S6.4: SUM-149 cells were treated with the supernatant collected from the hBMSC treated with complexes for 24 h.

Appendix F: siRNA Library Screening to identify complementary therapeutic pairs in triple negative breast cancer cells

A version of this chapter was published in:

Bindu Thapa, Remant Bahadur KC, Hasan Uludağ, "siRNA Library Screening to identify Complementary Therapeutics Paris in Triple-Negative Breast Cancer Cells", *RNA Interference and Cancer Therapy: Methods and Protocols in Molecular Biology*, 2019, 1974, 1-19.

F.1. Introduction

The coupling between rapid human genome sequencing and techniques for high-throughput screening has revolutionized the studies of gene function and their role in different diseases. Silencing of individual genes predicted from the genome sequencing provides a clear-cut way to systematically probe the role of individual genes in different diseases. Non-coding RNAs (ncRNAs) such as microRNA (miRNA) and short interfering RNAs (siRNAs) that participate in RNA interference (RNAi) mechanism have been developed as a new line of therapeutics for cancer gene therapy. siRNA silences a targeted gene by inducing natural RNAi pathway, which results in degradation or translational blockage of a complementary messenger RNA (mRNA). siRNA treatments have been used for functional genomics and to reveal the molecules involved in biochemical pathways [339]. The complex physiological changes associated with different diseases can be better understood by silencing specific genes associated with such diseases. Silencing with siRNA allows reversible deletion of individual participants in biochemical cascades, revealing their role and function in the investigated aspects of the diseases. Hence, siRNA library screens, in which large numbers of siRNAs have been compiled broadly (e.g., against genome-wide transcriptome) or with a specific focus (e.g., against apoptosis-regulating proteins) have been indispensable to identify therapeutic targets in different diseases [110].

Cancer is a particularly attractive disease for siRNA screens since aberrant changes in gene expression and/or regulation is the main cause of the disease and large numbers of aberrant transformations are likely to emerge in individual cancers. The outcome of siRNA screens can identify aberrant mediators that can serve as drug targets, in addition to providing specific siRNAs that can be employed in therapy. Genome wide screens against breast cancers have been attempted to provide an un-biased approach for target identification [426, 427]. Assessing the outcomes of

every possibility head-to-head can provide a more objective assessment of the relative importance of various targets, but handling large libraries is time consuming, requires significant resources and are more likely lead to false positive hits due to technical errors. Alternatively, we preferred to screen 'focused' libraries, such as the libraries against apoptosis-regulating proteins [110, 207], protein kinases [110], phosphatases [428] and protein regulators of cell cycle [429] in malignant cell lines, since less resources are required especially for subsequent validation studies. The findings have typically revealed that individual target's silencing altered the assessed feature of the malignant cells. Since the ultimate goal is to control unchecked growth, the screens have been most notably conducted to inhibit cellular growth (i.e., as a functional outcome). However, in most diseases, especially in cancer, where cellular transformation arises from the interplay or accumulation of multiple mediators, identifying and targeting single mediators may not be sufficient. Complex signaling network including redundancies, extensive crosstalk, compensatory and neutralizing activities in disease-causing cells, in addition to heterogeneity in the population of disease-causing cells, is responsible for the therapeutic limitations of mono-therapy [6, 8, 71]. To this end, combination therapy comprising multiple therapeutic agents, which target multiple pathways, has been developing as a promising approach in cancer gene therapy [71]. Three major approaches to combinational therapy include (i) inhibiting specific targets by multiple strategies, (ii) abolishing multiple components in a given pathway (to better eradicate a given pathway), and (iii) interfering with multiple mechanisms in tumor growth and metastasis [13]. The combination of therapeutic agents that generate the synergism via complementary effects with minimal overlapping of toxicity spectrum is an ideal model in therapeutic intervention. This modality may further attenuate the side effects associated with the clinical doses of individual drugs by reducing the doses of individual component [14, 430]. Therefore, here, we established a standard protocol

as a proof of concept to identify complementary therapeutic pair for cancer gene therapy using siRNA library screening in breast cancer cells. Triple negative breast cancer MDA-MB-231 cells were used as a model of breast cancer, given the lower therapeutic response (with current drugs) in the case of triple negative breast cancer.

F.2. Materials

F.2.1. Cell culture and seeding

1. Identity-authenticated triple negative breast cancer cells, MDA-MB-231.
2. Tissue culture media: Dulbecco's Modified Eagle's Medium (DMEM) supplemented with 10% fetal bovine serum and 100 U/ml penicillin and 100 μg/ml streptomycin.
3. Hank's Balanced Salt Solution (HBSS)
4. Tissue culture plates: sterile standard T75 tissue culture flask for adherent cells, 96-well transparent tissue culture plates
5. Instruments: Hemocytometer, brightfield microscope, cell culture incubator (5% CO_2, 37°C)

F.2.2. siRNA library screening with Drug

1. RNAase free sterile water.
2. Serum free culture medium, DMEM.
3. siRNA library: siGENOME Human Apoptosis library, G-003905. **See note 1.**
4. Positive and Negative control siRNAs. **See note 2.**
5. Drug: recombinant human TRAIL.

6. Transfecting reagent: lipid modified small molecular weight (MW 1200 Da) polyethyleneimine. **See note 3.**
7. Microplate seals
8. Instruments: Plate centrifuge, Perkin Elmer Janus Automated Liquid Handling System and "WinPREP" software

F.2.3. Final Read out Assay

1. 3-(4,5-dimethylthiazol-2-yl)-2,5-diphenyltetrazolium bromide (MTT)

2. Dimethyl sulfoxide (DMSO)

3. Instruments: Microplate reader (to measure absorbance), multichannel pipette, syringe and membrane filter.

F.3. Methods

The protocol we developed is semi-automated and optimized for triple negative breast cancer cells lines and an apoptosis-related siRNA library which contains 446 siRNAs related to apoptosis events. Some of the steps need to be modified depending on cell types and siRNA libraries. The experimental design is divided into following sections: Cell culture and seeding, Sample preparation, Transfection and drug treatment and Final read-out assay as outlined in **Figure F.1**. **See note 4** for additional information.

F.3.1. Cell culture and seeding

1. Aspirate 10 mL of pre-warmed cell culture medium into sterile 75-cm^2 cell culture flask inside laminar flow hood. Gently, swirl the flask to ensure even distribution of flask bottom

surface. Collect pre-warmed cell culture medium into 15 mL centrifuge tube. Put these two medium into incubator to keep warm until they are use.

2. Remove the frozen cell stock from liquid nitrogen, spray with 70% alcohol and wipe. Open the cap of cryotube for 2 second and close (to remove liquid nitrogen from cryotube) inside laminar flow hood. Immediately, thaw the cells in 37 °C water bath. **See note 5.**

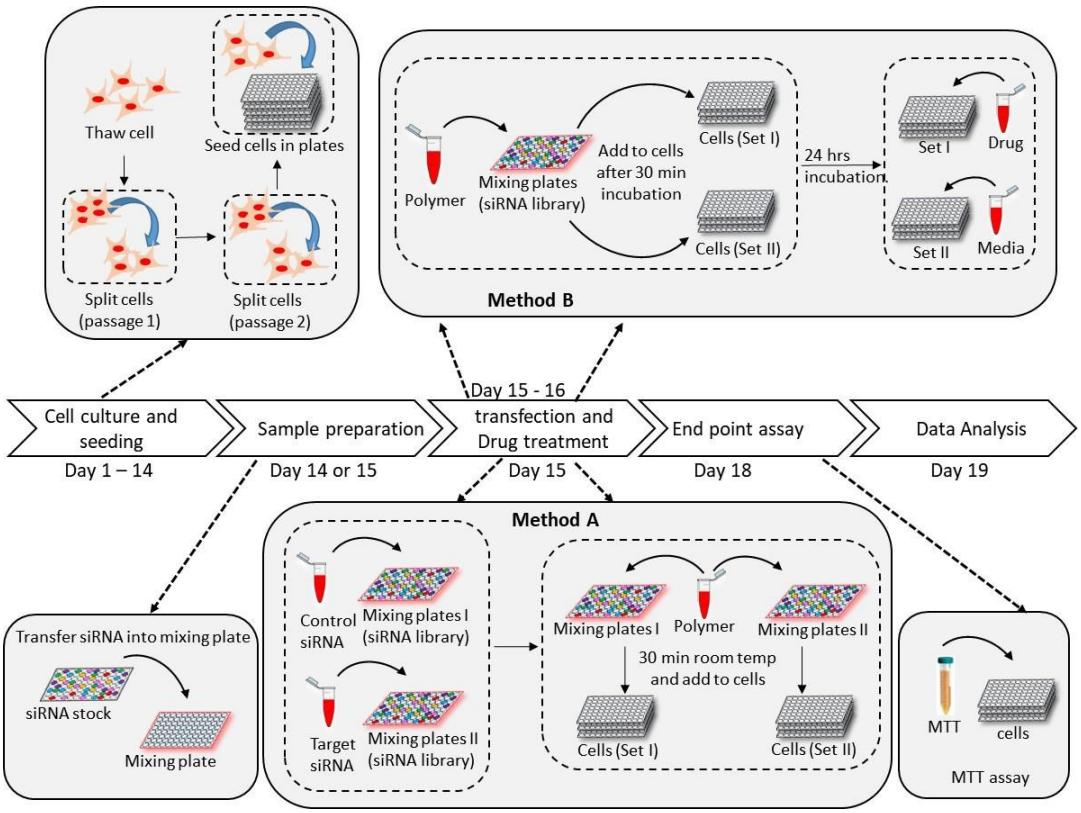

Figure F.1: Workflow and timeline for apoptosis siRNA library screening to identify complementary therapeutic pair of drug (TRAIL) or siRNA in triple negative breast cancer cells (e.g. MDA-MB-231 cells). Total time required from thawing cells is about 3 weeks in which first 2 weeks is for the cell thawing the subculturing. If cells are ready for testing, only one week is required to complete the library screening.

3. Pipette the cells from cryovial into centrifuge tube containing medium (prepared in step 1) and centrifuge at 600 rpm for 5 min. to remove the cell freezing medium. **See note 6.**

4. Remove supernatant, add 5 mL of complete DMEM medium, re-suspend the cells and transfer into 75-cm^2 cell culture flask (prepared in step 1) with vented cap.
5. Place the flask in incubator at 37°C, 5% CO_2 under humidified condition and allow cells to attach. Change the medium after 24 hr. Check the cells daily and allow it to grow until 80 to 90% confluence. **See note 7.**
6. Once cells reach 80- 90% confluent, aspirate the media, wash twice with of HBSS (~10 mL) and add 0.05% trypsin-EDTA (1 mL). Incubate it at room temperature until it starts to dislodge from the flask (~ 2 min.).
7. Add 10 mL of complete DMEM medium to stop the enzymatic activity of trypsin-EDTA. Over incubation with trypsin might digest the cells.
8. Collect the cells into 15 mL centrifuge tube and centrifuge at 72 X g for 5 min.
9. Remove supernatant and re-suspend cell in 10 mL complete DMEM medium.
10. Pipette 10 mL of complete DMEM medium into 75-cm^2 cell culture flask.
11. Add 2 mL of cell suspension into it (1:5 dilutions)
12. Gently swirl the flask to distribute the cells throughout the flask and allow them to grow.
13. Repeat the step 6 to 12 at least 2 times before seeding into plates for screening and proceed to step 14. **See note 8.**
14. Once the cells reached the 80 to 90 % confluence, aspirate the medium, wash HBSS and trypsinize (As explained in step 6).
15. Add 10 mL of complete DMEM to stop trypsinization, pipette cell suspension into 15 mL centrifuge tube, and centrifuge at 600 rpm for 5 min.
16. Remove supernatant and re-suspend cells in 10 mL of complete DMEM medium by careful pipetting the cell suspension up and down around 10 to 15 times to separate cells clumps.

If required, mix cells from other flask since the cells from single flask might not be enough. **See note 9.**

17. Count the cells on a Neubauer cell counting chamber.
18. Dilute cell suspension, which gives 5,000 cells in 90 µL of medium. **See note 10**.
19. Mix well and pour cell suspension into sterile flat bottom rectangular container prepared for loading into 96-well plate through liquid handling robot. **See note 11.**
20. Gently pipette 90 µL of cell suspension into each well using liquid handling robot. Gently shake the plates to ensure a uniform distribution of cells throughout the well surface. **See note 12.**
21. Move cell seeded 96-well plates into incubator at 37 °C, 5% CO_2 humidified atmosphere. Allow them to grow for 24 hr. Do not overlay the plates inside incubator.
22. Repeat step 20 and 21 until all the required 96-well plates were seeded.
23. Incubate cells overnight and check them under microscope. If the cells reached ~40% confluence, proceed transfection.

F.3.2. Sample preparation

1. Calculate how much siRNA is needed per well using the formula:

   $$\text{siRNA needed (µL)} = \frac{\text{Final volume (medium+compexes; µl) X dose of siRNA (nM)}}{\text{Concentration of stock siRNA (nM)}}$$

   Our siRNA stock concentration was 1 µM and the final volume was 100 µL. So, for 30 nM treatment concentration, 3 µL of siRNA was needed. **See note 13.**

2. Thaw the stock siRNA library and centrifuge to collect residual agents on surfaces. Pipette the required amount of siRNA from the stock siRNA plate (1 µM) into 96-well mixing plate (round bottom) using liquid handling robot in a sterile environment. First and last

column of all the plates was left empty where the same amount of control siRNAs (positive and negative control) and blank (saline) were pipetted as shown in **Figure F.2**. **See note 14.**

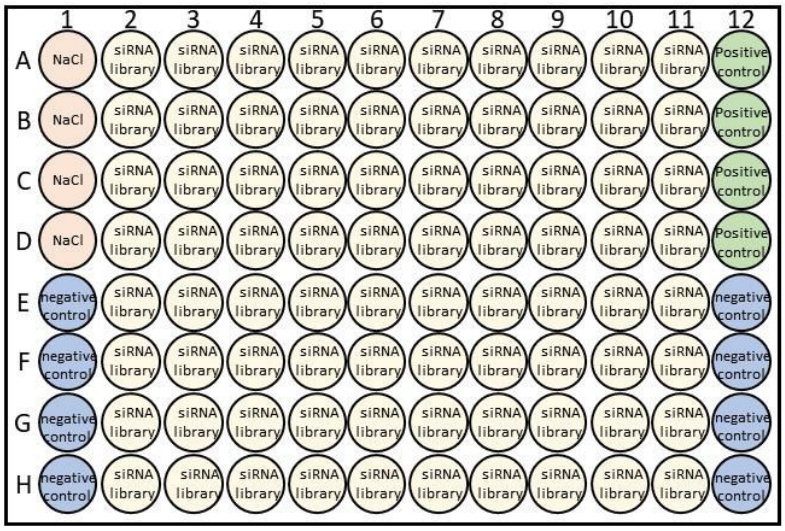

Figure F.2: Layout of 96-well mixing plate with siRNA printing.

3. Prepare polymer (lipid modified 1.2 kDa polyethyleneimine) solution in serum free DMEM medium (without serum). Prepare extra (~10%) polymer solution to encounter the dead volume while pipetting. Concentration of polymer should be calculated in such a way that polymer to siRNA weight ratio become 6 in total 10 μL of complexes per well. **See note 15.**

F.3.3. Transfection and drug treatment

Transfection procedure in this study was 'forward' transfection (i.e., cell addition is followed by siRNA complex) using aliphatic lipid-grafted low molecular weight (1200 Da) polyethylenimine (PEI-L) as transfecting agent [431]. This library screening is intended to find

out synergistic pairs of siRNA-siRNA molecules (Method A, **Figure F.1**) or siRNA-drug molecules (Method B, **Figure F.1**). In Method A, siRNAs were plated in 96-well mixing plate in two parallel sets of plates. A pre-determined desired siRNA was then added to each well of one set of prepared siRNA plates, while a negative control (scrambled) siRNA was added to each well of the other set of siRNA plates. In Method B, drug (TRAIL) treatment was performed after 24 hr. of transfection to one set while set remained without drug (TRAIL). Screening was performed in triplicate wells. Hence, sufficient complexes should be prepared for addition to 6 wells for each siRNA treatment (with 10% excess volume to account for pipetting losses).

Method A: To reveal synergistic pairs of siRNA-siRNA combinations.

(i) Take 2 sets of siRNA library plated in 96-well mixing plate (round bottom).

(ii) Add target siRNA (e.g. Mcl-1) to each well of one set and control siRNA to each well of another set. The following procedure is same for both sets. Label the mixing plates properly.

(iii) Mix well by pipetting and centrifuge them briefly.

(iv) Allow them to reach room temperature.

(v) Add previously prepared polymer into each well containing siRNAs. Make polymer to siRNA weight ratio 6. Now, total volume of complexes is 30 μL (for triplicate)

(vi) Pipette several times using liquid handling robot. **See note 16.**

(vii) Incubate these complexes for 30 min. at room temperature.

(viii) Repeat the steps 5 and 6 until all the siRNA were mixed with polymers. **See note 17.**

(ix) Mix the complexes well. Aspirate all of them and dispense 10 µL of complexes to each well of 96-well plate containing well-attached cells. Dispense remaining 10 µL complexes to replicate II and 10 µL to replicate III. **See note 18.**

(x) Gently tap the plates to distribute the complexes and return it back to incubator. Incubate for another 72 hr.

Method B: To reveal synergist pairs of siRNA-drug combinations.

1. Calculate and pipette siRNA solution enough for 2 sets of screening into round bottom 96-well mixing plate. Label the mixing plates properly.
2. Mix wells by pipetting and centrifuge them briefly.
3. Allow them to reach to room temperature.
4. Add previously prepared polymer solution into each well containing the siRNAs. Make polymer to siRNA weight ratio 6. Total volume of complexes would be 60 µL for the two sets of screening in triplicate (10 µL per well x 6 wells).
5. Pipette the complexes several times using liquid handling robot. **See note 16.**
6. Incubate the complexes for 30 min. at room temperature.
7. Repeat steps 4 and 5 until all the siRNA were mixed with polymers. **See note 17.**
8. Mix the complexes well. For set 1: Aspirate all of them and dispense 10 µL of complexes to each well of 96-well plate containing well-attached cells. Dispense remaining 10 µL complexes to replicate II and 10 µL to replicate III. For Set 2: Repeat the same procedure for this set as well. **See note 18**.
9. Gently tap the plates to distribute the complexes well in the plate and return it back to incubator and incubate for 24 hr.

10. Prepare drug (TRAIL) solution in complete DMEM medium. **See note 19.**
11. Add 20 µL of TRAIL solution into one set of cells (from step 8) treated with siRNA complexes (replicate I, II and III). To have a proper control, add 20 µL of complete DMEM medium into another set (from step 8) of cells with siRNA complexes (replicate I, II and III).
12. Gently tap the plates to ensure proper mixing of drug and return back to incubator. Incubate for another 48 hr.

F.3.4. End point assay and data analysis

1. Prepare MTT solution (5 mg/mL) in pre-warmed HBSS, filter through syringe membrane filter (pore size 0.2 µm). **See note 20.**
2. After 72 hr. of polymer/siRNA complexes treatment, add MTT solution to each well using multichannel pipette and incubate at 37^{o}C for 1.5 hr. Volume of MTT solution should be adjusted in such a way that final concentration becomes 1 mg/mL. **See note 21.**
3. Check the plate for MTT crystal generation and remove the media from well. If the crystal did not appear in non-treated group, then incubate for an extra time. **See note 22.**
4. Add 100 µL of DMSO to each well using multichannel pipette. Gently tap the plate to dissolve MTT crystal completely within a 10-min time window. **See note 23.**
5. Read the absorbance at 570 nm at plate reader and proceed to data analysis. **See note 24.**

F.3.5. Data analysis and selection of Hits

It is always not feasible to replicate the library screen therefore our confidence level in the identified targets from primary screening is low. Further validation is always needed to establish

effective hits. We performed the screening experiments in triplicate to maximize the sensitivity along with increasing the confidence in hits.

1. To identify the effective siRNAs, calculate relative cell viability of treated group as a percentage of cell growth in non-treatment control group on a per plate basis using following formula:

   Relative cell viability = $\frac{\text{O.D. of siRNA or Drug teated well}}{\text{O.D. of Non-treated well}}$ X 100%

   In calculating the O.D. of wells, background O.D. (i.e., that of DMSO) should be reduced from the measured O.D.s.

2. After calculating relative cell viability of each well of the entire plate, calculate mean and standard deviation of triplicate wells (plates) using excel or other suitable software.

3. Calculate significance by student's two-tailed t-test (assuming equal variance) and z score to identify the effective targets. A value of $p<0.05$ was considered significant and the outliers were noted by selecting responses with $-1.96 < z < 1.96$. Calculate z value using following formula:

   $z = \frac{xi-\mu}{s}$

   where xi is the percentage of cell growth compared to non-treatment cells for each well (relative cell activity), μ is the average and s is the standard deviation of all xi in the whole plate.

4. The targets which satisfies the criteria (i) relative cell viability < 70%, (ii) z-score < -1.96 and (iii) $p < 0.05$ was considered as hits in our screens.

5. Select the targets based on selection criteria mentioned above and prioritize the hits for validation. **See note 25 and 26** for detailed criteria to prioritize and validate selected targets.

6. Plot the correlation plots (between replicates) to assess the reproducibility and assess the quality control of the library screen. **See note 27** for details. See **note 28** for anticipated results.

F.3. Notes

1. To this end, different siRNA libraries are commercially available, adding possibilities of focused screening towards specific class of cellular molecules, which are more cost-efficient and increase the chances of new drug target discovery. Although we used focused siRNA libraries in this protocol, the protocol can also be applicable to genome-wide screens with appropriate instrumentation. This protocol requires high throughput liquid handler therefore experimental costs will increase with the increase in experiment size. On the other hand, high throughput screening instrumentation made the entire screen possible to set-up, run and evaluate in a reasonable time frame.
2. Scrambled siRNA is used as negative control siRNA to assess non-specific toxicity associated with siRNA, transfecting reagents and/or procedural steps. One can design or order it through different vendors. Negative control siRNA should have a chemical composition/size/architecture similar to the siRNA library members (e.g., a short 21 b.p. polynucleotide or long 27 b.p. DICER-substrate polynucleotide) that do not target any known transcript. Manufacturer-supplied scrambled siRNA should be also confirmed not to display any activity; despite best efforts, we still see some level of activity in separate assays when we use scrambled siRNAs. Keeping a low concentration/dose of siRNA is an effective way to minimize non-specific effects. Positive control siRNA, where strong efficacy of the siRNA is well-established, assures the accuracy of collective procedures during the screen, including

transfection, incubation, and endpoint assays. Therefore, careful selection of positive control is important. We recommend finding a proper positive control for particular cell line before screening. Using different positive control with different siRNA libraries is recommended. Since our aim is to find out the best targets, which cause breast cancer cell death, we use siRNA silencing CDC-20 (cell cycle protein) as positive control, which had already shown significant cell death of breast cancer cells.

3. The siRNAs used here are not chemically-modified, since such a modification makes library costs significantly higher, so that the screening will require an effective transfection reagent for intracellular delivery of siRNA. We rely on lipid-grafted low molecular weight (MW 1200Da) polyethylenimines (PEIs) obtained from RJH Biosciences Inc., Edmonton, Canada to undertake siRNA transfections in this protocol; while we found such PEIs to display an optimal efficacy over toxicity for a broad array of cells. Other transfection reagents could also be used in library screens. However, the choice of the polymer in our screens is facilitated by the availability of several polymeric analogues that allows us to match the performance of transfection reagent to the features of the cells, so that improved transfection efficiencies are obtained compared to generic transfection reagents commercially available [207, 432]. Polymeric delivery agent used for transfection is non-toxic and relatively easy to prepare. Unlike more cytotoxic liposomal reagents, the lack of toxicity by polymeric agents provides a clear advantage by maintaining normal physiology of the cells during testing. The availability of several analogues of the polymeric transfection reagents also enhances chances of success in specific cell types by employing an analogue with highest transfection efficiency in that cell type.

4. The protocol we developed is semi-automated and optimized for triple negative breast cancer cells lines and an apoptosis-related siRNA library which contains 446 siRNAs related to apoptosis. For each targeted gene, a pool of 4 non-overlapping siRNAs were included in the treatment. Some of the steps will need to be modified while adopting to other cell types and siRNA libraries. In order to optimize this protocol for other cell lines, thorough testing of each individual step with negative and positive controls is recommended. While setting up large-screens, advance planning and detailed scheduling are crucial for the success of the screening. Required materials, reagents and equipment need to be checked beforehand. Listing of every required reagents and planning for extra amount (overhead of 10%) is recommended. In this protocol, siRNA library screens are used to identify complementary pairs of therapeutic agents for cancer gene therapy. The synergism can be explored between the library members and a particular siRNA, a conventional chemotherapy drug or a protein drug used in cancer therapy. In order to identify complementary therapeutic pairs, two parallel siRNA library screenings are performed; in one screen, cells are treated with the library members alone (i.e., without a co-treatment) and, in a second screen, cells are treated with the combination of library members and a desired agent (e.g., TRAIL or a specific siRNA).
5. Cells should be thawed as fast as possible. While keeping in water bath, continuous shaking of the cell-containing cryotube by hand is recommended. Cells should be checked every half minute and keep in water bath until small portion of ice remains.
6. Centrifugal force and time should be optimized based on the size of the cells.
7. Cell culture condition such as metabolic activity, growth rate and cell cycle are crucial for the transfection efficiency [392, 433, 434]. Cells prior to seeding should never reach the confluence state ‘plateau’ phase, which may lower the metabolic activity in subsequent

generations. Over confluent cells will start to die and/or enter into senescence, which had reduced metabolic activity. This will substantially affect transfection efficiency. Beyond 80 to 90% of confluence MDA-MB-231 cell becomes round and detach from the flask. Therefore, cells should never grow more than 5 to 7 days. Cells with higher passage numbers (~20 to 25) are less metabolically active and should be avoided and some passage (e.g., at least twice) should be allowed for frozen cells before employing in screening.

8. Cells should be maintained in several flaks such that sufficient cells are generated for seeding into 32 plates (96-well) as described in this Protocol. To avoid experimental variation, those flasks should be prepared from the cells of same batch and passage. This protocol was optimized for 96-well plate format, which was considered an optimum scale to screen large numbers of samples at a reasonable cost (i.e., small enough for reagent amounts) and reproducibility (i.e., sufficient cell numbers). However, 384-well culture plate can also be used. Number of cells and medium per well should be adjusted accordingly.
9. Pipette slowly and avoid aspirating air to prevent the bubble formation in the suspension
10. Total cell suspension required for the entire plate should be prepared in a single container (500 mL bottle). Preparing in separate container may result in variation in cell numbers between plates. Always calculate for 110 wells instead of 96 well and prepare extra cell suspension. The cell culture condition and seeding density significantly influence the transfection efficiency and functional outcome of any siRNA library screening. Number of cells per well should be considered based on the size of well and type of cells and their growth speed. Cells should be seeded at such a density that the sham (non-treatment) group should grow exponentially but not to reach the over-confluence and plateau phase at the day of analysis. In addition, toxicity and transfection efficiency of polymer/siRNA complexes is closely related

to cell density. As an example, polymer and siRNA concentrations could be more than optimal and generate non-specific effects if the cell density is low, as compared with confluent cell cultures. Efficiency of siRNA may be reduced in high cell density. Therefore, optimization of cell density to achieve optimum transfection without inducing any toxicity is crucial. Since cell seeding density does not necessarily translate to attached cell density, optimization is recommended based on cell culture condition, speed of cell growth, handling process and passage number of the cell line. Sufficient dynamic range should be available to detect functional effects in both positive and negative directions. MDA-MB-231 cell is fast growing breast cancer cells therefore 5000 cells per well is optimal for 96-well plate in our case.

11. Programming of the robot should be done prior to cell suspension preparation. Label 96-well plate beforehand. Wipe workstation with 70% ethanol. Turn on lamina flow hood at least 15 before experiment.
12. Avoid moving anything over cell suspension container. Put the lid as soon as seeding is complete to avoid any possible contamination.
13. Always prepare 10% extra volume in order to compensate loss during pipetting.
14. siRNA can be aliquated into mixing plate and stored at -20°C beforehand to reduce work load at the day of transfection. It should be sealed tightly with aluminum plate sealer before storing and should be centrifuged before using. Each of the mixing plates were designed in such a way that positive and negative controls are accommodated. **See note 2** for details on positive and negative control. Positive and negative control should be included in all plates. Needless to say, concentration and cell exposure time of both positive and negative control siRNAs should be identical to the siRNA library members.

15. Polymer solution should be prepared fresh. Optimization of transfection conditions (e.g., cell density, polymer and siRNA concentration, polymer to siRNA ratio, etc.) in particular cell culture plates that is used during screening is crucial. We found polymer: siRNA weight ratio of 6 optimal for siRNA transfection in MDA-MB-231 cells. This can vary depending on the type of cells and polymers or transfecting reagents. **See note 3** for details.
16. Pipetting should be done gently. While mixing, pipette only fraction of mixture and discharge slowly. Repeat these processes at least 5 times. Avoid aspirating air, which creates bubble.
17. This type of library screening contains more than one siRNA mixing plates. Hence, in order to provide same incubation time with all the siRNAs, it is recommended to have an interval of 5 minutes between two plates.
18. Before adding to cells, check for air bubbles in each well. If any air bubble is present, wait until it bursts or use pipette tips to burst it. The speed of complex mixing is critical to avoid any air bubble formation. Centrifugation of the complexes is not recommended. The triplicate samples were placed in 3 separate plates, rather than added consecutively in the same plate, to improve reproducibility and confidence in the obtained results.
19. We aim to reveal the complementary therapeutic targets of TRAIL in the library screening. TRAIL induces apoptosis in MDA-MB-231 cells. Since the effect of the TRAIL was more after 48 hr. than 24 hr., we add TRAIL after 24 hr. of siRNA transfection, which allows total 48 hr. of incubation with TRAIL. For other drugs, time of treatment may vary and should be optimized before library screening. TRAIL protein loses its activity with repeated freeze-thaw cycles. Hence, it should be aliquated into small volumes and stored at -80°C according to manufacturer's instruction. Dilute TRAIL into complete medium just before adding to cells. Concentration of drugs used must be predetermined. Here, we used final concentration of 5

ng/mL of TRAIL. This will vary depending on drug and cells types. Always prepare an extra (around 10%) drug to compensate the pipetting error.

20. The MTT Assay was used for assessing cellular growth, which provides immediate results without further analysis, optimal signal-to-noise ratios and, more importantly, a read-out that is directly related to the desired clinical outcome in this therapeutic model. MTT must be dissolved in HBSS completely by vortexing and protect from light. Soluble versions (e.g., XTT) of the dye could be used to eliminate the organic solvent (DMSO) in the processing.
21. To synchronize the incubation time with MTT reagent, MTT reagent was added to each plate in 10 min intervals. In this way, sufficient time is provided to process and read the plate before the next plate is processed. This way addition of MTT solution and reading plate can be done parallel and total incubation time for each plate would be same. Incubation time with MTT reagent depends on number of cells and metabolic activity of the cells and should be optimized depending on cell type used in screening.
22. If media is aspirated, then care must be taken not to touch the cells and vacuum force should not be strong so that cells are lost. Alternatively, upside-down the cell culture plate to dump media and gently tap on tissue paper to remove media completely. Presence of even small amount of media could affect the absorbance.
23. Check each well and make sure crystals are completely dissolved. If the crystals are not dissolved completely, it will give false results. Shake the plate in plate shaker for 30 second if undissolved crystals are visible.
24. Plate reader should be turned on at least 10 minutes before reading plate. The O.D. measured corresponds to the total metabolic activity (mitochondrial dehydrogenase activity) in the well and can be used as a measure of cell numbers. Cell growth by the treated cells was expressed

as a relative percentage of the cells incubated with medium only (no treatment). It should be remembered that some agents can alter metabolic state of the cells (hence MTT signal) without affecting the cell numbers (growth), so that the possibility of false hits due to this complication should be considered.

25. Once hits were identified, multiple criteria should be utilized to prioritize the hits for validation. Druggability is one criteria to select if the aim is to find out the hits, which would represent the candidate drug targets. Function(s) of the identified targets can be obtained from the literature review if they are well known. In addition, different bioinformatics tools are available which can help to build functional network of hits and their interaction with other genes. Considering the expression and or mutational status of the hits focusing on cancer type in question is also important. Some databases such as Cancer Genome Atlas are available for this analysis. In addition, it is not advisable to select the hits based on the ranking from the investigated functional outcome (i.e., growth inhibition). Hits with weaker performance but strong association to the disease of interest pathway should always be prioritized. It should be kept in mind that the performance of the identified siRNAs can always be increased by optimizing siRNA sequences and transfection conditions. However, we advise to consider the hits with strong performance even the supporting evidences in disease of interest is missing. This may lead to identify the novel biomarker and to unforeseen insights into the biological pathway associated with disease.
26. Successful outcomes from siRNA library screening greatly depends on the optimization of the protocol. Experimental artifacts may be further exasperated from the use of high throughput screening which can be minimized by optimizing each step in overall protocol. Since pooled siRNAs were used in this protocol, there is always the possibility of non-specific effects arising

from individual siRNAs in the cocktail. At the same time, using pooled siRNA reduces the overall cost of siRNA library screening and increases the throughput of single screen. Finally, validation studies with independent siRNAs are needed; one can use the same source of siRNA for this purpose (e.g., from the same manufacturer of libraries) or prepare new siRNAs with different sequences against the same target. Either approach should lead to equivalent outcomes. The validation of identified targets with complementary assays is also accordingly required. See reference [207] for follow up validation studies in details for this particular study.

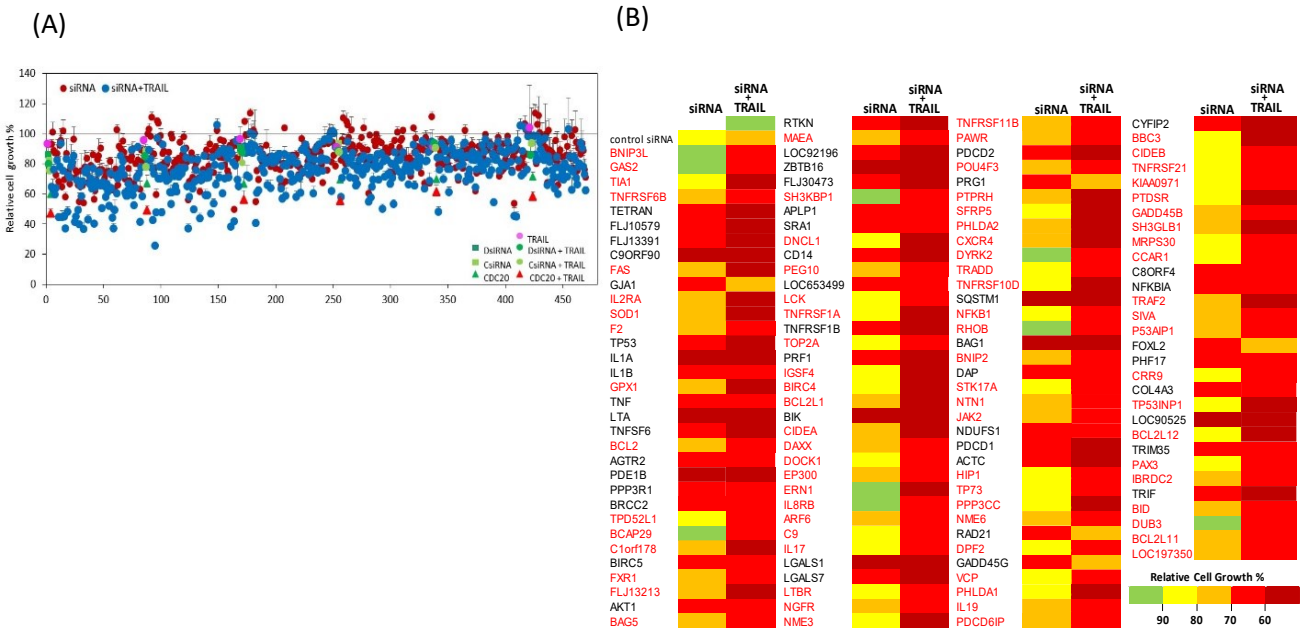

Figure F.3: (A) Human apoptosis siRNA library screen in MDA-MB-231 cells without and with TRAIL (5.0 ng/mL) treatment. The relative cell growth for treated cells was calculated as a percentage of cell growth of non-treated group. Final concentration of siRNA used for cell treatment was 30 nM. CDC-20 siRNA was used as positive control and two negative control siRNA were used; DsiRNA (27-mer) and CsiRNA (21-mer). CDC-20 siRNA is 27-mer DICER-substrate polynucleotide therefore DsiRNA is used as its control. siRNAs from library are 21-mer polynucleotide therefore CsiRNA is used as its control. (**B**) Heat map shows the siRNAs that induced significant cell death (relative cell growth < 70%) in MDA-MB-231 cells (without or with TRAIL). Many siRNAs, including BCL2L12, SOD1, BCL2L1, FLJ13391 and NTN1 and

FLJ13213, showed significant cell death in the presence of TRAIL. Figures are adapted from ref [5].

27. Quality control throughout the experiment is very important. Performance of positive and negative controls throughout plates, analysis of standard deviation and *p*-value derived from the triplicates, distribution of viability across the entire library and within plates are some parameters to assess the quality of outcomes. Exclusion of the outermost wells of each plate is also recommended to avoid edge effects (especially important if there is high evaporation from plates). For a successful screening, cells should be checked under microscope while screen is in progress to uncover potential technical problems such as edge effect, plate-to-plate variability or contamination. If the edge effect and other technical problems are obvious within a plate, then *B* score instead of *z* score can be used to exclude the wells or row/columns affected by such technical problems. *B* score is relatively robust to outliers and can be calculated using open-source BioConductor bioinformatics software [435].
28. This protocol was developed to identify two types of complementary therapeutic pairs, one involving siRNA-siRNA combinations and one involving siRNA-drug combinations, for cancer therapy using focused siRNA libraries in triple negative breast cancer cells (e.g. MDA-MB-231). Using this protocol, we identified synergistic combinations of therapeutic agents for protein-based anti-cancer drug TRAIL (**Figure F.3**). Optimization of experimental parameters such as cell density, concentration of therapeutic agents and composition of complexes (in particular polymer/siRNA ratio) are critical factors in performing this type of protocol. In siRNA-TRAIL combination study, post-transfection time for the addition of drug should be properly selected to get the optimum outcome. By fine-tuning operational parameters of conventional siRNA library screening protocols, we were able to identify promising siRNAs that can sensitize breast cancer cells to a drug (TRAIL) therapy.

F.4. Acknowledgements

BT was supported by Alberta Innovates Graduate Studentship. The authors RBKC and HU are the founder and shareholders in RJH Biosciences Inc. that are developing the lipopolymers for medical applications.

Appendix G: Content licence for figure 1.3

ELSEVIER LICENSE
TERMS AND CONDITIONS

Jul 28, 2019

This Agreement between Bindu Thapa ("You") and Elsevier ("Elsevier") consists of your license details and the terms and conditions provided by Elsevier and Copyright Clearance Center.

License Number	4637451160252
License date	Jul 28, 2019
Licensed Content Publisher	Elsevier
Licensed Content Publication	Trends in Molecular Medicine
Licensed Content Title	TRAIL on trial: preclinical advances in cancer therapy
Licensed Content Author	Daniel W. Stuckey,Khalid Shah
Licensed Content Date	Nov 1, 2013
Licensed Content Volume	19
Licensed Content Issue	11
Licensed Content Pages	10
Start Page	685
End Page	694
Type of Use	reuse in a thesis/dissertation
Portion	figures/tables/illustrations
Number of figures/tables/illustrations	1
Format	both print and electronic
Are you the author of this Elsevier article?	No
Will you be translating?	No
Original figure numbers	Figure 2
Title of your thesis/dissertation	Nucleic Acids and their Combination for Cancer Therapy
Expected completion date	Sep 2019
Estimated size (number of pages)	245
Requestor Location	Bindu Thapa 1-019 Research transition facility university of alberta Edmonton, AB T6G 2V4 Canada Attn: Bindu Thapa
Publisher Tax ID	GB 494 6272 12
Total	0.00 USD
Terms and Conditions	